

2014

Forces Generated by Cell Intercalulation Tow Epidermal Sheets in Mammalian Tissue Morphogenesis

Evan Heller

Follow this and additional works at: http://digitalcommons.rockefeller.edu/student_theses_and_dissertations



Part of the [Life Sciences Commons](#)

Recommended Citation

Heller, Evan, "Forces Generated by Cell Intercalulation Tow Epidermal Sheets in Mammalian Tissue Morphogenesis" (2014). *Student Theses and Dissertations*. 334.
http://digitalcommons.rockefeller.edu/student_theses_and_dissertations/334

This Thesis is brought to you for free and open access by Digital Commons @ RU. It has been accepted for inclusion in Student Theses and Dissertations by an authorized administrator of Digital Commons @ RU. For more information, please contact mcsweej@mail.rockefeller.edu.



FORCES GENERATED BY CELL INTERCALATION TOW
EPIDERMAL SHEETS IN MAMMALIAN TISSUE
MORPHOGENESIS

A Thesis Presented to the Faculty of
The Rockefeller University
in Partial Fulfillment of the Requirements for
the degree of Doctor of Philosophy

by

Evan Heller

June 2014

FORCES GENERATED BY CELL INTERCALATION TOW EPIDERMAL SHEETS IN MAMMALIAN TISSUE MORPHOGENESIS

Evan Heller, Ph.D.

The Rockefeller University 2014

Underlying the dramatic tissue movements of development—the bending, folding, squeezing, pushing, pulling, mass movements, and individual movements—are processes of cell migration. Throughout our lives, cell migration plays a role in the maintenance and regeneration of our tissues, and even in the development and progression of disease. To carry out the complex tasks of development and tissue morphogenesis, cells must coordinate their behaviors and migrate collectively. Insights into these collective behaviors have come from elegant studies of gastrulation movements in model organisms such as flies, frogs, and fish, uncovering conserved cellular and molecular mechanisms. However, the extent to which these mechanisms are refined, reiterated, and combined in the complex tissue environments of late development and adulthood is not well understood, highlighting the need for new models. Here, I develop a model of collective cell movements in late mammalian development by studying embryonic eyelid closure in mice, a process in which an epithelium locally reshapes, expands, and moves over another epithelium. Using a combination of lineage tracing and genetic ablation facilitated by ultrasound-guided lentiviral injection, I establish that the migratory cells of the eyelid front are derived from the epidermis rather than the periderm, and that the periderm is not required in the process as previously hypothesized. Quantitative analyses of cell proliferation, including inhibition of cell divisions *in vivo*, reveal that closure is primarily driven by cell motility rather than by proliferation. Optimizing conditions for the culture and live imaging of skin explants *ex vivo*, I reveal that cells of the eyelid front elongate perpendicularly to the axis of closure, extend mediolateral protrusions, and intercalate along this axis. Laser ablation and quantitative analyses of tissue deformation reveal that it is this intercalation, and not assembly and constriction of a supracellular actin cable, that drives eyelid closure. This mechanism is a novel mode of epithelial fusion

in which forces generated by cell intercalation are leveraged to tow the surrounding tissue. Functional analyses *in vivo* show that this mechanism requires $\alpha_5\beta_1$ integrin/fibronectin and myosin II-dependent cell motility, is potentially organized by non-canonical Wnts/PCP, and is supported by a concomitant reduction in cadherins through localized Wnt/ β -catenin signaling. These studies establish eyelid closure as a model in which well-described mechanisms of collective cell movement are integrated into a complex morphogenetic process, set the stage for future study of the interplay between canonical and non-canonical Wnts/PCP in regulating cell motility and intercalation, and present an opportunity to uncover novel regulators of collective migration.

To childlike wonder, tempered immaturity, unfettered enthusiasm, and a lack of moderation, which, in my mentors and colleagues, have been a joy and inspiration.

Acknowledgments

In science, no work is fully our own, nor should it be. Concepts start out partially formed, and through the scrutiny of our peers, the incorporation of some ideas and the rejection of others, and of course through experimentation, they emerge as something coherent and, with any luck, enlightening. There are thus many people to whom this work also belongs. Foremost, there is my advisor, Elaine Fuchs, who gave me the latitude to propose and explore my own ideas before I had any measure of scientific credibility. She in many ways let me feel like my own PI in her lab, reining me in to help me when I clearly needed it and always wholeheartedly supporting my work. Her tireless dedication to science and demanding standards have been an inspiration, and her promotion of a collaborative, intellectual workplace whose mission is for everyone to achieve their best work has been a privilege.

I am also indebted to my thesis committee, Sandy Simon, Mary Beth Hatten, and Jen Zallen, who took an interest in my work and whose suggestions have been invaluable along the way. I am, alas, a terrible student, who never much cared for classes and meetings. But once I got over the nervousness of presenting (which happened anew at every meeting), I found that discussing my work with them was an absolute pleasure, and I always left with newfound inspiration and purpose. I will, in particular, always admire Sandy's style of teaching and approach to science—he encouraged me early on to run, and have fun with, this project.

On the scientific side, this work would not be what it is without the help of my collaborators in Dresden, Vijay Krishnamurthy and Stephan Grill, two generous biophysicists who agreed to work with us in revising our paper. Nor without the Fuchs lab mouse staff, particularly Nicole Stokes and Dan Oristian, who are constantly mating mice for me and who in general make my life a lot easier. Shiva Bhuvanendran and Alison North, who work in the university's Bio-imaging Center, were also of great help in getting my imaging experiments started.

Then there are the postdocs and students in the lab who have been a second family of

sorts. Boba Beronja took me under his wing as a rotation student and got me started in the lab. He is a brilliant and creative thinker, endlessly and unreasonably optimistic, and very likely one of the great ones. Irina Matos, my dear friend, whose love and enthusiasm for science (and mitosis in particular) have been a beacon. Scott Williams, my long-suffering baymate, who bore the brunt of my sarcasm, surly humor, and irredeemable untidiness. Chen Luxenburg, a cynical man but a great colleague, who always came by to share ideas with me from conferences he'd been to. Ya-Chieh Hsu, who is always ready for a good discussion, is always full of good advice, and who, with her stash of candy and snacks, kept me well-fed during long experiments. Brice Keyes and Amma Asare, my link to the world of bioinformatics and two of the funniest people in the lab. And last but not least, some of the newer students and postdocs in the lab, who have been a lot of fun to work with, including Tamara Ouspenskaia, Kenneth Lay, Cynthia Alexander, and Aaron Mertz.

Last of all, I would like to thank my best friend and lifelong partner, my wife, Rebeca Tenney, for holding me in high estimation and always rounding up.

Table of Contents

1	Introduction	1
1.1	Basic principles of cell migration	2
1.2	Regulated adhesion: the basis of collective cell movement	6
1.2.1	Cell-cell adhesion	6
1.2.2	Cadherin-based adhesion and the adherens junction.	7
1.2.3	Actomyosin dynamics at the adherens junction	8
1.2.4	Beyond the adherens junction	10
1.3	Cell migration and adhesion in morphogenesis	11
1.3.1	Epithelial to mesenchymal transition (EMT)	12
1.3.2	Cell sorting and cadherin-dependent migration	14
1.3.3	A case of cadherin-dependent cell migration: border cell migration	18
1.4	Conserved morphogenetic movements	21
1.4.1	Cell shape changes in morphogenesis	22
1.4.2	Epithelial sheet movement	23
1.4.3	Cell intercalation and convergent extension movements.	29
1.4.4	Planar cell polarity	35
1.4.5	Collective cell movements in organogenesis	39
1.4.6	Emerging technologies in live imaging	40
1.5	The skin as a model system	42
1.5.1	Temporary epithelial fusions	46
1.5.2	Outline of this work	47
2	Developing Eyelid Closure as a Model	52
2.1	Cell types contributing to eyelid closure	54
2.1.1	Keratin and integrin expression in the eyelid	57

TABLE OF CONTENTS

2.1.2	Genetics and lentiviral technology in the skin	60
2.1.3	Lineage tracing of the epidermis and periderm	62
2.1.4	Ablation of the periderm.	64
2.2	Cell motility and proliferation	64
2.2.1	Culture conditions for live imaging explanted eyelids	66
2.2.2	Cell proliferation in eyelid closure	68
2.2.3	The acquisition of motile properties by front cells	73
2.2.4	Global and individual cell behaviors in eyelid closure	76
2.3	Discussion	81
2.4	Experimental procedures	85
2.4.1	Lentiviral constructs	85
2.4.2	Mouse lines and lentiviral injections	85
2.4.3	Antibodies	86
2.4.4	Immunofluorescence and fixed tissue imaging	86
2.4.5	Image analysis and quantification	87
2.4.6	Culture and live imaging of eyelid explants	88
2.4.7	RT-PCR profiling of eyelid front cells	91
2.4.8	Statistical analysis	92
3	A Towing Mechanism of Eyelid Closure	93
3.1	Cell movement and tissue deformation	94
3.1.1	Cell intercalation and apicobasal polarity in the eyelid front	95
3.1.2	Quantitative analyses of tissue deformation	97
3.2	Laser ablation studies in support of a towing mechanism	103
3.2.1	Coordinated movement and cell elongation in the eyelid epidermis .	104
3.2.2	Laser ablation of the eyelid front	106
3.2.3	Laser ablations to rule out alternative mechanisms	109
3.3	Discussion	113
3.4	Experimental procedures	118
3.4.1	Laser ablation	118
3.4.2	Image analysis and quantification	118
3.4.3	Tissue strain rate analysis	119
3.4.4	Statistical analysis	120
4	Molecular mechanisms underlying eyelid closure	121
4.1	Integrin and cadherin-based adhesion in eyelid closure	123
4.1.1	Loss of integrin-fibronectin adhesion prevents eyelid closure	123

4.1.2	The sufficiency of front cell intercalation for eyelid closure	128
4.1.3	Cadherins in eyelid closure	130
4.2	Canonical and non-canonical Wnts	136
4.3	Discussion	143
4.4	Experimental procedures	149
4.4.1	Mouse lines	149
4.4.2	Immunofluorescence	151
4.4.3	Lentiviral constructs	151
4.4.4	Statistical analysis	152
5	Summary and Perspectives	153
5.1	Eyelid closure as a model system	155
5.2	Cell intercalation in eyelid closure	157
5.3	Beyond eyelid closure	159
	Bibliography	161

List of Figures

1.1	Actin purse strings in tissue morphogenesis	28
2.1	Juxtaposition of cell types in the eye	55
2.2	Overview of eyelid closure	56
2.3	Keratin expression in the eyelid suggests a functional separation	58
2.4	Unique keratins in the eyelid front	59
2.5	Integrin expression in the eyelid	61
2.6	Ultrasound-guided <i>in utero</i> lentiviral injection	63
2.7	The periderm is not required for eyelid closure	65
2.8	Culture conditions supporting eyelid closure <i>ex vivo</i>	67
2.9	Setup for live imaging eyelid closure	69
2.10	Cell proliferation in eyelid closure	70
2.11	Eyelid closure progresses in the absence of cell division	72
2.12	Eyelid closure completes in the absence of cell division <i>in vivo</i>	73
2.13	Cell morphology in the eyelid front	75
2.14	FACS isolation and RT-PCR profiling of eyelid front cells	77
2.15	Global and individual cell behaviors in eyelid closure	78
2.16	Dermal cell movements do not contribute to eyelid closure	80
2.17	Cell segmentation and tracking efficiency	90
3.1	Opposing cell movements in the eyelid front	96
3.2	Quantitative analysis of tissue deformation in the eyelid	102
3.3	Cell intercalation is coupled to translocation of the eyelid	103
3.4	Coordinated movements and elongation of the eyelid epidermis	105
3.5	Targeted tissue ablation with a multiphoton laser	107
3.6	Laser ablation of front cells suggests they generate a pulling force	108

3.7	Eyelid front cells are required for eyelid closure	110
3.8	Additional ablations to distinguish possible modes of eyelid closure	111
3.9	The eye is pushed below the eyelids during closure	112
4.1	Knockdown of fibronectin, α_5 integrin, and myosin IIA in the skin	125
4.2	Cell intercalation depends on integrin-fibronectin adhesion	126
4.3	Knockdown of additional integrins	127
4.4	Conditional ablation of myosin IIA in the skin	129
4.5	Front cells are sufficient to drive eyelid closure	131
4.6	Eyelid closure primarily depends on integrin rather than on cadherin-based adhesion	134
4.7	E-cadherin is not upregulated in the absence of fibronectin or α_5 integrin	135
4.8	Epithelial cohesion is necessary for eyelid closure	137
4.9	Canonical Wnt signaling in the eyelid	139
4.10	Non-canonical Wnts/PCP in the skin are required for eyelid closure	140
4.11	Eyelid front cells are specified but fail to intercalate in PCP mutants	142
4.12	Proposed mechanism of eyelid closure	150

List of Illustrations

1.1	The cell migration cycle	4
1.2	Integrin-based adhesion	5
1.3	The structure and formation of adherens junctions	9
1.4	Border cell migration	19
1.5	Apical constriction	24
1.6	Modes of cell intercalation in development	31
1.7	The core PCP pathway	37
1.8	The architecture of mammalian skin	44
3.1	Models of eyelid closure and expected patterns of tissue deformation	101
3.2	Relationship between tissue deformation and the strain-rate tensor	120

Chapter 1

Introduction

Cell migration is a fundamental process to organisms as simple as the amoeba and as complex as mammals. Since the first observations of amoeboid motility in cells with the advent of optical microscopy, the intricacies of cell movement have captivated cell and developmental biologists, biochemists, and physicists alike. While the primary role of migration for unicellular organisms is to find food, multicellular organisms have systems in place to instruct individual cells, each with the capacity to migrate autonomously, to work collectively within sheets or clusters in carrying out the complex morphogenetic tasks of development and in maintaining the integrity of adult tissues. The past fifty years have seen tremendous advances in our understanding not only of the mechanics and biochemistry underlying cell locomotion, but of the great diversity of processes in development, tissue morphogenesis, and disease driven by temporally and spatially-regulated cell motility. Not surprisingly, while the basic machinery and core molecular players of cell migration are conserved between all organisms, the specifics of how they are regulated and compartmentalized within different cell types, and how their activities are coordinated across entire tissues to achieve different ends remain an area of intense, interdisciplinary research.

The study of cell movement is directly relevant to human health. In development, defects in migration are associated with congenital abnormalities of the brain and heart (Xu et al., 1998), and in adults they are implicated in many of the most prevalent diseases of our time, including vascular disease (Adams and Alitalo, 2007) and cancer metastasis (Friedl et al.,

2012). By developing new tools and techniques for the real-time visualization of signaling and forces acting within and between cultured cells and their substrates, we continue to advance our understanding of the basic mechanics of cell movement. Likewise, new imaging modalities and computational tools allow the visualization and quantitative analysis of cell movements within developing embryos (Keller et al., 2010), adult tissues of living animals (Rompolas et al., 2012), and even within growing tumors (Sahai, 2007). Pushing the limits of these techniques and applying them to the study of increasingly complex systems not only gives us detailed insight into basic mechanisms of cell movement and tissue morphogenesis, but also as to how these mechanisms are elaborated upon in different contexts in embryonic and adult development, and how they are misappropriated in the progression of disease.

1.1 Basic principles of cell migration

The mechanisms of cell migration have been elucidated in beautiful detail at the level of individual cells on planar substrates (Abercrombie et al., 1970a,b,c; Gail and Boone, 1970; reviewed in Ridley et al., 2003). At its simplest, migration involves the polarization of a cell in the direction of a migratory stimulus, the extension of actin-based protrusions that adhere to the extracellular matrix (ECM) or to an adjacent cell, the translocation of the cell body, and the disassembly of adhesive contacts at the rear ([Illustration 1.1](#)). This process is mediated by integrin-family transmembrane receptors that link the cell via its actin cytoskeleton to the ECM through a vast network of adapter proteins and effectors in structures called focal adhesions (FAs) [Geiger and Yamada, 2011; Heath and Dunn, 1978; Hynes and Destree, 1978]. Integrins function as heterodimers whose α and β subunits dimerize and aggregate in response to binding ECM proteins such as fibronectin, collagen, and laminin ([Illustration 1.2](#)). While both subunits contribute to ligand specificity, the cytoplasmic tails of β -integrins are primarily responsible for establishing the link between the cytoskeleton and ECM through recruitment of FA proteins, including focal adhesion kinase (FAK), α -actinin, talin, and vinculin (Geiger et al., 1980; Horwitz et al., 1986; Jockusch et al., 1995).

1.1. BASIC PRINCIPLES OF CELL MIGRATION

Activation of Src-family kinases by FAK also sets the stage for downstream signaling by Ras and MAP kinases, Rap1, and c-Jun N-terminal kinase (JNK), which have complex roles in signaling and transcription (Danen and Sonnenberg, 2003; Ilić et al., 1997). Integrins thus provide a mechanochemical link between a cell and its environment in a wide range of contexts, enabling it to both exert traction on its surroundings and respond to external forces (Schwartz and Simone, 2008; Wang et al., 1993).

Acting both up- and downstream of integrins are members of the Rho-family GTPases that regulate the assembly and turnover of FAs by modulating actin polymerization and myosin II-dependent contractility (Hall and Nobes, 2000). Initial polarization of a cell in response to a migratory cue is in large part mediated through the Rho GTPase Cdc42 (Nobes and Hall, 1995). Along with Par proteins and aPKC, which also play an essential role in establishing apicobasal polarity in stationary epithelial cells, Cdc42 positions the microtubule organizing center (MTOC) and Golgi in front of the nucleus, polarizing membrane traffic (Etienne-Manneville, 2008). Cdc42 also recruits the cell's actin polymerization machinery to the leading edge both directly, through WASP/N-WASP-mediated activation of the Arp2/3 complex, and through recruitment of the GTPase Rac, which promotes actin polymerization through the WAVE/Scar family of Arp2/3 activators (Ridley et al., 2003). Together, Cdc42 and Rac mediate the polarized extension of actin-based protrusions, lamellipodia and filopodia, in the direction of cell migration, which in turn are stabilized by integrin-mediated adhesion to the ECM (Pollard and Borisy, 2003).

To complete a cycle of locomotion, a cell must couple formation of new adhesive contacts at the front to translocation of the body and disassembly of contacts at the rear. This is primarily mediated by RhoA, which, due to mutual antagonism with Rac, accumulates at the sides and rear of the cell. RhoA modules the activity of myosin II through its main effectors, Rho kinase (ROCK) and myosin light chain kinase (MLCK), promoting the formation and contraction of actomyosin bundles that generate the tension required for productive migration and disassembly of cell-ECM contacts at the rear (Chrzanowska-Wodnicka and

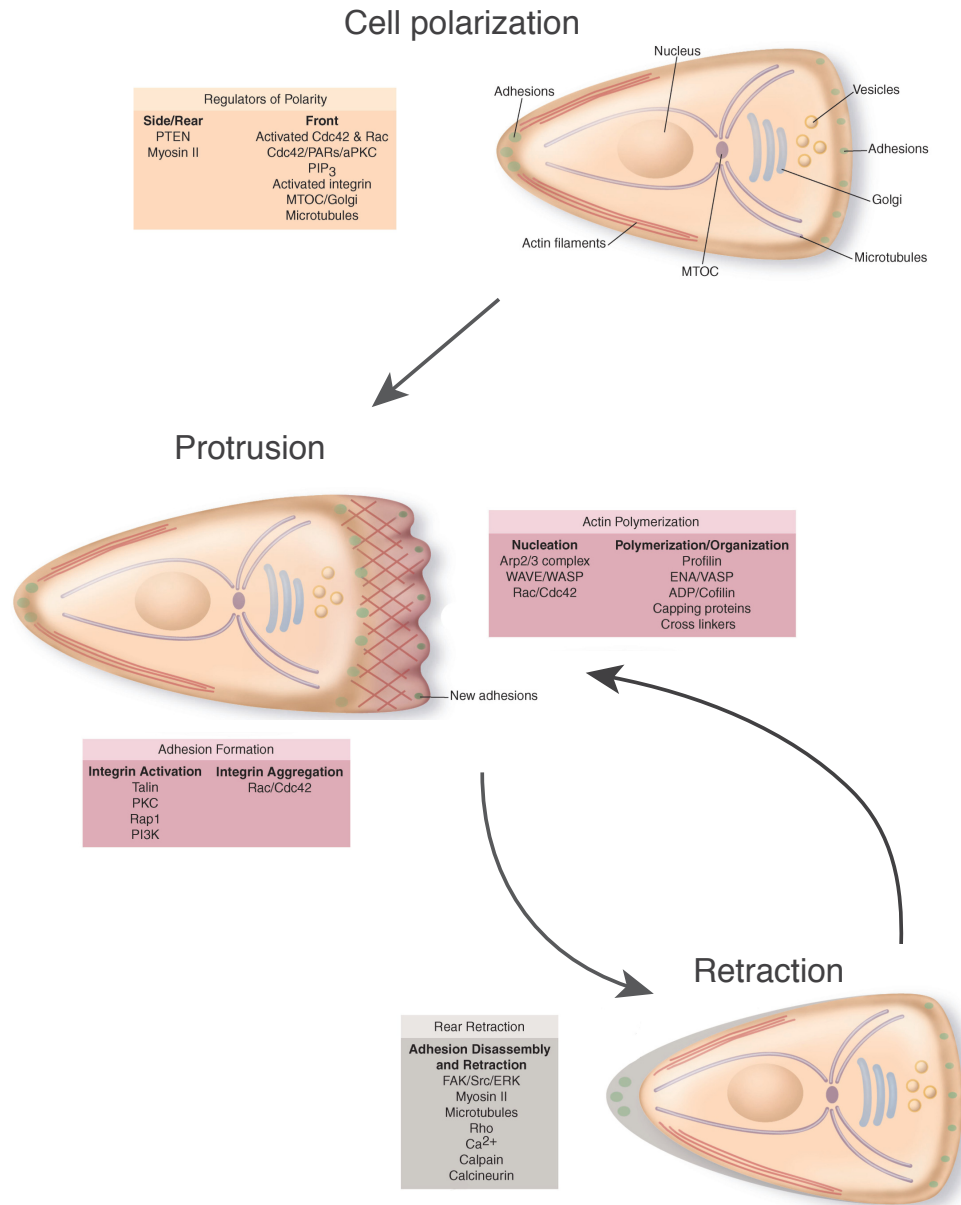


Illustration 1.1: The cell migration cycle. In response to a stimulus, a cell polarizes its microtubules, MTOC, and Golgi. This involves the Rho GTPase Cdc42 and components of the Par polarity complex, and results in polarized vesicle trafficking. Among the targets of Cdc42 and Rac are WASP/WAVE proteins, which activate Arp2/3 at the front of the cell to stimulate actin polymerization, pushing against the membrane. This generates cell protrusions that are stabilized by the formation of integrin-based adhesions to the ECM. Myosin II-dependent contractility downstream of Rho mediates the forward propulsion of the cell and the disassembly of adhesive contacts at the rear. Illustration adapted from Ridley et al. (2003).

1.1. BASIC PRINCIPLES OF CELL MIGRATION

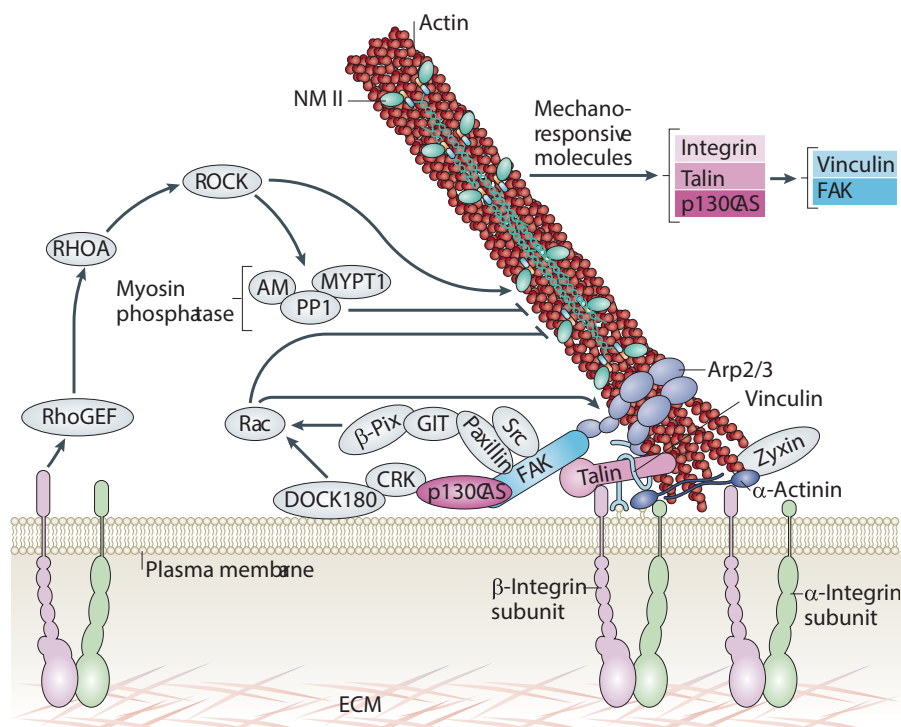


Illustration 1.2: Integrin-based adhesion. Adhesion to the ECM is mediated through integrins, a ubiquitous family of heterodimeric transmembrane receptors. Following the clustering and activation of integrins upon binding to ECM proteins such as fibronectin, collagen, and laminin, the cytoplasmic tails mediate the assembly of macromolecular adhesion complexes known as focal adhesions. Tensin and FAK are likely the first to be recruited, followed by α -actinin, talin, vinculin, and Src-family kinases. Integrin cytoplasmic tails are linked directly to the actin cytoskeleton through talin, α -actinin, and tensin, and indirectly through vincullin and paxillin. These initial events set the stage for the recruitment of more than 50 factors as well as the activation of downstream signaling molecules such as Ras and MAP kinases, Rap1, and Jun-kinase (JNK). Illustration reproduced from Vicente-Manzanares et al. (2009).

Burridge, 1996).

While the full details of cell migration are immensely complex even in the case of a single cell, this basic machinery—mediators of polarity, actin polymerization, and contractility—is the foundation of all examples of cell movement, from that of single-celled organisms to the complex, highly orchestrated movements of animal development. The study of cell movement in the complex environments of developing embryos and adult tissues is thus a study of how this machinery operates when cells are interconnected to varying degrees in tissues, and of the upstream pathways that organize and compartmentalize its activity.

1.2 Regulated adhesion: the basis of collective cell movement

Rather than individual cells, many examples of cell movement in development, adult tissues, and diseases such as cancer involve movements of cell sheets or clusters, in which cells remain connected to their neighbors. In this way, a tissue can harness the power of cell motility to shape entire organs and remain coherent while it is remodeled. The one great exception, of course, is development of the nervous system, which relies on the guidance of individual cells to their final destinations (Bate, 1976; Letourneau, 1975; O'Donnell et al., 2009). Individual cell migration is thus regulated by increasingly complex spatiotemporal cues and constraints in the different tissues of an organism, many of which are not preserved *in vitro*.

1.2.1 Cell-cell adhesion

Cells of both simple and stratified epithelia form three main types of cell-cell junctions: adherens junctions (AJs), desmosomes, and tight junctions (TJs). Adherens junctions are the first to form at initial sites of cell-cell contact and facilitate the formation of the other two. As dynamically regulated structures, adherens junctions are also arguably the most important: their rapid remodeling is essential to many processes in embryonic development, including the sorting of cells into distinct tissue layers, the formation of tissue boundaries, shape changes associated with cell rearrangement, and the conversion of stationary epithelial cells

1.2. REGULATED ADHESION: THE BASIS OF COLLECTIVE CELL MOVEMENT

to a migratory fate (Gumbiner, 2005; Hammerschmidt and Wedlich, 2008). Desmosomes endow the cell with mechanical stability by anchoring the membrane to the intermediate filament network, and are particularly important in organs subjected to mechanical stress, such as the skin and heart (Garrod and Chidgey, 2008). Tight junctions, on the other hand, serve to form tight seals between epithelial cells to control paracellular permeability as well as to create a barrier to protein diffusion across apical and basolateral membrane domains (Shin et al., 2006). In addition to partitioning the cell membrane, TJs also play an active role in establishing apicobasal polarity by recruiting members of the Crumbs and Par apical polarity complexes. All three classes of junctions, in addition to their structural roles, are important signaling centers, interact in some way with the actin cytoskeleton, and exhibit a considerable degree of crosstalk between one another, in addition to mediating integrin/ECM adhesion by recruiting shared scaffolding proteins and GTPases that regulate actin dynamics and contractility (Yamada and Nelson, 2007).

1.2.2 Cadherin-based adhesion and the adherens junction.

Whereas integrins are the basis of cell adhesion to the ECM, cadherins form the major basis of cell-cell adhesion. Cadherins are a large superfamily of transmembrane proteins that mediate calcium-dependent adhesion between cells in virtually all solid tissues (Hyafil et al., 1981; Takeichi, 1977; Yoshida and Takeichi, 1982; reviewed in Gumbiner, 2005). They are expressed in tissue-specific, partially overlapping patterns, and their dynamic, physiological regulation at the cell surface and roles in signaling are essential to development and tissue morphogenesis (Jamora and Fuchs, 2002; Maître et al., 2012; Zhong et al., 1999). Classical cadherins, including E- (epithelial), N- (neural), R- (retinal), and VE- (vascular-endothelial) cadherin are homophilic, single-pass transmembrane proteins associated with various forms of adherens junctions and are characteristically linked to the actin cytoskeleton. A subfamily of cadherins, the desmocollins and desmogleins, also mediate the formation of desmosomes, while tight junctions mediate calcium-independent adhesion through separate classes of ad-

hesion molecules, namely claudins, occludins, and junctional adhesion molecules (JAMs) (Shin et al., 2006). Finally, cadherin-like proteins that contain variable numbers of cadherin repeats in their extracellular domains and do not fall neatly into a subfamily, including Fat, Dachsous, and Flamingo, play important roles in patterning, establishment of planar polarity, and tumor suppression (Zallen, 2007).

Similarly to focal adhesions, adherens junctions are intimately associated with the actin cytoskeleton through a set of adapter proteins, some of which are shared with focal adhesions, and are regulated both at the level of cadherin ligation and membrane turnover (Illustration 1.3A). Classical cadherins, such as E-cadherin, form parallel *cis* dimers in the membrane that interact with dimers in adjacent cells to form a homophilic bond (Overduin et al., 1995). Like integrins, their cytoplasmic domains aggregate, which promotes the binding of accessory proteins, including β -catenin and p120, that ultimately link them to the cytoskeleton via α -catenin (Harris and Tepass, 2010). α -catenin in turn has been found to bind directly to actin filaments as well as indirectly through vinculin, VASP, α -actinin, and ZO-1 (Drees et al., 2005; Kobiela and Fuchs, 2004). That these proteins are also found in focal adhesions implies that both cell-cell and cell-ECM adhesion complexes use analogous mechanisms to respond to and exert tension on their surroundings (le Duc et al., 2010).

1.2.3 Actomyosin dynamics at the adherens junction

The formation of cell-cell adhesions in many ways parallels that of cell-ECM adhesion. It utilizes many of the same regulators of the cell's actin polymerization and contractile machinery to generate membrane protrusions, but stabilizes them in cadherin-based adhesions to an adjacent cell rather than the ECM. Both Arp2/3, which promotes actin branching and lamellipodia formation, and formin-1, which promotes linear actin polymerization and extension of filopodia, are associated with the cadherin complex (Kobiela et al., 2004; Verma et al., 2004). E-cadherin, with p120-catenin, has been shown to activate Arp2/3 via phosphatidylinositol 3-kinase (PI3K) and Rac (Kovacs et al., 2002), while formin-1, which can

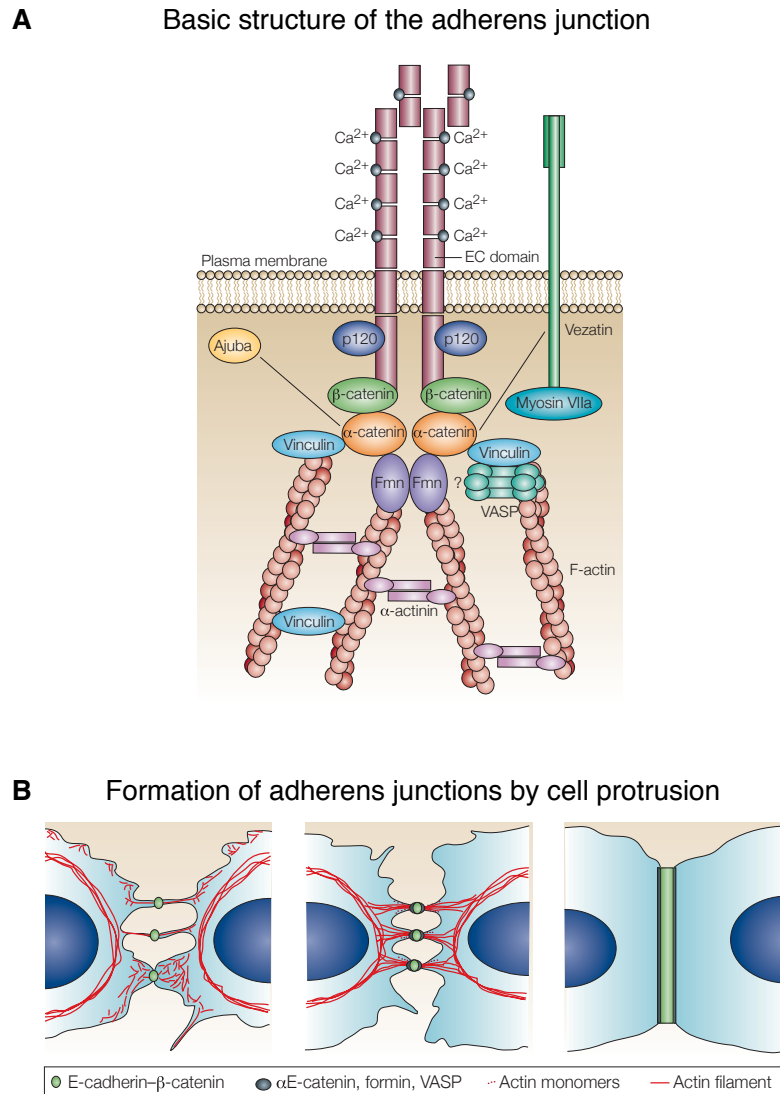


Illustration 1.3: The structure and formation of adherens junctions. (A) Cell-cell adhesion is mediated through members of the cadherin superfamily. Classical cadherins are calcium-dependent, single-pass transmembrane proteins that form homophilic bonds between cells. Similarly to focal adhesions, their cytoplasmic domains associate with the actin cytoskeleton through a large complex of accessory proteins. Chief among them are α - and β -catenin. Direct binding of β -catenin to the cytoplasmic tail recruits α -catenin, which can directly bind actin, while p120 stabilizes cadherins at the membrane by inhibiting their endocytosis. β -catenin also has a well-known role in Wnt signaling. (B) The formation of AJs in epithelial cells involves the extension of actin-based protrusions into adjacent cell membranes. Recruitment of PI3K and Rac to cadherins activates Arp2/3 and generates lamellipodial protrusions, while formin-1, through α -catenin, generates filopodia. Actin polymerization and remodeling through VASP, vinculin, and zyxin result in the coalescence and maturation of nascent adhesions, highlighting the connection between integrin- and cadherin-based adhesions. Illustrations reproduced from Kobiela and Fuchs (2004).

nucleate actin in response to Rac, Rho, and Cdc42, interacts with α -catenin (Kobielak et al., 2004). There is also evidence that β -catenin can interact with PI3K (Woodfield et al., 2001). Both lamellipodial and filopodial protrusions are likely to mediate junction formation in different contexts.

In epithelial cells, initiation of adherens junction formation involves extension of actin-based protrusions into the membrane of an adjacent cell, forming cadherin-rich puncta (Illustration 1.3B; Vaezi et al., 2002; Vasioukhin et al., 2000). Double rows of these puncta form intermediate adhesion structures called adhesion zippers, which associate with radial actin fibers in cultured cells and recruit VASP, zyxin, Mena, and vinculin. Local actin polymerization and contractility result in the coalescence of these structures into a linear adhesion and their eventual remodeling into a cortical actin belt associated with mature adherens junctions. In different contexts, the same family of scaffolding proteins, Rho-family GTPases, and mediators of actin polymerization and myosin II-based contractility thus drive both basic cell locomotion and the formation of adhesive contacts between cells.

1.2.4 Beyond the adherens junction

While the coupling of cell-cell junctions to the actin cytoskeleton is a general feature of epithelial cells, it is likely not essential for the formation of a basic adhesive bond between cells. Two naturally-occurring cadherins, T-cadherin (found in the heart) and LI (liver-intestine)-cadherin lack the typical cadherin cytoplasmic domain, but still mediate effective adhesion (Kreft et al., 1997; Vestal and Ranscht, 1992). Likewise, mouse E-cadherin mutants that lack the entire cytoplasmic domain are still able to promote effective cell aggregation, as do C-cadherin mutants in *Xenopus* lacking the binding site for β -catenin (Ozawa and Kemler, 1998). Likely the most important role for coupling adherens junctions to the cytoskeleton is to generate forces to drive cell shape change, cell movement, and the polarization and organization of cells within an epithelium. It is also important to note that cadherins function effectively as cell adhesion molecules even outside of well-defined adherens junctions,

1.3. CELL MIGRATION AND ADHESION IN MORPHOGENESIS

particularly in non-epithelial cells, such as those of neural tissues and the embryonic mesoderm. In these tissues, cadherins are likely dispersed throughout the cell and not fully linked to the cytoskeleton (Levi et al., 1991).

To achieve the great diversity of collective cell movements in development and tissue morphogenesis, the strength, location, and timing of cell-cell adhesion are carefully regulated. This is achieved through patterned expression of cadherins with different binding affinities, regulation of the conformation and clustering of cadherin dimers in the membrane by the catenins, and cadherin trafficking. Cadherin internalization rates are known to be modified in response to external stimuli such as growth factor signaling (Brieher and Gumbiner, 1994; Krieg et al., 2008), and cadherin turnover is essential for the long-term maintenance of cell-cell junctions (de Beco et al., 2009). Control of cadherin endocytosis is in turn linked to regulators of actin reorganization at the junction, which can either stimulate or inhibit the clathrin-mediated uptake of cadherins. p120-catenin, for example, stabilizes adherens junctions by inhibiting cadherin endocytosis (Davis et al., 2003), while in endothelial cells, activation of Rac and Pak by VEGF promotes endocytosis through recruitment of β -arrestin (Gavard and Gutkind, 2006). By fine-tuning levels of cadherin expression, stability at the membrane, and rates of turnover within and between tissues, a great diversity of behaviors that drive the sweeping shape changes, epithelial fusions, and mass cell movements of tissue morphogenesis can be achieved.

1.3 Cell migration and adhesion in morphogenesis

Perhaps the most striking feature of embryonic development is the variety of collective cell movements that take place. In different contexts, cells move as individuals, small clusters, sheets, and tubes, each of which utilize force-producing actin polymerization, contractility, and adhesion to different extents. Our knowledge of the diversity of cell movements that drive morphogenesis is illuminated by studies of gastrulation in model organisms such as the fly, frog, fish, and mouse. This is the process by which the single-layered blastula

gives rise to the three germ layers, the endoderm, mesoderm, and ectoderm, from which all the adult tissues of an animal are derived (Solnica-Krezel and Sepich, 2012). While the cell movements that occur differ from tissue to tissue and between organisms in analogous phases of development, they share governing principles and are driven by common cellular and molecular mechanisms. Although variations of these general mechanisms have been found to play a role in organogenesis, tissue regeneration, and cancer metastasis (Friedl and Gilmour, 2009), we are only beginning to understand the modes of collective cell movement used throughout an organism's life.

1.3.1 Epithelial to mesenchymal transition (EMT)

The process of cell movement is inextricably linked to fate specification. All of our tissues and organs are derived from a single-layered epithelium in gastrulation. Like most epithelia, cells are tightly interconnected by adherens and tight junctions, and are polarized along their apical–basal axis. A major early event in gastrulation is a process known as emboly, in which a subset of these cells, the mesodermal and endodermal progenitors, are internalized through an opening in the embryo called the blastopore in *Xenopus* and primitive streak in amniotes. Following internalization, cells typically migrate as individuals away from the blastopore to different regions of the embryo, where they generate the internal organs including mesodermally-derived muscle, bone, circulatory system, connective tissue, and notochord (which forms part of the nervous system), and endodermally-derived stomach, liver, intestines, and lungs (Solnica-Krezel, 2005). The process by which stationary epithelial cells break free of their surroundings and become migratory, known as an epithelial to mesenchymal transition (EMT), is essential in development, and was previously the predominant framework for understanding cell movements in embryonic development.

EMT is characterized by the loss of cell-cell adhesion, often through transcriptional downregulation of E-cadherin, with a corresponding increase in cell-ECM adhesion, loss of apicobasal polarity, cytoskeletal reorganization to promote delamination and migration,

1.3. CELL MIGRATION AND ADHESION IN MORPHOGENESIS

and degradation of the basement membrane, the specialized ECM at the basal surface of most epithelia (Cano et al., 2000; Greenburg and Hay, 1982; Hay, 1995; Nakaya et al., 2008). An EMT is initiated by localized signaling in development. In mouse and chick development, mesodermal and endodermal progenitors are internalized through the primitive streak as individual cells in a process known as ingression (in contrast to *Drosophila* and *Xenopus* embryos, in which adherent cells are internalized by invagination and involution, respectively). These cells respond to canonical Wnt signaling, downstream of which members of the TGF- β superfamily, Nodal and Vg1, induce EMT and ingression (Varlet et al., 1997). Signaling through FGF receptors plays an important role in maintaining the EMT (Mathieu et al., 2004). Together, these signaling molecules activate transcription factors that produce the main features of an EMT, the most important of which are the transcriptional repressors Snail, Twist, and Slug, that mediate the downregulation of E-cadherin and other junctional proteins, and the expression of mesenchymal markers.

Migration of cells as individuals following an EMT plays an important role throughout development. In *Drosophila*, although the mesoderm is initially internalized by a process of inward folding to create the ventral furrow, cells subsequently break away and migrate along the inside surface of the future ectoderm (Leptin, 1999). In chordates, following neural tube closure, neural crest cells on the roof plate delaminate and migrate peripherally to form diverse cell lineages including melanocytes, cartilage, smooth muscle, peripheral neurons, and glia (Duband et al., 1995; Weston, 1963). It is important to note that, in addition to promoting the dispersal of cells and their development into diverse tissues, groups of cells that migrate as individuals can also contribute to the overall shaping of tissues. In *Xenopus*, following internalization, the movement of individual axial mesoderm cells away from the blastopore and toward the head contributes to axis extension. Likewise, in zebrafish embryos, a ventral-to-dorsal gradient of BMP signaling contributes to axis elongation by establishing a reverse gradient of cell adhesion, which directs the dorsal convergence of mesodermal cells by lamellipodia-driven migration (von der Hardt et al., 2007). Directed

migration can thus contribute, with other mechanisms of *bona fide* collective cell movements, to large-scale shape changes in tissue morphogenesis.

Outside of embryonic development, EMTs are also important in wound healing and tissue repair, and are known to contribute to pathogenesis. In adult skin, wound healing involves an EMT to promote motility of epidermal cells at the wound border, as well as to generate myofibroblasts that remodel the interstitial ECM and promote wound contraction (Martin, 1997; Yan et al., 2010). Diseases such as renal fibrosis are associated with EMTs and with the conversion of epithelial cells into myofibroblasts (Iwano et al., 2002), and it is believed that EMT can play a role in dissemination of tumor cells in metastatic cancer (Labelle et al., 2011; Yang et al., 2004). However, while EMTs and the migration of individual cells are essential to numerous processes in development, they simply do not account for the full range of morphogenetic cell movements observed. Many, if not most, of the large-scale movements that shape the developing embryo involve cells that retain some degree of cell-cell adhesion. Accumulating evidence from live imaging studies of tumor cells in 3D culture and within intact tumors also indicates that cells can invade and spread as connected strands or clusters (Friedl et al., 2012). Rather than a sharp transition, the process of EMT is perhaps best considered as occurring along a spectrum, encompassing both individual and collective cell behaviors.

1.3.2 Cell sorting and cadherin-dependent migration

On the opposite end of the spectrum is cell movement and rearrangement driven predominantly by cadherin-dependent cell-cell adhesion. The idea that differences in the adhesive and mechanical properties of cells can direct their sorting and assembly into distinct tissues dates from the classic experiments of Townes and Holtfreter, in which mixtures of cells from embryos were found to self-organize (Townes and Holtfreter, 1955). However, only recently have we begun to understand the molecular basis of a cell's mechanical properties and to incorporate mechanical models into studies of tissue morphogenesis *in vivo*.

Theories of cell sorting

Cell sorting involves the segregation of a mixture of cells with different fates and mechanical properties into distinct domains, and the maintenance of this segregated state. While tissues rarely begin as truly random mixtures of different cell types *in vivo*, cell sorting has important functions in forming and maintaining tissue boundaries in embryonic, adult, and diseased tissues. A number of theories have been proposed to explain cell sorting, each of which accounts for different aspects of the process at play in different developmental contexts. The simplest model is that the cells of an aggregate behave as the molecules of a mixture of immiscible liquids, where the molecules with stronger intermolecular attraction (higher surface tension) coalesce and separate from the bulk to minimize their surface free energy (Foty et al., 1996; Steinberg, 1962). The equivalent of intermolecular forces for a mixture of cells would be their relative adhesiveness, a function of the number and identity of cadherin molecules at the membrane. While the surface tension of a tissue is indeed correlated with the expression of cadherins, and in some circumstances such a model is sufficient to account for the sorting that occurs (Foty and Steinberg, 2005), cell contractility also influences its surface tension and, in combination with other active processes, is likely to be important for cell sorting in the majority of cases.

Other models of cell sorting account for both adhesion and actomyosin contractility at the cortex. In the differential surface contraction hypothesis (Harris, 1976), contractility at the free surface of a cell serves to increase surface tension, while adhesion at cell-cell junctions reduces cell adhesion and thus decreases surface tension. Either higher contractility at the free surface or lower contractility at cell-cell junctions (but not both) would result in the liquid-like segregation of cells on the basis of surface tension. Lending direct support to this model is a study in zebrafish embryos, in which atomic force microscopy (AFM) was used to measure the adhesiveness and cortical tension in cells of the ectoderm, mesoderm, and endoderm (Krieg et al., 2008). When isolated from the embryo and mixed in culture, cells of the ectoderm sort to the inside of the aggregate, with the mesoderm and endoderm cells on

the outside. Rather than the relative adhesiveness of the cell types, actomyosin contractility dictated the outcome of sorting, highlighting the role of contractility at specific cell interfaces in driving cell sorting.

Perhaps the most realistic model, at least in theory, is the differential interfacial tension model (Brodland, 2002). This treats tissues not as liquids, but as a set of cell-cell interfaces, each subject to adhesive forces that act to expand the interface, and cortical tension that tends to shrink it. Such a model is attractive because terms can be introduced to account for various other properties of a cell, including elasticity and viscosity. This framework has been utilized to accurately describe packing geometries in the development of the *Drosophila* wing imaginal disk and to predict cell rearrangements that occur during tissue growth in different regimes of cell contractility, adhesion, and elasticity (Farhadifar et al., 2007). Likewise, simulation of cell shapes in the *Drosophila* eye using a model that accounts for cell-cell adhesion and cortical contractility was able to recapitulate the arrangement of pigment and cone cells in both wildtype and mutant conditions (Hayashi and Carthew, 2004; Hilgenfeldt et al., 2008).

Cell sorting in development

Regardless of the mechanics underlying it, aspects of cell sorting play a major role in development. In the early stages of mouse blastocyst formation, pluripotent epiblast cells and prospective endoderm cells are initially specified at random positions and sorted into distinct domains (Plusa et al., 2008). This is thought to have an important role in fate specification later in development, as it establishes the positions of cell populations within the long-range signaling gradients that evolve. As cells adopt different fates, differences in surface tension are thought to play a role in keeping them separate. Following the internalization of mesoderm and endoderm in gastrulation, this is at least part of what keeps the germ layers from intermixing, a role that appears to also apply to different regions of the mesoderm (Ninomiya et al., 2004) and to neural crest and epidermal cells (Davis et al., 1997).

1.3. CELL MIGRATION AND ADHESION IN MORPHOGENESIS

The process of epiboly, the thinning and spreading of the epiblast that occurs concurrently with gastrulation, involves the movement of cells from deep to superficial layers in a process of radial intercalation (Keller, 1980). In zebrafish, this is known to require E-cadherin and regulators of E-cadherin endocytosis such as the EGF pathway, implicating a role for cell sorting in either driving or maintaining the positions of cells following radial intercalation (Kane et al., 2005). Finally, cell sorting can play an active role in the generation of polarized embryonic structures. Studies of chick development have revealed that the limb bud forms by a process of cell segregation from the somatopleural mesoderm, where FGF signaling triggers both changes in cell surface tension as well as proliferation (Damon et al., 2008). The *Drosophila* wing disk, a polarized structure that is compartmentalized along the anterior-posterior as well as dorsal-ventral axes, likewise requires cell sorting downstream of Decapentaplegic (Dpp, a homolog of BMP) and Notch signaling to form and maintain tissue boundaries. Both proper expression of E-cadherin and other adhesion molecules as well as regulation of cell cortex tension are known to play a role (Landsberg et al., 2009). A similar process of boundary formation is believed to be at play in vertebrate development in the formation of the somites, paired blocks of mesoderm on either side of the notochord that give rise to the skeleton, skeletal muscles, and parts of the dermis (Baker et al., 2008). However, in this case, differences in surface tension alone are unlikely to fully account for the compartmentalization observed, and processes of cell attraction and repulsion mediated by Eph-Ephrin signaling also contribute (Durbin et al., 1998).

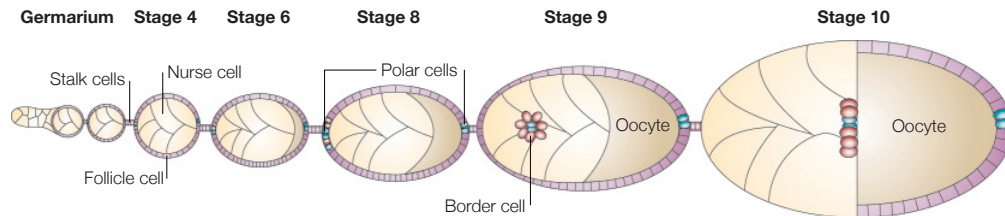
While other processes are likely to contribute to cell sorting *in vivo*, such as chemotaxis, differences in cell migration rates, and cell attraction and repulsion (such as through Eph-Ephrin signaling), cell sorting on the basis of adhesion and surface tension alone represents an important class of collective cell movements in tissue morphogenesis.

1.3.3 A case of cadherin-dependent cell migration: border cell migration

Although apparently rare, an intriguing and well-studied example in which a group of cells delaminate from a stationary epithelium and migrate using only cadherin-based adhesion is the process of border cell migration in *Drosophila* oogenesis ([Illustration 1.4](#); reviewed in Montell, 2003). The *Drosophila* egg chamber consists of 650 post-mitotic follicle cells that surround sixteen germline cells, of which one differentiates into the oocyte and the others into nurse cells that provide nutrients and cytoplasm to the oocyte. In the process of egg chamber formation, the follicle cells rearrange themselves such that most adopt a columnar morphology around the oocyte, while those that surround nurse cells spread out into a thin squamous layer. As this occurs, a group of 6–10 cells, including two specialized cells at the anterior end of the chamber, the polar cells, detach from the follicular epidermis and invade the germline tissue. The border cell cluster is guided to the oocyte where it forms the micropyle, the pore through which sperm enters during fertilization, and produces factors such as *torso-like* that contribute to the anterior-posterior patterning of the embryo (Savant-Bhonsale and Montell, 1993). It is thus an essential process for the fertility of female flies and the proper patterning of embryos.

What makes border cell migration such an important model is that it is a true case of tissue invasion that occurs naturally in development, with potential parallels to the acquisition of invasive properties by tumor cells. As a model, it offers insight into signaling pathways that direct the acquisition of motile properties by epithelial cells as well as into cellular and molecular mechanisms of the collective migration of a free group of cells (Wang et al., 2006). Unlike examples of EMT, in which cells increase integrin-based adhesion to the ECM, there is no ECM or “empty” space into which border cells migrate—they utilize nurse cells as a substrate. Among the genes found in screens for defects in the process, E-cadherin was found to be required in both border cells and nurse cells for effective migration, indicating that cadherin-mediated adhesion is likely the sole means by which border cells gain the necessary traction for migration. This is unusual, as high cadherin expression is typically

Egg chamber development in the *Drosophila* ovary



Overview of border cell migration

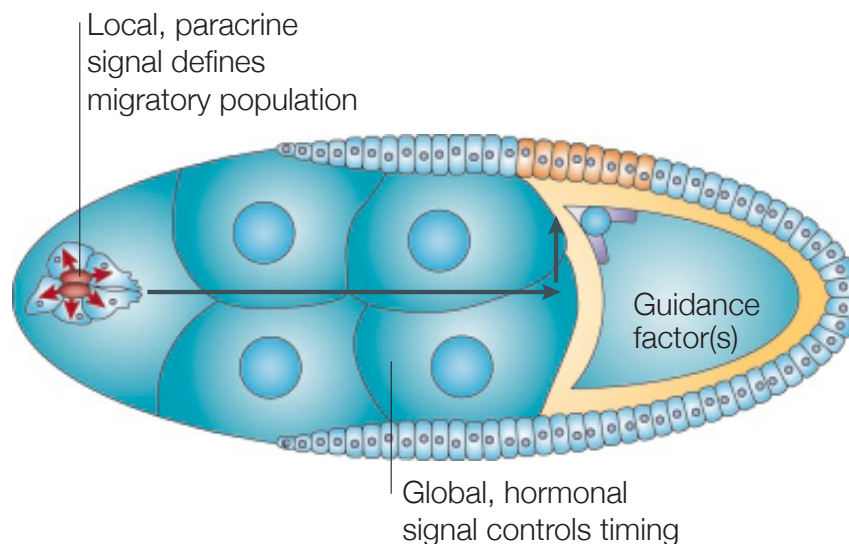


Illustration 1.4: Cadherin-dependent migration: border cell migration. The *Drosophila* egg chamber consists of ~650 follicle cells surrounding sixteen germline cells, of which one becomes the oocyte and the others nurse cells that feed the oocyte. As the egg chamber develops to stage 9, the follicle cells on the anterior side assume a squamous morphology and spread over the nurse cells. A group of these, including two specialized polar cells and 6–10 border cells, detach from the follicular epidermis and invade the group of nurse cells. They migrate as a free group of cells across the chamber to the oocyte, where they fuse to form the micropyle (sperm duct). Controlling their movements are *Slbo*, a homolog of mammalian C/EBP proteins, which controls their delamination from the follicular epidermis, Jak-Stat signaling to stimulate their active migration, and Pvf1 (homologous to VEGF and PDGF) and Vein (an EGF ligand), two chemoattractants produced by the oocyte. Border cell migration is an important model of epithelium-on-epithelium migration and the signaling pathways involved in the acquisition of invasive properties. Illustrations reproduced from Montell (2003).

correlated with a less motile phenotype, although it is becoming increasingly appreciated that, in some contexts, cadherins can actually promote cell migration (Martinez-Rico et al., 2010; Shih and Yamada, 2012).

Among the other genes found to regulate the process are the *Drosophila* homolog of the mammalian CCAAT enhancer binding protein (C/EBP), *Slbo*, a transcription factor controlling the acquisition of motile properties and the detachment of border cells from the follicular epidermis (Montell et al., 1992), and the Jak-Stat pathway, which activates transcription downstream of growth factor signaling and is well-known to promote cell migration both in tissue culture and a variety of developmental contexts (Hou et al., 2002). Downstream targets of *Slbo* include E-cadherin, FAK, and the pointed-end directed motor, myosin VI, thought to stabilize the E-cadherin/ β -catenin complex (Geisbrecht and Montell, 2002). The C/EBP pathway is thus likely to control the mechanics of border cell migration at least in part by the dynamic regulation of cadherins. Jak-Stat signaling, on the other hand, is required to recruit border cells around the polar cells and stimulate their active migration (Silver and Montell, 2001). Polar cells produce the cytokine Unpaired, which activates Jak-Stat in neighboring border cells, necessary both for effective migration and the recruitment of the correct number of border cells to the cluster. In contrast to long-range chemotactic signals, this may function to promote group over individual cell migration. Finally, controlling the directed migration across the egg chamber are chemoattractants originating in the oocyte: Pvf1, which has some homology to both VEGF and PDGF, and Vein, an EGF ligand (Duchek et al., 2001), both of which are sensed by cognate receptors in border cells.

In contrast to the collective rearrangement of cells by sorting on the basis of surface tension, border cell migration illustrates an example in which mediators of cell-cell adhesion are used to drive active cell migration. This serves to highlight the incredible plasticity of cells within epithelia and the diversity of morphogenetic behaviors that can be achieved by the simple activation of individual cell motility or by modulating levels of cell adhesion and contractility. Not only are the behaviors of cells diverse in different developmental contexts,

1.4. CONSERVED MORPHOGENETIC MOVEMENTS

so too are the basic means by which they exert traction on their surroundings to promote cell movement. While extremely useful as models to understand basic principles of integrin and cadherin-dependent cell movement and segregation into tissue domains *in vivo*, the processes of EMT is in many ways on the opposite end of a spectrum to cell sorting and border cell migration. On the one side is EMT, the adoption of motile properties that characterize the crawling motility of cells exhibited in culture; on the other are processes that predominantly involve cell-cell adhesion. In reality, tissue morphogenesis in development and homeostasis involves a subtle interplay between cell-cell and cell-matrix adhesion whose intricacies we are only beginning to unravel, involving motile behaviors downstream of developmental signaling pathways and thermodynamic forces generated by differential adhesion and contractility.

1.4 Combining cell motility and adhesion: conserved morphogenetic movements in development

The basic force-producing machinery of actin polymerization and myosin II-dependent contractility can be used in combinatorial fashion to achieve varying degrees of epithelial stability or cell movement. In spite of the apparent diversity of cell movements, variations of a surprisingly small number of evolutionarily conserved cellular and molecular mechanisms have been found to drive many of the most substantial tissue movements that take place in development. Underlying them all is a simple, unifying framework in which the force-producing activity of actomyosin contractility is compartmentalized within cells and coordinated across tissues, and harnessed to produce global changes in tissue morphology through mechanical coupling of cells at cell-cell junctions. The intricate spatial regulation of actomyosin dynamics and the stability of cadherin-based junctions, in many cases by highly conserved pathways, can thus be considered the organizing principle of morphogenesis, underlying collective cell movements common to the development of all multicellular organisms and accounting for the subtle differences between them.

1.4.1 Cell shape changes in morphogenesis

The crawling motility of individual cells either in tissue culture or following an EMT *in vivo* can be considered a specialized case of a larger set of cell shape changes of which cells are capable. A common process in which epithelial tissues harness the power of shape changes in a subset of cells to produce folds and invaginations is apical constriction ([Illustration 1.5](#)). This has been studied extensively in *Drosophila* mesoderm invagination (Sweeton et al., 1991), vertebrate neuralation (Kölsch et al., 2007), and in *Xenopus* bottle cells in the formation of the blastopore (Lee and Harland, 2007). It likely also plays a role in the formation of a wide variety of epidermal appendages. In the case of invaginating mesodermal cells in *Drosophila*, apical constriction occurs by a process of rapid, pulsed constrictions that are stabilized between pulses to drive a continuous decrease in apical area (Martin et al., 2008). The force for constriction comes from the repeated formation and coalescence of myosin II foci on the apical actin network, found to immediately precede an apical constriction. These pulses are eventually stabilized by maintenance of high levels of myosin II at the apical surface, generating a pulling force on adjacent cell-cell junctions. This results in their redistribution from a subapical to apical region of the cortex and the inward bending of the tissue.

Apical constriction is controlled by many of the expected regulators of myosin II activity. Rho-kinase, activated by RhoGEF2 and Rho, is required for the process in both flies and mice (Nikolaidou and Barrett, 2004), while in amphibians, it requires the Rho GTPase Rap1 rather than Rho itself (Haigo et al., 2003). Like the process of cell migration, apical constriction is a polarized process, in this case requiring the compartmentalized activation of actomyosin contractility at the apical surface. This occurs through the apical anchoring of RhoGEF2 and its activation by the $G_{\alpha 12\alpha 13}$ –Concertina (Cta) pathway (Kölsch et al., 2007). In cultured cells, RhoGEF2 is known to bind the microtubule (MT) plus-tip-binding protein, EB1, and to be released by $G_{\alpha 12\alpha 13}$ -Cta. The fact that astral microtubules concentrate at the cell apex and MT plus-ends are oriented apically suggest this as the means by which RhoGEF2 is targeted there. This is likely a conserved mechanism, as RhoGEF2

1.4. CONSERVED MORPHOGENETIC MOVEMENTS

and $G_{\alpha12\alpha13}$ -Cta are required for gastrulation and cortical remodeling, and a mammalian homolog of RhoGEF2, PDZ-RhoGEF (ARHGEF11), was recently found to play a role in apical constriction during neural tube closure in mice (Nishimura et al., 2012). Proper organization of the apical actin network, in which RhoGEF plays a role, is also essential, along with the Abelson kinase (Abl), which inhibits the Ena/VASP family of actin regulators, and Shroom, an actin-associated protein that binds and recruits ROCK to the apical membrane (Haigo et al., 2003).

Interestingly, apical constriction in *Drosophila* mesoderm invagination requires the two major effectors of EMT, Twist and Snail. Whereas Snail is required for myosin coalescence at the apical cortex, Twist is necessary to stabilize pulsed contractions produced by Snail activity to sustain the process (Martin et al., 2008). This is likely through a role in actin remodeling, as *twist* mutants fail to form a dense apical actin meshwork. This involvement of a pathway classically considered to promote individual cell motility highlights a major theme of morphogenesis: the use of a core set of molecular force generators in a spatially-controlled manner to promote a diversity of collective behaviors. The compartmentalization of myosin II activity by the spatial restriction of ROCK through RhoGEFs is widespread in development, and many of the pathways regulating their localization are conserved. Importantly, that apical constriction involves pulsatile actomyosin contraction rather than a continuous process of constriction underscores the role of dynamic, polarized actomyosin flows in driving morphogenesis.

1.4.2 Epithelial sheet movement

One of the best-studied types of collective cell movement, both in simplified cell culture models and in elaborate processes *in vivo*, is epithelial sheet movement. As a model, it is a perfect example of the combined use of cell migration, cell-cell adhesion, and the assembly of specialized actomyosin structures to achieve a complex morphogenetic task: cell movement in a scenario where epithelial integrity is required. Cultured epithelial and endothelial cells

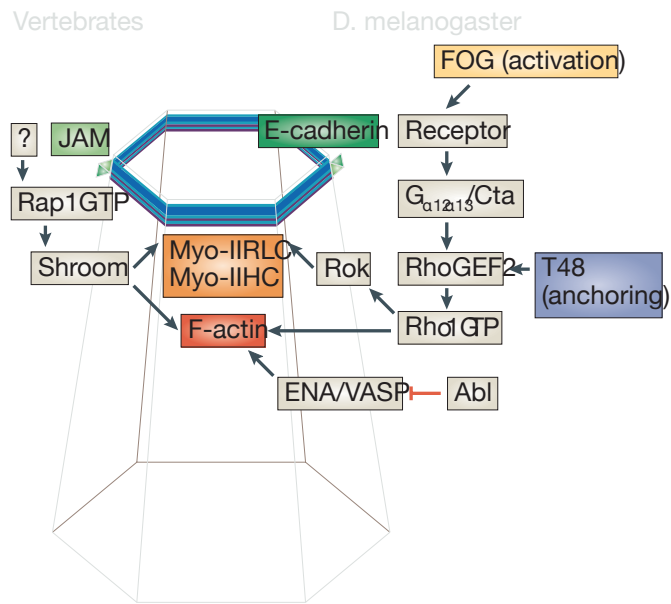
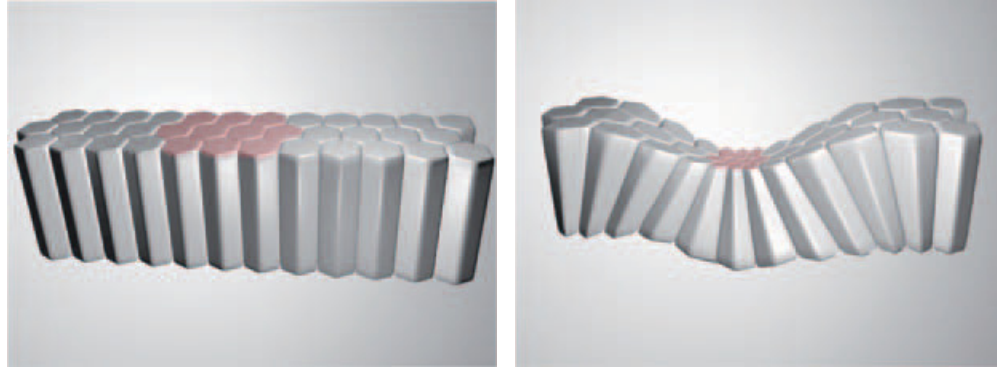


Illustration 1.5: Apical constriction: an individual cell behavior driving tissue shape change. Apical constriction illustrates how the shape changes of a few cells within a stable epithelium can drive substantial tissue movement. Apical anchoring and activation of RhoGEF2 by the $G_{\alpha 12 \alpha 13}$ -Cta pathway, along with the ROCK and actin-binding protein Shroom, compartmentalize ROCK and myosin II activity along the apical membrane. The process of constriction itself involves rapid, pulsatile actomyosin contractions that are stabilized by maintenance of high levels of apical myosin II. Illustrations reproduced from Lecuit and Lenne (2007).

1.4. CONSERVED MORPHOGENETIC MOVEMENTS

perform sheet migration in response to a stimulus, such as creating a gap in a monolayer (a scratch-wound assay), or in response to growth factors such as FGF (Vitorino and Meyer, 2008).

Basic principles

Cell culture studies have uncovered a number of basic principles of the process likely to play a role *in vivo*, including the specification of more migratory “leader” cells (Omelchenko et al., 2003), active motility in cells throughout the sheet, coordination of cell movement, and the non-essential role of proliferation (Poujade et al., 2007). Despite the connectivity of cells and greater protrusive activity of leader cells, it is truly a group phenomenon—every cell can contribute (Farooqui and Fenteany, 2005). As is the case for cells migrating in isolation, cells both at the front and within a migrating sheet polarize their microtubules and microtubule organizing center (MTOC) [Yvon et al., 2002]. They also require all the familiar regulators of cell migration, including Rho GTPases, Arp2/3 components, and regulators of contractility, such as ROCK (Vitorino and Meyer, 2008). A global increase in motility by uniform application of a growth factor, for example, increases the overall rate of sheet movement. The process is thus achieved by harnessing the power of individual cell motility by directing and coordinating cell movements over large distances. Rather than drive the whole process, leader cells are predominantly required to direct the motility of cells within the sheet in response to a stimulus. Loss of FGFR in endothelial cells, for example, inhibits directional cell movements without affecting random cell motility. Cadherins and components of adherens junctions, such as α -catenin, on the other hand, are necessary to maintain the “follower” behavior of cells within the bulk of the sheet by coordinating their movements (Vitorino and Meyer, 2008). In this way, the whole of the process is greater than the sum of its parts.

The specification of specialized leader cells, the active contribution of follower cells, and the emergence of group phenomena from the coupling of cells are found in numerous ex-

amples of epithelial sheet movement in development and tissue maintenance. For example, migration of the zebrafish lateral line, a group of several hundred proliferating cells that deposits groups of sensory cells as it travels the length of the embryo, involves the specification of leader cells that direct the migration of intrinsically motile followers (Haas and Gilmour, 2006). Similarly, while in some organisms the first mesodermal cells internalize by an EMT, the bulk of the mesoderm and endoderm do so as a multilayered sheet (Keller et al., 2000). A study of the collective movement of zebrafish mesoderm cells found that, while isolated cells were capable of directed movement, adequate cell-cell adhesion was required when cells were part of a group (Arboleda-Estudillo et al., 2010). This suggests a universal role for adhesion in mediating group behavior. In skin wound healing, keratinocytes at the wound border alter their integrin expression and migrate as a sheet across a provisional ECM (Martin, 1997). While many other process contribute to effective healing, including epidermal proliferation and contraction of specialized fibroblasts at the wound site, the initial process of re-epithelialization is a classic example of sheet migration, underscoring it as a fundamental, conserved morphogenetic mechanism.

Epithelial fusion and spreading

Epithelial sheet movement in development often involves the integration of forces from multiple tissues and the assembly of a supracellular actomyosin ring around the gap. This is perhaps due to the size of gap that must be closed and the magnitude of the forces required. A classic example is *Drosophila* dorsal closure, the sealing of a naturally-occurring epithelial gap that forms as a result of germband retraction in gastrulation (Jacinto et al., 2002b). Movement and fusion of the epidermal sheets on either side is driven by the combined activity of a contractile actomyosin “purse string” assembled by cells bordering the gap, apical constriction of amnioserosa (AS) cells, the extra-embryonic tissue exposed by the gap, and extension of filopodia between apposing sheets (Figure 1.1A).

Although the exact signals that initiate the process are not well understood, activation of

1.4. CONSERVED MORPHOGENETIC MOVEMENTS

the JNK pathway and Dpp signaling, which have wide-ranging roles in cell migration, are known to regulate formation of the actomyosin cable (Arias and Jacinto, 2007). This cable acts both as a source of circumferential tension to pull the epidermal sheets forward and as a ratchet to stabilize transient pulling forces generated by apical constriction in the AS (Hutson et al., 2003; Solon et al., 2009). Pulsed apical constriction in the AS begins before the onset of dorsal closure, and its amplitude decreases as dorsal closure proceeds. The pulsing of AS cells is also coordinated in space, with cells 1–2 diameters apart pulsing together in an anti-phase relationship. This suggests the conversion of forces from apical constriction into forward sheet movement through a cooperation of AS cells and the actin cable. In support of this, JNK mutant embryos that fail to assemble an actin cable fail to complete dorsal closure, while apical constrictions in the AS are equivalent to wild-type embryos (Jacinto et al., 2002a; Solon et al., 2009). Throughout the process, cells at the leading edge become highly elongated along the axis of closure and extend lamellipodia and filopodia into the gap. Cell elongation actively contributes to forward movement throughout the process (Gorfinkiel et al., 2009), while the extension of protrusions plays a role in aligning and zippering the sheets after they are brought into close apposition (Millard and Martin, 2008). As a whole, dorsal closure is an illuminating example of how numerous manifestations of cell motility are combined in a carefully orchestrated process of collective cell movement.

The function of a supracellular actomyosin cable as a purse string and ratchet is common to many examples of epithelial closure and spreading in development (Figure 1.1B). In zebrafish gastrulation, the spreading of the enveloping layer (EVL) over the yolk cell during epiboly is driven by an actin cable assembled by cells of the yolk syncytial layer (YSL), a group of epithelial cells on the surface (Behrndt et al., 2012). The EVL is tethered to the YSL by tight junctions and is pulled over the yolk cell by a combination of circumferential tension from constriction of the actin cable and retrograde actomyosin flow within the YSL. This flow, opposite to the direction of sheet movement, is resisted by friction from the actin cable, leading to an additional force driving EVL spreading. Supracellular actomyosin

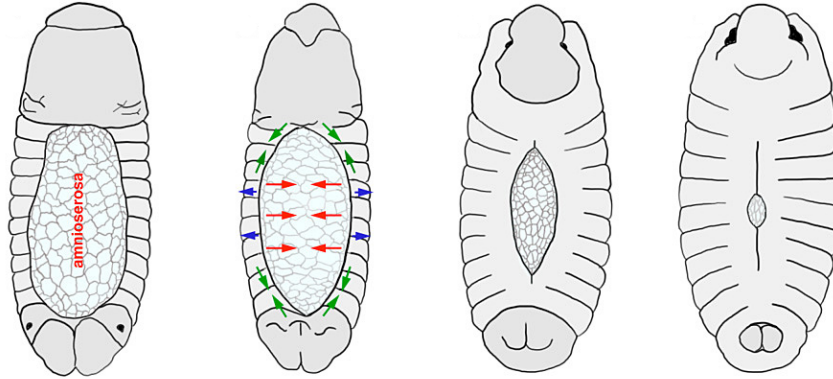
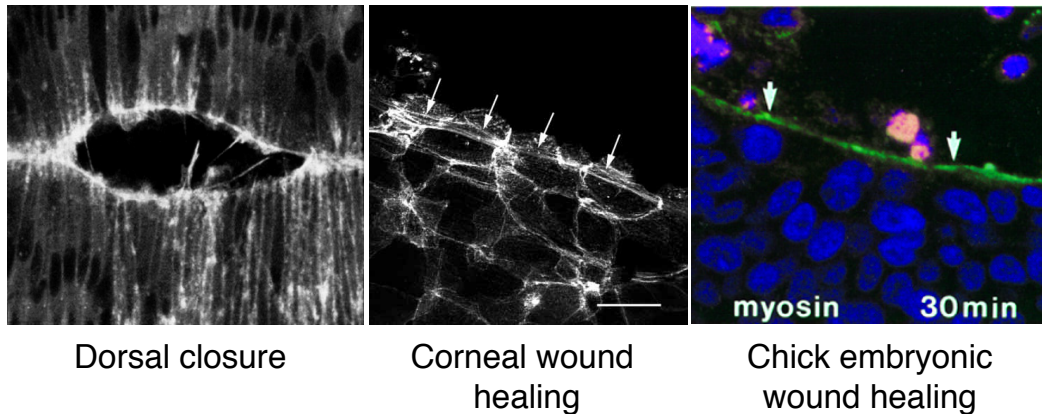
A *Drosophila* dorsal closure, a model epithelial fusion**B** Supracellular actin cables in epithelial fusion

Figure 1.1: Actin purse strings in tissue morphogenesis. (A) Schematic of *Drosophila* dorsal closure, perhaps the best-known example of epithelial fusion driven by an actin purse string in development. The process involves closure of a gap on the dorsal epithelium formed during germband retraction, and requires assembly of a supracellular actomyosin cable, known to require JNK signaling, pulsed apical constriction in the underlying amnioserosa, and extension of filopodia between cells of apposing sheets. The actin cable is believed to generate centripetal tension to pull the surrounding epidermis as well as stabilize the pulsed apical constriction of cells in the amnioserosa. Filopodia are believed to play a role in sealing the sheets once they are brought together. (B) Examples of actin purse strings driving tissue morphogenesis and homeostasis across the animal kingdom. Examples include not only dorsal closure, but corneal wound healing in mice and healing of the embryonic chick wing bud. Illustration in (A) from Nicole Gorfinkiel. Images in (B) reproduced from Jacinto et al. (2002a), Brock et al. (1996b), and Danjo and Gipson (1998), respectively.

1.4. CONSERVED MORPHOGENETIC MOVEMENTS

cables also contribute to embryonic wound healing in *Xenopus* (Bement et al., 1999), chick (Brock et al., 1996a), and mouse (McCluskey et al., 1993), as well as corneal wound healing in adult mice (Danjo and Gipson, 1998), although their precise role has not been fully elucidated.

1.4.3 Cell intercalation and convergent extension movements.

Polarized cell movements leading to the ordered rearrangement of cells within a tissue are a major force in shaping the body plan during embryogenesis. Among the best-studied large-scale morphogenetic movements in development are convergent extension movements, which drive axis elongation in the dorsal mesoderm and neural tissues of *Xenopus* and zebrafish, the notochord of mice, and the germband of *Drosophila*. Few other processes are as ubiquitous in animal development or as responsible for such a degree of active tissue remodeling and passive deformation. These movements are driven by cell intercalation, a highly regulated process of neighbor exchange leading to the narrowing of a tissue along one axis and extension along another. Although the mechanisms by which cells intercalate are substantially different between epithelial and mesenchymal tissues and even vary between mesoderm-derived tissues, they are driven by the same fundamental machinery that fuels cell migration and cell shape change. Common to both are the compartmentalization of protrusive activity and myosin II-dependent contractility within cells and across tissues.

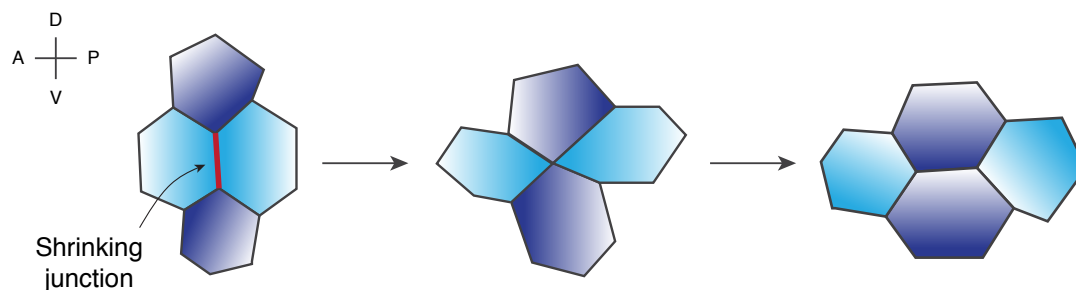
Epithelial cell intercalation.

Cell intercalation in epithelial tissues involves the planar polarized remodeling of apical cell junctions, perhaps best illustrated in the process of germband elongation in *Drosophila* gastrulation (Irvine and Wieschaus, 1994). As the mesoderm and endoderm are internalized, the outer epithelium, known as the germband, nearly doubles its length in the absence of cell division over the course of two hours. This occurs by the intercalation of cells along the dorsal-ventral (D-V) axis, narrowing the tissue in this direction while extending it along

the anterior-posterior (A–P) axis. Similar to apical constriction, this involves the compartmentalized activity of myosin II and is characterized by pulsatile actomyosin flows that are stabilized by accumulation of myosin II, only instead of constricting the apical surface of the cell, they are directed to specific junctions oriented along the D–V axis (Bertet et al., 2004; Rauzi et al., 2010; Zallen and Wieschaus, 2004). Shrinkage of these junctions results in cell intercalation by a T1 process (using terminology from the study of topology, Weaire and Rivier, 2006). This involves the sequential transition from a type 1 configuration, a grouping of four cells in which cells along the A–P axis are in direct contact while cells along the D–V axis are not, to a type 2 configuration in which the four cells share a common vertex, and finally to a type 3 configuration, in which a new junction forms between cells along the D–V axis. This results in intercalation along the D–V axis and extension of the tissue along the A–P axis (see [Illustration 1.6A](#)). However, these transitions do not account for the full range of cell intercalations observed in the germband. Nearly two-thirds of cell junctions with high levels of myosin are associated with actomyosin cables that span multiple junctions, similar to those that drive processes of epithelial fusion and spreading (Fernandez-Gonzalez et al., 2009). Contraction of multiple, linked junctions along the D–V axis forms multicellular rosettes whose directional resolution (similar in principle to a T1 process) elongates the tissue by multiple cell diameters (Blankenship et al., 2006). The combined effect of both by the same underlying mechanism are likely responsible for the great speed at which the germband elongates.

Anisotropic myosin II activity is directed by well-established asymmetries between A–P and D–V junctions established by A–P patterning genes (Irvine and Wieschaus, 1994). Whereas F-actin, ROCK, and myosin II preferentially accumulate along the A–P axis (Zallen and Wieschaus, 2004), Par3, E-cadherin, and β -catenin accumulate along the D–V axis, a polarization necessary for proper germband extension (Blankenship et al., 2006). F-actin is the first to polarize and is able to do so when D–V polarity is disrupted, suggesting that A–P polarity is established prior to or independently of D–V polarity (Blankenship et al.,

A Cell intercalation in epithelial tissues



B Mediolateral intercalation in mesodermal tissues

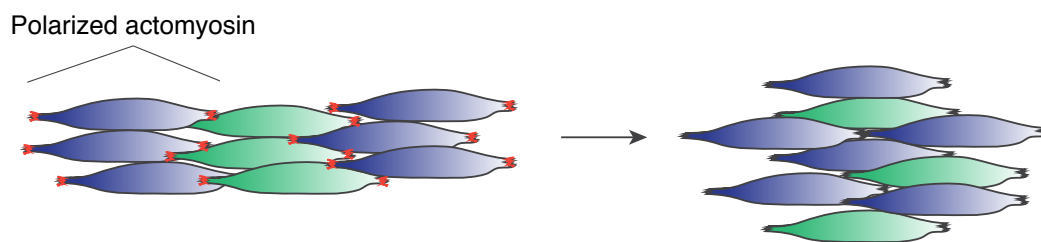


Illustration 1.6: Modes of cell intercalation in development. (A) The basic process of epithelial cell intercalation by the planar-polarized remodeling of cell-cell junctions. Pulsatile myosin II flows directed towards junctions along the D–V axis (or, equivalently, on the A–P sides of cells) cause their preferential shrinkage. This enables cells along the D–V axis that were not previously in contact to form a junction, resulting in their intercalation between two cells along the A–P axis. Using terminology from mathematical topology, this is known as a T1 process (Weaire and Rivier, 2006). A similar process involving the shrinkage of multiple linked junctions leads to multicellular rosette formation, whose resolution leads to even greater extension along the A–P axis. (B) Mesodermal cell intercalation. Rather than the myosin II-dependent remodeling of cell junctions, the more loosely-connected cells of mesodermal tissues intercalate by a process of polarized motility. Highly elongated cells extend protrusions along their mediolateral axis, thought to allow them to exert traction on their neighbors. Cells pull each other into file, elongating the tissue along the A–P axis. This model has recently been called into question by the discovery of preferential junction shrinkage in the *Xenopus* mesoderm (Shindo and Wallingford, 2014).

2006; Zallen and Wieschaus, 2004). This polarity is reinforced by Rho GTPase, ROCK, and Shroom, which promote contractility along the A–P axis and inhibit cell adhesion by excluding Par3 (Simões et al., 2010, 2014), as well as by Abl, which promotes the turnover of β -catenin at shrinking junctions (Tamada et al., 2012). These asymmetries direct the anisotropic flow of myosin along the A–P, where lower levels of E-cadherin likely modulate the local actin meshwork (Rauzi et al., 2010). In support of this, uncoupling E-cadherin from the cytoskeleton by knockdown of α -catenin is sufficient to disrupt the planar polarization of both E-cadherin and myosin II. However, it is unclear if pulsatile actomyosin flows are strictly necessary for cell intercalation or whether they simply characterize local myosin II activity. As a whole, the process illustrates how pathways regulating tissue patterning compartmentalize actomyosin contractility within cells, driving large-scale tissue remodeling through the additive effect of cell intercalation in small groups of cells.

Mesodermal cell intercalation

Convergent extension movements in mesodermal tissues are a major driving force in the anterior-posterior elongation of the vertebrate embryo. Unlike epithelia, the cells of the mesoderm are not polarized along their apicobasal axis and are often only loosely connected. As such, convergent extension in these tissues involves polarized cell movements that drive the mediolateral intercalation of cells rather than the remodeling of specific cell junctions ([Illustration 1.6B](#); Keller et al., 1989; Shih and Keller, 1992). Mesodermal cells elongate along their mediolateral axis and extend bipolar, mediolaterally-oriented lamelliform and filiform protrusions. These protrusions are thought to be tractive, allowing cells to form transient adhesions that enable them to crawl over and pull each other into file (Keller et al., 2000). Similarly to neighbor exchanges in epithelial convergent extension, intercalation of cells mediolaterally narrows the tissue along this axis while extending it along the A–P axis. The local formation and rapid remodeling of adhesive contacts allows cells to intercalate effectively while forming a stiff array capable of resisting deformation from

1.4. CONSERVED MORPHOGENETIC MOVEMENTS

surrounding tissues and evolving substantial pushing forces that drive tissue elongation. Indeed, biomechanical measurements of Keller explants, mesodermal tissue explants from the dorsal involuting marginal zone that autonomously converge and extend, indicate that the tissue stiffens by a factor of three to four times along the A–P axis as it extends, and generates forces upwards of $0.5 \mu\text{N}$ (Moore et al., 1995). This effectively pushes the anterior away from the posterior regions of the embryo in axis elongation, and has an important developmental role in the internalization of mesodermal and endodermal tissues as well in the functioning of organs that require an elongated shape, such as the notochord and gut (Keller et al., 2000).

Mediolateral intercalation contributes to tissue elongation in two distinct ways depending on the presence of tissue boundaries. Early in gastrulation, bipolar protrusive activity throughout the dorsal mesoderm, with cells acting as substrates for each other, directs its elongation. As gastrulation proceeds, however, the notochord-somite boundary (NSB) forms within this population of intercalating cells, after which cells within the notochord exhibit monopolar protrusive activity and elongate the tissue by a “boundary capture” mechanism (Elul and Keller, 2000; Keller et al., 1989). As cells within the notochord reach the NSB, one side of the cell adheres to it and ceases protrusive activity at that interface. Continuing, monopolar protrusions at the other interface exert traction on cells in the interior of the notochord, “capturing” and pulling them into the boundary. This leads to mediolateral intercalation and tissue elongation by a similar, though distinct, mechanism. The boundary is thought to be formed by the inhibition of cell-cell adhesion between the notochord and the surrounding presomitic mesoderm downstream of Eph-ephrin signaling, preventing these cells from intercalating with each other (Fagotto et al., 2013). This is followed by the deposition of a specialized ECM including fibrillin and laminin at the boundary, likely mediating the attachment of cells and cessation of protrusive activity by integrin-based adhesion (Veeman et al., 2008). Monopolar cell intercalation can also occur by the directional bias of cell motility toward (rather than away from) a tissue boundary, as occurs in the neural

plate (Elul and Keller, 2000).

Cell intercalation in loosely-connected mesodermal tissues involves a complex and poorly understood interplay between cell protrusion, contractility, and adhesion. Similar to epithelial cell intercalation and apical constriction, pulsed actomyosin contractions were found to occur as mesodermal cells elongate in *Xenopus* development, suggesting that they have a function in generating cell shape changes or stabilizing tractive adhesions (Kim and Davidson, 2011). Both cadherin and integrin-based adhesion are required for proper convergent extension. Cadherins are typically downregulated in converging and extending tissues, but either overexpression or loss of cadherins in mesodermal or neural tissues leads to defective intercalation, suggesting that their levels must be maintained within a permissive range (Delarue et al., 1998). Supporting this notion, protocadherins expressed specifically in intercalating tissues, paraxial protocadherin (PAPC) in the dorsal mesoderm and axial protocadherin (AXPC) in the notochord are essential for their role in regulating cadherin-based adhesion. PAPC in particular cannot itself mediate cell-cell adhesion but is known to disrupt C-cadherin-based adhesion in *Xenopus* and to localize to active cell protrusions (Chen and Gumbiner, 2006). Similarly, integrin-ECM adhesion is required for both monopolar cell intercalation in boundary capture as well as bipolar intercalation. In *Xenopus*, $\alpha_5\beta_1$ -fibronectin adhesion is necessary for the mediolateral polarization of cell protrusions (Davidson et al., 2006) and to reduce levels of cadherin-based adhesion in the mesoderm (Marsden and DeSimone, 2003).

Cell intercalation driving convergent extension is a testament to the power of compartmentalized actomyosin dynamics within cells. Despite a radical difference in execution, epithelial and non-epithelial tissues share a fundamental strategy of tissue elongation by the coordinated intercalation of cells. The ubiquity of this strategy in development and the fact that all of its manifestations involve pulsatile actomyosin flows and the modulation of cell contractility and adhesion suggest a deep evolutionary conservation. A recent study performing a detailed quantification of myosin II polarity and actomyosin dynamics in the

1.4. CONSERVED MORPHOGENETIC MOVEMENTS

Xenopus mesoderm even suggests that the same mechanism may operate in both tissue types (Shindo and Wallingford, 2014). In addition to the mediolateral extension of lamellipodia, actomyosin flow mediating the specific remodeling of D–V-oriented junctions was found to drive cell intercalation by a T1 process, as occurs in epithelial convergent extension. Although it is difficult to imagine how this would drive mediolateral intercalation in tissues exhibiting monopolar protrusions, it is possible that it operates in combination with other processes of cell motility to achieve tissue elongation in different scenarios.

1.4.4 Planar cell polarity

An important discovery of the last twenty years is that a key pathway that establishes planar polarity in *Drosophila* also regulates convergent extension movements in vertebrates. Known as the planar cell polarity (PCP) pathway, its molecular determinants are conserved from flies to humans (Seifert and Mlodzik, 2007; ?), and it is responsible for the compartmentalization of actin protrusion and myosin II-dependent contractility fundamental to many processes of tissue morphogenesis.

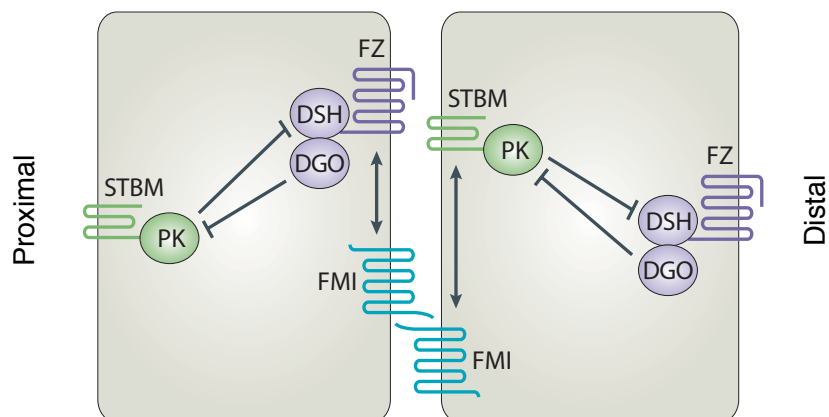
PCP involves the coordination of cells within a tissue to orient themselves, either individually or as groups, across a two-dimensional plane. First identified in *Drosophila*, core PCP proteins including Frizzled (Fzd), Strabismus (Stbm), and Flamingo (Fmi), which are membrane bound, and Dishevelled (Dsh), Diego (Dgo), and Prickle (Pk), which are cytoplasmic but membrane-associated, were found to be responsible for the precise distal orientation of wing hairs and the orientation of photoreceptor clusters in the eye. Acting in parallel to these core proteins, a second PCP cassette consisting of Fat (Ft) and Dachshous (Ds), two protocadherins, and Four-jointed (Fj) has recently been identified as reinforcing correct establishment of planar polarity in these tissues, although its relationship to the Fzd/Fmi pathway is still open to debate. In mice, orthologs of these proteins including Fzd3 and 6, Vangl2 (Strabismus), Celsr1 (Flamingo), and Dishevelled (Dvl1–3) similarly control the orientation of stereocilia bundles in the inner ear (Montcouquiol et al., 2006) and the orientation of body

hairs (Devenport and Fuchs, 2008).

Although mechanistic details of how PCP proteins give rise to planar polarity and regulate migration are lacking, genetic studies in *Drosophila* and other model organisms have uncovered a number of key requirements for their activity (Illustration 1.7A). The initial cue for generating planar polarity comes from local differences in Frizzled activity, thought to be generated by either an external gradient of a Wnt (5b or 11, in vertebrates only), or generated locally by Fj, Ft, and Ds (or an unknown mechanism) and propagated from cell to cell (Zallen, 2007). PCP proteins are first localized to the apical surface of a cell, where they segregate into mutually antagonistic subcomplexes likely via directional transport along polarized microtubules. In the *Drosophila* wing, the subcomplexes consist of Fzd, Dsh, and Dgo on the distal surface, antagonizing Pk activity, and Pk and Stbm on the proximal surface, antagonizing Dsh. In the mouse inner ear, PCP proteins similarly segregate into mutually antagonistic complexes, but they do not distribute in exactly the same way (Wang, 2006). For example, Fzd3 and 6 co-localize with Vangl2 (Stbm) instead of in separate complexes, and Dvl2 localizes opposite to Fzd instead of co-localizing with it. These differences in the localizations of PCP proteins in mammalian tissues has not been extensively studied.

In addition to polarity defects, PCP mutants exhibit severe defects in conserved developmental cell movements, including convergent extension in vertebrates (Wallingford et al., 2000) and dorsal closure in *Drosophila* (Kaltschmidt et al., 2002). While there is not a perfect correspondence between establishment of planar polarity in epithelia and regulation of developmental cell migrations by the PCP pathway, in both scenarios, downstream effectors of Dsh, such as Rho GTPases and ROCK, compartmentalize the activity of myosin II and actin polymerization, leading to polarized cell behaviors. This has multiple roles in morphogenesis, including orienting cell protrusive activity, regulation of cadherins, and the polarized deposition of ECM components. All three are likely involved in convergent extension movements. In the *Xenopus* mesoderm, Dishevelled localizes to mediolateral protrusions along with Arp2/3 and Rac (Kinoshita et al., 2003) and is required both for the elongation of

A Mutual antagonism between core PCP proteins



B Localization of PCP proteins in epithelial and non-epithelial tissues

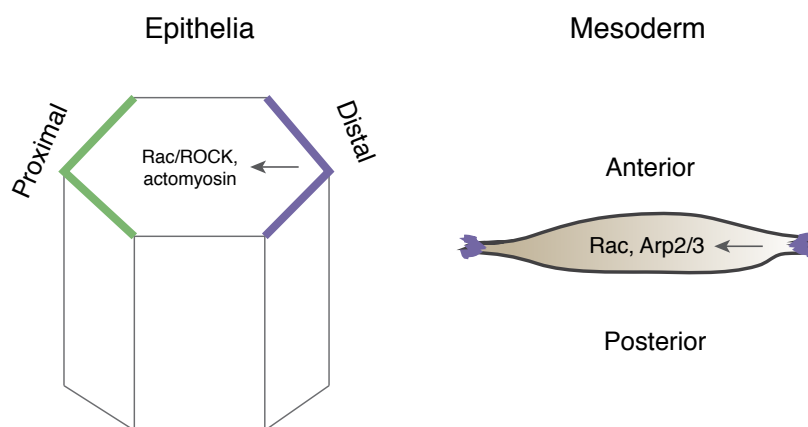


Illustration 1.7: The core PCP pathway. (A) Following their apical localization, PCP components distribute into mutually antagonistic complexes, consisting of Frizzled, Dishevelled, and Diego at the distal end, and Strabismus (Vangl2) and Prickle at the proximal end in *Drosophila* wing cells. PCP proteins are recruited into the region of the adherens junction by the atypical cadherin Flamingo (Celsr1). The end result of PCP is determined through effectors of Dishevelled, including the Rho family GTPases and ROCK. (B) In epithelia, PCP proteins control the precise distal orientation of wing hairs in *Drosophila*, and the A–P orientation of body hairs and organization of seterocilia bundles of the inner ear in mice. Although the pathway is not essential for convergent extension in the *Drosophila* germband, it is known to regulate cell intercalation in the neuroepithelium in mice, and the mediolateral intercalation of the dorsal mesoderm in *Xenopus* and zebrafish, where Dishevelled has been found to localize to mediolateral protrusions. Illustration in (A) reproduced from Seifert and Mlodzik (2007).

cells and the polarization of protrusive activity (Illustration 1.7B). This is thought to involve both a direct role of Dishevelled in regulating cell motility as well as the local remodeling of the fibronectin matrix (Goto et al., 2005). In the notochord, disruption of Fz, Stbm, or Pk likewise results in an abnormal distribution of fibronectin that causes inappropriate cell intercalation. However, the interplay between PCP and ECM assembly is likely complex, as a syndecan-4-dependent interaction of cells with fibronectin was also found to feed back into establishment of PCP (Munoz et al., 2006). PCP signaling through Wnt11 and Frizzled-7 was also found to downregulate cell-cell adhesion in two ways: by affecting cadherin endocytosis through Rab5 in zebrafish (Ulrich et al., 2005), and by either the sequestration of cadherins in the membrane through PAPC or by direct competition with cadherin dimerization in *Xenopus* (Kraft et al., 2012). PCP thus has multiple roles in regulating protrusive activity, matrix organization, and the active remodeling of junctions to create a dynamic environment for directed motility.

Interestingly, the PCP pathway is not required for planar polarity and epithelial cell intercalation in the *Drosophila* germband, which instead relies on a separate A–P patterning system (Irvine and Wieschaus, 1994; Zallen and Wieschaus, 2004). However, highlighting its conserved role in the spatial regulation of actomyosin dynamics, the process of neural tube closure in mice requires PCP both in epithelial cell intercalation to narrow and extend the neural plate and for anisotropic apical constriction to form the tube (Baker and Schroeder, 1967; Nishimura et al., 2012; Schoenwolf, 1984; Stein and Rudix, 1953). This involves the asymmetric localization of Celsr1 along the A–P axis, leading to the polarized accumulation of ROCK through Dsh, Daam1, and PDZ-RhoGEF. Similarly to the *Drosophila* germband, local activation of myosin preferentially shrinks D–V-oriented junctions, driving mediolateral cell intercalation and tissue extension along the A–P axis. This is thought to simultaneously generate anisotropic apical constriction that bends the narrowing neural plate to form a tube (Nishimura et al., 2012). PCP proteins were also recently discovered to polarize components of the septin cytoskeleton in the *Xenopus* mesoderm, di-

1.4. CONSERVED MORPHOGENETIC MOVEMENTS

recting actomyosin flow to specific cell junctions and mediating their shrinkage (Shindo and Wallingford, 2014). Specifically, Sept7 was found to localize to mediolateral vertices downstream of Dvl, stabilizing cortical actin at these interfaces and excluding myosin activity. As a consequence, actomyosin flow is biased toward D–V-oriented junctions, driving cell intercalation by junction remodeling as observed in epithelial tissues. PCP thus represents a ubiquitous and evolutionarily conserved means by which the fundamental force-producing machinery of individual cells are coordinated within tissues to drive morphogenesis.

1.4.5 Collective cell movements in organogenesis

The study of collective cell movement has in large part focused on gastrulation movements in lower organisms such as flies, frogs, and fish because of the ease of live imaging and genetic manipulation. However, such movements are by no means limited to early development. Branching morphogenesis to form a tubular network in organs such as the trachea, mammary and salivary glands, and pancreas, for example, integrates numerous types of collective cell movement (Lu and Werb, 2008). In the *Drosophila* trachea, apical constriction and invagination of a group of around 80 epithelial cells first forms a placode. This is followed by the acquisition of invasive properties and active migration of a group of leader cells to partially extend the tube (Ghabrial et al., 2003). The majority of the tube, however, elongates by the intercalation of “follower” cells, known to require PCP and finely-tuned levels of E-cadherin endocytosis, combined with cell proliferation. Finally, a complex, reiterative process elaborates these structures into highly branched trees. A similar process likely operates in the formation of the mammary and salivary glands. Elongation of the collecting ducts in the vertebrate kidney was also recently found to occur by a process of epithelial cell intercalation (Lienkamp et al., 2012). As in the formation of the trachea in *Drosophila* and in vertebrate neural tube closure, PCP is required for the formation and proper resolution of multicellular rosettes.

While cell proliferation is traditionally considered the major driving force of tissue growth

in development and homeostasis, its conspicuous absence in driving these examples of tissue morphogenesis in late development suggests that it is more important behind the scenes. Similar combinations of conserved mechanisms of collective cell movement, first uncovered in gastrulation, may also play a role in the rapid sculpting of tissues in adult homeostasis, regeneration, and disease. Indeed, in polycystic kidney disease, a common disorder in humans leading to the formation of multiple cysts in nephrons, conditions known to favor cell intercalation in development prevent cyst formation (Nishio et al., 2010). This suggests the possibility that, in some cases, cell intercalation may either be the cause of or used to treat certain diseases.

1.4.6 Emerging technologies in live imaging

Our understanding of the cellular and molecular mechanisms driving tissue morphogenesis has grown hand-in-hand with improvements in imaging technology and computational tools to analyze the dynamics of complex developmental processes. The past ten years have seen the widespread adoption of two-photon microscopy for deep tissue imaging in live animals and the long-term imaging of embryos. In contrast to conventional imaging by exciting fluoreophores with visible wavelengths, two-photon imaging relies on the simultaneous absorption of two photons in the infrared or near-infrared range generated by high-power, femtosecond pulsed lasers (Denk et al., 1995). Because the probability of absorbing two photons is extremely low except at the focal plane, this restricts excitation to a small volume, minimizing the effects of photobleaching and photodamage inherent to visible excitation. At high powers, two-photon lasers can also be used for tissue ablation by generating a small volume of plasma at the focus (Jiang and Tsai, 2003; Yalcin et al., 2010). Combined with advances in techniques to stabilize animals and reduce motion artifacts from the heartbeat and respiration, this has enabled live imaging at spatial resolutions comparable to those achieved in cell culture models, as well as an opportunity to probe the contributions of different cell populations to a process. In neurobiology, this has allowed the imaging of neuronal migra-

1.4. CONSERVED MORPHOGENETIC MOVEMENTS

tion as well as changes in neuronal morphology in response to various pathologies (Zhang and Murphy, 2007). Perhaps most exciting, it is finding continued use in visualizing the behaviors of cells in living tumors and stem cells within their niche, shedding light on the processes of tumor outgrowth, intravasation, and metastasis (Tozluoğlu et al., 2013), as well as the dynamics of stem cells in tissue self-renewal (Rompolas et al., 2012).

Another advance that has only recently become commercially available is light sheet microscopy, a technique that allows multiple views of a living specimen to be acquired simultaneously (Huisken et al., 2004). A light sheet is generated by focusing a laser in only one direction using a cylindrical lens, illuminating a thin region of a specimen that is imaged by perpendicularly-facing detectors. This affords better contrast and faster acquisition than scanned confocal or multiphoton microscopy, and has ushered in an era of *in toto* imaging, in which all of the cells of a developing embryo are imaged and tracked over the course of development. Combined with sophisticated image registration and analysis software, this technique has been used to digitize the early development of zebrafish (1.5 to 30 hours post fertilization, hpf) and *Drosophila* embryos (3 to 18.5 hpf), mapping the movements and divisions of all cells (Keller et al., 2008a; Tomer et al., 2012). This allows both focusing on specific developmental processes, such as internalization events in gastrulation, as well as the dynamics of large populations of cells, such as waves of cell division that lead to early symmetry breaking. Very recently the technique has been used in the real-time monitoring of brain activity in zebrafish using the calcium indicator GCaMP5G, revealing populations of neurons with coordinated activities (Ahrens et al., 2013). While the technique holds incredible promise, it operates at the bleeding edge of what is possible with today's acquisition hardware and computing power, and requires considerable expertise in image and data processing.

With the acquisition of increasing complex, quantitative datasets has come the need for mathematical modeling and computer simulation to explain the observed phenomena. Simulations based on the principle of minimizing surface energy have been used to explain the

configuration of cone cells in the *Drosophila* eye (Hilgenfeldt et al., 2008), packing geometries in the wing imaginal disk (Farhadifar et al., 2007), and the formation of dorsal appendages in the eggshell (Osterfield et al., 2013). Finite element modeling, a technique in which a structure is represented as a latticework of discrete elements with well-defined physical properties, has been used to understand how contractility in a small group of cells drives tissue invagination in sea urchin and *Drosophila* embryos (Davidson et al., 1995; Pouille and Farge, 2008), and how forces from constrained proliferation lead to vilification of the gut (Shyer et al., 2013). Similarly, cell tracking techniques and principles of soft matter physics have been applied to map the evolution of tissue deformation as a result of cell shape changes and intercalation (Blanchard et al., 2009). As biology becomes increasingly multidisciplinary, the development of such models and analytical tools will allow us to understand the physical basis of morphogenetic processes.

Finally, innovations in techniques to support the growth of embryos and tissues *ex vivo* continues to expand the possibilities for imaging tissue morphogenesis in the complex tissue environments of mammalian development. Methods to image whole mouse embryos have clarified the cellular origins of the gut endoderm (Kwon et al., 2008), mechanisms of left-right patterning in the early embryo (Viotti et al., 2012), and the role of PCP and cell intercalation in neural tube closure (Nishimura et al., 2012; Pyrgaki et al., 2010). Techniques to maintain skin explants at an air-liquid interface have also been used to study the targeting of melanoblasts to hair follicles, shedding light on a process of cell migration in a complex, 3D environment (Li et al., 2011). Continuing to push the envelope in the realm of imaging modalities, computational tools, and methods to culture embryos, tissues, and organs will greatly expand our understanding of tissue dynamics in scenarios relevant to human health.

1.5 The skin as a model system

The skin epidermis and its appendages, including hair follicles, sweat glands, and sebaceous glands, provide a protective barrier against physical trauma, microbes, dehydration, and

1.5. THE SKIN AS A MODEL SYSTEM

ultraviolet irradiation. Under constant assault, it is able to perform these functions by continually renewing itself through reserves of stem cells, which maintain a careful balance of proliferation and differentiation (Fuchs, 2008). In the service of maintaining a barrier, it has enormous morphogenetic potential both in embryogenesis, where it initiates hair follicle formation and mediates processes of epithelial fusion to protect the eye and internal organs, and in adulthood, where it retains a remarkable capacity to mobilize keratinocytes to heal wounds (Bement, 2010). In mice, these properties, along with its accessibility to imaging and genetics, make it ideal for the study of tissue morphogenesis and homeostasis in mammals.

The mammalian epidermis is a stratified squamous epithelium consisting of an undifferentiated, proliferative basal layer, followed by successively differentiated suprabasal layers (Illustration 1.8). The basal layer adheres to a specialized ECM rich in growth factors and proteoglycans, the basement membrane, which separates it from the underlying dermal mesenchyme. The basal layer gives rise to the successive layers of the skin by a carefully orchestrated differentiation program, in which cells withdraw from the cell cycle and progressively move outward, where they are eventually sloughed off the surface (Fuchs, 2008). Cells in each layer of the skin, representing different stages of the differentiation program, are characterized by unique morphologies, gene expression patterns, cytoskeletal elements, and adhesion molecules that can be used as markers (Fuchs and Green, 1980). The basal layer is characterized by its cuboidal morphology, high expression of the keratins K5 and K14, and attachment to the basement membrane by hemidesmosomes, integrin-based adhesions tethered to the keratin cytoskeleton. These properties are in large part responsible for the skin's characteristic mechanical strength, as disrupting the K5/K14 filament network or attachment to the basement membrane through $\alpha_6\beta_4$ integrin in mice results in skin blistering (Dowling et al., 1996; Vassar et al., 1991), explaining the phenotypes of the human skin disorder epidermolysis bullosa simplex (Coulombe et al., 2009).

As basal cells progress through their differentiation program, they form three distinct

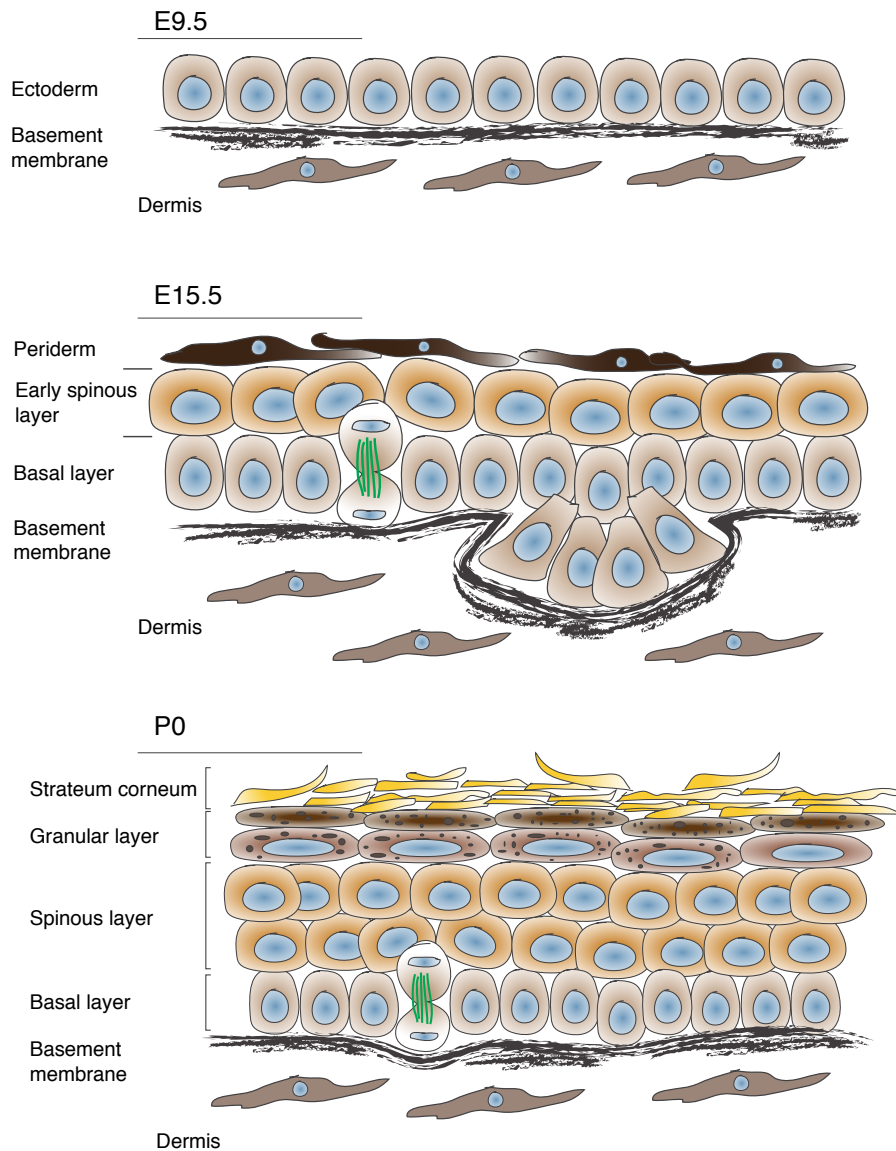


Illustration 1.8: The architecture of mammalian skin. In mice, the skin develops from a single layer of ectodermal progenitors following neural tube closure at E9.5. Between E10.5 and E12.5, the periderm, a transient layer of tightly-connected squamous cells, develops to protect the embryo until the skin has fully differentiated and acquired its barrier function. Differentiation begins between E14.5 and E15.5 with the onset of asymmetric cell division. At this stage, the skin is also morphogenetically active, characterized by the onset of hair follicle placode formation and temporary epithelial fusions, including eyelid closure, digit fusion, and fusion of the ear to the scalp. By P0, the skin has fully differentiated into layers with distinct morphologies, cytoskeletal elements, and gene expression patterns. The result is a mechanically robust, water-permeable tissue that protects against constant environmental assault.

1.5. THE SKIN AS A MODEL SYSTEM

suprabasal layers in the skin: the spinous and granular layers, and the stratum corneum (Illustration 1.8). The spinous layer is characterized by a switch from K5/K14 expression to K1 and K10, the adoption of a flattened, squamous morphology, and formation of desmosomes connecting cells within the layer and to the underlying basal layer (Fuchs and Cleveland, 1998). In the granular layer, keratinocytes begin the process of cornification essential for the barrier function of the skin. This involves the formation of keratohyalin granules, which play a role in the aggregation of keratin filaments into microfibrils through the proteins filaggrin and loricrin (Lynley and Dale, 1983), and lamellar bodies, which contain lipids that are secreted into the extracellular space during cornification (Schmitz and Muller, 1991). Granular cells also begin the synthesis of cornified envelope proteins. Finally, the membranes of keratinocytes are transformed into a tough, waterproof envelope, the stratum corneum. This occurs through the digestion of the nucleus and cytoplasm, precipitating the release of lipids, and the protein cross-linking actions of loricin and transglutaminase (Harding, 2004).

In mice, the skin develops from a single-layered sheet of ectodermal progenitors following neural tube closure at E9.5. Prior to the onset of differentiation around E14.5, a barrier function and mechanical stability are thought to be provided by the periderm, a transient layer of tightly-connected, squamous cells that develops between E9.5 and E12.5 in a regional manner (Nakamura et al., 1979). Initial expansion of the epidermis occurs by symmetric cell division, in which basal cells divide parallel to and retain contact with the basement membrane. Following a period of uniform growth, the onset of differentiation is marked by the transition from predominantly symmetric to predominantly (>70%) asymmetric cell division, which partitions the cell into one basal and one suprabasal daughter. This continues until the completion of stratification at E18.5 and is a major driving force of differentiation in the skin (Lechler and Fuchs, 2005; Williams et al., 2011). The process is regulated by a conserved set of proteins known to regulate spindle orientation, asymmetric cell division, and differentiation in *Drosophila* neuroblasts (Schober et al., 1999). In the

skin, their recruitment to the apical cortex similarly controls spindle orientation, promoting differentiation through Notch signaling (Williams et al., 2011).

1.5.1 Temporary epithelial fusions

Taking place concomitantly with asymmetric cell division and differentiation are a number of dramatic morphological changes in the skin. Among them are the formation and down-growth of hair follicle (HF) placodes and temporary epithelial fusions. In large part due to their complexity, none of these processes are fully understood. HF placodes are thought to be induced by a process of epithelial condensation involving FGFs and BMP inhibitors secreted by the dermis, and activation of Wnt/ β -catenin signaling in the epidermis (Sennett and Rendl, 2012). Recent evidence from live imaging suggests that the process of down-growth involves directed cell migration and intercalation downstream of Eda/NF- κ B and Wnt signaling, and only a minor role of cell proliferation (Ahtiainen et al., 2014). However, apical constriction, cell sorting, and the spatial control of proliferating cells may also be involved (Devenport and Fuchs, 2008).

Temporary epithelial fusions, as the name implies, involve the fusion of epithelial structures in development and their subsequent reopening. Common to all mammals, this includes digit fusion, fusion of the ears to the scalp, and eyelid closure, all of which take place between E14–16, reopening about two weeks after birth (Harris and McLeod, 1982; Maconnachie, 1979). Early studies using electron microscopy and conventional histology revealed the presence of a ridge of rounded periderm cells at the border of the eyelids, digits, and ears, extending numerous filiform protrusions between each other. This has led to the hypothesis that fusion is mediated by the proliferation and streaming of peridermal cells to “glue” the epidermal structures together (Maconnachie, 1979). Differentiation and keratinization of the underlying epidermis after birth is thought to then cause their separation.

Eyelid closure is perhaps the best-studied of these process, largely because defects, manifesting as an eyelid-open-at-birth (EOB) phenotype, are easy to spot. In mice, eyelid devel-

1.5. THE SKIN AS A MODEL SYSTEM

opment begins at E11.5, and, as in other processes of temporary fusion, is accompanied by an accumulation of rounded periderm cells at the leading edge (Findlater et al., 1993). The peridermal and epidermal layers of the eyelid extend over the cornea and fuse between E15 and E16, when the two eyelids meet at the center of the eye. Among the genes known to play a role are those encoding regulators of growth factor signaling, such as EGFR, FGF10, and c-Jun (Mine, 2005; Tao et al., 2005; Zenz et al., 2003), contractility, such as ROCK (Shimizu et al., 2005; Thumkeo et al., 2005), and epithelial-mesenchymal crosstalk (Huang et al., 2009). Despite the wealth of genetic information, most studies have focused on delineating the signaling pathway that culminates in the activation of Rho kinases to promote F-actin assembly. The downstream cellular and molecular mechanisms that physically drive eyelid closure, however, are not well understood. Current models include possible roles for the periderm and cell proliferation, as well as cell migration and actomyosin contractile processes similar to embryonic wound healing and dorsal closure. Taken together, the skin and its appendages provide a unique opportunity to understand the integration of proliferation and the regulation of cell movement in the complex tissue environments of mammalian development.

1.5.2 Outline of this work

It is becoming increasingly clear that collective cell movement is a major driving force of tissue morphogenesis in development, regeneration, and disease. Insights into mechanisms of collective cell movement have come from extensive studies of gastrulation movements in model organisms including flies, frogs, fish, and to a lesser extent, mice. This has uncovered a conserved set of cellular and molecular mechanisms that variously drive the elongation, spreading, and fusion of tissues. However, to what extent these mechanisms operate later in development and in adulthood is not well understood. There is thus a great need of new model systems, particularly in mammals, to understand how evolutionarily conserved mechanisms of collective movement are refined, reiterated, and combined and in the increasingly

complex tissue environments of late development and adulthood. The lack of such models is in part due to the difficulty of live imaging mice—embryos cannot be maintained in static culture past E10.5, and live imaging adult mice requires a sophisticated stage setup to immobilize the animal and hardware to carefully time image acquisition to avoid motion artifacts from respiration.

For my thesis work, I set out to develop eyelid closure as a model system. Eyelid closure is a process of temporary epithelial fusion in the skin. Common to all mammals, it involves migration of the eyelids over the surface of the cornea to promote development of the eye. In mice, it is an ideal model of collective cell movements because it occurs rapidly on the surface of the embryo (within 24 hours), making it amenable to live imaging. As a process of epithelial fusion, it can also be productively compared to similar processes in other organisms, such as *Drosophila* dorsal closure and wound healing to identify common principles and important differences. As a migration of epithelial cells, it is also accessible to all the tools used in the study of mammalian skin, including a large variety conditional knockouts, a technique of lentiviral-mediated *in vivo* RNAi developed by my lab, and the ability to study migration of keratinocytes out of skin explants and individually in culture. This combination of mouse mutants, RNAi, and multiple avenues to assay migration position eyelid closure as a powerful system to understand the mechanics and regulation of collective cell movement in a physiologically relevant context.

In the first part of this work, I define the basic parameters of eyelid closure in terms of the cell types that contribute, their morphological and genetic properties, and the behaviors they display. To achieve this, I characterized the eyelid front in terms of its expression of epidermal differentiation markers and integrins, and performed lineage tracing of the epidermis and periderm to determine its origin. Combined with genetic ablation of the periderm, this establishes the eyelid front is derived from the epidermis.

To determine the relative contributions of cell motility and proliferation to eyelid closure, I performed a detailed, quantitative analysis of cell proliferation in the eyelid front

1.5. THE SKIN AS A MODEL SYSTEM

and surrounding epidermis, including inhibition of cell division *in vivo*. This provided evidence overwhelmingly in support of cell migration over proliferation in driving the process. Finally, to better understand the motile properties of front cells, I analyzed the actomyosin cytoskeleton in and the morphology of front cells at high magnification in whole-mounts, optimized conditions for the culture and live imaging of eyelid explants *ex vivo*, and conducted a rudimentary RT-PCR analysis of FACS-purified front cells. These analyses revealed that front cells become highly elongated perpendicular to the axis of eyelid closure, extend mediolateral protrusions, and intercalate along this axis. Supporting a transformation to a motile fate, RT-PCR analysis along with immunostaining for traditional markers of an EMT reveal an upregulation of markers of motile epithelia, including α_5 integrin and fibronectin, and a downregulation of E-cadherin and epidermal keratins, but not the telltale signs of an EMT. By simultaneously imaging epidermal and dermal cells, I rule out potential contributions from the dermis, suggesting that cell intercalation plays an important role in eyelid closure.

Having implicated a role for cell intercalation in eyelid closure, I go on to detail the cellular mechanism of eyelid closure by combining live imaging and quantitative image analysis with laser ablation experiments. Using *K14-H2B-GFP*-expressing embryos to visualize and track nuclei during eyelid closure, I map the relative movements of cells in the eyelid front and surrounding tissue. This reveals that cells with opposing movements are distributed throughout the front while cells in the surrounding epidermis appear to be displaced passively. In collaboration with Vijay Krishnamurthy and Stephan Grill, two biophysicists at the Max Planck Institute, I quantify how these relative movements contribute to tissue deformation in the eyelid by computing the strain-rate tensor, which describes the magnitude and orientation of deformation as a function of position. This uncovers a region of active shear in the front but little deformation in the surrounding epidermis. Further, it reveals that the rates of tissue compression and extension are roughly equal throughout the front, suggesting a process similar to convergent extension, but localized to a small region of tissue. This pattern of tissue strains is fundamentally incompatible with the action of a contractile

actin cable, which would display a region of exclusively compression at the front, setting eyelid closure apart from other models of epithelial fusion.

Following this analysis, I tested the functional importance of the eyelid front by performing a series of laser ablation experiments. This indicated that the front is required for the forward movement of the eyelid, and that it is the source of a pulling force that deforms the eyelid epidermis over long timescales. Together with ablations to rule out alternative possibilities, this suggests a mechanism of closure in which forces from cell intercalation are leveraged to tow the surrounding epidermal sheets.

In the last part of this work, I explore the molecular mechanisms underlying eyelid closure by analyzing its dependence on integrin- and cadherin-based adhesion, and highlight potential roles for canonical and non-canonical Wnt signaling. Using lentiviral-mediated RNAi to knock down α_5 integrin and fibronectin in the skin, I document a reduction in the intercalation speed of front cells leading to defective eyelid closure. To determine whether integrin-fibronectin adhesion is required directly for cell intercalation or indirectly by fine-tuning levels of cadherins, I similarly depleted cadherins in the skin. Reducing cell-cell adhesion in the eyelid front by knockdown of E-cadherin has no effect on eyelid closure, and conversely, knockdown of fibronectin and α_5 integrin does not cause an upregulation of cadherins. This suggests a direct role for integrin-fibronectin adhesion in cell intercalation, perhaps as a means for cells to gain traction.

To rule out a potential role of fibronectin in stimulating the transformation of epidermal cells to a motile fate, I also ablated myosin IIA globally in the skin as well as specifically in the eyelid front. I achieved specific targeting of the eyelid front by designing and injecting a lentiviral *K17-Cre* construct into myosin IIA conditional knockout mice. Lack of defects in epidermal architecture and adherens junction formation but the loss of hair follicles in the skin suggests that myosin IIA has a morphogenetic rather than a structural role. The eyelid closure defects in both cases combined with the observation that front cells still adopt their characteristic, bipolar morphology indicates that $\alpha_5\beta_1$ integrin and myosin II-dependent

1.5. THE SKIN AS A MODEL SYSTEM

cell motility within the eyelid front is the driving force of the process.

Finally, I document the presence of localized Wnt/ β -catenin signaling in the eyelid front and a specific requirement of non-canonical Wnt/PCP signaling for eyelid closure. Whereas canonical Wnts likely mediate specification of the eyelid front, PCP appears to regulate cell intercalation either directly or through the organization of fibronectin.

Chapter 2

Developing embryonic eyelid closure as a model of collective cell movements in late mammalian development

By studying cell movements in model morphogenetic processes, we can gain insight into the diversity of cellular behaviors that shape tissue and organs in embryogenesis, and contribute to tissue homeostasis and disease in adulthood. Elegant studies in model organisms including *Drosophila*, *Xenopus*, and zebrafish have revealed both significant commonalities and important differences in the cellular and molecular mechanisms underlying convergent extension movements and processes of epithelial fusion. However, such studies have largely not been extended to mammals, in part because no simple, genetically tractable system has been developed. To bridge this gap, I have adopted embryonic eyelid closure as a model of epithelial fusion in mice and assembled a toolkit for its analysis.

Eyelid closure defects are the hallmark of mice with mutations in genes that regulate cell motility and cell growth, and have been documented in studies for nearly 20 years, beginning with mutations in the EGF pathway (Luetteke et al., 1993; Miettinen et al., 1995). In addition to growth factor signaling, pathways mediating actin cable assembly, such as the JNK pathway (Zenz et al., 2003; Zhang et al., 2003), and regulators of contractility, such as ROCK, have also been implicated (Shimizu et al., 2005; Thumkeo et al., 2005). However, it has been difficult to integrate these insights into a comprehensive model of eyelid closure because they variously affect proliferation, differentiation, and migration. Potential roles have been suggested for the periderm, cell proliferation, and constriction of an actomyosin

cable analogous to *Drosophila* dorsal closure and embryonic wound healing. In particular, early electron microscopic studies of eyelid closure and other examples of temporary epithelial fusion have revealed numerous filopodia extending between cells of the periderm, which pile up over the epidermis during fusion, suggesting they may have a general role in sealing epidermal appendages (Harris and McLeod, 1982; Maconnachie, 1979).

In this chapter, I detail the basic components of the process in terms of the cell types that contribute, their origins, and their behaviors. To do so, I perform an immunohistological analysis of the eyelid, revealing a clear functional separation of the eyelid front from the surrounding epidermis in terms of its integrin and keratin expression. Whereas the papebral epidermis, the epidermis covering the surface of the eyelid, shows signs of early differentiation at E15.5, the eyelid front remains basal in character and uniquely expresses fibronectin and α_5 integrin. Lineage tracing of the epidermis and periderm indicates that the front is clearly of epidermal rather than peridermal origin, and genetic ablation of the periderm has no effect on eyelid closure, indicating that striking morphological changes it exhibits are a consequence rather than a cause of eyelid closure. A quantitative analysis of cell proliferation in the eyelid front and surrounding epidermis combined with inhibition of cell division *in vivo* similarly rules out an essential contribution of proliferation to the process.

Focusing on the epidermal cells of the eyelid front, high magnification imaging of cell morphology and the actomyosin cytoskeleton in whole-mounts reveals that, rather than assemble a supracellular actin cable at the border, front cells display predominantly cortical actin and myosin, elongate perpendicular to the axis of closure, and pack together in a multicellular sheet. To analyze their behavior in detail, I optimized methods to culture and live image eyelid explants *ex vivo*. Using a combination of *K14-H2B-GFP*-expressing embryos and *Rosa26^{mT/mG}* embryos injected with low-titer *LV-Cre* to sparsely-label cells with membrane-targeted GFP, I visualized both the global movements of cells as well as the dynamics of individual cells. Consistent with their elongated morphology, front cells display mediolateral protrusive activity and intercalate with each other. By also imaging cell

movements in the dermis and quantifying their speed relative to the epidermis, I rule out a potential contribution of dermal cell proliferation or streaming into the region. These results establish the intercalary behavior front cells as an essential feature of eyelid closure.

2.1 Cell types contributing to eyelid closure

The formation of eyelid primordia begins around E11.5 and is followed by a period of growth up to E14.5. At this stage, the eyelid is a fold of the skin that partially extends over the eye, including both epidermis and dermis (illustrated in [Figure 2.1](#)). The epidermis on the upper side of the eyelid, the papebral epidermis, is continuous with the headskin and follows the same differentiation program as the rest of the skin. Underneath the eyelid, the epidermis differentiates to form the conjunctiva, a stratified, non-keratinized epithelium that lubricates the eye by producing mucus and tears. The conjunctiva is in turn continuous with the cornea, a third epithelium that forms the surface of the eye. Covering the entire surface of the embryo are cells of the periderm. The eyelid thus rests at the junction of multiple, distinct epithelial populations that could contribute to eyelid morphogenesis and closure.

At E15.5, a population of eyelid cells migrates over the cornea, leading to fusion of the eyelids by E16.5 (an overview is presented in [Figure 2.2](#)). A particularly interesting aspect of this process is that it involves movements of a multilayered epithelium consisting of an undifferentiated basal layer, differentiated suprabasal layers, and a superficial layer of periderm cells. To assess which cells of the eyelid become migratory and ultimately contribute to closure, I performed immunohistochemistry and whole-mount immunofluorescence using a battery of epidermal differentiation markers and integrins on eyelids harvested from mice prior to the initiation of eyelid closure at E14.5, during closure at E15.5, and after fusion of the eyelids at E16.5. To directly test the contributions of different epithelial cell types to the eyelid, I also performed lineage tracing experiments over the course of development.

2.1. CELL TYPES CONTRIBUTING TO EYELID CLOSURE

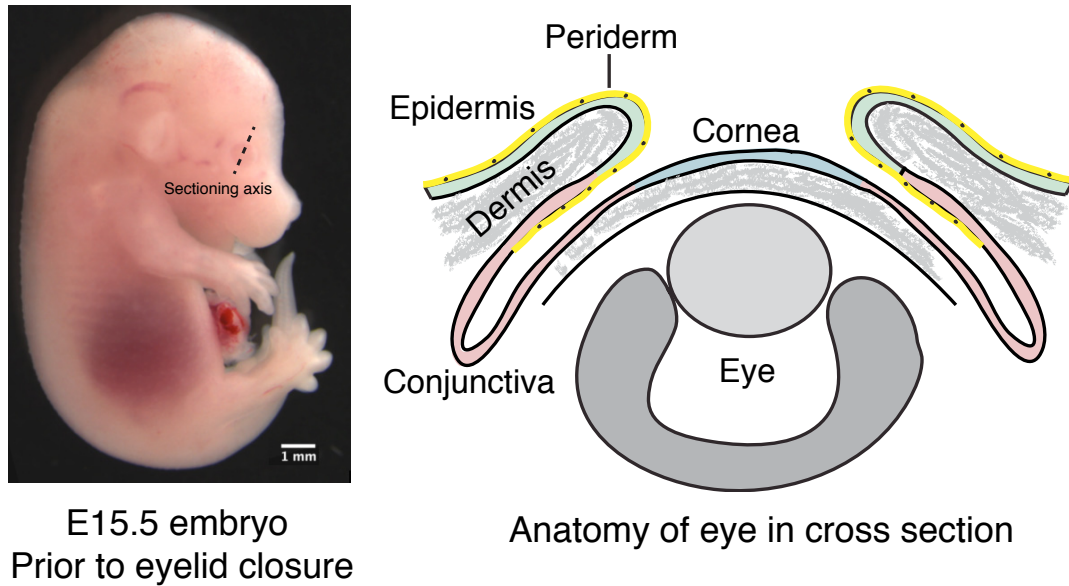


Figure 2.1: Juxtaposition of cell types in the eye. Schematic of the eye at E15.5 in sagittal section, revealing the epithelial cell types that could contribute to eyelid closure. The eyelid consists of a differentiating epidermis, underlying dermis, and superficial periderm layer. The upper eyelid (papebral) epidermis is continuous with the conjunctiva, a stratified, non-keratinized epithelium, which, in turn, is continuous with the cornea. The eyelids rest on the surface of the eye.

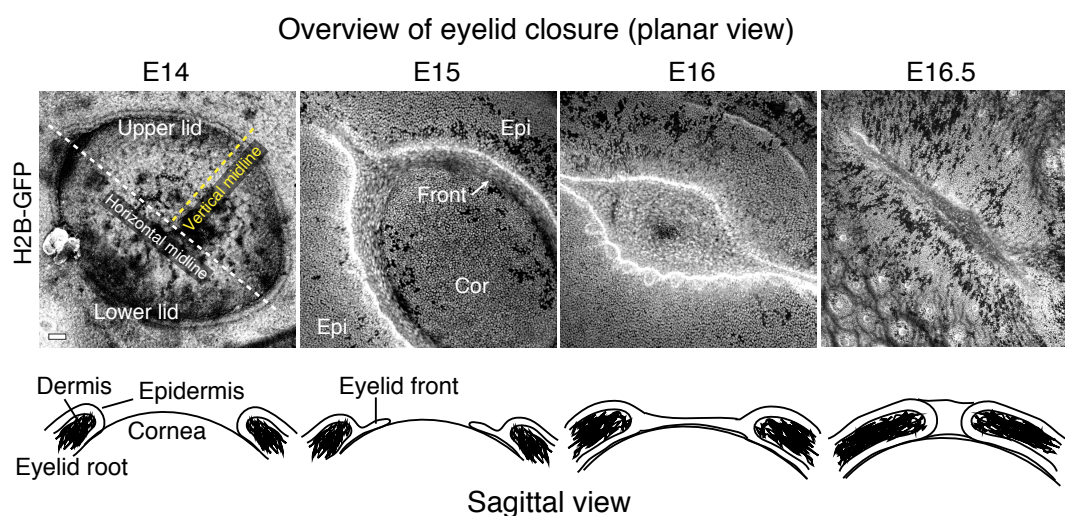


Figure 2.2: Overview of eyelid closure. The process is illustrated in planar (upper, fluorescence images) and sagittal view (lower, schematic). For reference, the horizontal and vertical midlines are indicated, as well as the corneal epithelium (Cor), eyelid front, and surrounding epidermis (Epi). Eyelid closure takes place between E15 and E16, and involves the extension and movement of eyelids over the surface of the eye. It is an example of a temporary epithelial fusion in the skin, along with digit fusion and fusion of the ears to the scalp. The eyelids remain fused until ~2 weeks after birth.

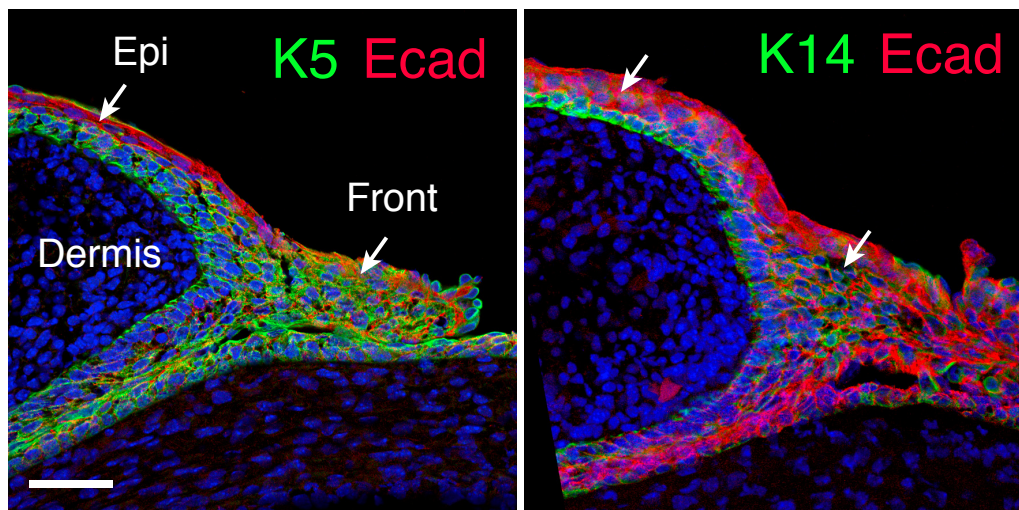
2.1. CELL TYPES CONTRIBUTING TO EYELID CLOSURE

2.1.1 Keratin and integrin expression in the eyelid

As basal cells of the skin commit to differentiation, they form three distinct layers: the spinous and granular layers, and the stratum corneum, each of which expresses different sets of keratins, adhesion molecules, and other proteins (Section 1.5; Fuchs, 2008). Keratin and integrin expression in the eyelids prior to and during closure reveals the presence of a distinct cell population contributing to closure. At E14.5, prior to extension of the front, the eyelid epidermis resembles normal, undifferentiated skin epidermis in its expression of only the basal keratins K5 and K14 (Figure 2.3). With the beginning of eyelid closure at E15.5, the papebral epidermis shows the initial signs of differentiation, including a spinous layer expressing K1 and K10, whereas cells of the extending eyelid front only express basal keratins, indicating that migrating cells retain the properties of undifferentiated epidermis. Consistent with a functional separation of the eyelid front from the surrounding epidermis, K17, a marker of morphogenetically active epithelia expressed in the hair follicle placode (McGowan and Coulombe, 1998), and K6, a marker of hyperproliferative keratinocytes typically associated with wounded epidermis and proliferative compartments of adults hair follicles (Wong, 2003), are specifically expressed at the front (Figure 2.4). Importantly, K15, a marker of the conjunctiva (Zhang et al., 2013), is not expressed, indicating that migratory cells are epidermal rather than conjunctival in nature.

This functional separation is further supported by integrin expression in the eyelid. Consistent with the expression of K5 and K14 and the maintenance of an undifferentiated state, α_6 integrin, which pairs with β_1 -integrin in the basal layer, is expressed throughout the eyelid front, though at lower levels than basal cells of the surrounding epidermis (Figure 2.5, Figure 2.14B). α_2 and α_3 integrins, which have roles in adhesion to collagen and laminin and are both highly expressed in basal layer cells, however, are expressed at low levels in the front. Instead, as early as E14.5, the small population of cells that will form the eyelid front are marked by an upregulation of α_5 integrin and its ligand, fibronectin (Figure 2.5). These differences in integrin expression become more pronounced during migration of the

Basal layer keratins



Suprabasal keratins

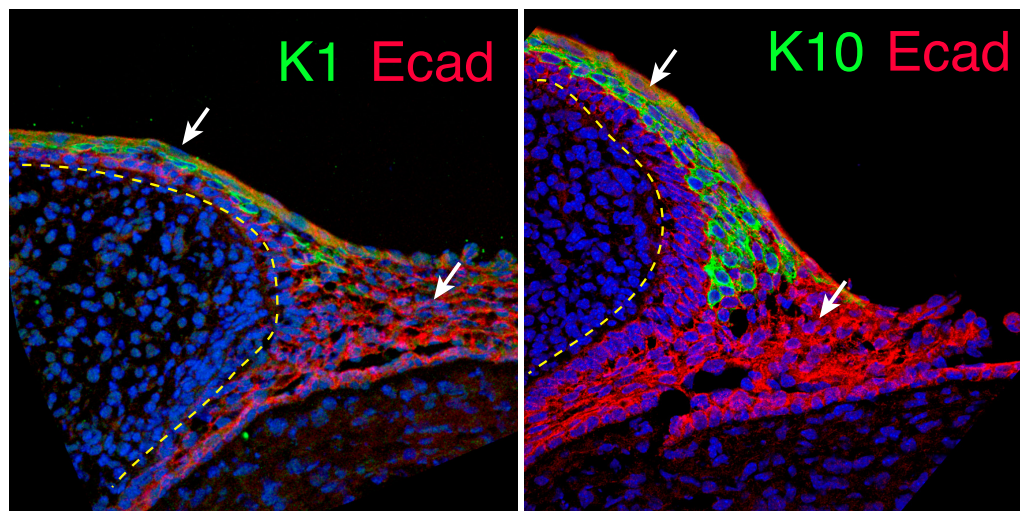


Figure 2.3: Keratin expression in the eyelid suggests a functional separation. Immunofluorescence of eyelid sagittal sections at E15.5 reveals that the epidermal cells extending over the eye retain expression of basal-layer keratins, including K5 and K14 (upper panels). By contrast, cells of the surrounding epidermis have already begun differentiating and express K1 and K10 (lower panels). In all images, keratin expression in the palpebral epidermis (Epi) should be compared to the front. E-cadherin (red) is used to label all epidermal cells. Scale bars, 50 μm .

2.1. CELL TYPES CONTRIBUTING TO EYELID CLOSURE

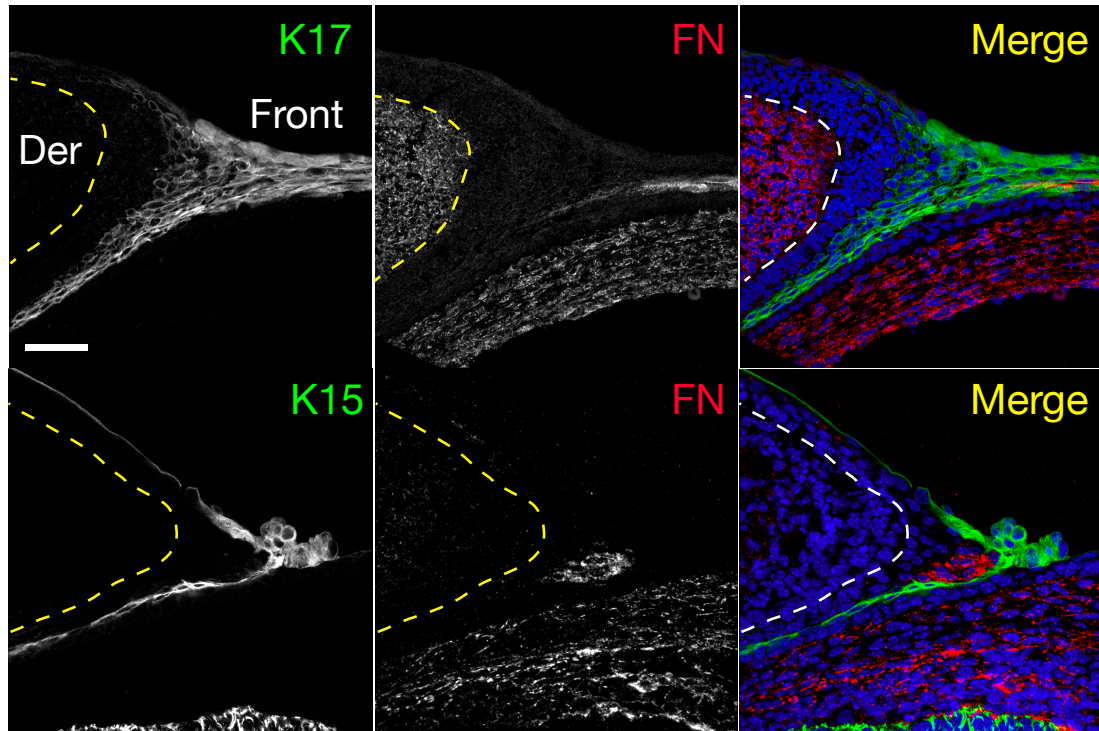


Figure 2.4: Unique keratins in the eyelid front. Consistent with a functional separation of the eyelid, cells in the front express K17, a marker of morphogenetically-active epithelia in development also expressed in developing hair follicles, teeth, and nails. Lack of K15 expression, a conjunctival marker, indicates it is a distinct population derived from the epidermis. Scale bars, 50 μm .

eyelids at E15.5 and persist through eyelid fusion at E16.5, with the highest α_5 integrin and fibronectin expression at the leading edge. The acquisition of motile properties by cells of the eyelid thus coincides with maintenance of an undifferentiated state and a shift in integrin expression profile. Although the importance of these changes are not well understood, the eyelid closure defect of TGF- α knockout mice, in which eyelid closure either fails to initiate or is delayed, has been suggested to be due to an attenuated upregulation of α_5 integrin and fibronectin in the eyelid front (Luetkeke et al., 1993). Similarly, misexpression of α_5 integrin in the eyelid results in failure of the eyelids to fuse, suggesting that coordinated expression of this integrin and fibronectin are required for proper migration (Carroll et al., 1998).

2.1.2 Genetics and lentiviral technology in the skin

While the genetic tools available in mice are not as sophisticated as in simpler organisms such as yeast and flies, studies in mice are perhaps the most relevant to human development and disease. With the widespread application of transgenic and gene targeting technologies, and the deposition of mouse strains into public repositories over the last thirty years, we now have an impressive array of conditional knockout mice, reporter lines, and mice expressing fluorescent fusion proteins at our fingertips. In the skin, use of the K5 and K14 promoters has enabled the skin-specific expression of numerous proteins, including GFP-actin to visualize actin dynamics (Vaezi et al., 2002), H2B-GFP to label nuclei and identify label-retaining stem cells in hair follicles (Tumbar et al., 2004), and both Cre and CreER, used in combination with floxed lines for lineage tracing and to generate skin-specific knockouts. However, standard genetic techniques in lower eukaryotes, such as the creation of genetic mosaics to analyze clones of mutant cells in otherwise wildtype tissue or generating double and triple knockouts, while technically possible, is cumbersome at best. In spite of the wide variety and availability of mouse lines, mouse genetics is also by comparison a slow process due to a 19 day gestation period and approximately eight weeks until sexual maturity.

An important advance in the use of skin as a model system was the recent development

2.1. CELL TYPES CONTRIBUTING TO EYELID CLOSURE

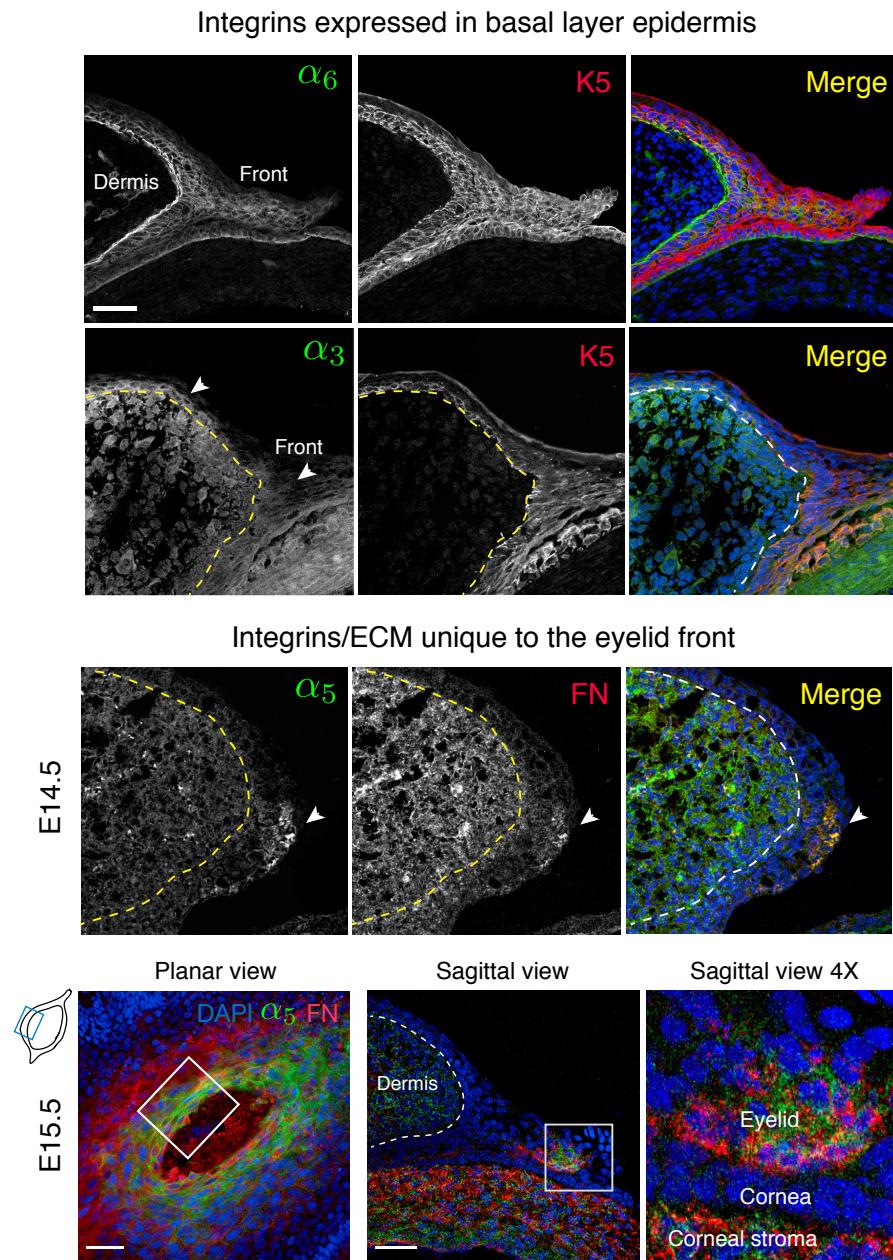


Figure 2.5: Integrin expression in the eyelid reveals the specific upregulation of α_5 integrin and fibronectin. Immunofluorescence staining for basement membrane receptors reveals differences in the integrin expression profile of eyelid front cells. Whereas α_6 integrin is expressed throughout the front, although at lower levels than the epidermal cells behind it, α_3 , which mediates adhesion to collagen and laminin and has a role in organizing the basement membrane, appears nearly absent by comparison (upper panels). Instead, fibronectin and its receptor α_5 integrin become specifically and locally upregulated as early as E14.5, becoming more pronounced as eyelid closure proceeds. Note that fibronectin remains compartmentalized within the eyelid epidermis. There are no signs of ECM or an organized basement membrane between the eyelid and underlying corneal epithelium (lower panels). Scale bars, 50 μm .

of ultrasound-guided lentiviral injection to achieve skin-specific transgene expression *in vivo* (Beronja et al., 2010). This is a relatively simple surgical procedure that involves microinjection of concentrated lentivirus into the amniotic sacs of E9.5 embryos (Figure 2.6). In combination with an shRNA library from The RNAi Consortium (TRC), which contains multiple hairpins for over 15,000 genes in the mouse genome (Root et al., 2006), this affords unparalleled ease in quickly silencing genes for which no genetic mutant exists, knocking down multiple genes simultaneously, and performing rescue experiments *in vivo*. In addition to facilitating the study of embryonic development in mice by greatly reducing the time and effort required to genetically manipulate animals, it has enabled genome-wide RNAi screening for regulators of normal and oncogenic growth in the embryonic epidermis (Beronja et al., 2013). Only a few years ago, this would have been unthinkable. The further use and development of such genetic tools, very likely by improving on RNAi with CRISPR/Cas9 technology, along with methods to culture and image whole embryos and skin explants, will continue to advance the complexity of studies in the mouse into the realm of simpler organisms.

2.1.3 Lineage tracing of the epidermis and periderm

Temporary epithelial fusions that occur on the surface of the embryo are thought to be mediated by periderm, a superficial layer of tightly-connected, squamous cells that develops between E9.5 and E12.5 to protect the embryo until the skin has stratified and differentiated (Section 1.5). Previous studies of eyelid closure using electron microscopy have shown that peridermal cells appear to stream out and pile up over the eye, where they are loosely packed and extend numerous cytoplasmic protrusions (Findlater et al., 1993; Maconnachie, 1979). To systematically explore the role of the periderm in eyelid closure, I used antibodies against the simple epithelial keratins K8 and K18, expressed by the periderm but not the underlying epidermis (Lu et al., 2005), to examine its localization throughout eyelid closure. Although the clumping of peridermal cells at the eyelid front is striking, they remained on the surface

2.1. CELL TYPES CONTRIBUTING TO EYELID CLOSURE

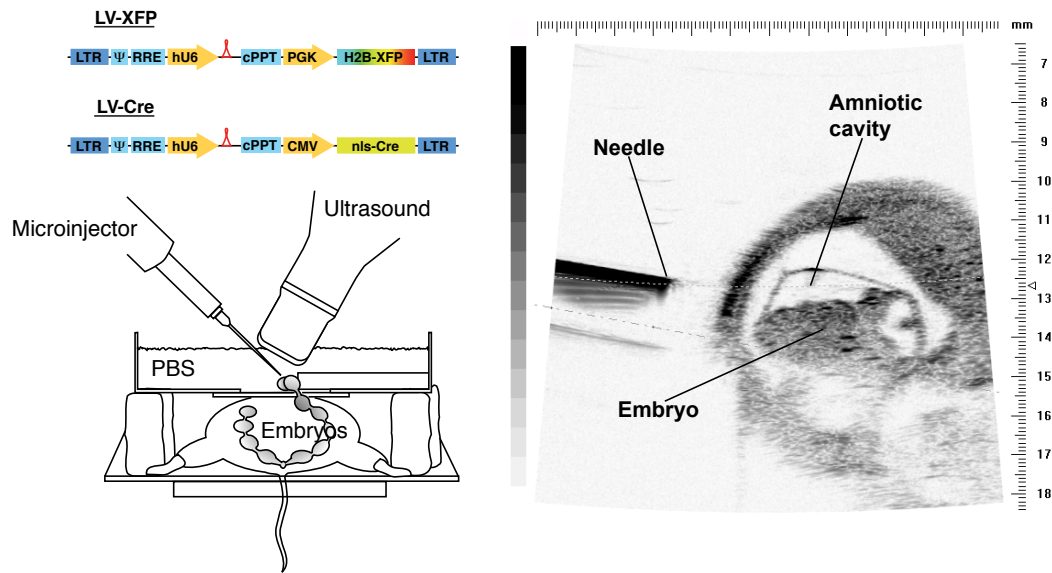


Figure 2.6: Ultrasound-guided *in utero* lentiviral injection system. This technique allows rapid, skin-specific transgene expression in mice, and involves microinjecting concentrated lentivirus into the amniotic sacs of E9.5 embryos. A pregnant mouse is anaesthetized and maintained on a heated platform, while embryos are removed into a PBS-filled dish. Using an ultrasound probe to visualize embryos, a glass microinjection needle is targeted to the amniotic cavity. Because of the simplicity of the procedure, it has been used successfully in studies of gene function in early skin development as well as genome-wide RNAi screening for regulators of normal and oncogenic growth. Images courtesy of Slobodan Beronja and Geulah Livshits.

of an extending sheet of epidermal cells throughout eyelid closure (Figure 2.7A).

Despite the absence of simple epithelial keratins, it is possible that the unique, migratory cells of the eyelid front are derived from the periderm in development. To test this hypothesis, I performed lineage tracing experiments using the lentiviral injection system developed by my lab. Exploiting the fact that lentivirus transduces the first cell layer it contacts *in vivo* (Beronja et al., 2010), I selectively labeled the periderm and its progeny by delivering *nls-Cre* lentivirus into E11.5 *Rosa26^{YFP}* Cre-reporter embryos. At E16.5, YFP was present in superficial K8/K18-positive periderm cells, but not the eyelid epidermis, demonstrating that eyelid cells are not derived from the periderm. To show that eyelid epidermal cells are instead derived from epidermis, I performed a lineage trace using the *K14-Cre* line, in which Cre expression is initiated around E13.5, after specification of the periderm. At E16.5, YFP was present in eyelid epidermis, but not superficial periderm cells (Figure 2.7B).

2.1.4 Ablation of the periderm.

Although the periderm neither gives rise to nor intermixes with epidermal cells during eyelid closure, the striking morphological changes it exhibits suggest that it may cooperate with or guide the underlying cells. To test the functional importance of the periderm in eyelid closure, I utilized a Cre-inducible diphtheria toxin system (Breitman et al., 1990) to specifically ablate the periderm in development. Transduction of E11.5 *Rosa26^{DTA}* embryos with high-titer *LV-nls-Cre* resulted in complete ablation of the periderm by E15.5, but did not prevent eyelid closure (Figure 2.7C). This indicates that the elaborate and dynamic changes in the periderm that accompany the process are not essential to the mechanism.

2.2 The relative contributions of cell motility and proliferation

Tissue morphogenesis often requires cell proliferation and migration, as exemplified by vertebrate gastrulation, where axis elongation requires not only cell intercalation, but also oriented cell divisions regulated by the PCP pathway (Gong et al., 2004; Wei and Mikawa,

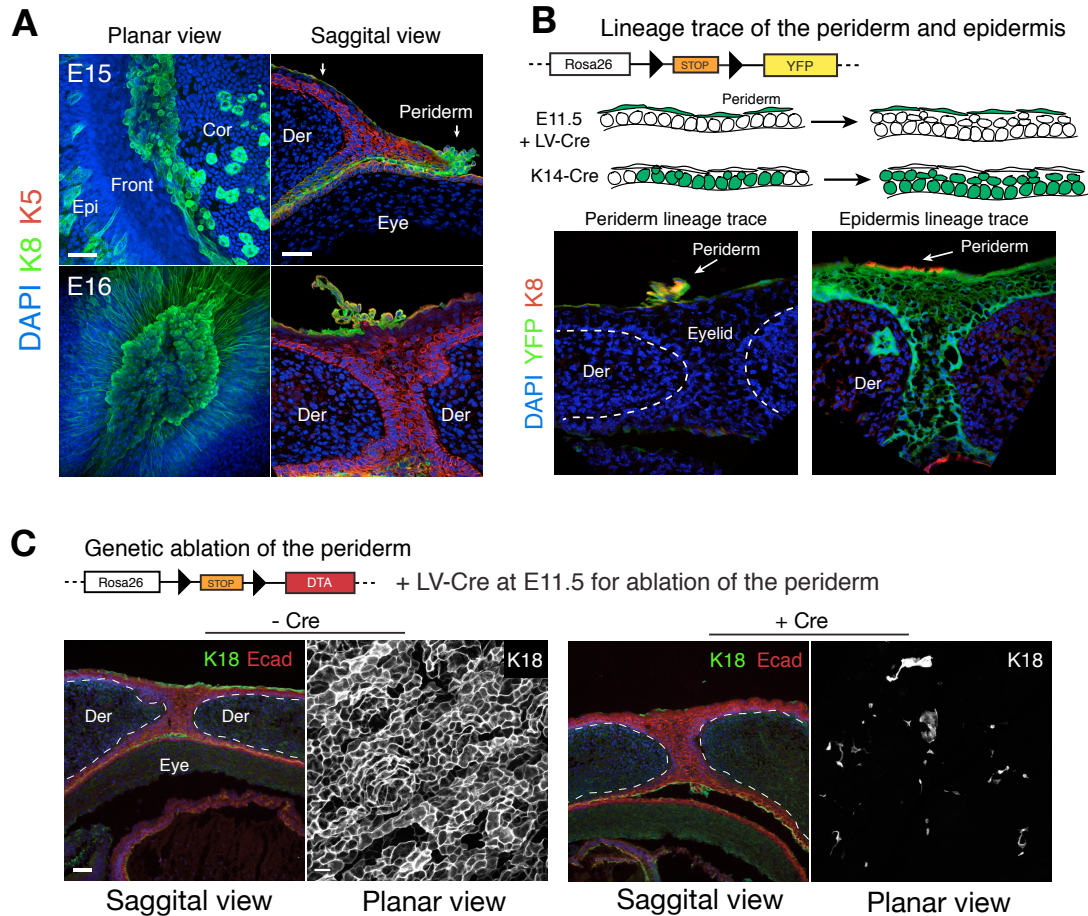


Figure 2.7: The periderm is not required for eyelid closure. (A) The extending eyelid consists of both undifferentiated K5/K14+ epidermal cells (eyelid front) and K8/K18+ superficial peridermal cells (arrows). (B) Lineage tracing by injection of *LV-Cre* into the amniotic sacs of *Rosa*^{YFP} embryos or expression of *K14-Cre*. Selective transduction of the periderm at E11.5 shows that only periderm is marked, and that it does not contribute the eyelid tissue (left). Labeling epidermal progenitors with *K14-Cre*, expressed after formation of the periderm at E13.5, labels the eyelid epidermis, demonstrating that it is derived from the epidermis rather than periderm (right). (C) Selective ablation of periderm does not affect eyelid closure. Periderm was ablated by injecting *LV-Cre* into the amniotic sacs of E11.5, *Rosa*^{DTA} embryos. Immunostaining of periderm with K18 shows that despite >90% ablation of superficial periderm cells, eyelids still close. Sagittal sections are of the eyelid, planar views are of backskin, illustrating ablation of the periderm over the entire surface of the embryo. Scale bars, 50 μ m.

2000). To understand the dynamics of eyelid closure and to gain a quantitative understanding of the interplay between cell migration and proliferation, I optimized conditions for imaging eyelid closure *ex vivo*.

2.2.1 Culture conditions for live imaging explanted eyelids

While roller bottle culture can support the development of E7.5 mouse embryos for up to three days (Rivera-Pérez et al., 2010), and it is possible to maintain whole embryos up to E10.5 in static culture for 18–24 h using specially-prepared rat serum (Jones et al., 2002; Piliszek et al., 2011), culture of later-stage embryos has proven notoriously difficult. To circumvent these difficulties, organ culture techniques that rely on keeping tissue at an air-liquid interface have been successfully utilized for the lung, kidney, heart, intestine, forebrain, mandible, and skin (Kashiwagi and Huh, 2005). However, as this involves floating the organ on a filter membrane, combining these techniques with live imaging has been challenging because of drift and detrimental effects on tissue health from the evaporation of media. Only very recently have successful attempts been reported to live image embryonic skin, one using Trowell-type culture dishes, a gas bubbler to prevent evaporation, and imaging on an upright confocal microscope (Ahtiainen et al., 2014), the other sandwiching skin explants between a gas-permeable membrane and a filter membrane in a closed, media-filled dish, and imaging on an inverted microscope (Li et al., 2011). Both techniques are limited to the use of air objectives.

To explore methods for live imaging eyelid closure at various magnifications and resolutions, I assessed the viability of explanted eyelids after prolonged culture both submerged and at an air-liquid interface. Whereas culture at an air-liquid interface supports long-term, low-magnification imaging, even the short-term maintenance of tissue within culture media would enable the use of higher-power and resolution dipping lenses or, alternatively, culture in glass-bottom dishes and the use of oil immersion objectives. As a measure of tissue health, I quantified the number of apoptotic cells as indicated by active caspase-3 staining and an-

2.2. CELL MOTILITY AND PROLIFERATION

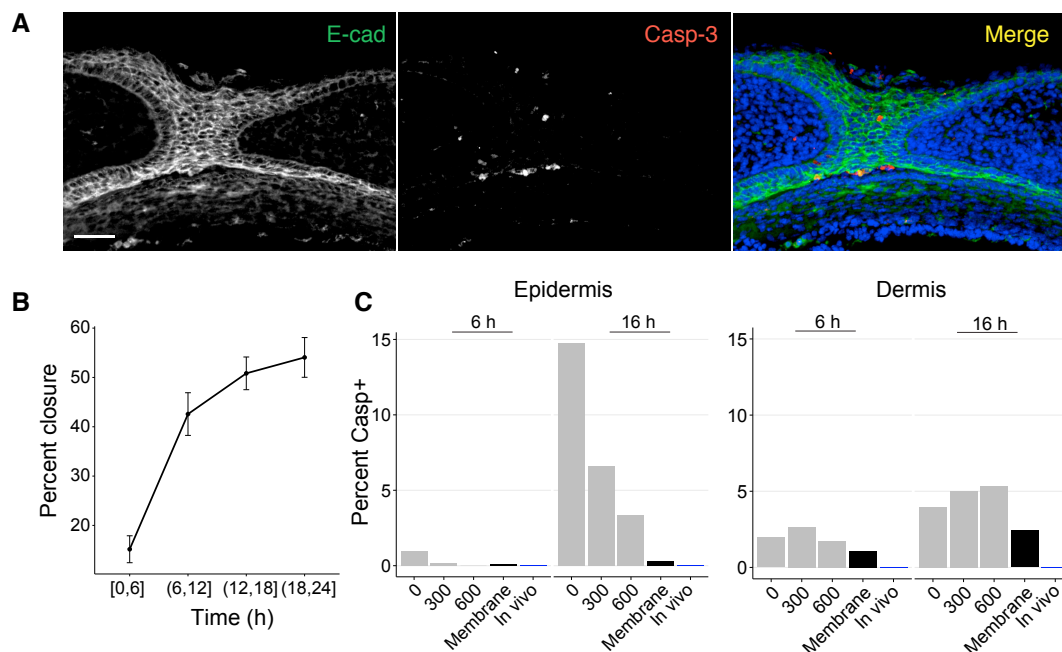


Figure 2.8: Culture conditions supporting eyelid closure *ex vivo* (A) Analysis of tissue morphology and cell viability after 12 h culture at an air-liquid interface. Eyelids are able to fuse *ex vivo* with a minimal increase in apoptosis or changes in cell morphology, indicated by E-cadherin and active caspase-3 staining, respectively. (B) Kinetics of eyelid closure *ex vivo*, illustrating that the process can be followed reliably for periods up to 12 h. Progression of eyelid closure was quantified by measuring the uncovered area of the eye. (C) Measurements of apoptosis in the epidermis and dermis under different culture conditions. In addition to a requirement for a high calcium concentration, cell viability in both the epidermis and dermis depends on culture at an air-liquid interface (membrane). More apoptosis was observed in the dermis than the epidermis. Scale bars, 50 μm .

alyzed tissue morphology by immunofluorescence. At an air-liquid interface, eyelid closure proceeded reliably for up to 12 h, with minimal apoptosis and no obvious morphological defects (Figure 2.8A-B). On the other hand, when explants were fully submersed in media, eyelid closure did not proceed for more than a few hours, and the skin displayed substantially more apoptosis than observed *in vivo*. In both cases, more apoptosis was observed in the dermis than in the epidermis (Figure 2.8C).

Based on these observations, I imaged eyelid closure at an air-liquid interface. To minimize the potential for tissue movement and microscope drift and the detrimental effects of

media evaporation, I sealed eyelid explants against a gas-permeable membrane and imaged them on an inverted scanning or spinning disk confocal (Figure 2.9). Spinning disk has the advantage for long-term, 3D imaging for its fast acquisition rate, which minimizes photo-bleaching and phototoxicity, but with thick samples suffers from high background due to pinhole crosstalk. While not an issue for imaging bright structures such as nuclei, imaging the dynamics of membranes, actin, or microtubules after E14.5 requires a scanning confocal or multiphoton microscope. When imaged this way, the overall rate of closure *ex vivo* ($\sim 10 \mu\text{m}/\text{h}$) is similar that observed *in vivo* ($\sim 300 \mu\text{m}/24 \text{ h}$). By using explants from *K14-H2B-GFP*-expressing embryos, this afforded sufficient resolution to observe the overall movement of eyelids during closure, to track individual cell movements, and even to monitor the progression of mitoses (Figure 2.9). Using explants from *Rosa26^{mT/mG}* or *Rosa26^{YFP}* embryos transduced *in utero* with low-titer *LV-Cre*, it also permitted observation of the dynamics of individual cells. As a proof-of-principle, I also successfully imaged eyelid closure by submersing explants in a small volume of media and using dipping lenses on an upright confocal. While it was considerably more difficult to stabilize and only supported the process for periods of 3–6 h, it suggests that this method is potentially suitable to observe the dynamics of the cells on short timescales.

2.2.2 Cell proliferation in eyelid closure

To explore the of cell proliferation in eyelid closure, I combined a quantitative analysis of cell proliferation with administration of cell cycle inhibitors *in vivo*. Monitoring the incorporation of the nucleotide analogue 5-Ethynyl-2'-deoxyuridine (EdU) over a 12 hour period between E14.5 and E15.5 as well as antibody staining for Ki67, a general marker of cycling cells, revealed which cells of the eyelid proliferate during closure. Consistent with previous observations (Shimizu et al., 2005), while the cornea and embryonic skin surrounding the eye were highly proliferative, epithelial cells at the eyelid front showed little or no proliferation (Figure 2.10A).

2.2. CELL MOTILITY AND PROLIFERATION

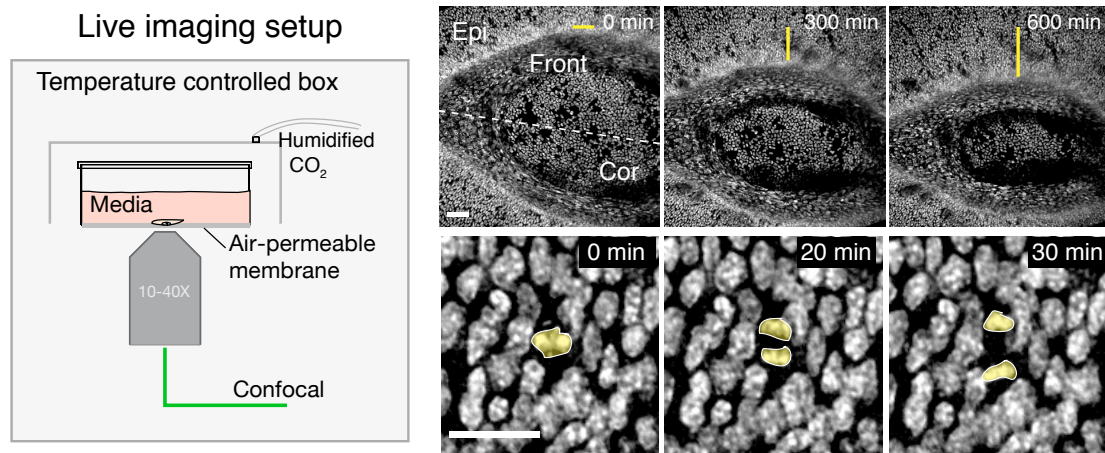


Figure 2.9: Setup for live imaging eyelid closure. Eyelid explants are imaged at an air-liquid interface by sealing them against a teflon-bottomed dish using a small volume of matrigel. Eyelids are imaged for periods up to 16 h on an inverted spinning disk or scanning confocal microscope house in a temperature-controlled box. To prevent evaporation and maintain a physiological pH, humidified 5% CO₂ is supplied. This enables live imaging with kinetics comparable to those *in vivo*. Using *K14-H2B-GFP* or other fluorphore-expressing mice, the progression of eyelid closure, behaviors of individual cells, and even the progression of mitoses can be monitored. Scale bars, 50 μ m.

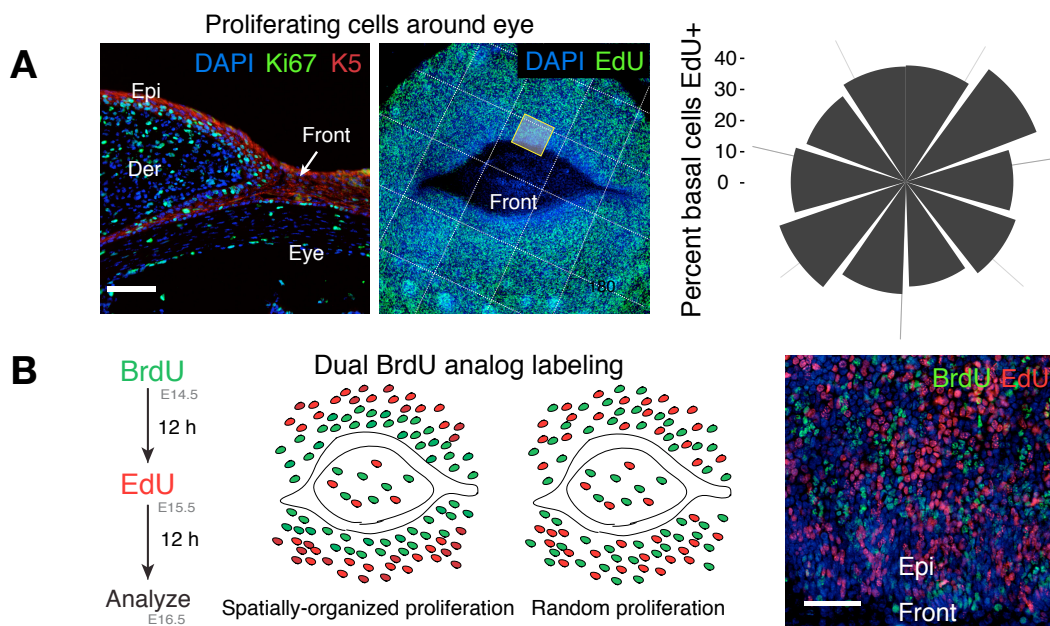


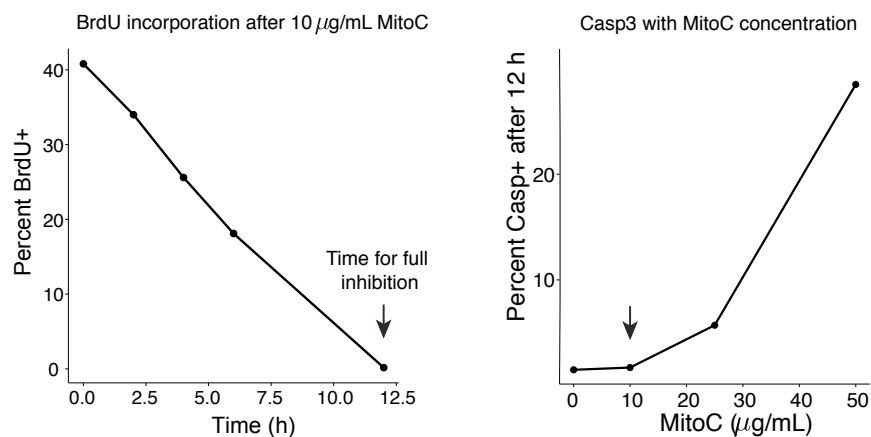
Figure 2.10: Cell proliferation in eyelid closure. (A) Front cells do not proliferate during eyelid closure. Left: Immunolabeling for Ki67, a general marker of cycling cells. Note that while the cornea and surrounding epidermis are highly proliferative, K5-positive eyelid front cells are not. Right: Tiled, 3D imaging of an eyelid explant pulsed for 2 h with EdU reveals no asymmetry of cell proliferation around the eye. The number of EdU-positive cells was calculated in 36-degree regions with ~600 segmented cells per region. (B) Dual BrdU-analog incorporation scheme. If a subpopulation of proliferative cells were driving asymmetric tissue growth, incorporation of the two analogs in distinct regions would be expected. Instead, they are incorporated randomly throughout the tissue.

2.2. CELL MOTILITY AND PROLIFERATION

Since eyelid front cells did not appear to proliferate, I next addressed whether asymmetric growth of the surrounding tissue might push eyelids over cornea. To test this possibility, I pulsed embryos for 2 h with EdU prior to dissection of eyelids and performed tiled 3D imaging. Automated counting of EdU-positive cells in 36 degree regions around the eye revealed uniform proliferation (Figure 2.10A). To test whether spatially-organized cell proliferation might contribute to asymmetric tissue growth over time, I utilized a dual BrdU analog incorporation scheme, injecting EdU at the beginning of eyelid closure, BrdU 12 h later, and labeling the two with different fluorophores (Figure 2.10B). If asymmetric tissue growth were occurring, the analogs should be incorporated in distinct bands around the eye. Instead, an essentially random incorporation was observed, consistent with uniform tissue growth.

Finally, to directly test whether proliferation is required for the process, I inhibited cell division *in vivo* by administering mitomycin-C (mito-C), an irreversible inhibitor of DNA synthesis, to living embryos. In culture, 10 $\mu\text{g}/\text{mL}$ mito-C completely inhibited keratinocyte mitoses by 12 h with a minimal increase in apoptosis (Figure 2.11A). Prior to 12 h, a number of cell divisions can still be observed in the skin, and cells still incorporate BrdU. The effects of inhibiting cell proliferation on eyelid closure were therefore assessed in two ways. First, mito-C was administered at late E14.5 to completely inhibit proliferation by the onset of eyelid closure at E15.5, and the progression of closure as well as the number of cell divisions occurring in the skin were monitored by live imaging over a period of six hours. This revealed that, in spite of an $\sim 75\%$ reduction in cell division compared to untreated embryos, eyelid closure progressed normally (Figure 2.11B). Second, mito-C was administered at the very beginning of eyelid closure at E15.5, and the process was allowed to proceed *in vivo* up to late E16.5. In spite of the complete inhibition of proliferation, evidenced by lack of EdU incorporation and a substantially-reduced embryo size at E16.5, eyelids fully closed (Figure 2.12). Taken together, these results suggest that eyelid closure is accomplished primarily by cell migration rather than proliferation.

A Determination of mitomycin C concentration *in vitro*



B Injection of mitomycin C *in vivo*

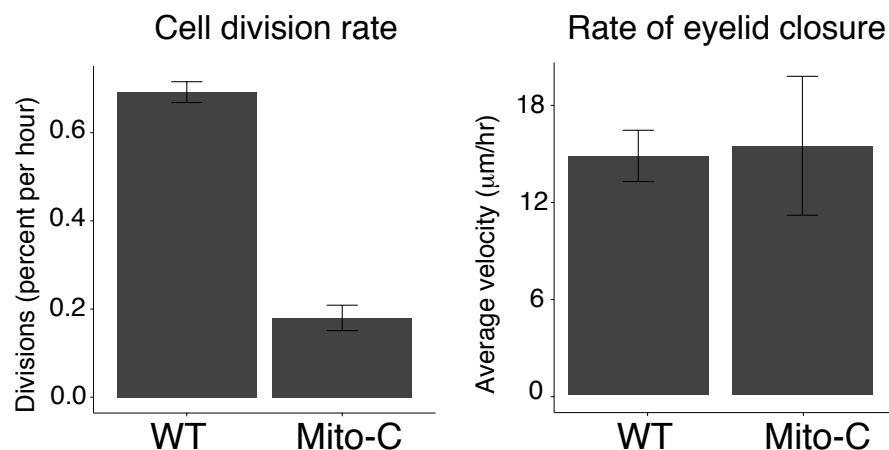


Figure 2.11: Eyelid closure progresses in the absence of cell division. (A) Calibration of mitomycin-C dosage to inhibit cell division. Left: Timecourse of BrdU incorporation during continuous culture in 10 $\mu\text{g/mL}$ mito-C, illustrating that 12 h is required for full inhibition of cell proliferation. Right: Quantification of apoptosis with increasing concentrations of mito-C, illustrating a stark increase at concentrations above 20–30 $\mu\text{g/mL}$. (B) Progression of closure was quantified by measuring the average displacement of the eyelid border over the eye. At the same time, cell proliferation was quantified by manually counting the number of dividing cells in regions of equal area (comprising ~ 4000 cells) over the course of 20 frames and expressed as the fraction of cells in the region per hour. H2B-GFP transgenic embryos were exposed *in utero* to mito-C for 12 h prior to live imaging and quantitative analysis. Reductions of cell divisions by $>75\%$ ($p = 0.0011$) did not affect eyelid closure rates ($p = 0.90$, $n = 3$ mito-C treated, 2 WT embryos).

2.2. CELL MOTILITY AND PROLIFERATION

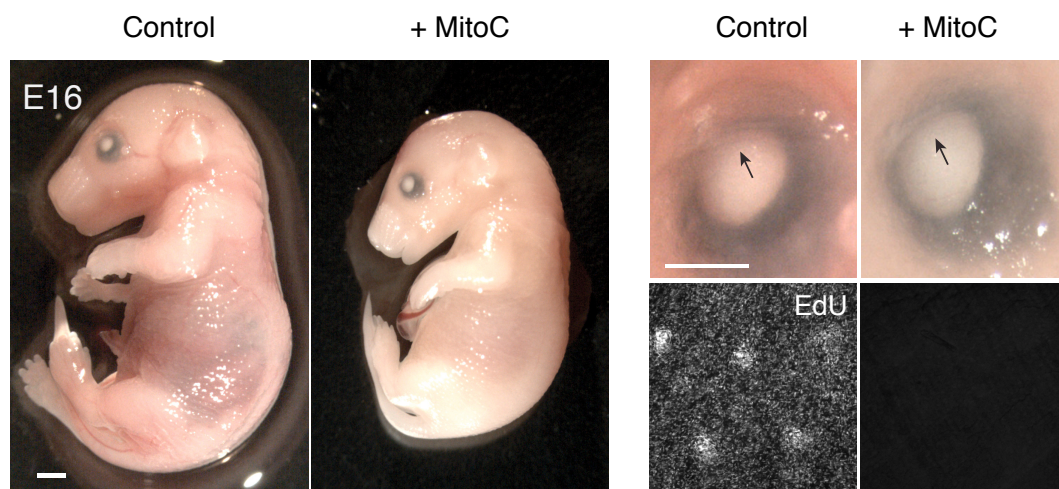


Figure 2.12: Eyelid closure completes in the absence of cell division *in vivo*. Mitomycin-C was injected into the amniotic sacs of early E15.5 embryos, at the very beginning of eyelid closure, and mice were harvested at late E16.5 after completion of the process. In spite of a vastly-reduced embryo size and full inhibition of cell division, evidenced by lack of EdU incorporation, eyelid closure completes normally. Scale bars, 1 mm.

2.2.3 The acquisition of motile properties by front cells

Observing little, if any, role for periderm or proliferation in eyelid closure, I focused on the non-proliferative cells at the eyelid front. Immunofluorescence of sagittal sections revealed prominent actin fibers at the eyelid tip, an observation which has led researchers to posit that eyelid closure is driven by assembly and constriction of an actomyosin cable in a purse-string fashion (Shimizu et al., 2005). Supracellular actin cables are polarized structures that span multiple junctions in cells bordering epithelial gaps and play an essential role in wound healing and *Drosophila* dorsal closure (Section 1.4.2). However, by whole-mount imaging, I found that instead of a polarized, supracellular actin cable in a single row of cells at the leading edge, the eyelid front consisted of highly elongated cells that organized their actomyosin cytoskeleton mediolaterally and packed together vertically in multiple layers (Figure 2.13A; compare with the actin cables in Figure 1.1B, page 28). This differed markedly from epidermal cells behind the front, which formed a honeycomb-like lattice with a characteristic cortical actomyosin network. To confirm that these highly-elongated cells were indeed of

epidermal origin, I performed a lineage trace of the epidermis by mating *K14-Cre* mice to the *Rosa26^{mT/mG}* Cre-reporter line, in which expression of membrane-bound tdTomato switches to membrane-bound GFP (mGFP) upon Cre activation (Muzumdar et al., 2007). mGFP expression by these highly elongated eyelid cells traced their derivation to the mGFP-positive epidermal cells and not mTomato-positive peridermal or dermal cells (Figure 2.13B).

To examine the morphology and behavior of cells in the extending eyelid in greater detail, I sparsely labeled the skin with mGFP by injecting low-titer *LV-Cre* into *Rosa26^{mT/mG}* embryos. High magnification confocal imaging of eyelid whole-mounts from these mice revealed the highly elongated, bipolar morphology of individual cells in the front, features more often associated with mesenchymal than epithelial cells (Figure 2.13B). Quantification of their aspect ratio at different positions within the front revealed a gradient of cell elongation from the eyelid base to the front, consistent with the pattern of α_5 -integrin and fibronectin expression in the eyelid (Section 2.1.1) and suggesting a corresponding gradient in motility. Live imaging of explants labeled in similar fashion at E14.5 and E15.5 revealed that, both prior to and during eyelid closure, occasional cells from the epidermis enter the front, upon which they rapidly elongate. A representative example at E15.5 is documented in Figure 2.13C. This suggests that these dramatic shape changes occur in response to cues from the local microenvironment and that the collective reorganization of cells in the eyelid front is an active process.

The highly specific upregulation of α_5 integrin in eyelid front cells immediately suggested it as a means to isolate and transcriptionally profile them to understand their unique morphological and motile properties. Isolation by fluorescence activated cell sorting (FACS) and RT-PCR profiling revealed that, consistent with a transition to a motile state, $\alpha_5\beta_1$ -high eyelid front cells displayed a transcriptional downregulation of E-cadherin as well as the epidermal keratins K14 and K5 in comparison to cells of the surrounding epidermis (Figure 2.14A-B). Of additional note was their elevated expression of genes encoding tenascin-C, K6, K17, fascin-1, and C/EBP α , hallmarks of morphogenetically-active tissues in development and

2.2. CELL MOTILITY AND PROLIFERATION

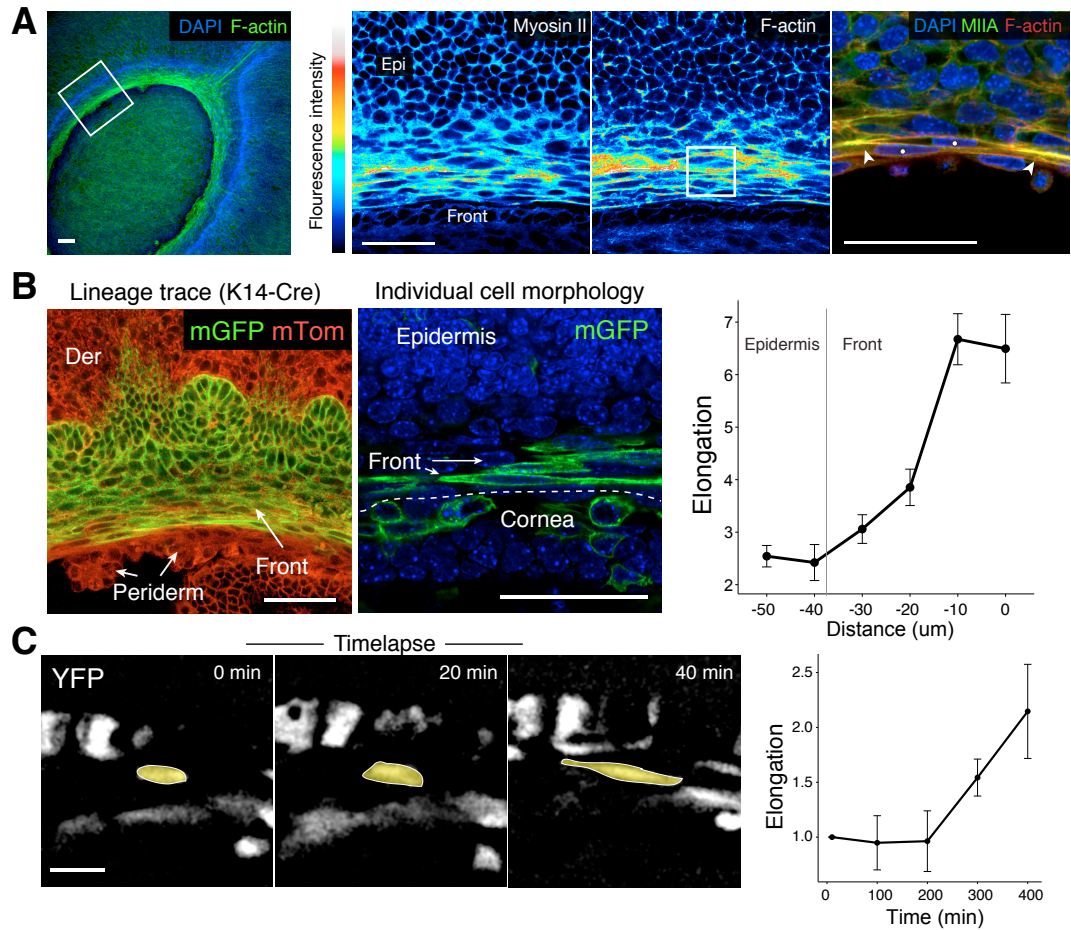


Figure 2.13: Cells in the eyelid front adopt an elongated, bipolar morphology, and pack in a multicellular sheet. (A) Analysis of eyelid morphology by whole-mount phalloidin staining and myosin IIA-GFP expression. Quantification of fluorescence intensity shows that actomyosin is enriched in eyelid front cells (middle panels). Note that intensity is greatest at elongated bipolar tips rather than along eye border (rightmost panel). In contrast, surrounding epidermal cells exhibit a characteristic, honeycomb architecture and show uniform, cortical localization of actin and myosin. (B) Left: Elongated, mesenchymal-like cells of the eyelid front are derived from epidermis, as determined by analyzing *K14-Cre* \times *Rosa26^{mT/mG}* embryos. Eyelid front cells are mGFP+, indicating that they are epidermal, while periderm and dermal cells are mTomato+. Right: Sparse-labeling of eyelid front cells permit morphological analysis of individual mGFP cells. Quantification of cell elongation by aspect ratio reveals a gradient from eyelid front to the base ($n = 116$ cells, 11–26 per bin). (C) Live imaging of individual cytoplasmic YFP+ labeled epidermal cells within the eyelid. Occasional capturing of actively elongating cells near the surrounding epidermis suggests that they undergo an active shape change (right: quantification of relative elongation, $n = 3$ cells). Scale bars, 50 μm .

disease (McGowan and Coulombe, 1998; Minn et al., 2005; Wang et al., 2006). The upregulation of K17 is particularly interesting for its parallels to early hair follicle formation, while C/EBP α is a master regulator of border cell migration in *Drosophila*. Interestingly, however, vimentin and other classical markers of an epithelial-mesenchymal transition (EMT) were not detected (Figure 2.14C). Taken together, these results indicated that developing eyelid cells possess unique properties that enable them to be motile for eyelid closure, but without undergoing a full EMT.

2.2.4 Global and individual cell behaviors in eyelid closure

Immunolabeling of ECM components in sagittal sections showed no signs of an organized basement membrane between the eyelid and cornea, suggesting that front cells migrate directly over the single-layered corneal epithelium (Figure 2.5). Along with their bipolar, elongated morphology and local secretion of fibronectin, this suggested that they adopt a mode of collective cell movement rather than migrate as individual cells over the eye. To explore this in detail, I performed live, 3D imaging of eyelid closure using explants from *K14-H2B-GFP*-expressing embryos to visualize and track global cell movements, and from *Rosa26^{TFP}* or *Rosa26^{mT/mG}* embryos transduced *in utero* with low-titer *LV-Cre* to observe the dynamics of individual cells. This revealed that, although the overall movement of eyelids was centripetal, individual front cells appeared to move perpendicularly to this axis (Figure 2.15A). Moreover, when the average velocity of these cells was measured and contrasted with the movement of surrounding epidermis, it was clear that eyelid front cells moved considerably faster, suggesting that their movement was at least in part independent of the other epidermal cells.

These key features were more readily visualized by averaging the azimuthal component of cell movements in regions around the eye. This revealed substantial movements perpendicular to the closure axis within the eyelid front, but not the surrounding epidermis (Figure 2.15A, right). Likewise, histograms of the overall orientation of cell movements

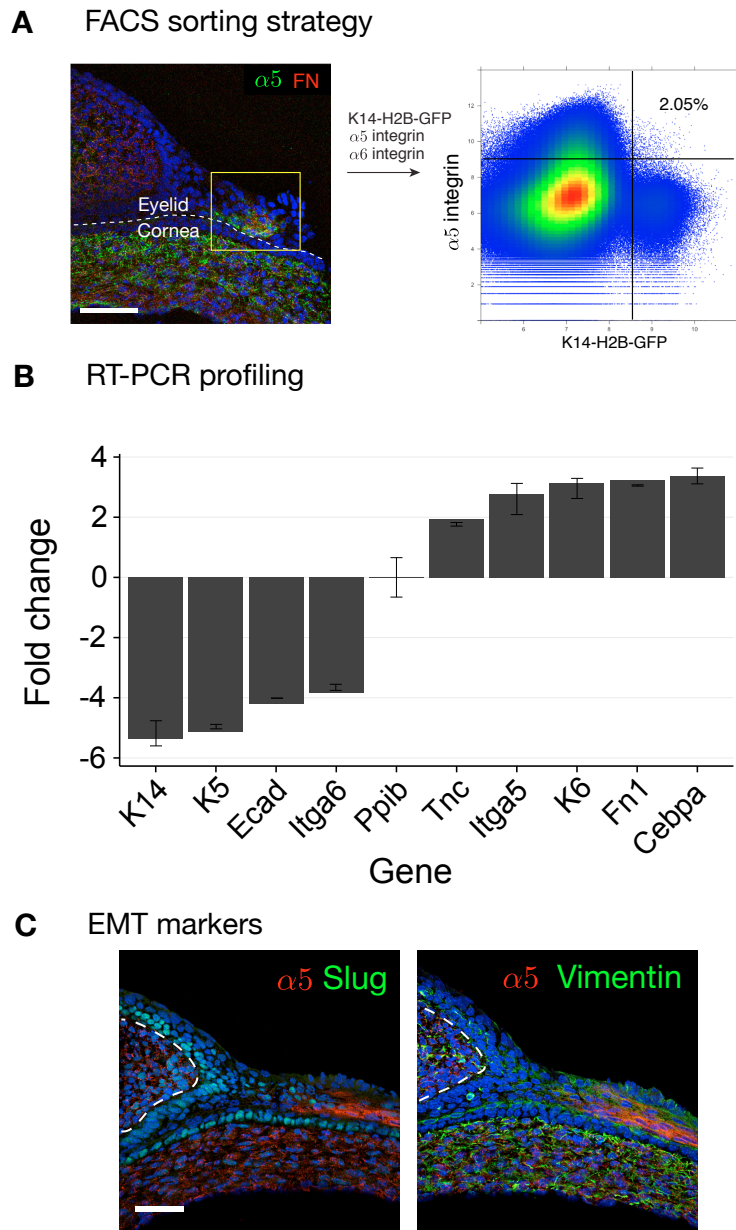
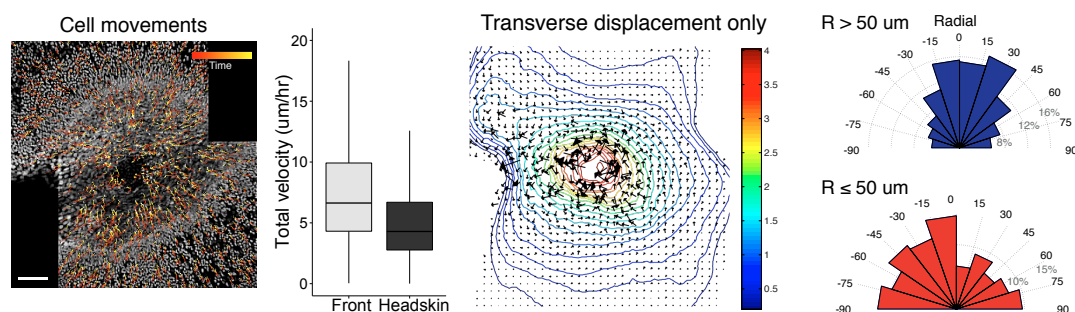


Figure 2.14: FACS isolation and RT-PCR profiling of eyelid front cells. (A) Sorting strategy of front cells based on *K14-H2B-GFP* and α_6 integrin expression following dissection of E15.5 eyelids. ~20,000 cells can be obtained from a single litter. This is sufficient for RT-PCR, but requires pooling of litters or the use of low-input amplification techniques for low-input for genome-wide transcriptional profiling. Front cells (*K14-H2B-GFP*^{hi}; α_5 integrin^{hi}) are compared to *K14-H2B-GFP*^{hi} α_5 integrin^{lo} cells of the surrounding epidermis. (B) RT-PCR profiling of eyelid front cells, revealing a transcriptional downregulation of E-cadherin and other basal epidermal markers, and upregulation of genes associated with cell motility, including C/EBP α , fibronectin, and tenascin-C. (C) Immunofluorescence analysis of markers of an epithelial-to-mesenchymal transition. In spite of a reduction in E-cadherin levels and expression of K17, two markers of a classical EMT, vimentin and slug, are not obviously upregulated. Scale bars, 50 μ m.

A Global cell movements in eyelid closure



B Individual cell movements

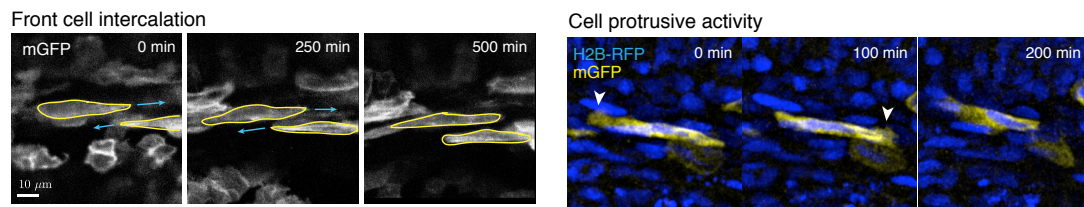


Figure 2.15: Global and individual cell behaviors in eyelid closure. (A) 3D tracking of cells in the eyelid and surrounding epidermis reveals cells with significant tangential movements despite an overall radial trajectory. The average speed of front cells is substantially greater than surrounding epidermal cells ($p < 0.0001$, $n = 7000\text{--}10000$ tracks), suggesting an active role in closure (left). A strong velocity component of the eyelid front, but not surrounding epidermis, is oriented perpendicularly to the closure axis (right). Average tangential velocity of cells in $256 \mu\text{m}^2$ regions are plotted as contours, with arrows indicating average direction of movement (length is proportional to speed). Histograms of the overall orientation of cell movements relative to the center of the eye indicate that, far from the center, movements are primarily radial (blue), while at the front, most cells move completely orthogonally (red). (B) Live-imaging of eyelids sparsely-labeled with mGFP reveals mediolateral protrusive activity and cell intercalation. Arrows indicate the direction of cell intercalation, arrowheads indicate mediolaterally-oriented cell protrusions. Scale bars, $50 \mu\text{m}$ (A) and $10 \mu\text{m}$ (B).

2.2. CELL MOTILITY AND PROLIFERATION

relative to the center of the eye revealed that cell movements far from the center were primarily radial, while most cells at the front moved orthogonally. To visualize the cellular behaviors behind these tangential movements, I imaged small clones of mGFP-labeled front cells, revealing mediolateral protrusive activity and intercalation of cells with their neighbors (Figure 2.15B). The behavior was highly reminiscent of convergent extension movements in mesodermal tissues, in which cells interact with along their mediolateral faces through membrane protrusions. Importantly, cells showed no signs of concerted or pulsatile contraction, indicating that cell movement rather than the contraction of cells was driving eyelid closure.

Given the juxtaposition of multiple cell types in the eyelid, I performed live imaging experiments to assess their relative contributions, labeling either the periderm or dermis separately from the epidermis. Using a membrane dye to selectively label superficial cells of the periderm in *K14-H2B-GFP*-expressing embryos and live imaging, I found that, in contrast to the substantial movements of epidermal cells in the eyelid, cells of the periderm moved very little relative to each other and gave the appearance of being carried along (not shown). To rule out potential contributions from underlying dermal tissue, I imaged embryos from a *K14-Cre* \times *Rosa26^{mT/mG}* mating, in which mGFP-expressing epidermal cells could be readily distinguished from mTomato-expressing dermal cells (Figure 2.16A). Particle Image Velocimetry (PIV) revealed that average flow velocities in the dermis (red) and surrounding eyelid epidermis (green) were essentially equivalent ($2.3 \mu\text{m/h}$ vs. $2.8 \mu\text{m/h}$, $p = 0.16$). Moreover, these velocities were substantially lower than those of intercalating layers of green front cells ($4.3 \mu\text{m/hr}$, $p < 0.001$), consistent with the previous analysis of cell speeds by tracking nuclei (Figure 2.16B-C). In total, these results identified the acquisition of intercalary behavior in the epidermal cells of the front as a key feature of eyelid closure, and raised the question of whether they were actively driving the process or a consequence of other forces in the region.

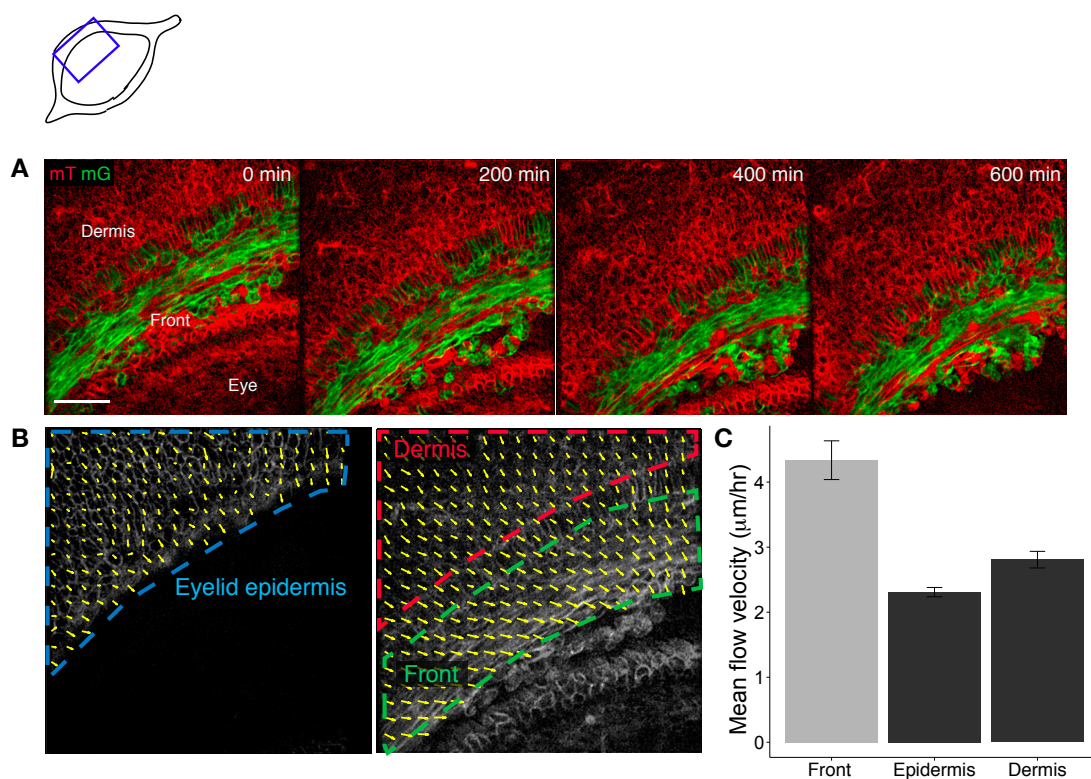


Figure 2.16: Dermal cell movements do not contribute to eyelid closure. (A) Frames from a timelapse of eyelid closure using *Rosa26^{mT/mG}* embryos, in which epidermal cells are labeled in green and dermal cells in red. No substantial movement of dermal cells is observed by visual inspection. (B-C) PIV analysis was used to separately estimate the velocity of the eyelid epidermis, underlying dermis, and intercalating cells. The velocity of the dermis is essentially equivalent to that of the overlying epidermis, both of which are substantially lower than the velocity of intercalating cells. This implies that the eyelid epidermis and dermis are moving as a coherent unit. Scale bars, 50 μm .

2.3 Discussion

The establishment of a model morphogenetic process and a toolkit for its analysis is a natural follow-up to the development of lentiviral technology for the rapid genetic manipulation of the skin. This technique enables the rapid, convenient expression of fluorescent proteins and the silencing of genes either throughout the skin or in small clones by adjusting viral titer. Combined with the wide-availability of conditional knockout mice, transgenic overexpressors, and mice expressing fluorescent reporters, it is now possible to probe the dynamics and regulation of skin morphogenesis in unprecedented detail. As a stereotyped process of epithelial fusion, eyelid closure offers a unique view into how aspects of cell motility and collective migration are utilized in the context of a differentiating tissue in late mammalian development. The potential value of such a model for uncovering basic principles of tissue morphogenesis is easy to appreciate—no study of wound healing does not draw inspiration from *Drosophila* dorsal closure, and no study of the collective invasion of cancer cells does not draw parallels to border cell migration.

Establishing a system requires a careful delineation of its parameters, namely what cells are involved, where they come from, and what they are doing. To date, most studies of eyelid closure have assumed a role of the periderm due to the striking morphological changes it exhibits in the region of the eye. This has led to a model in which the cells of the eyelid front originate from proliferation of periderm cells, which then migrate across the cornea and fuse. Despite the attractiveness of this hypothesis, the role of the periderm in eyelid closure has remained correlative. Similarly, analyses of actomyosin organization only in tissue section or at low magnification in whole-mounts have led to the comparison of eyelid closure to dorsal closure or embryonic wound healing, suggesting either constriction of a supracellular actin cable at the epidermal border or forward migration of a growing epithelial sheet across the cornea. Substantiating evidence comes from genetic studies, which show essential roles for Rho-associated kinases 1 and 2 (ROCKs 1 and 2) and their relative, LIMK2 (Rice et al., 2012; Shimizu et al., 2005; Thumkeo et al., 2005). Further strengthening the notion that

actin cable formation is essential for eyelid closure is that EGF cannot stimulate myosin light chain (MLC) phosphorylation when ROCK1 is absent (Shimizu et al., 2005), and LIMK2-deficient keratinocytes *in vitro* show reduced actin filaments (Rice et al., 2012).

Although the wide range of mouse mutants that exhibit eyelid closure defects clearly shows that the process integrates aspects of cell migration, without context, it has been difficult to decide exactly what it is a model for. Eyelid closure defects have been reported for mice harboring mutations in a diverse array of signaling proteins, including EGF and TGF α (Luetkeke et al., 1993; Miettinen et al., 1995), and both canonical and non-canonical Wnt signaling (Gage et al., 2008; Huang et al., 2009; Wu et al., 2012). By activating the MAPK-ERK signaling pathway, growth factors have been implicated in epidermal proliferation as well as migration (Huang et al., 2009; Mine, 2005; Tao et al., 2005). Thus, in addition to exactly which cell types are contributing, it has never been clear to what extent proliferation, differentiation, and migration play a role.

Using a simple toolkit consisting of whole-mount immunofluorescence, live imaging of skin explants, and genetic ablation, all facilitated by lentiviral injection, I set out to better understand the basic architecture of the eyelid and the cellular behaviors involved in its closure. This has helped to provide the necessary context to evaluate the role of the many genes implicated in the process and to firmly establish eyelid closure as a basic model of collective movement and cell intercalation in the mouse. Lineage tracing of the epidermis and periderm clearly revealed that the extending eyelid is derived from the epidermis, and both live imaging and genetic ablation indicate that the striking accumulation of rounded periderm cells over the eye is a consequence rather than an essential component of the process. This of course raises the question as to the role of the periderm in development, as its presumed protective functions appear to dispensable. The presence of microvilli and pinocytotic vesicles at the surface of periderm cells suggests a potential role in influencing the composition of the amniotic fluid or in nutrient resorption (M'Boneko and Merker, 1988). Another possibility is that it reinforces apicobasal polarity in the skin prior to the onset of

2.3. DISCUSSION

differentiation. This intriguing possibility was raised by a study of palate fusion in the mouse, an example of a permanent tissue fusion in which apposing epidermal layers of the palatal shelves undergo an EMT to allow mesenchymal continuity (Jin and Ding, 2006). It found that preventing desquamation of the periderm by inhibition of TGF- β caused epidermal cells to retain apicobasal polarity and fail to undergo an EMT (Wu et al., 2013; Yoshida et al., 2012). This suggests that the differentiation of the periderm, resulting in its desquamation between E15.5 and E18.5, may actually promote the acquisition of motile properties by the eyelid front.

While proliferation is necessary for the formation of eyelids in development, administering mitomycin-C *in vivo* prior to and at the onset of eyelid closure revealed that it is not necessary for their closure. This is perhaps not surprising, as many of the most dramatic large-scale tissue movements in development are known to occur in the absence of cell division, and in many cases it is actively suppressed. In *Drosophila*, extension of the anterior part of the *Drosophila* germband occurs in the absence of cell division, and in ventral furrow formation, inhibition of mitosis is specifically required for the cell shape changes that drive invagination (Grosshans and Wieschaus, 2000). Likewise, the transient inhibition of cell division is a necessary feature of convergent extension in the *Xenopus* dorsal mesoderm (Leise and Mueller, 2004; Shih and Keller, 1992) and appears to be important for the formation of hair follicles in the skin (Ahtiainen et al., 2014). However, while a common theme in morphogenesis, the absence of cell proliferation is not universal: oriented cell divisions are essential to elongate dorsal tissues in zebrafish gastrulation (Gong et al., 2004), in the posterior region of the *Drosophila* germband, where it contributes to the fast rate of tissue extension (da Silva and Vincent, 2007), and potentially in formation of the avian primitive streak (Wei and Mikawa, 2000).

The adaptation and optimization of explant culture and live imaging techniques have made it possible to study the dynamics of eyelid closure both at the level of populations and individual cells. As with all developmental processes, the simple observation of cellular be-

haviors by live imaging provides vital insight into how cell motility is integrated into a large-scale process that cannot be obtained any other way. Imaging of *K14-H2B-GFP*-expressing embryos to visualize and track global cell movements and genetic sparse-labeling with cytoplasmic and membrane markers to observe the dynamics of individual cells revealed that, quite surprisingly, cells within the eyelid front elongate perpendicular to the axis of closure and intercalate in the fashion of mesodermal cells. By using schemes to rule out contributions from the periderm and dermis, it was clear that this intercalation behavior was the defining feature of the process. Eyelid closure is thus more than a simple model of cell migration—it is a model of the specification of motile cells within a vertically stratifying epithelium and of cell intercalation driving substantial tissue movement.

A detailed analysis of keratin and integrin expression and cell morphology suggests a clear transformation of eyelid front cells and the acquisition of mesenchymal-like properties, including the local expression of fibronectin and α_5 integrin. This is supported by FACS isolation and RT-PCR profiling, revealing a transcriptional downregulation of E-cadherin and the epidermal keratins K5 and K14, and an upregulation of ECM components including fibronectin and tenascin-C ([Section 2.2.3](#)). While this, along with a previous study documenting FGF10 expression in the eyelid mesenchyme (Tao et al., 2005), immediately suggested an EMT, classical markers including vimentin and Slug are not obviously upregulated in the eyelid front, and an EMT is at odds with the necessity for the fused eyelids to form a continuous epidermal seam to protect the eye in postnatal development. The maintenance of K6 and K17 expression is similarly not typically associated with a full EMT, but rather with “morphogenetically active” epithelia during processes such as wound healing and hair follicle downgrowth. However, it is becoming increasingly clear that EMTs are more of a loose framework than a well-defined transition ([Section 1.3.1](#)), and in this regard, the transformation of the eyelid front certainly qualifies. A better understanding of this transition and the signaling pathways that mediate it will require building on my admittedly limited profiling data either by including a complete set of EMT markers for RT-PCR profiling

2.4. EXPERIMENTAL PROCEDURES

or performing whole-genome transcriptome analysis. Currently, 10–20,000 front cells can be isolated from a litter of embryos, yielding ~4 ng RNA, which would likely require low-input amplification techniques for RNASeq. While well within reason, improvements to my sorting strategy by using *K17-GFP* mice should increase the yield of cells.

The combination of live imaging and transcriptional profiling in eyelid closure holds great promise not only for understanding how the intercalation of a small population of cells drives a process of epithelial fusion and how cell intercalation is regulated in the unique context of late mammalian development, but the identification of novel genes that mediate the transformation to a motile fate. In the following chapters, I will lay the groundwork for exploring these opportunities further by detailing the cellular mechanism of eyelid closure and the basic requirements for productive cell intercalation in this system. As these techniques are by no means limited to the study of eyelid closure, the hope is that they will pave the way for future studies of tissue dynamics in the skin.

2.4 Experimental procedures

2.4.1 Lentiviral constructs

All lentiviral constructs utilized the pLKO.1 backbone from The RNAi Consortium. Construction of *LV-nls-iCre* and *LV-H2B-RFP* has been described previously (Beronja et al., 2010).

2.4.2 Mouse lines and lentiviral injections

The *K14-H2B-GFP* (Tumbar et al., 2004), *ROSA^{mT/mG}* (Gt(ROSA)26-Sor^{tm4}(ACTB-tdTomato,-EGFP)^{Luo}, JAX 007576), *ROSA^{YFP}* (Gt(ROSA)26-Sor^{tm1}(EYFP)^{Cos}, JAX 006148), and *ROSA^{DTA}* (Gt(ROSA)26-Sor^{tm1}(DTA)^{Lky}, JAX 009669) (Breitman et al., 1990) mouse lines have been described and are publicly available from Jackson Laboratories. Mice were maintained as homozygotes and mated to CD1 females from Charles River Laboratories for experiments. Ultrasound-

guided lentiviral injections were performed using previously-published protocols (Beronja et al., 2010).

To inhibit cell divisions *in vivo*, mitomycin-C was administered into the amniotic sacs of E14.5-E15.5 embryos using the same microinjection setup used for lentiviral injection. Injection volumes from a 2 mg/mL stock were determined based on estimated volumes of amniotic fluid in mouse development (McCafferty, 1955). To achieve a final concentration of 30–50 μM , 1.5–2 μL was injected into E14.5 embryos, while 2.5–3 μL was used for E15.5 embryos.

2.4.3 Antibodies

Antibodies were used at the following dilutions: K5 (rabbit, 1:1000, Fuchs Lab), K14 (rabbit, 1:500, Fuchs laboratory), K10 (rabbit, 1:1000, Covance), K8/TROMA-I (rat, 1:500, DSHB), K17 (rabbit, 1:1000, Fuchs laboratory), K18 (rabbit, 1:2000, Fuchs laboratory), E-cad (rat, 1:500, Fuchs laboratory), α_5 integrin (rat, 1:500, BD clone 5H10-27), β_1 integrin (rat, 1:500, BD clone 9EG7), α_6 integrin (rat, 1:1000, BD clone GoH3), α_3 integrin (mouse, 1:500, BD clone 42/CD49c), α_v integrin (rabbit, 1:500, Chemicon), cellular fibronectin (mouse IgM, 1:1000, Sigma FN-3E2), Laminin 5 (rabbit, 1:1000, Fuchs laboratory), myosin IIA (rabbit, 1:500, Covance), active caspase 3 (rabbit, 1:500, R&D), BrdU (mouse, 1:100, Life Technologies clone MoBU-1), and BrdU (rat, 1:500, Abcam). Secondary antibodies coupled to Alexa Fluor 488, 546, or 647 (Life) were diluted 1:1000 and incubated for 1 h at room temperature. Nuclei were stained with Hoechst 33342 (1:5000). Sections were mounted in ProLong Gold antifade, whole-mounts in SlowFade Gold with DAPI (Life).

2.4.4 Immunofluorescence and fixed tissue imaging

For immunofluorescence of sagittal tissue sections, whole embryos were embedded in OCT, sectioned (10 μm) on a Leica cryostat, and fixed for 15 min in 4% paraformaldehyde in PBS. Because of the location of the eyes on either side of the head, sagittal sections of eyelids

2.4. EXPERIMENTAL PROCEDURES

were obtained by decapitating embryos and mounting the head nose-first in OCT, such that sectioning occurred along the cranial-caudal axis. Sections were blocked and permeabilized for 1 h in blocking buffer (0.3% Triton X-100, 1% BSA, 1% fish gelatin, 5% donkey serum, and 5% goat serum in PBS). Primary antibodies were incubated overnight at 4°C.

For whole-mount immunofluorescence, embryos were fixed for 1 h in 4% PFA. Eyelids or skin explants were dissected and blocked/permeabilized for 5 h-overnight in blocking buffer. Primary antibodies were diluted 1:200, secondaries 1:500, and incubated for 24 h at 4°C, followed by at least 5 h of washing in 0.1% Triton in PBS, exchanged every ~30 minutes. F-actin was labeled using Alexa Fluor 546 or 647-conjugated phalloidin (Life), diluted 1:500 and incubated for 2 h at room temperature.

Low-magnification imaging was performed on a Zeiss Axioplan2 using a Plan-Apochromat $\times 20/0.8$ air objective. High magnification images were collected on a Zeiss LSM 780 or 510 Meta using Plan-Apochromat $\times 63/1.4$ oil or C-Apochromat $\times 40/1.2$ W objectives. Tiled Z-stacks were collected using Zeiss ZEN software or PerkinElmer Volocity.

2.4.5 Image analysis and quantification

Basic image analysis, including contrast enhancement, maximum projection, and all manual measurements, was performed in Fiji/ImageJ. 3D reconstructions were made in Bitplane Imaris. Quantification of proliferation and apoptosis rates in tissue sections and whole-mounts was performed using adaptive thresholding and watershed segmentation in semi-automated fashion using custom ImageJ macros. To assess tissue viability following prolonged culture *ex vivo*, eyelid explants were fixed in 4% PFA for 45 min and embedded in OCT. Sagittal sections of the eyelid were stained for E-cadherin to label the epidermis, active caspase-3 to label apoptotic cells, and Hoechst to label all nuclei. Multichannel images were acquired at $\times 20$ magnification, and E-cadherin staining was used as a mask to separate epidermal from dermal cells. Nuclei were filtered using a 2×2 median filter and thresholded using the Bernsen algorithm with a 7 pixel circular window. A watershed transform

was used to separate touching cells, and the number of caspase 3-positive cells was counted in over ten non-overlapping fields of eyelid skin from at least three embryos using ImageJ's particle counter function. The amount of apoptosis is expressed as a percent of total cells in either the epidermis or dermis, and typically included ~ 5000 cells.

Measurements of the density of proliferating cells in regions of embryonic skin around the eye were performed by pulsing *K14-H2B-GFP* embryos for 1 h with EdU to label proliferative cells. Ultra-high resolution images of the entire eye and surrounding epidermis were obtained by tiled, 3D imaging at $\times 63$ magnification on a Zeiss LSM780 or PerkinElmer Volocity spinning disk confocal. The z -position of the basal layer within each image stack was determined manually, and the x, y positions of both EdU-positive and negative nuclei in the basal layer were determined using the segmentation techniques described earlier. The percent of EdU-positive cells was calculated in 30-degree regions of skin around the eye and plotted as a radial histogram.

2.4.6 Culture and live imaging of eyelid explants

Eyelids were explanted from mid-to-late E15.5 embryos into warm media (Defined Keratinocyte Serum-free Media supplemented with $600 \mu\text{m}$ calcium and 5% w/v penicillin-streptomycin, Life Technologies). This media was determined to best support progression of eyelid closure and overall tissue health *ex vivo* by trial-and-error; however, skin explants can also be maintained in 3:1 DMEM/F12 supplemented with 5% FBS. Calcium concentration must be maintained above $300 \mu\text{m}$ to support epidermal integrity and viability of the dermis (in general, the dermis tended to be more sensitive to calcium concentration as far as apoptosis rates). Embryos were kept warm under a 250 W heat lamp (GE), and care was taken to explant tissue as rapidly as possible. For live imaging, we used methodology previously described for embryonic skin explants (Li et al., 2011). Using a small volume of growth factor-reduced matrigel, allowed to polymerize for 25 min at 37°C , we sealed eyes against a Lumox teflon-bottom dish (Sarstedt). Eyelid closure was imaged for periods of

2.4. EXPERIMENTAL PROCEDURES

6–24 h in 5% CO₂ on a PerkinElmer Volocity spinning disk system equipped with a heated enclosure and gas mixer (Solent) and $\times 20/0.75$ CFI Plan-Apo objective, or a Zeiss LSM 780 system with a stage-top incubator and Plan-Apochromat $\times 20/0.8$ objective. In both cases, CO₂ was bubbled through water to prevent evaporation of media.

For analyzing cell movements in eyelid explants, I developed a custom MATLAB-based pipeline. Image stacks were deconvolved using the Richardson-Lucy algorithm and filtered using a 3D bandpass filter. This serves to filter out pixel noise, background, and any features smaller than the characteristic size of a nucleus. Nuclei were then segmented in 3D using a simple region-growing algorithm modified from Keller et al. (2008a), which allocates pixels in an image to objects in a stepwise fashion by considering neighboring pixels at increasing threshold levels. This allows the calculation of the centroid positions of nuclei in each frame of a timelapse, as well as filtering of objects based on their mean intensity, size, or morphology.

Tracking of nuclei was performed using the tracking module from the Danuser lab's *μ Track* software package, which features robust handling of track splitting and merging (Jaqaman et al., 2008). Segmentation and tracking efficiency were determined by manual verification in two movies (Figure 2.17). For segmentation efficiency, the number of false positives and false negatives were counted manually in three frames, and the total efficiency expressed as 100% - (percent false positive + percent false negatives). Tracking efficiency was evaluated by plotting histograms of frame-to-frame linking distance and track lengths. To avoid mistracking of cells, the histogram of linking distances should fall off gracefully before reaching the maximum distance a cell is expected to move between frames (empirically determined to be 6 μ m). The histogram of track lengths, on the other hand, gives a sense of how long individual cells can be followed. By both metrics, cell tracking in eyelid closure was satisfactory, although cells in the crowded region of the eyelid front proved more difficult than cells of the surrounding epidermis to follow for long periods. Downstream analysis of cell speed and visualization of cell tracks was performed using custom MATLAB routines.

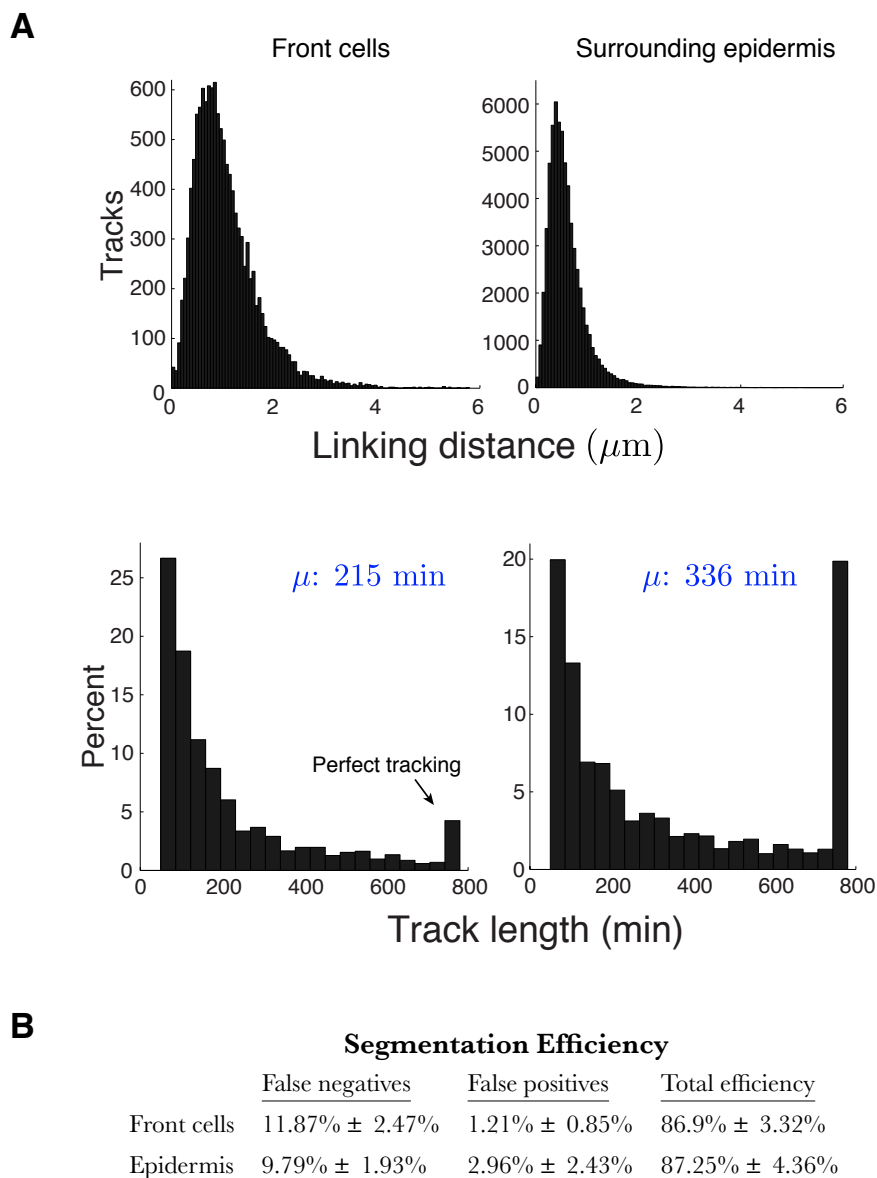


Figure 2.17: Cell segmentation and tracking efficiency. (A) Histograms of frame-to-frame linking distance (top) and track length (bottom) for eyelid front cells and cells of the surrounding epidermis. The histogram of linking distances falls off before an empirically-determined upper limit of 6 μm , indicating that a frame rate of 1/10 min is sufficient to accurately track cells. While the slower-moving cells of the eyelid epidermis can be tracked for longer than front cells, both can be monitored over periods of a few hours. (B) Efficiency of detection of nuclei based on manual controls from 3 frames in two independent movies.

2.4. EXPERIMENTAL PROCEDURES

For the analysis of eyelid closure following mito-C treatment to inhibit cell proliferation, closure rates were measured by tracing the border of the eyelid in 10-frame intervals and measuring the average displacement over time. Cell divisions were counted manually in regions of approximately equal area (comprising about 4000 cells) in eyelid samples over the course of 20 frames. The rate is expressed as a percent of total cells (counted by automatic segmentation in the first frame) dividing over time.

2.4.7 RT-PCR profiling of eyelid front cells

Eyelids from E15.5 *K14-H2B-GFP* embryos were dissected and digested in 0.25% collagenase (Sigma) in HBSS for 1 h at 37°C. Epidermis was separated from dermal cells by filtering through a 70 μ m filter and digested in 0.25% Trypsin/EDTA for 15 min at room temperature. Cells were sorted by FACS on the basis of *K14-H2B-GFP* and α_5 integrin expression, mRNA was isolated using an Absolutely RNA Purification Kit (Stratagene), and cDNA was synthesized using Superscript VILO and random hexamer primers (Life). Real-time PCR was performed on a Roche LightCycler 480 or 7900HT Fast Real-Time PCR System (Applied Biosciences). Relative quantification of transcript levels was performed by generating calibration curves for all primer pairs. Each measurement was performed in triplicate.

Primer sequences were as follows:

Fn1 forward: 5'-ATGTCGGGACCAGTAGGACA-3', reverse: 5'-CGATATTGGTGAATCGCAGA-3';
Itga5 forward: 5'-CACCATTCAATTTGACAGCAA-3', reverse: 5'-ATGTCGGGACCAGTAGGACA-3';
Itgb1 forward: 5'-TGGCAACAATGAAGCTATCG-3', reverse: 5'-ATGTCGGGACCAGTAGGACA-3';
Itgav forward: 5'-GGTGTGGATCGAGCTGTCTT-3', reverse: 5'-CAAGGCCAGCATTACAGTG-3';
Itga6 forward: 5'-TTTGGAGCCCCAGGGACTTAC-3', reverse: 5'-GCACCCCCGACTTCACCAT-3';
K14 forward: 5'-CGCCGCCCCTGGTGTGG-3', reverse: 5'-ATCTGGCGGTTGGTGGAGGTCA-3';
K5 forward: 5'-AACATTTTGGGGTCTGGGTCAC-3', reverse: 5'-GGCCCACAGAGACTGCTTCTTT-3';
K6 forward: 5'-CCCTGCAGAAGGCCAAACAG-3', reverse: 5'-AAGAGCTGAGGCCACCAGAAGA-3';
Cebpa forward 5'-CATCTGCGAGCACGAGACGT-3', reverse: 5'-GGGCTCCCGGGTAGTCAAA-3';

Ecad forward 5'-GATGATGCCCCCAACACTCC-3', reverse: 5'-CTCTCGAGCGGTATAAGATGTGATTT-3';

Ppib forward: 5'-GTGAGCGCTTCCCAGATGAGA-3', reverse: 5'-TGCCGGAGTCGACAATGATG-3'.

2.4.8 Statistical analysis

All statistical analyses were performed in the R statistical environment (R Core Team, 2013). A two-tailed, unpaired t-test was used to assess the level of significance between two experimental conditions, while multiple conditions were compared using ANOVA followed by Tukey's HSD test. Normality of distributions was tested visually using histograms or quantile-quantile plots. A Mann-Whitney-Wilcoxon test was used for any non-normal data. All means are reported \pm s.e.m. unless otherwise indicated. Plots were produced in MATLAB or R using the ggplot2 package (Wickham, 2009) and assembled in Adobe Illustrator.

Chapter 3

Insights into collective cell movements in embryonic skin: cellular mechanisms of eyelid closure

While many processes of epithelial fusion and spreading are mediated by a supracellular actin “purse string,” the eyelid front exhibits no such structure. Contractile actin cables are typically polarized within epithelial cells bordering a gap or wound and span multiple cells ([Section 1.4.2](#), [Figure 1.1](#)). Although their assembly is often accompanied by protrusive activity and a loss of apicobasal polarity in leading edge cells (Bahri et al., 2010), the majority of cells retain their epithelial characteristics. Contraction of the cable over the course of closure also typically leads to the substantial elongation of cells bordering the gap in direction of closure or, in some cases, passive intercalation and spreading of the tissue over the gap. Cell protrusions oriented along the axis of closure cooperate with constriction of the actin cable to seal apposing epithelial sheets.

In stark contrast, cells of the eyelid front actively elongate *perpendicular* to the axis of closure, pack together in a thin, multilayered sheet, and exhibit actomyosin dynamics and intercalary behavior reminiscent of convergent extension movements in mesodermal tissues. Throughout the sheet, actomyosin in front cells is predominantly cortical, although enriched mediolaterally, and thus bears little resemblance to the continuous actomyosin cable tethered at cell-cell junctions observed in other processes of epithelial fusion. Together, these observations suggest that the intercalation of front cells plays an active role in eyelid closure. To test this hypothesis, I performed a detailed analysis of cell intercalation movements

and cell polarity within the eyelid front, including a quantitative analysis of tissue deformation that arises as a result of these movements in collaboration with a team of biophysicists at the Max Planck Institute. These analyses expose the pattern of tissue strain—regions of compression, extension, or both—that uniquely characterizes a morphogenetic process (Blanchard et al., 2009). In the eyelid, this uncovers a region of active shear in the front, in which the rates of tissue compression and extension are equal throughout, but little deformation in the surrounding epidermis. This argues that the eyelid front is a region of active intercalation and distinguishes it from processes driven by a contractile actin cable, which are characterized by a region of predominantly tissue compression at the front.

To validate the functional importance of the eyelid front, I conducted a series of laser ablation experiments after determining a laser power and dwell time that would effectively ablate a targeted region of skin without causing non-specific damage to the surrounding tissue. This shows that the eyelid front is required for the forward movement of the eyelid and the source of a pulling force that both tows the surrounding epidermis and stretches epidermal cells in close proximity along the axis of closure. I performed a number of additional experiments targeting different regions of the eyelid to rule out other potential mechanisms of closure. In combination, these results suggest a model of closure in which forces from cell intercalation are leveraged to tow the eyelids over the eye.

3.1 Quantitative analysis of cell movement and tissue deformation in eyelid closure

In order to analyze patterns of cell movement within the eyelid and surrounding epidermis, I imaged eyelid closure in *K14-H2B-GFP*-expressing embryos. Tracking nuclei, mapping the trajectories of cells, and measuring regional differences in cell speed all helped to elucidate how front cells are able to drive the large-scale tissue movements required for the process.

3.1. CELL MOVEMENT AND TISSUE DEFORMATION

3.1.1 Cell intercalation and apicobasal polarity in the eyelid front

Although cell intercalation was observed throughout the eyelid front, the tendency of the surrounding tissue to be drawn toward the center gave the appearance of domains of movement in a single direction. I explored this further by examining the spatial orientation of cell movements in early and mid/late closure (Figure 3.1A). Color-coding the azimuthal movements of cells based on their overall direction revealed that, in early closure, cells migrating in opposing directions were distributed throughout the front. By averaging velocities of front cells such that movements with equivalent speeds but opposite directions negate each other, it was clear that these movements largely opposed each other. Although a similar analysis of mid/late closure revealed distinct domains of movement, these regions were peripheral to the fastest-moving, most-elongated cells near the center. There, cell movements largely opposed each as observed at earlier stages. These analyses suggested the possibility that cell intercalation within the front was the driving force of eyelid closure.

Cells of the embryonic skin are strongly polarized along their apicobasal axis. Segregating the membrane into apical and basolateral domains are the Par3/Par6/aPKC complex, which organizes the apical surface, and the Scribble (Scrib)/Discs-Large (Dlg)/Lethal Giant Larvae (Lgl) complex that organizes the basolateral domain. Members of these two complexes are mutually antagonistic, with Scrib excluding members of the Par complex, and the Par complex, through recruitment of Crumbs (Crb), excluding Scrib (Margolis and Borg, 2005). Along with the polarization of these two complexes, epithelial cells polarize their centrosome and Golgi apically, which may play a role in polarized membrane trafficking or signaling associated with the primary cilium (Ezratty et al., 2011). Migrating cells, on the other hand, utilize many of the same components to establish front/back polarity. Components of both the apical Par complex and basolateral Scrib complex co-localize with Cdc42 at the leading edge to mediate polarity and directional migration (Etienne-Manneville, 2008). The centrosome and Golgi are similarly polarized, although whether they are positioned in front of or behind the nucleus depends on cell type (Yvon et al., 2002). In the skin, keratinocytes

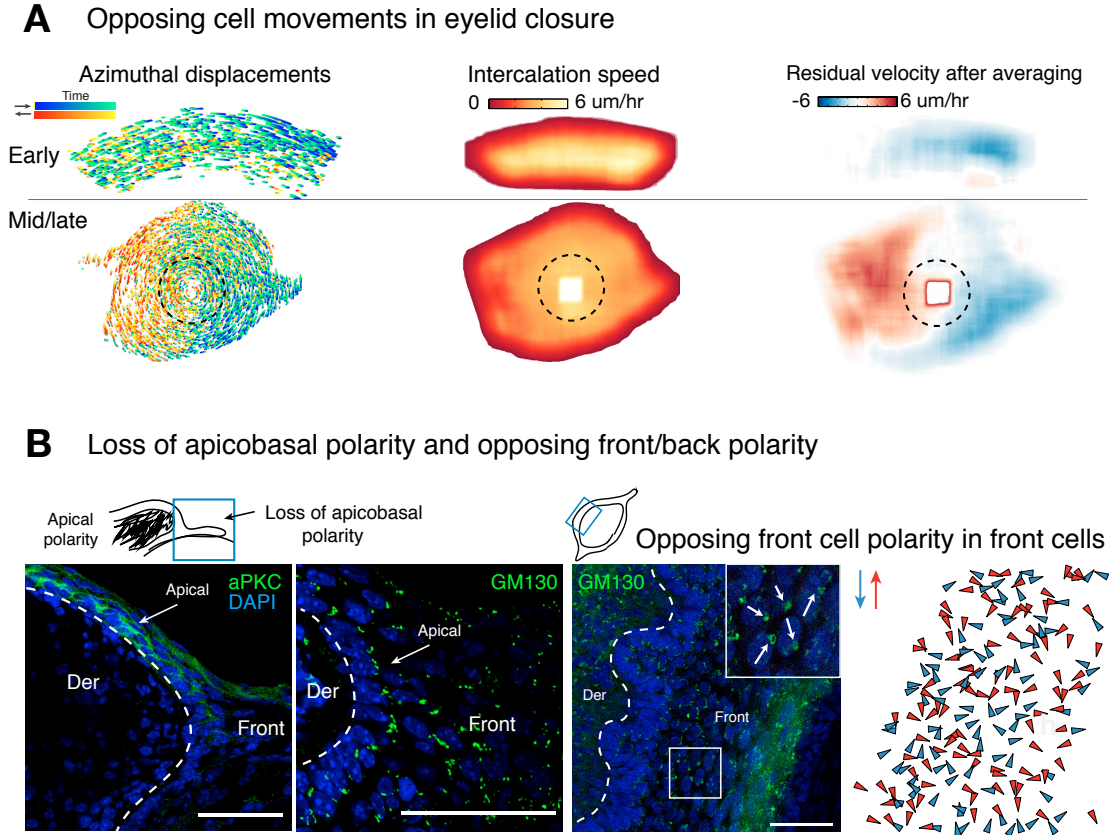


Figure 3.1: Opposing cell movements in the eyelid front. (A) Orientation of cell movements in early and mid/late eyelid closure. Left: Color-coded plots of the transverse displacements of front cells from live imaging data indicates that cells with opposing movements are distributed throughout the front. Middle: Heat maps of overall front cell speed. The fastest moving cells are nearest the border of the eye. Right: Plot of residual azimuthal velocity after averaging in $32 \times 32 \mu\text{m}$ regions throughout the front. Although domains of movement in a single direction appear as closure progresses, these are restricted to peripheral regions. Near the center, corresponding to the fastest-moving, most elongated cells, movements almost completely oppose each other as observed in early closure. (B) Immunolabeling of GM130 and aPKC in sagittal sections of eyelids reveals the clear apicobasal polarity of cells in the surrounding epidermis, but its loss in the eyelid front (left). *In vivo* whole-mount immunolabeling for Golgi marker GM130 was used to create a map of front cell polarities, revealing that they are strongly polarized along their mediolateral axis, but that cells with opposing polarities are distributed throughout the front (right). Scale bars, $50 \mu\text{m}$.

3.1. CELL MOVEMENT AND TISSUE DEFORMATION

have been found to polarize their centrosome and Golgi in a context-dependent manner. *In vitro*, migrating keratinocytes polarize them in the direction of migration, while in explant outgrowth assays, they localize behind the nucleus.

Accompanying their changes in morphology, integrin expression, and transcriptional profile, eyelid front cells lose their apicobasal polarity and acquire front/back polarity. Immunofluorescence staining of cell polarity markers in sagittal section revealed the robust apical localization of Par3 and aPKC in the epidermis around the eye, but an absence in the front, along with a disorganization of the Golgi marker GM130. To examine the polarity of front cells in detail, I performed high-magnification imaging of eyelid whole-mounts stained with GM130 or pericentrin to define an approximate axis of polarity for cells throughout the tissue. Consistent with a mechanism of cell intercalation in which small transverse displacements contribute to substantial overall tissue movements, the polarity of front cells was strongly oriented along their mediolateral axis, but with cells in a given region frequently displaying opposite polarities (Figure 3.1B). Such movements further underscored the striking differences between eyelid closure and a purse-string or wound-closure mechanism in that active cell intercalation within a small region of tissue appeared to drive the process.

3.1.2 Quantitative analyses of tissue deformation

Cell intercalation can be an active, force-generating process, driving the spreading and elongation of tissues in development, or a passive response to external forces. Many morphogenetic processes occurring over large regions of an embryo involve a combination of both. For example, explanted tissue from the *Xenopus* dorsal mesoderm can autonomously converge and extend, generating pushing forces upwards of $0.5\ \mu\text{N}$ (Moore et al., 1995). This likely contributes actively to the internalization of mesoderm and endoderm, as well as closure of the blastopore. At the same time, however, the overlying neuroectoderm and superficial endoderm likely extend passively as a result of mediolateral intercalations in the underlying tissues (Shih and Keller, 1992). Much of the tissue stretching observed in wound

healing or *Drosophila* dorsal closure is also expected to be a passive response to contraction of an actomyosin cable or forces generated in other tissues.

Of course, it is impossible to simply observe the forces evolved within cells and their transmission through tissues in living organisms. However, whether a process of cell intercalation or shape change is active or passive can be distinguished by combining direct biophysical measurement with a quantitative assessment of tissue strain (deformation), the response of a tissue to the combined effect of internally-generated and external forces. An approach that has been used to great success in describing morphogenesis in epithelia is computer simulation based on the principle of minimizing surface free energy. By representing an epithelium as a network of vertices and edges and evolving its configuration according to a well-defined set of rules informed by biophysical measurement, it is possible to make predictions about the mechanism of a morphogenetic process. For example, by simulating the equilibration or “settling” of an epithelium in response to cell division within different regimes of cell elasticity, adhesion, and contractility, it is possible to predict its final packing geometry (Farhadifar et al., 2007). This has been used to account for the evolution of the *Drosophila* wing imaginal disk from an irregularly-packed soft network to the hexagonal array observed in late development, and the arrangement of cone and pigment cells in the ommatidium (Hilgenfeldt et al., 2008). A similar method was used to explain how regional differences in contractility and stiffness and the assembly of actomyosin cables along specific cell interfaces drives the formation of dorsal appendages in the *Drosophila* egg (Osterfield et al., 2013).

A drawback of these methods is that they rely on the analogy of tissues to foams and represent tissue remodeling as a series of discrete changes in cell-cell connectivity. While they make perfect sense for describing morphogenetic processes driven mainly by differences in cortical tension or remodeling of cell junctions, they are not well-suited for processes driven by a combination of cell movement and shape change. An alternative approach based on the continuous sliding of cells between each other uses ideas from tensor analysis

3.1. CELL MOVEMENT AND TISSUE DEFORMATION

to measure strain rates within tissues. This essentially uses the relative movement and speed of cells to describe how quickly and in which directions a region of tissue is deforming. With measurements of cell shape change, it can be used to understand how combinations of cell intercalation and processes such as apical constriction generate the characteristic patterns of tissue convergence and extension of a given morphogenetic process. Applied to *Drosophila* dorsal closure, for example, it reveals predominantly tissue compression generated by asymmetric cell shape change in the amnioserosa in line with this as a major driving force of the process (Blanchard et al., 2009). In germband elongation, a process known to be driven by cell intercalation, it identifies both A–P-oriented intercalation and cell elongation as contributing. On the other hand, in the zebrafish neuroectoderm, cells converge medially without substantially elongating the tissue along the A–P axis. An analysis of strain rates suggests that this is because cell shape changes along this axis resist tissue elongation from cell intercalation. Tissue strain rates thus yield a “signature” of tissue compression and extension that provides mechanistic insight into a morphogenetic process.

The hypothesis that eyelid closure is driven by the movements of cells in the front has a number of predictions that can be distinguished by an analysis of strain rates. Most importantly, it would reveal a region of significant deformation at the front, but little in the surrounding tissue. The pattern of deformation within the front, in turn, would provide mechanistic insight into how front cells mediate closure.

A priori, the opposing cell movements observed in the eyelid front are consistent with a number of possible mechanisms (Illustration 3.1). If a supracellular actin cable that had simply evaded detection were acting in cells bordering the eye, a region of exclusively tissue compression should be observed within the front corresponding to contraction of the cable. Behind this region, both tissue compression and extension would be observed if the actin cable were driving the passive intercalation of cells behind it, whereas uniform compression would be observed if it were simply squeezing cells of the front together. A second model is that opposing cell movements throughout the front create a global purse string. In this

case, one would observe uniform tissue compression throughout the front and a separate region of extension in the surrounding epidermis, similar to the expectation in dorsal closure, where apical constriction in the amnioserosa subsequently elongates cells of the lateral epidermis. Finally, cell intercalation in the front could drive convergent extension movements, in which the rates of tissue compression and extension are roughly equivalent. This, in turn, could lead to spreading of the eyelid epidermis over the eye, or be coupled to translational movement of the entire eyelid.

To determine the role of cell intercalation in eyelid closure, I performed a tissue strain rate analysis in collaboration with Vijay Krishnamurthy and Stephan Grill at the Max Planck Institute, using particle image velocimetry (PIV) to measure the tissue flow field and quantify the rate and direction of tissue deformations (Figure 3.2A-B). Consistent with the hypothesis that eyelid closure is driven by the movements of front cells, it identified a region of active shear exclusively at the front coinciding with peak actomyosin intensity and cell elongation (Figure 3.2C). Both the average rate of tissue compression and extension displayed sharp peaks at the front, indicating that in this region, the tissue was maximally compressed perpendicular to and extended along the axis of closure (Figure 3.2B). Importantly, compression and extension rates were similar throughout the front. This indicates that the eyelid front is a region of active intercalation rather than exclusively tissue compression, and based on the relatively little deformation observed in the surrounding epidermis, implies that intercalation plays an active role in eyelid closure.

The pattern of deformation observed in the eyelid front is consistent with either the expansion and spreading of the front over the eye or the conversion of forces from cell intercalation into forward translational movement. To distinguish between these possibilities, I examined long-term changes in tissue dimensions by live imaging (Figure 3.3). By measuring the axial length of the front as the eyelid closed, I found that, in comparison to the amount of forward movement, it spread comparatively little over the eye (Figure 3.3A). Remarkably, it instead appeared to compress, thickening vertically in the process. Consistent with this was

3.1. CELL MOVEMENT AND TISSUE DEFORMATION

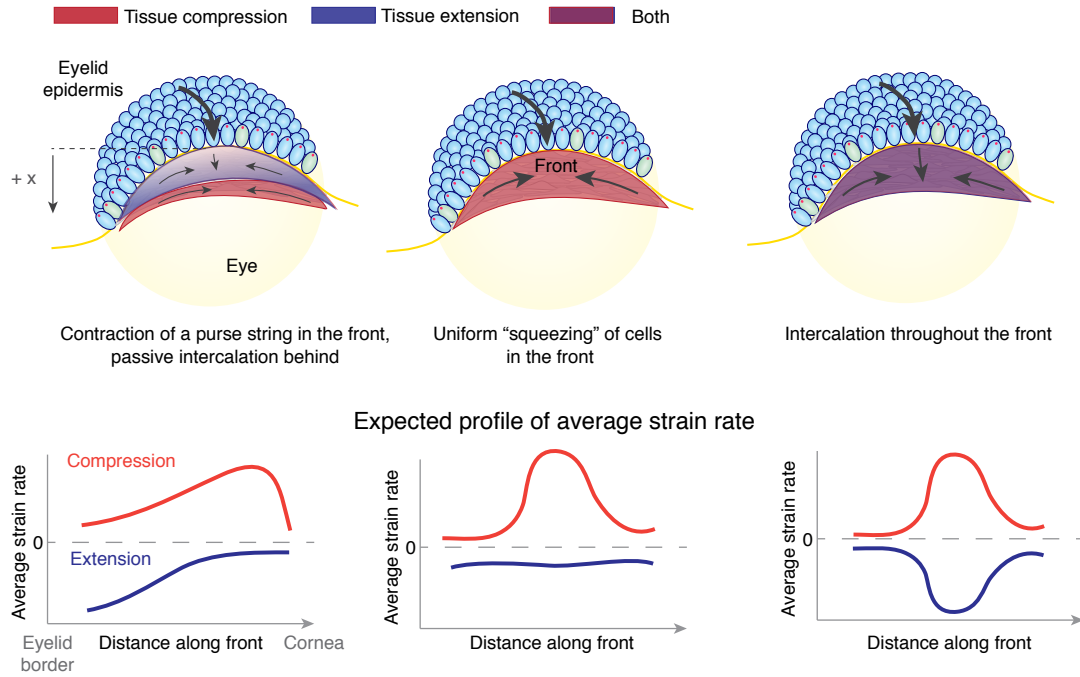


Illustration 3.1: Models of eyelid closure and expected patterns of tissue deformation.

Quantitative analysis of the relative movements and speeds of cells can be used to reveal patterns of deformation in a tissue. Based on ideas from tensor analysis, it involves computation of tissue strain rates, which quantify the magnitude and direction of tissue compression and extension. The pattern of tissue strain can be used to distinguish between possible cellular mechanisms of eyelid closure. If a conventional actomyosin cable were driving closure, then a region of tissue compression corresponding to contraction of the cable would be observed immediately abutting the eye (left panel). This would likely drive the passive intercalation of cells behind it, revealed as a region of both tissue compression and extension (purple region). If the relative movements of cells were simply constricting the eyelid front, predominantly compressive strain would be observed, with very little local extension (middle panel). Finally, active cell intercalation could generate a region of tissue convergence and extension, in which the rates of tissue compression and extension would be roughly equivalent throughout the front (right panel). In the lower panels, expected profiles of azimuthally-averaged strain rates in the front are provided as a function of distance from the eyelid border.

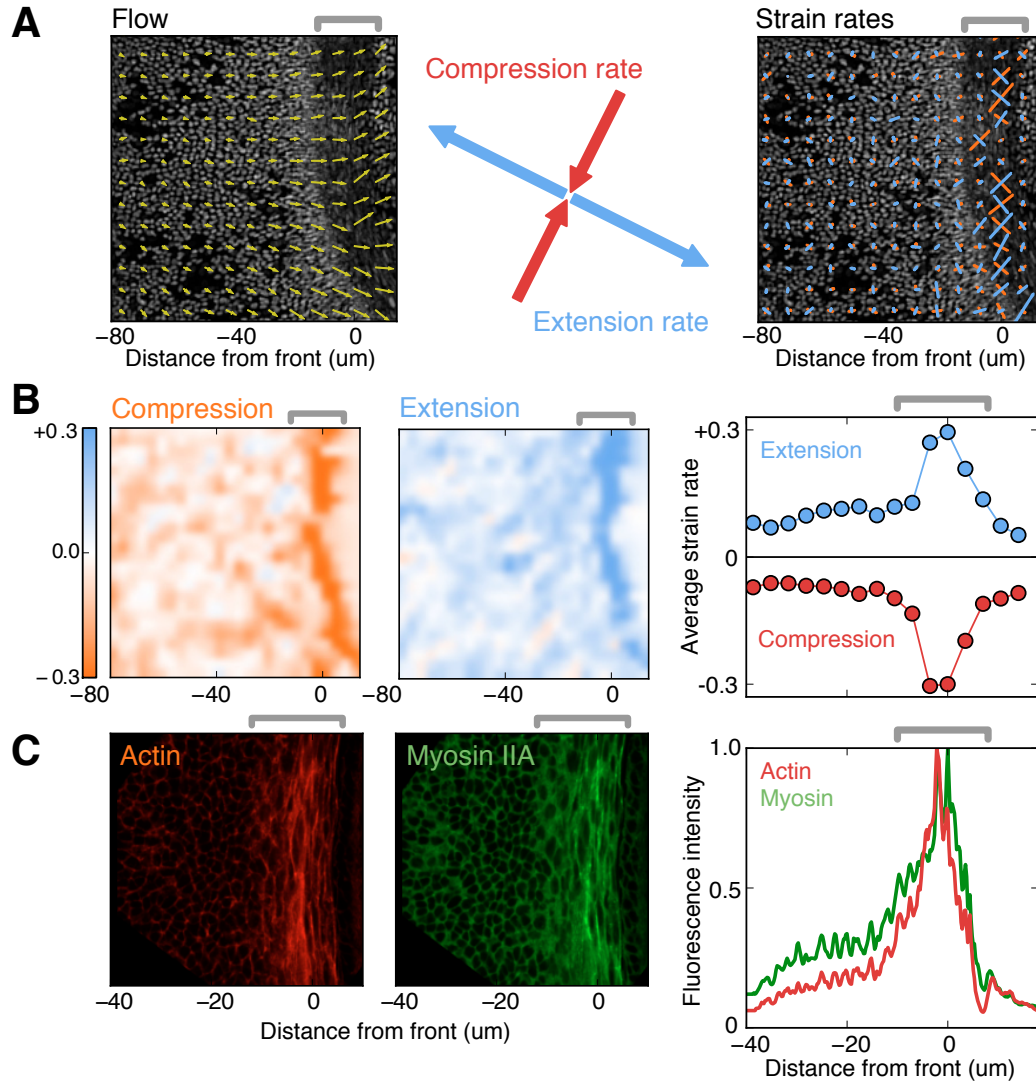


Figure 3.2: Quantitative analysis of tissue deformation in the eyelid. (A) Particle image velocimetry (PIV) was used to measure the tissue flow field and to quantify deformation and shear in the eyelid and surrounding epidermis. The eigenvectors of the symmetrized velocity gradient tensor (strain rate tensor) identify the principal axes of deformation during flow, while the eigenvalues specify the rates of tissue deformation along these principal directions. In the right panel, the two strain rates are depicted as red (compression) and blue (extension) lines, with length proportional to magnitude. (B) The profile of average tissue compression and extension displays a sharp peak in the region of active cell intercalation, indicating that the eyelid front is maximally compressed perpendicular to, and extended along, the closure axis. Note that the two strain rates have similar magnitude but opposite sign throughout the front, suggesting tissue convergence and extension rather than uniform contraction. The presence of a sharp peak of both extension and compression at the front also argues against the action of a contractile actomyosin cable. (C) The region of maximum tissue compression and extension coincides precisely with peak actin and myosin intensity and mediolateral cell elongation in the eyelid front.

3.2. LASER ABLATION STUDIES IN SUPPORT OF A TOWING MECHANISM

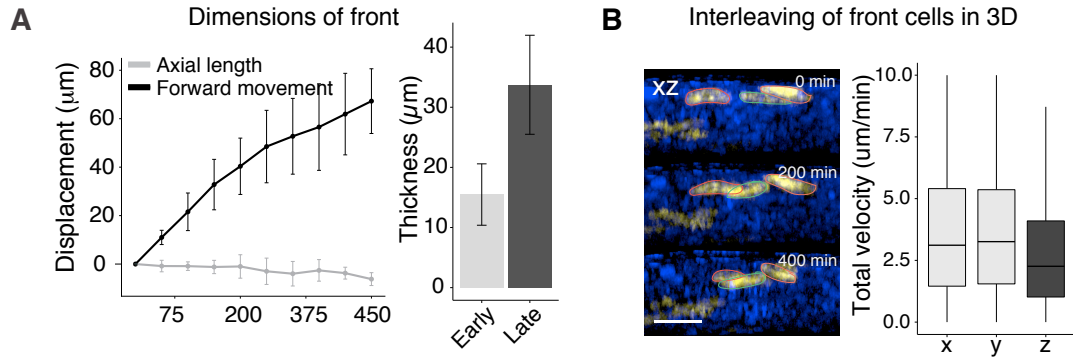


Figure 3.3: Cell intercalation is coupled to translocation of the eyelid. (A) As the eyelid moves over the eye, the axial length of the layer of front cells remains relatively constant, and the density of cells in a fixed region increases linearly ($n = 3$ eyelids). This is accompanied by an overall thickening of the eyelid front between E15 and E16 in vivo ($p = 0.0044$; $n = 8$ early, 5 late eyelids). (B) View of the eyelid along the xz axis with three individual cells highlighted, illustrating convergence of cells along this axis. The slower speed along the z axis relative to the xy axis implies that thickening is a consequence of mediolateral intercalation. Together, this suggests that cell intercalation in the front is coupled to forward translational movement of the eyelid rather than tissue spreading. Scale bars, $50\ \mu\text{m}$.

an increase in cell density over the course of closure. Visualizing individually-labeled cells in 3D similarly revealed convergence along the xz as well as the xy axis, although quantification of cell velocities indicated that movements in the z -direction were significantly smaller and unlikely to be an active part of the process (Figure 3.3B). Together, these observations support a mechanism in which forces from cell intercalation are translated into a pulling force on the surrounding epidermis. Conceptually, this mechanism is equivalent to purse-string closure, but is achieved through cell movements rather than contraction of an actin cable.

3.2 Laser ablation studies in support of a towing mechanism

My analysis of strain rates suggests that the large-scale tissue movements of eyelid closure are driven by cell intercalation in the front, with little to no relative movement of cells in the surrounding epidermis. To directly test the importance of intercalating cells, I combined

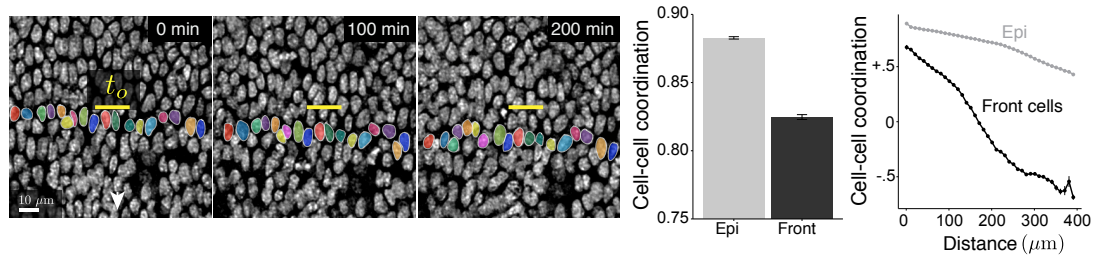
the targeted ablation of front cells with an analysis of the movements and morphology of cells in the epidermis behind them.

3.2.1 Coordinated movement and cell elongation in the eyelid epidermis

If mechanical forces generated by the eyelid front effectively pull the eyelids over the eye, I would expect to observe significant translational but little relative movement of cells in the surrounding tissue, as well as a slight deformation of the epidermis over long timescales, particularly in the region immediately adjoining the front. As illustrated by the colored row of cells in [Figure 3.4A](#), over the course of closure, cells largely maintained their relative positions despite significant translational movement toward the eye. Moreover, by comparing the velocity of epidermal cells to their nearest-neighbors and to cells at increasing distances, I found that cells within surrounding epidermis were highly coordinated over distances of hundreds of microns, while eyelid front cells were relatively uncoordinated, reflecting their mesenchymal-like behavior.

To explore the expectation that the epidermis deforms as a result of pulling forces in the eyelid front, I performed a quantitative analysis of cell morphology *in vivo* and tracked the deformation of the epidermis over time. Mating *K14-Cre* to *Rosa26^{mT/mG}* mice to uniformly label cell membranes in the skin with mGFP, I acquired tiled, high-magnification images of the entire eye and surrounding epidermis and used segmentation techniques to measure the elongation of cells ([Figure 3.4B](#)). This revealed that epidermal cells in close proximity to the eyelid front were elongated along the axis of closure, which became more pronounced between E15 and E16. These observations extended those of my strain rate analysis in their support of pulling forces generated by the front and identified essential features of eyelid closure that could be used as readouts in perturbation experiments. In particular, laser ablation of the eyelid front could distinguish whether cells of the surrounding epidermis were elongating autonomously or as a consequence of forces generated by the front.

A Movement of cells in the surrounding epidermis



B Cell elongation in surrounding epidermis

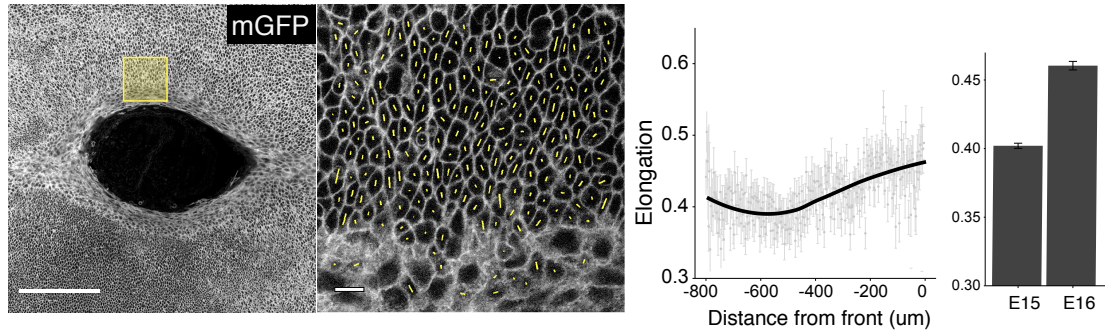


Figure 3.4: Coordinated movements and elongation of the eyelid epidermis. (A) Behind the eyelid front, cells in the epidermis and the underlying dermis move as a coherent unit. Individual frames from a timelapse of basal epidermal cells located behind the eyelid front (arrow denotes direction, yellow bar denotes spatial reference). A row of epidermal cells is colored to appreciate that epidermal cells surrounding the eye maintain their relative positions and move as a unit during closure (left). Cells throughout the eye were tracked individually and their velocity vectors were compared to their nearest-neighbors and to cells at increasing distances (right). These measurements underscore the high degree of coordination (cosine similarity) over large distances that epidermal cells behind the front display in comparison to the intercalating cells ($p = 0.001$, Wilcoxon test). (B) Analysis of cell elongation in the surrounding epidermis by tiled imaging of eyelid whole-mounts in which cells were uniformly labeled with mGFP (left). Cells in close proximity to the eye are elongated along the axis of closure. This elongation increases between E15 and E16 (right). Scale bars, 10 μm (A), 300 μm (B, left), 50 μm (B, right).

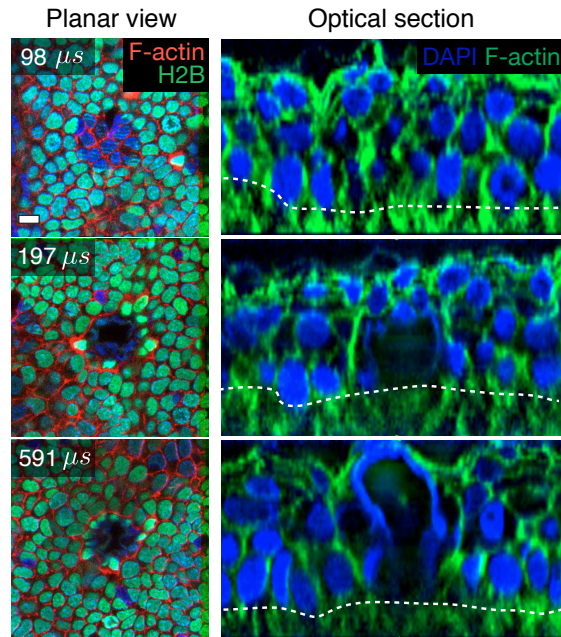
3.2.2 Laser ablation of the eyelid front

Given the unique morphological and motile properties of eyelid front cells, I set out to compromise their activity through physical perturbation. Using a two-photon laser, I first determined a laser power and dwell time that allowed me to specifically target and ablate a multicellular region of embryonic skin without causing non-specific damage to surrounding tissue (Figure 3.5A). An analysis of tissue morphology in skin explants following the ablation of a region of basal layer cells revealed that laser powers around 90% and dwell times of $\sim 200 \mu\text{s}$ could be used to ablate specific layers of skin epidermis without causing cavitation or changes in morphology to surrounding cells. In the eyelid, I verified that laser ablation both removed targeted cells as well as local ECM without inducing apoptosis in surrounding cells (Figure 3.5B).

Having established parameters for effective tissue ablation, I targeted cells in the eyelid front and analyzed the consequences to the progress of closure and the elongation of cells in the surrounding epidermis. As expected if the front were pulling the eyelid over the eye, ablation of the front resulted in a relaxation of epidermal cells behind this zone, returning them to the shape of epidermal cells more distant from the eye (Figure 3.6A). To evaluate whether forces generated by front cells not only stretch cells in the immediate vicinity, but also pull the eyelid epidermis forward, I ablated a rectangular region $\sim 40 \mu\text{m}$ behind the front and measured the effects both at the wound site and in the tissue located between the wound and eye (Figure 3.6B). Following laser ablation, the epidermis between the wound site and the eye was stretched forward over time, and the ablation site itself widened toward the eye until a wound healing response was initiated to close it. This provides explicit evidence of a pulling force generated by cell intercalation in the front.

Finally, I directly tested the importance of front cells to eyelid closure by ablating a region of intercalating cells along one eyelid and measuring the immediate effect on the translational movement of the adjacent epidermis (Figure 3.7). In these experiments, the second, unablated eyelid serves as an internal control. Using a scheme to measure the displacement

A Calibration of laser ablation



B Ablation of eyelid cells

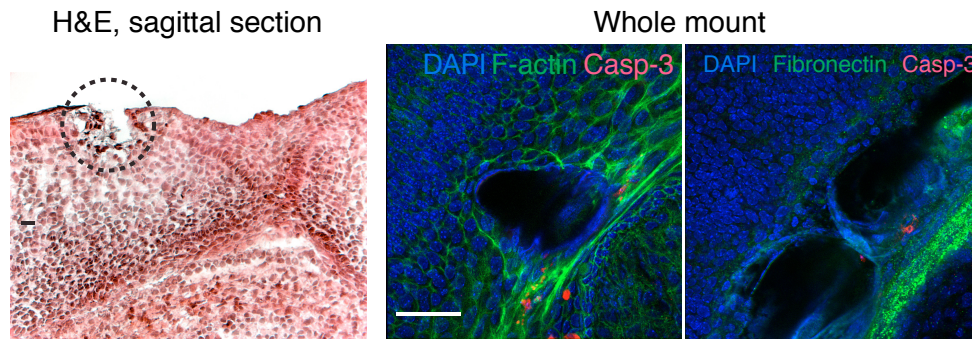


Figure 3.5: Targeted tissue ablation with a multiphoton laser. (A) Assessment of tissue damage as a function of laser dwell time. A pulsed, femtosecond laser at maximum power was used to ablate a $\sim 30 \mu\text{m}$ circular region of the epidermis. Sub-threshold doses resulted in bleaching but not ablation (top), while excessive doses causes broad tissue damage (bottom). Both power and dwell time were thus calibrated on a per-experiment basis using these values as a starting point. (B) Ablation of regions of the eyelid. Successful ablation was confirmed by cryosectioning and H&E staining (left). Staining for caspase-3 and fibronectin in whole-mount was used to confirm that laser ablation removed both cells and ECM without causing non-specific damage to the surrounding tissue (right). Scale bars, $10 \mu\text{m}$ (A) and $50 \mu\text{m}$ (B).

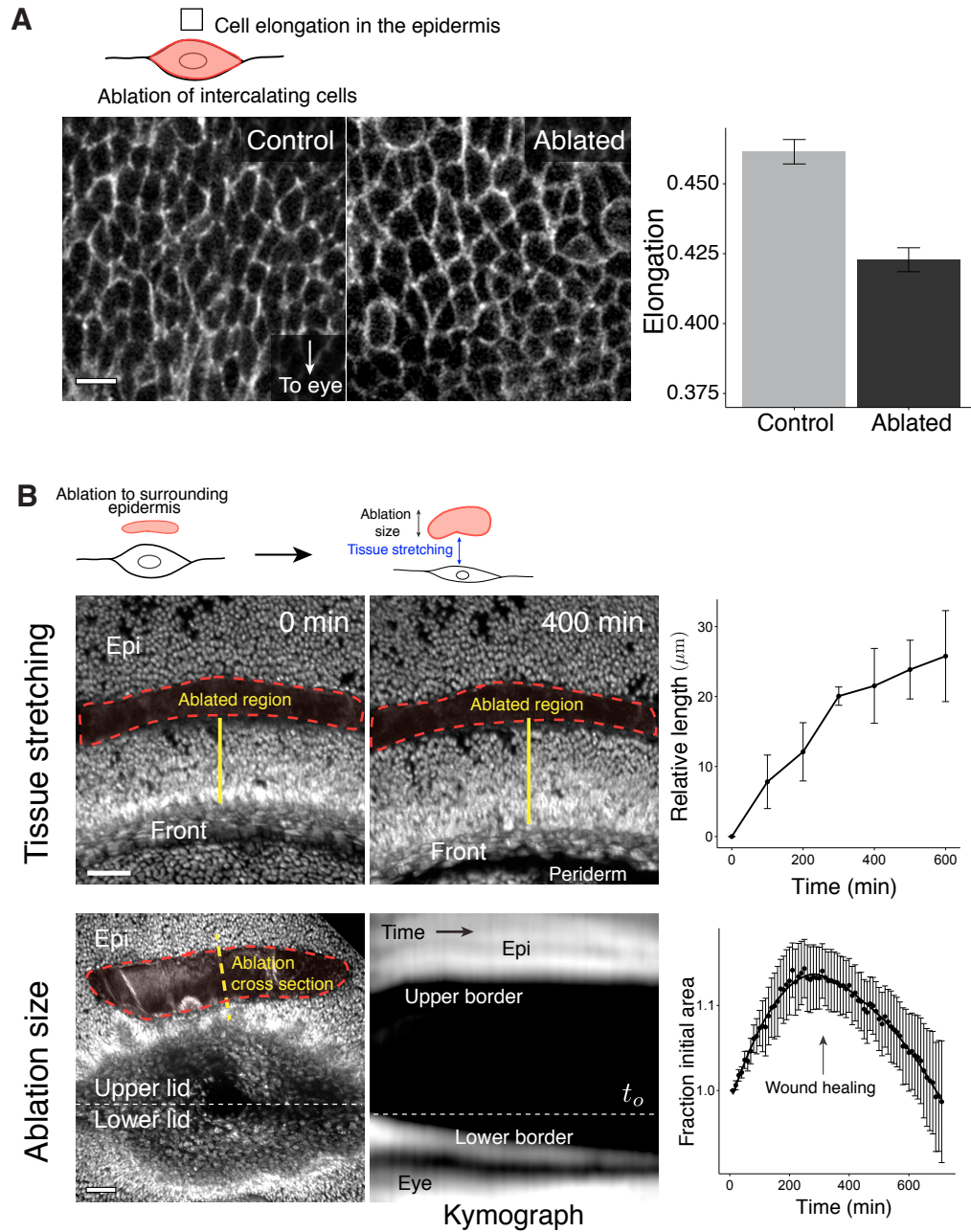


Figure 3.6: Laser ablation of front cells suggests they generate a pulling force. (A) Following laser ablation of the eyelid front, cells of the surrounding tissue become significantly less elongated in comparison to those of unablated control eyelids ($p < 0.0001$; $n > 1000$ cells pooled from 5 eyelids per condition). Shown are representative images of these shape changes. (B) When a region $\sim 40 \mu\text{m}$ from the eye is ablated, the epidermis in front of the gap is pulled toward the eye (upper). Frames from a timelapse sequence and quantifications illustrate that the tissue band broadens (yellow line, $n = 3$ eyelids). At the same time, the wound itself widens toward the eye until a wound healing response is initiated (bottom). Scale bars, $10 \mu\text{m}$ (A), $50 \mu\text{m}$ (B).

3.2. LASER ABLATION STUDIES IN SUPPORT OF A TOWING MECHANISM

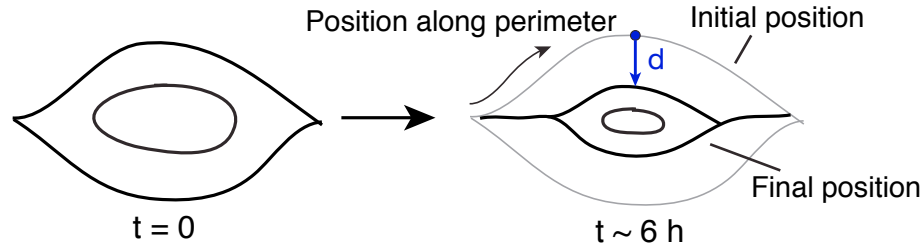
of an eyelid at every point along its perimeter, I found that, in contrast to the control eyelid, the epidermis directly behind a region of ablated front cells failed to move effectively over the eye. Similarly, ablating a region of epidermis immediately adjacent to the front, effectively untethering the front from the surrounding epidermis, revealed a substantial impairment in the forward movement of the eyelid. Pooling analogous ablations revealed a reproducible reduction in the rate of closure compared to unablated tissue. This indicates that the eyelid front is essential for the movement of eyelids and suggests cell intercalation as a means of generating force to achieve a process of epithelial fusion.

3.2.3 Laser ablations to rule out alternative mechanisms

A variety of additional ablations followed by live imaging further differentiated between multiple possible modes of eyelid closure (Figure 3.8). Ablating cells on the underside of the eyelid had little or no effect on closure, suggesting that it is not driven by cell shape changes (such as apical constriction) that bend the eyelid over the eye. Ablation of corneal epithelial cells or eyelid canthi likewise had no observable effect, arguing against contributions from the cornea or a zipper mechanism. High-speed imaging of cells in the cornea expressing *Kl4-actin-GFP* also revealed no evidence of pulsed apical constriction (not shown), suggesting that the cornea is a passive substrate. 3D reconstructions of the eyelid during closure instead suggest that the entire eye is pushed below the eyelids without substantial cell shape change in the cornea (Figure 3.9).

The lack of corneal effects differed markedly from similar studies of *Drosophila* dorsal closure, where ablation of the underlying amnioserosa had dire consequences to the process (Hutson et al., 2003). Overall, eyelid closure shares a few characteristics with dorsal closure, in particular the elongation of cells surrounding the gap (although the elongation is significantly smaller), but also exhibits striking differences in the lack of an actomyosin cable and contributions from apical constriction in the underlying tissue. It also bares some resemblance to convergent extension movements in that the rates of tissue compression and

A Quantification scheme



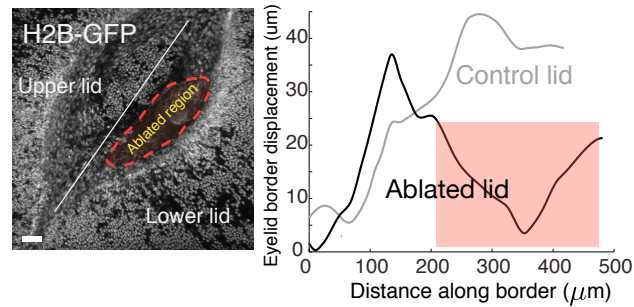
B Ablation of front cells

Ablation of intercalating layer

Control

Ablated

Ablated region



C Untethering intercalating cells

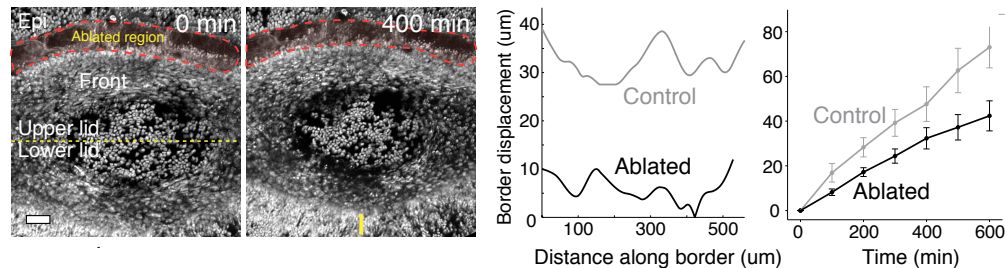


Figure 3.7: Eyelid front cells are required for eyelid closure. Ablation of a region of the eyelid front (indicated in red) prevents that region of the eyelid from moving over the eye. (A) Scheme to measure the effects of a laser ablation by plotting translocation of the eyelid at each position along the perimeter. (B) Plot of the average distance moved by each position along the eyelid border. The epidermis adjacent to a region of ablated front cells fails to move over the eye (black line), while surrounding, unablated tissue is unaffected (gray line). (C) A similar result is achieved when a region of the eyelid immediately adjacent to the front is ablated, effectively untethering front cells from the surrounding tissue. Although the front cells continue to intercalate, the eyelid fails to translocate over the eye (left). The overall rate of eyelid closure is reduced when results from similar ablation experiments are pooled, suggesting the result is representative (right, $n = 9$ unablated, 13 ablated eyelids). Scale bars, 50 μm .

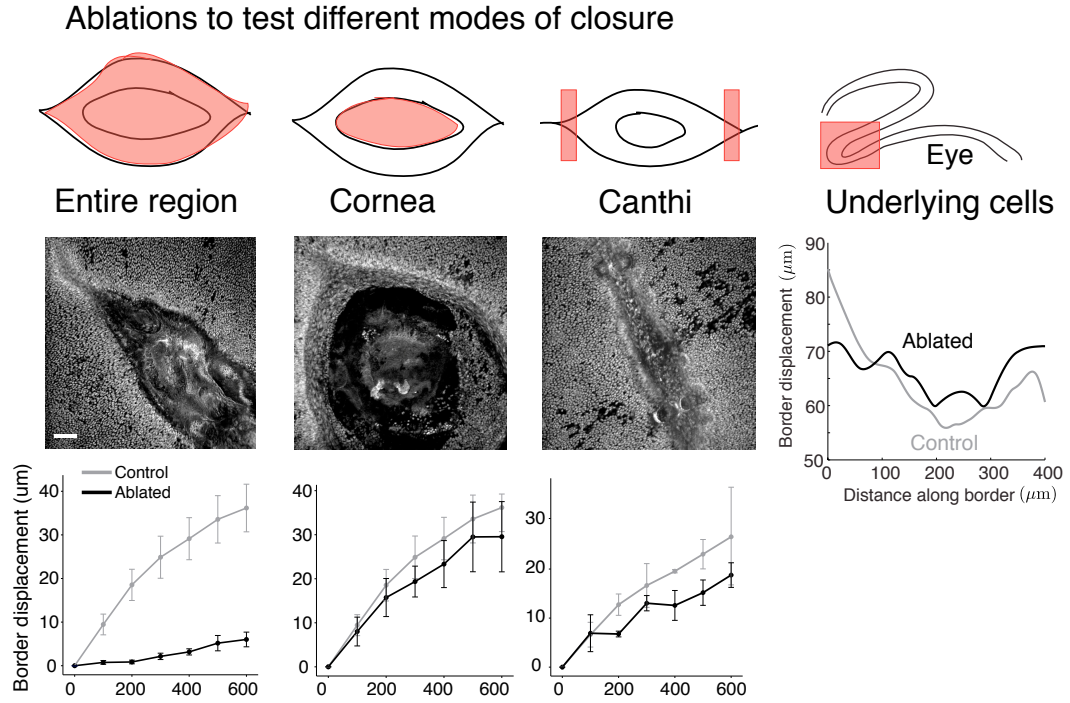


Figure 3.8: Additional ablations to distinguish possible modes of eyelid closure. Ablations were made to the entire region, cornea, and eyelid canthi, indicating that eyelid closure is primarily driven by the actions of intercalating cells. The cornea does not appear to contribute in the same way the amnioserosa contributes during *Drosophila* dorsal closure, and ablation of the eyelid canthi indicates that zippering does not contribute substantially to eyelid movement. Graphs indicate average translocation of the eyelid border over time ($n \geq 3$). Ablation of the conjunctival cells on the bottom of the eyelid does not affect eyelid closure, arguing against a mechanism in which cell shape changes bend the eyelid over the eye (graph indicates translocation a single eyelid border along its perimeter compared to the opposite, unablated eyelid). Scale bars, $50 \mu\text{m}$.

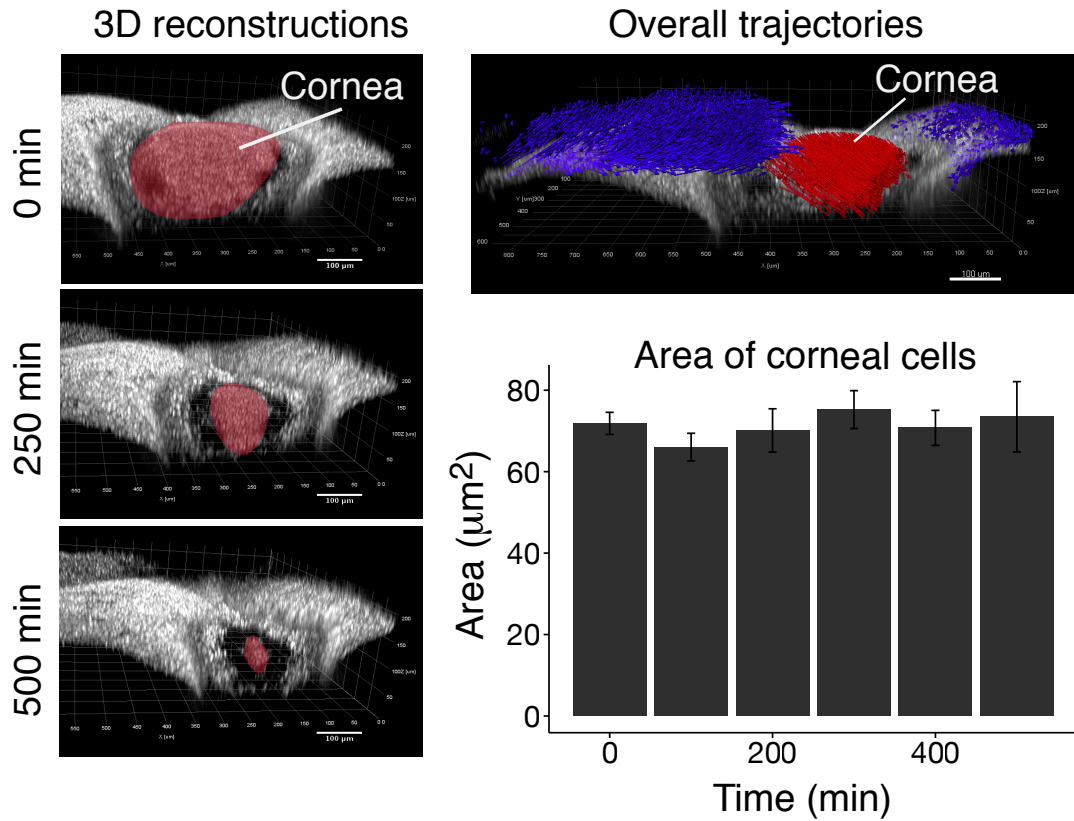


Figure 3.9: The eye is pushed below the eyelids during closure. 3D reconstructions of the eye during eyelid closure indicate that the eye is pushed beneath the eyelids without substantial cell shape changes in the cornea. Low-magnification imaging of eyelid closure in explants labeled with *K14-H2B-GFP* reveals that cells of the cornea move below the eyelids during the process (left, cornea labeled in red). Visualizing the overall trajectories of cells similarly reveals the downward movement of corneal cells (right, top). However, this movement is not accompanied by apical constriction or a reduction in the area of corneal cells, quantified over time in a live imaging experiment by manually tracing cells labeled with mGFP (right, bottom). Scale bars, 100 μm .

3.3. DISCUSSION

extension have similar magnitudes in the eyelid front. However, whereas convergent extension typically involves the reshaping of large, homogeneous regions of tissue, in this case it is restricted to a small region bordering the eye. Taken together, these results best fit a model whereby a pulling force generated by eyelid front cells is responsible for towing the epidermis behind it.

3.3 Discussion

In striking contrast to other models of epithelial fusion, cells of the eyelid front do not assemble a supracellular actin cable, which is typically polarized within the single row of epithelial cells bordering a gap or wound and tethered at the level of adherens junctions (Danjo and Gipson, 1998). Constriction of this cable is thought to generate circumferential tension to pull the surrounding epithelial sheets over the gap and to stabilize external sources of tension, such as from apical constriction of the amnioserosa in *Drosophila* dorsal closure. In many cases, epithelial is facilitated by the extension of filopodia along the axis of closure, as in dorsal closure, corneal wound healing, and the healing of epithelial monolayers *in vitro*, but they are not strictly required, as in the chick wing bud (Brock et al., 1996b). In the eyelid, the elongation of cells perpendicular to the axis of closure, loss of apicobasal polarity, packing together in multiple layers beyond the epidermal margin, and mediolaterally-oriented protrusions suggests that the forces to close the eyelids are generated by a fundamentally distinct mechanism.

By mapping the displacements of cells in the eyelid, I found that cells move in opposing directions throughout the front rather than in distinct domains. Supporting this, an analysis of polarity markers *in vivo* revealed a strong mediolateral polarization of front cells, but with cells in a given region frequently displaying opposite polarities. Although this analysis does not distinguish which side of the cell is the front or the back, as cells polarize their Golgi and MTOCs either in front of or behind the nucleus in different contexts (Yvon et al., 2002), it does suggest that opposing movements or forces are distributed throughout the front. This

could be clarified by live imaging eyelid closure with a genetically-expressed centrosomal marker, such as centrin-GFP, and determining if centrosome position is correlated with the direction of movement. That cells closer to the surrounding epidermis acquire a radial bias to their movement as eyelid closure progresses also provided a first indication that active intercalation in the front was driving more passive movement behind. These observations distinguished eyelid closure from other examples of epithelial fusion by the presence of a domain of opposing cell movements bordering the gap.

In all morphogenetic processes, a key, but often challenging question is who is pulling or pushing whom. Constituting the great fascination of development are the mass movements, sweeping shape changes, and collective remodeling of tissues that take place, but not all of them are active, force-generating processes. Decades of research into the gastrulation movements of the frog, fish, and chick have clearly indicated that the active remodeling of certain tissues contributes to substantial passive deformation throughout the embryo (Keller, 2002). Mediolateral intercalation in the mesoderm and neural tissues essentially deforms the whole of the initially spherical embryo, narrowing and extending it and thereby establishing an elongated body plan. Tissue explants from the dorsal mesoderm of *Xenopus*, for example, autonomously converge and extend, and biophysical measurements reveal that it stiffens in the process, generating pushing forces around of $0.5 \mu\text{N}$ (an order of magnitude higher than the force a cell exerts on its substrate at a focal adhesion). Explants of the overlying epithelial cells, however, converge and extend only when placed on a layer of mesodermal tissue (Elul and Keller, 2000). This suggests that the superficial epithelial layers of the embryo are deformed and carried along by active intercalation in the underlying tissue. Similarly, in the formation of the chick primitive streak, cell intercalation in the medial region of the epiblast also appears to drive the passive movement of lateral cells, pulling them toward the midline (Voiculescu et al., 2007). Thus, in both epithelial and mesodermal tissues, although the mechanism is distinct, cell intercalation can be an active, force-producing process or a passive response to remodeling in neighboring tissues.

3.3. DISCUSSION

A quantitative analysis of cell movements within the eyelid front and in the surrounding epidermis yielded important insight into whether the observed cell intercalation was an active process contributing to eyelid closure or a passive response to forces generated elsewhere. Measurement of tissue strain rates, which describe the magnitude and orientation of local deformation, identified two distinct regimes in the eyelid consistent with the functional separation revealed by differences in cell morphology and gene expression—a region of active shear in the front, and comparatively little deformation in the epidermis behind it. This immediately distinguished it from classic examples of convergent extension or epithelial sheet movement driven by an actin purse string. While cell intercalation is often found to passively deform surrounding tissues, the intercalation itself occurs throughout a broad, relatively homogeneous region, deforming its surroundings along a gradient (i.e. the closer you are, the more you are deformed). This is in contrast to the sharp transition observed in the eyelid, where cell intercalation and virtually all the tissue compression and extension are observed in the front. Monitoring cells in epidermis behind the front during eyelid closure revealed a high degree of coordination between cells even at large distances and few relative movements, supporting the notion that the process is driven by the specific activities of front cells rather than a tissue-level reorganization.

A careful consideration of the pattern of tissue compression and extension in the eyelid front sheds light on the mechanism of closure. Cell intercalation in the front is consistent with a number of possible modes of closure. If the cells of the front were squeezing together to generate circumferential tension in the manner of a global purse string, then the front would be characterized predominantly by tissue compression and little, if any, extension. This is analogous to the situation in dorsal closure, where the combined activities of the actin cable and amnioserosa generate a region of almost exclusively compressive deformation at the front (Blanchard et al., 2009). The presence of a contractile actomyosin ring would similarly reveal a region of predominantly tissue compression bordering the eye, even if it were driving passive cell intercalation behind it. Instead, roughly equal tissue compression

and extension are observed throughout the front, similar to what is observed in convergent extension of the *Drosophila* germband and *Xenopus* mesoderm, but restricted to a small region of tissue. Moreover, the profiles of azimuthally averaged strain rates reveal a sharp peak in both compression and extension, indicating that the tissue transitions from a region of very little deformation to a region in which it is maximally compressed perpendicular to and extended along the axis of eyelid closure. By contrast, a global purse string mechanism would display no such peak in tissue extension in the front, while the constriction of an actin cable is expected to reveal a gradual increase in tissue compression and a corresponding decrease in extension toward the front (see [Illustration 3.1](#)). Combined with an analysis of the spreading of the eyelid front over long timescales, this indicates that cell intercalation is coupled to forward translational movement rather than tissue spreading and elongation.

While helpful in identifying the cellular mechanism of eyelid closure, my analysis of strain rates has important limitations. For one, an analysis of the rates of tissue compression and extension captures half of the picture, the other half being the strains associated with cell shape change. Because of the packing of eyelid front cells in multiple layers and the limited resolution afforded by live imaging at an air-liquid interface, it has proven extremely difficult to track cell shape changes in an imaging experiment. While a visual inspection of the behaviors of individual cells reveals no signs of continuous or concerted cell contraction, it remains a distinct possibility that shape changes over the course of several hours cooperate with cell intercalation to drive eyelid closure. In the future, this analysis may be facilitated by genetic sparse-labeling with multiple membrane-targeted fluorophores, either by injecting embryos with a mixture of lentivirus or using “Brainbow” mice (Livet et al., 2007).

An analysis of strain rates also makes no claim as to the sufficiency of front cells for eyelid closure. Ideally, such an argument would be made by a combination of simulation informed by biophysical measurements and functional analyses *in vivo*. Simulating intercalation in varying regimes of cell-cell adhesion would yield valuable insight into the balance of cell motility and adhesion necessary to translate cell intercalation into the forward movement of

3.3. DISCUSSION

a tissue. If the relative adhesion of front cells to each other and to the surrounding epidermis could be quantified along with the force required to move the eyelid, perhaps by measuring the deflection of a calibrated glass pipette (Francis et al., 1987), it would also indicate whether the opposing movements observed throughout the front are sufficient to drive the process.

As these physical measurements would likely be difficult to obtain and simulations would take considerable time to develop, I focused instead on the arguably more important experimental validation of the hypothesis that front cell intercalation drives eyelid closure. Laser ablation of subsets of cells in the eyelid provided direct evidence that the front is necessary for the forward movement of the eyelid and the source of a pulling force that stretches the tissue toward the eye. It also ruled out potential contributions from the underlying corneal epithelium, cell shape changes in the conjunctiva, and forces from filopodial zippering in eyelid canthi.

While the elongation of epidermal cells in close proximity to the front along the axis of closure was useful as a means of testing the presence of a pulling force, it is important to note that, although significant compared to distant cells, it was minor in comparison to the stretching of the lateral epidermis that occurs in dorsal closure (Kiehart et al., 2000). This is consistent with the conversion of pulling forces into translational movement of the whole eyelid rather than the stretching of epidermal cells over the eye. As cells likely become elongated only over long timescales, it is also consistent with the comparatively low rates of tissue compression and extension observed behind the front during live imaging.

In support of this, ablating a region of the epidermis immediately adjacent to the front, untethering the population of intercalating cells from the eyelid, resulted in a decreased rate of closure. This indicates that intercalating cells need to be physically connected to the eyelid to drive closure and suggests a complex interplay between cell-cell and cell-ECM adhesion in maintaining tissue cohesion while permitting active cell movement. In total, the combination of a quantitative analysis of cell movement and tissue deformation with laser ablation to test their functional importance supports a model in which forces from active

cell intercalation are leveraged to tow the surrounding epidermal sheets. It is the functional equivalent of a purse string achieved by a fundamentally distinct mechanism.

3.4 Experimental procedures

3.4.1 Laser ablation

Tissue ablations were performed on a Zeiss LSM 510 NLO system using a Ti:sapphire laser (Chameleon Ultra, Coherent Scientific) tuned to 800 nm. Laser power and dwell time were calibrated per experiment, but were typically performed between 80–100% transmission using scan speed 6 and 50–75 repetitions (~ 90 – 140 μ s dwell time; see [Figure 3.5](#)). Quantification of the effects of ablations was performed by manually tracing the border of the eyelid every 10 frames, fitting a spline to the points, and calculating the average distance traveled using numerical integration in MATLAB.

3.4.2 Image analysis and quantification

Immunostaining and imaging were performed as described earlier. Global analysis of cell polarity in the eyelid was performed by 3D imaging of whole-mounts from *K14-H2B-GFP*-expressing embryos stained with GM130 or pericentrin. Nuclei were filtered using a 3D bandpass filter, and GM130 or pericentrin spots were filtered using a median filter to merge puncta into a single region. Both channels were segmented independently in 3D, and pericentrin spots were assigned to the nearest nucleus. A cell’s axis of polarity was defined by the vector connecting the centroid of a nucleus to the location of the nearest GM130 or pericentrin spot.

Measurements of cell elongation around the eye were performed using custom MATLAB scripts, in which cells were segmented based on cortical actin staining or mGFP expression using a watershed algorithm. Each watershed region was considered a cell, and the elongation and orientation of cells were determined by computing central moments us-

3.4. EXPERIMENTAL PROCEDURES

ing built-in functions of the MATLAB Image Processing Toolbox. Elongation is defined as $1 - W/L$, where W and L are the major and minor axes, such that very elongated cells take on values close to one.

For determining cell-cell coordination in eyelid front cells and the surrounding epidermis, a Delaunay triangulation was used to connect cells to their nearest neighbors. The cosine similarity between velocity vectors of cell pairs at varying distances was computed using $\cos\theta = \frac{\mathbf{v}_1 \cdot \mathbf{v}_2}{|\mathbf{v}_1||\mathbf{v}_2|}$. With this metric, cells moving with similar speeds and directions take on positive values, while those moving in opposite directions take on negative values.

PIV analysis was performed in PIVLab (Thielicke, W., and E. J. Stamhuis., 2013).

3.4.3 Tissue strain rate analysis

To quantify tissue deformations during eyelid closure, I collaborated with Vijay Krishnamurthy and Stephan Grill at the Max Planck Institute. We used PIV to infer the velocity field of the tissue, $\mathbf{v} = (v_x, v_y)$, where v_x and v_y are the components along the x and y -directions, respectively. We next computed the velocity gradient tensor L , defined by

$$L = \begin{pmatrix} \partial_x v_x & \partial_y v_x \\ \partial_x v_y & \partial_y v_y \end{pmatrix}$$

The components of L measure the variation of the velocity field in space. For example, $L_{xy} = \partial_x v_y$ is the variation of v_y along the x -direction. The strain-rate tensor ε is the symmetric part of L . It is defined by

$$\varepsilon = \frac{(L + L^T)}{2}$$

where L^T is the transpose of L . The eigenvalues λ_i and the eigenvectors \vec{u}_i of ε characterize the local deformation of the tissue. The eigenvectors indicate the principal directions of deformation, while the eigenvalues give the rate at which the tissue deforms along these

$$\varepsilon \cdot \vec{u}_i = \lambda_i \vec{u}_i$$

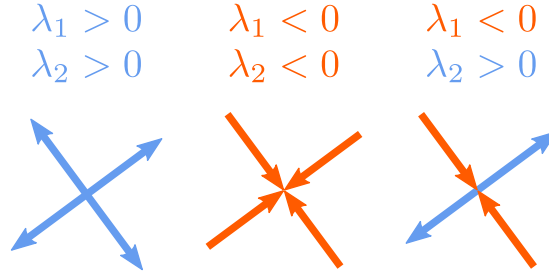


Illustration 3.2: Relationship between tissue deformation and the strain-rate tensor. When both the eigenvalues $\lambda_i > 0$, the tissue extends locally, while if both $\lambda_i < 0$, there is local compressive deformation. The tissue experiences a shear deformation when the eigenvalues are of the opposite sign.

principal directions. Specifically, a positive eigenvalue indicates that locally the tissue is extending while a negative eigenvalue indicates local compressive deformation of the tissue along the direction corresponding to the respective eigenvector (Illustration 3.2).

Notice that since the velocity field \mathbf{v} varies with position, the strain-rate tensor is also a function of position in the tissue. Thus at each coordinate (x, y) , we calculate the eigenvalues (λ_1, λ_2) and the eigenvectors (\vec{u}_1, \vec{u}_2) of the strain-rate tensor ε . A spatial plot of the \vec{u}_i with their lengths proportional to the absolute value of the eigenvalues $|\lambda_i|$ appears in Figure 3.2A. The eigenvectors \vec{u}_i are colored red when $\lambda_i < 0$ and in blue when $\lambda_i > 0$. As is evident from Figure 3.2B, the shear rates $|\lambda_i|$ take on their maximal values in the region of active intercalation. This is also evident from the peak in Figure 3.2B, which shows the variation of the strain-rates (averaged along the transverse direction) with distance from the eyelid front.

3.4.4 Statistical analysis

All statistical analyses were performed as described in Chapter 2.

Chapter 4

Molecular mechanisms underlying eyelid closure

Cell intercalation is one of the most powerful and ubiquitous instruments of tissue deformation in development. In the *Xenopus* mesoderm, it is almost solely responsible for pushing the head from the tail and establishing the elongated body plan of the embryo (Keller et al., 2000). It functions similarly in epithelial tissues, driving germband elongation in *Drosophila* and formation of the primitive streak in amniotes (Voiculescu et al., 2007). In mice, it is required to narrow the two sides of the neural plate, enabling it fold and form a tube, with deadly consequences if it fails to do so (Nishimura et al., 2012). Given the variety of tissues in which cell intercalation operates, it is perhaps not surprising that the details of its execution vary. In epithelial tissues, it typically involves a planar-polarized remodeling of D–V-oriented cell junctions, leading to the formation of multicellular rosettes whose resolution elongates the tissue along the A–P axis. By contrast, more loosely-connected mesodermal tissues intercalate by polarizing their movements along the D–V axis. It is thought that these cells extend tractive, mediolaterally-oriented protrusions that allow cells to pull each other into file. Whereas disruption of epithelial cell intercalation involves a loss of polarized myosin II activity along D–V junctions, defects in mediolateral intercalation often involve a randomization of cell protrusive activity (Davidson et al., 2006). In certain contexts, the non-canonical Wnt/PCP pathway regulates both modes of intercalation (the exception being germband elongation).

The morphology of eyelid front cells and their extension of mediolateral protrusions

naturally suggest that they intercalate by an analogous mechanism to mesodermal cells, with integrin–fibronectin adhesion serving as a means for cells to gain traction on their neighbors. However, even in mesodermal tissues, the role of integrin adhesion is complex. In *Xenopus*, it has been suggested that $\alpha_5\beta_1$ integrin/fibronectin adhesion attenuates cadherin-based cell–cell adhesion (Marsden and DeSimone, 2003), and that both overexpression and depletion of cadherins causes defects in convergent extension (Delarue et al., 1998). Thus, a complex interplay between integrin- and cadherin-based adhesion is likely at play in cell intercalation. PCP appears to be involved both directly, in orienting cell protrusive activity and cell–cell adhesion, and indirectly, in organizing the fibronectin matrix with which mesodermal cells have contact (Dzamba et al., 2009).

To explore the molecular mechanisms underlying eyelid closure, I examined the relative roles of integrin and cadherin-based adhesion using a combination of lentiviral-mediated knockdowns and conditional knockout mice. I found that, whereas $\alpha_5\beta_1$ and myosin II-dependent cell motility is required for eyelid closure, further reducing levels of cell–cell adhesion in the eyelid by knockdown of E-cadherin has no effect. I substantiate this further by analyzing the knockdown of P-cadherin, which is redundant with E-cadherin in the skin but not well-expressed in the eyelid front, and the combined loss of E-cadherin and P-cadherin. Even when epidermal architecture is compromised by the loss of both cadherins in the skin, eyelid closure proceeds to some extent, suggesting that the process is more reliant on cell intercalation mediated by integrin-fibronectin adhesion. Finally, I explore potential roles for Wnt/ β -catenin signaling and PCP in eyelid closure. Both prior to and during eyelid closure, canonical Wnt signaling is indeed active, particularly at the junction where the eyelid epidermis meets the front. This suggests a role for Wnt signaling upstream of the cell intercalation driving eyelid closure, perhaps in mediating the formation of the front. PCP, on the other hand, affects cell intercalation in the eyelid but not specification of the front. This suggests an intriguing interplay between these two pathways in orchestrating eyelid closure.

4.1 Integrin and cadherin-based adhesion in eyelid closure

If intercalation of front cells were truly the driving force of eyelid closure, as my mathematical analyses and laser ablation studies suggested, then perturbing the molecular processes underlying their movement should halt the process. One of the most significant changes that occurs in the eyelid front at the onset of closure is the specific upregulation of fibronectin and its receptor $\alpha_5\beta_1$ -integrin, and a concomitant downregulation in E-cadherin expression (Section 2.1.1 and 2.2.3). This, along with the mediolateral protrusive activity observed by live imaging, suggested a mode of cell intercalation not by the planar polarized remodeling of cell junctions, as typically observed in epithelial tissues, but a mode reminiscent of convergent extension movements in mesodermal tissues. Although mediolateral intercalation in these tissues primarily utilizes integrin adhesion either as a source of traction or to orient cell protrusive activity, they must retain some level of connectivity through cadherin-based adhesion, and both overexpression and downregulation of cadherins lead to defects in convergent extension (Lee and Gumbiner, 1995; Zhong et al., 1999). Integrin expression has also been linked to an indirect role in reducing cell–cell adhesion to a permissible level (Marsden and DeSimone, 2003). To explore these parallels further, I performed *in vivo* loss-of-function experiments of both integrins and cadherins.

4.1.1 Loss of integrin-fibronectin adhesion prevents eyelid closure

The loss of fibronectin and α_5 integrin in mouse embryos leads to early embryonic lethality. The embryos exhibit severe mesodermal defects, with incomplete development of the notochord and somites, as well as defects of the heart and brain (George et al., 1997; Yang et al., 1993). As a result, the role of α_5 integrin and fibronectin in skin morphogenesis has not been examined. To generate a skin-specific loss-of-function, I injected lentivirus carrying shRNAs against fibronectin and α_5 integrin into E9.5 embryos. I first evaluated the mRNA knockdown efficiency of the shRNAs targeting each gene available from the Broad Institute's TRC library by RT-PCR in cultured keratinocytes (Figure 4.1). This typically identified at

least two hairpins with efficiencies greater than 85%. I then cloned the strongest two hairpins into a vector expressing H2B-RFP from a separate promoter to label cells receiving the shRNA *in vivo*, and verified the knockdown in eyelids by whole-mount immunofluorescence. As revealed by the presence of rare, untransduced cells within highly infected eyelid tissue, these shRNAs also resulted in robust knockdown at the protein level (Figure 4.1).

The loss of either fibronectin or α_5 integrin in the skin resulted in a striking eyelid closure defect at E16.5. This was the only obvious defect in the skin, consistent with its established dependency on $\alpha_3\beta_1$, $\alpha_6\beta_4$, and laminin instead of on $\alpha_5\beta_1$ and fibronectin. On close examination, eyelid front cells still displayed their characteristic bipolar, elongated morphology and organized into a multilayered sheet (Figure 4.1). However, tracking cell movements in the eyelid front revealed that these cells moved considerably more slowly than cells transduced with a scrambled-sequence control shRNA (Figure 4.2; $1.73 \mu\text{m/h}$ average speed of transverse movements vs. $\sim 1.3 \mu\text{m/h}$ for mutants, $p < 0.001$). This decrease in cell movement was accompanied by a significantly reduced overall rate of eyelid closure ($6.30 \mu\text{m/h}$ average speed for wild-type vs. $3.61, 2.57, 4.25 \mu\text{m/h}$ for myosin II, fibronectin, and α_5 integrin KD, respectively), based on measurements of eyelid border translocation over time, as well as reduced cell elongation in the surrounding epidermal tissue (0.46 vs. ~ 0.4 for mutants, $p < 0.001$). Thus, a similar result to laser ablation of the eyelid front is achieved by inhibiting cell intercalation through the loss of fibronectin and α_5 integrin.

To further test the specific importance of α_5 integrin, I also knocked down α_v integrin, a fibronectin receptor that has been reported to be expressed in migrating but not stationary epidermal cells (Marchisio et al., 1991). Despite efficient knockdown, no eyelid closure phenotype was observed at E16.5 (Figure 4.3). By contrast, depletion of β_1 integrin, the partner of α_5 , also showed an open eye defect, although its effects were broader, consistent with its partnership with the major epidermal integrin α_3 (Raghavan et al., 2000). These results are in line with the specific importance of α_5 integrin and fibronectin in a wide variety of morphogenetic cell movements in development and homeostasis.

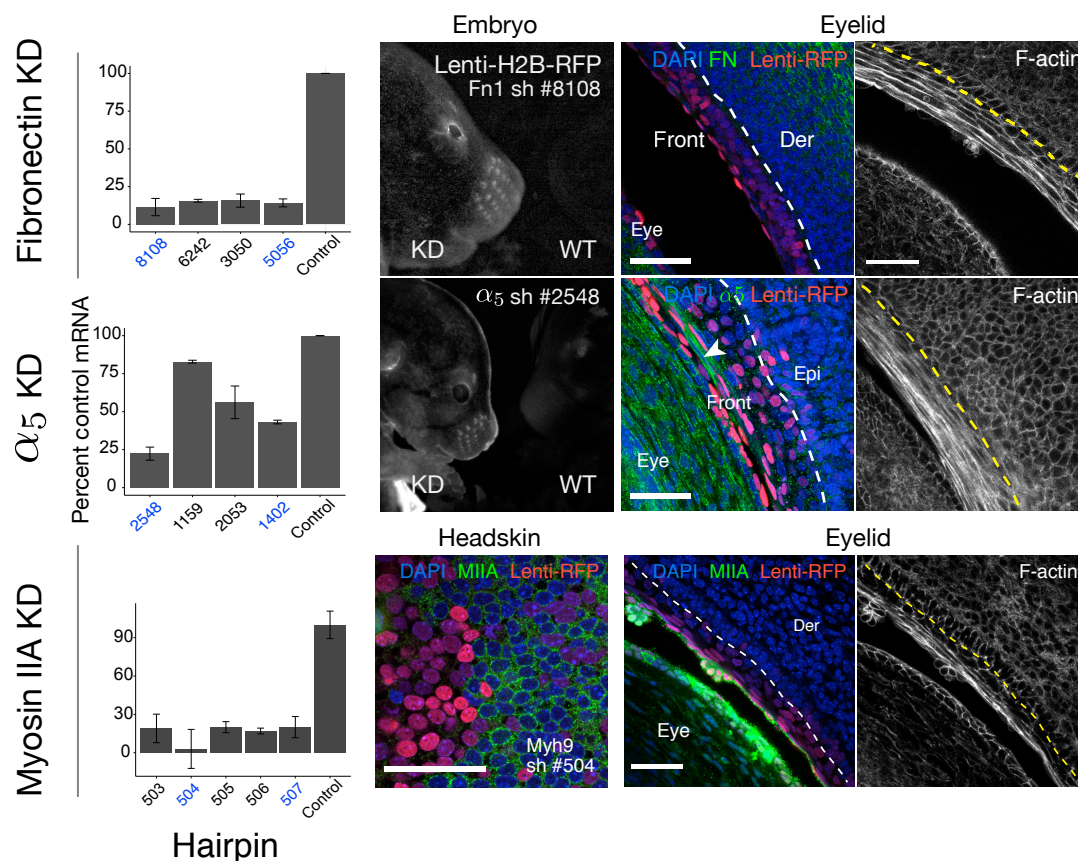


Figure 4.1: Knockdown of fibronectin, α_5 integrin, and myosin IIA in the skin. Left: Quantification of shRNA-mediated knockdown of fibronectin, α_5 integrin, and myosin IIA *in vitro* by RT-PCR. Right: Targeting of embryonic skin is verified by lentiviral H2B-RFP expression in embryos. For each gene, knockdown is illustrated by immunofluorescence in tissue whole-mounts. For α_5 integrin and fibronectin, which are specifically expressed in the eyelid, knockdown is illustrated by loss of staining in the eyelid front. Rare, non-transduced cells exhibiting a positive staining are indicated with arrowheads to confirm the specificity of the knockdown. For myosin II, a mosaic region of the headskin epidermis is shown to illustrate the specificity and effectiveness of the shRNAs used. Whole-mount phalloidin staining illustrates that eyelid front cells still acquire their elongated, bipolar morphology, indicating that motility, rather than specification, is affected. Scale bars, 50 μm .

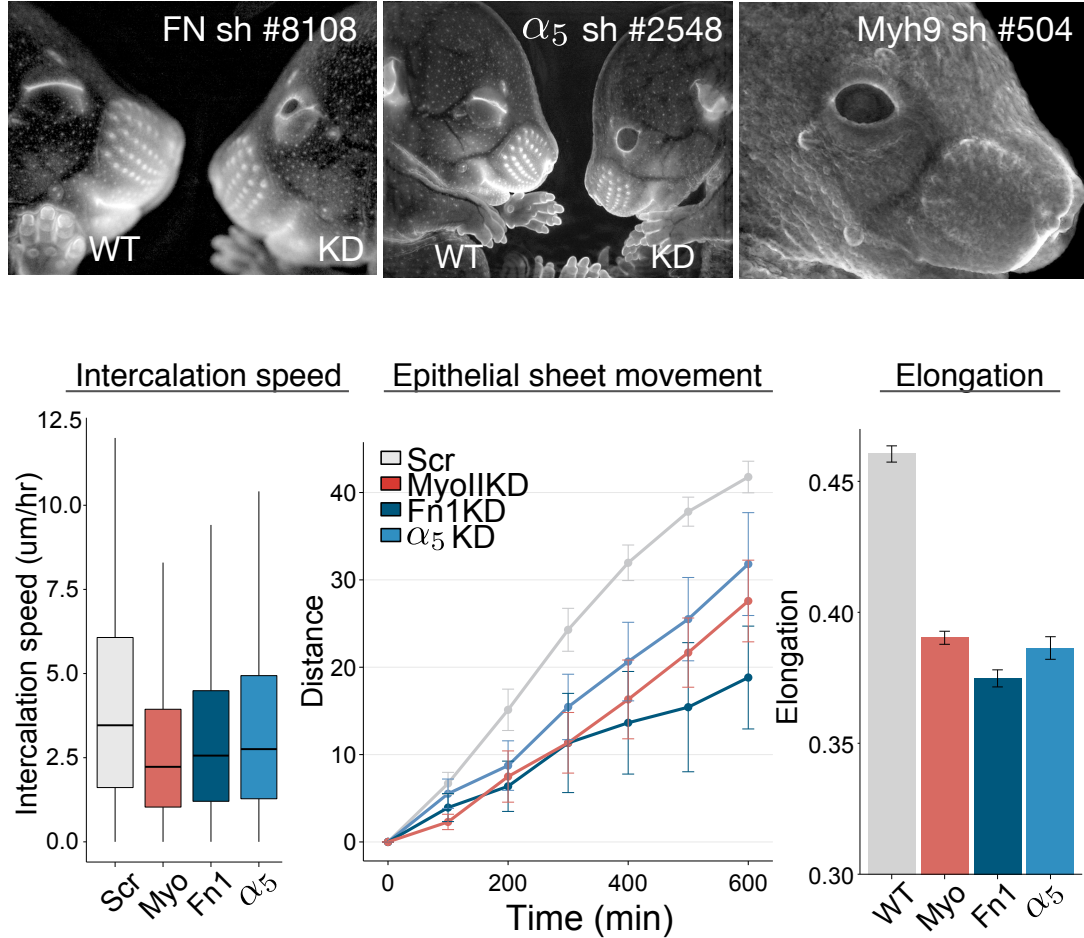


Figure 4.2: Cell intercalation depends on integrin-fibronectin adhesion. The most striking defect in the skin following knockdown of fibronectin, α_5 integrin, and myosin II is the failure of eyelid closure at E16.5 (upper panels). Myosin II KD embryos also exhibit defects in hair follicle morphogenesis and occasional errors in cell division (see also [Figure 4.4](#)). A detailed analysis of eyelid closure reveals that for all mutants, the speed of cell intercalations is substantially reduced compared to a scrambled-sequence control hairpin ($p < 0.001$, ANOVA followed by Tukey's HSD). The overall rate of eyelid closure, measured by following the border of the eye over time, is similarly reduced upon knockdown of either gene ($p = 0.023, 0.0042, 0.071$ for WT vs. myosin II, fibronectin, and α_5 KD, respectively, $n \geq 3$). Analogous (and comparable) to laser ablation of intercalating cells, the elongation of cells in the surrounding epidermis is also reduced ($p < 0.001$).

4.1. INTEGRIN AND CADHERIN-BASED ADHESION IN EYELID CLOSURE

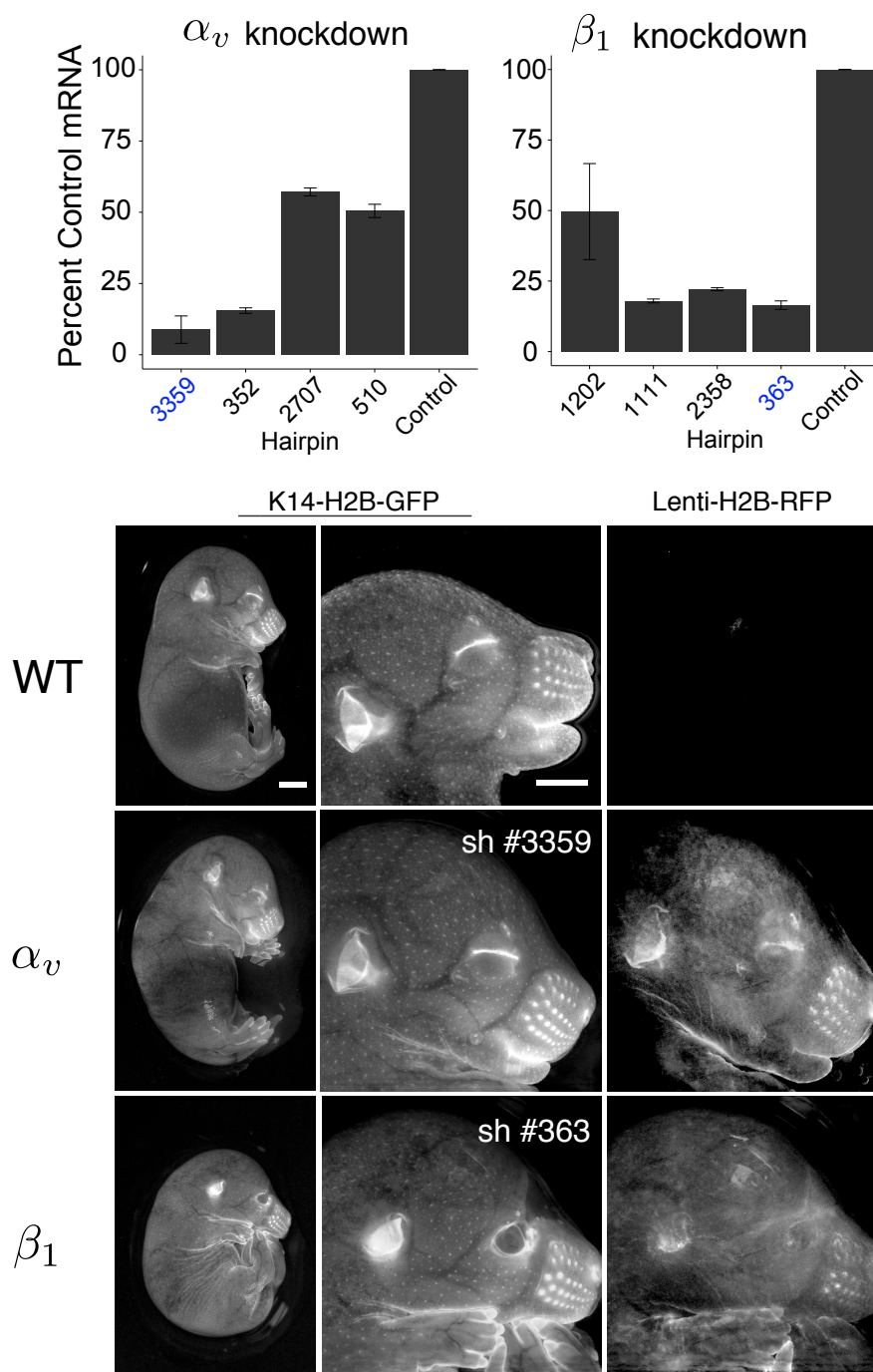


Figure 4.3: Knockdown of additional integrins indicates a specific requirement for α_5 integrin. Knockdown of α_v integrin, a fibronectin receptor that is expressed in the skin but not unregulated in the eyelid, has no effect on eyelid closure. However, knockdown of β_1 integrin, the major part of α_5 , results both in a failure of eyelid closure and in a broad range of skin defects, consistent with its role in adhesion to the basement membrane. This underscores the specific importance of integrin-fibronectin adhesion in mediating eyelid closure through α_5 integrin. Scale bars, 1 mm.

The presence of fibronectin and α_5 integrin at the eyelid front could indirectly promote eyelid closure by stimulating the migration of cells out of the surrounding epidermis rather than by promoting cell intercalation. To address this, I also targeted myosin IIA in the skin, reasoning that this would disrupt cell motility without significantly affecting local signaling or ECM deposition in the eyelid. Similarly to the loss of fibronectin and α_5 integrin, the most obvious defect was a strong inhibition of eyelid closure at E16.5. The epidermis was largely intact and the overall cell architecture, adhesion to basement membrane, and cell–cell junctions were not noticeably perturbed (Figure 4.4), although occasional errors in cell division and a block in hair follicle formation were observed. Tracking of cell movements in the eyelid revealed an even more significant reduction in the speed of cell intercalation, leading to an overall decrease in the rate of closure and significantly reduced cell elongation in the surrounding tissue relative to wild-type (Figure 4.1). This implies a direct role of integrin-ECM adhesion in mediating cell intercalation rather than in acting as a localized signal.

4.1.2 The sufficiency of front cell intercalation for eyelid closure

The lack of defects in the interfollicular epidermis on loss of myosin IIA suggests that, even in skin development, it has a fairly specific role in mediating processes of cell motility. The targeting of myosin IIA specifically in the eyelid front is thus an ideal test of the sufficiency of cell intercalation in driving eyelid closure. To achieve this specificity, I generated lentiviral constructs expressing *Cre* downstream of either the *K17* or *Pax6* promoter. Whereas K17 is expressed in both the eyelid front and hair placodes, Pax6 is expressed in the cornea, lens, and eyelid tissues. To test the specificity of these constructs, I injected *LV-K17-Cre* or *LV-Pax6-Cre* into *Rosa26^{YFP}* Cre-reporter mice and examined the expression of YFP in the eyelid front by whole-mount immunofluorescence. Whereas *Pax6-Cre* was expressed throughout the cornea, front, and surrounding eyelid epidermis, *K17-Cre* was expressed specifically in the eyelid front and hair follicles, and co-localized nicely with K17 protein

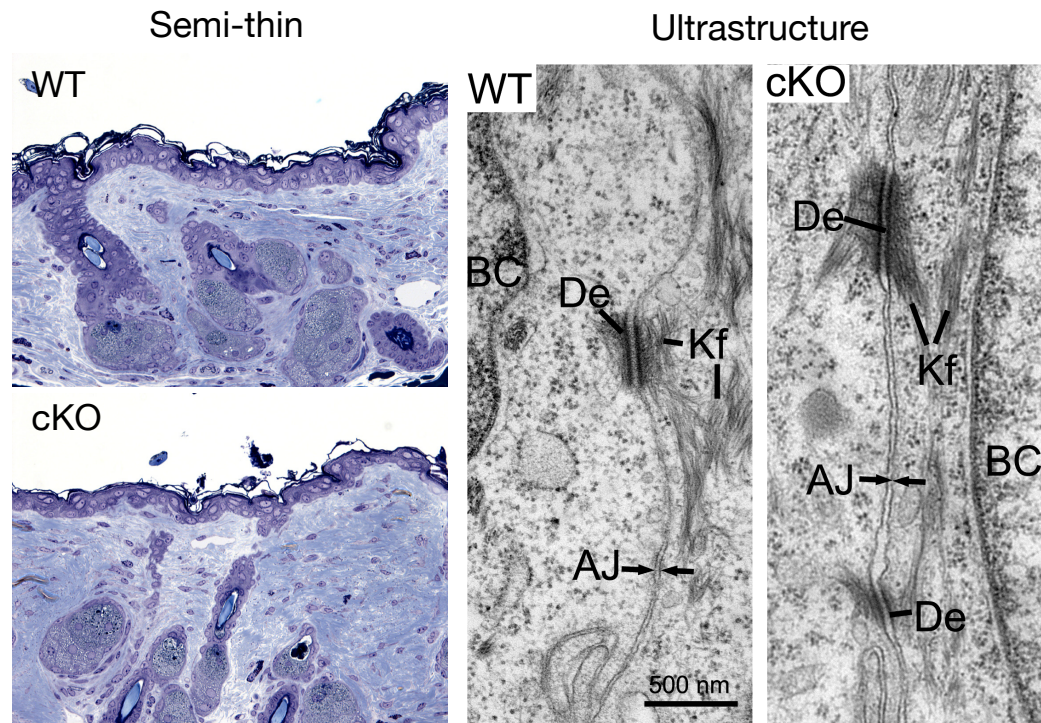


Figure 4.4: Conditional ablation of myosin IIA in the skin does not affect epidermal integrity. Left: Epidermal architecture and differentiation are grossly normal in semi-thin sections from P1 epidermis transduced with shRNAs targeting *Myh9*, indicated by the presence of superficial squamous layers. The most obvious defects are an eye-open-at-birth phenotype, lack of hair follicles, and occasional defects in cell division. Right: Transmission electron microscopy analysis of basal layer cells in P1 epidermis in which myosin IIA is conditionally ablated by mating K14-Cre and *Myh9^{fl/fl}* mice. Cell membranes are completely sealed, and both adherens junctions and desmosomes appear normal. AJ, adherens junction; De, desmosome; Kf, keratin filament. EM images courtesy of Amalia Pasolli.

expression (Figure 4.5A). However, as the K17 promoter is quite large in comparison to Pax6, transduction efficiency was correspondingly lower, although still within an acceptable range.

To abrogate myosin IIA specifically in the eyelid front, I injected *Myh9*^{*fl/fl*} embryos with *LV-K17-Cre* at E9.5. Whole-mount phalloidin staining of eyelids revealed a significant, reproducible defect in closure at E16.5, suggesting that cell movement in the eyelid front is sufficient to drive the process (Figure 4.5B). These results confirm and extend my laser ablation studies, revealing that eyelid closure is driven by localized myosin IIA and $\alpha_5\beta_1$ -dependent cell intercalation.

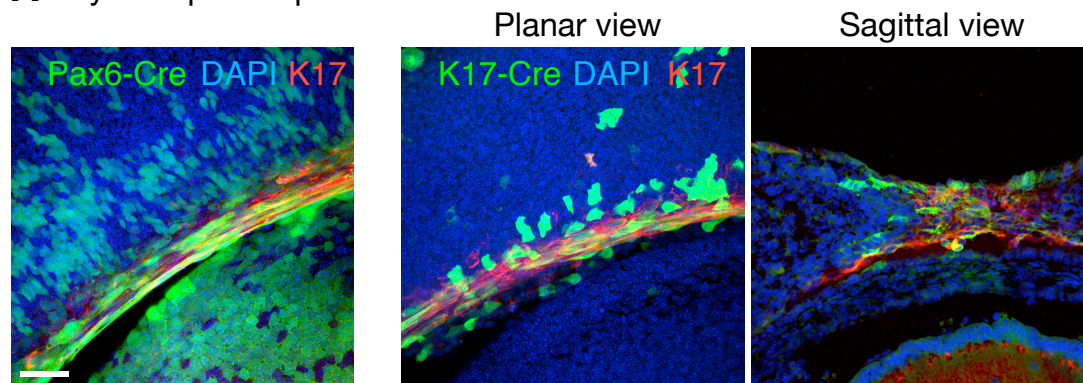
4.1.3 Cadherins in eyelid closure

Previous studies of convergent extension movements suggest that fibronectin can have multiple roles in regulating cell intercalation movements. On the one hand, integrins and fibronectin could be actively required for the necessary shape changes and movements, either for cells to gain traction on their neighbors and the surrounding ECM or to orient protrusive activity. On the other, cell intercalation could primarily be mediated by remodeling of cadherin-based junctions, with integrin-fibronectin signaling functioning passively to reduce cell-cell adhesion to a permissible level (Marsden and DeSimone, 2003). Both scenarios are consistent with an essential role for myosin II.

Adherens junctions and integrins have well-established opposing roles, both in convergent extension movements and in skin development (Livshits et al., 2012). An essential feature of hair follicle morphogenesis, for example, is the downregulation of E-cadherin and concomitant upregulation of P-cadherin (Hirai et al., 1989). If E-cadherin is overexpressed in the skin, hair follicle placodes do not form (Jamora et al., 2003). E- and P-cadherin are the predominantly-expressed cadherins in the skin and are partially redundant. Loss of E-cadherin is only mildly phenotypic due to a compensatory upregulation of P-cadherin, leading to progressive hyperplasia and degeneration of certain layers of the hair follicle in

4.1. INTEGRIN AND CADHERIN-BASED ADHESION IN EYELID CLOSURE

A Eyelid-specific promoters



B Eyelid-specific knockdown of myosin IIA

Myh9^{fl/fl} + LV-K17-Cre



Assay eyelid closure
at E16.5

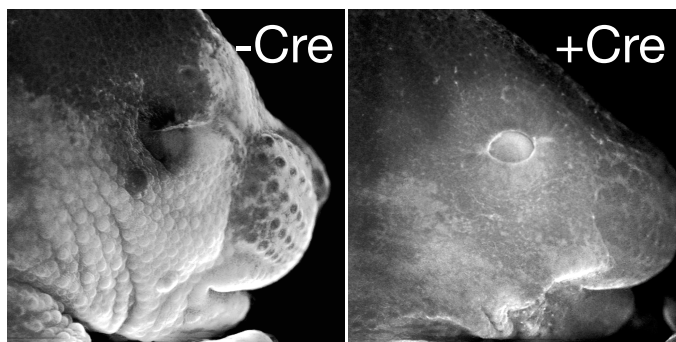


Figure 4.5: Front cells are sufficient to drive eyelid closure. (A) Cre expression was specifically targeted to the eyelid front by generating lentiviral constructs in which *nls-Cre* is driven by the Pax6 or K17 promoter (*LV-K17-Cre* and *LV-Pax6-Cre*, respectively). Injection of these constructs into *Rosa26^{YFP}* Cre-reporter mice reveals that, while Pax6 drives Cre throughout the front and surrounding eyelid epidermis (left), K17-Cre is expressed specifically in the front (right). (B) Injection of *LV-K17-Cre* into *Myh9^{fl/fl}* embryos results in an open-eye phenotype at E16.5 and a loss of hair follicle bumps (4/4 injected embryos vs. 6 WT littermates). This indicates that cell intercalation in the eyelid front is sufficient to drive the process.

adulthood (Tinkle et al., 2004). Likewise, in P-cadherin KO mice, the only major phenotype reported is a precocious development of mammary glands (Radice, 1997). Only the combined loss of both cadherins or the loss of α -catenin, which links the cadherin complex to the actin cytoskeleton, lead to defects in AJ formation and epidermal integrity (Tinkle et al., 2008).

Given the upregulation of fibronectin and α_5 integrin and the transcriptional downregulation of E-cadherin in the eyelid, I examined the potential role of cadherins in eyelid closure. While FACS isolation and RT-PCR profiling revealed a transcriptional downregulation of E-cadherin (Section 2.2.3), it was still clearly visible throughout the eyelid front by immunofluorescence in sagittal sections and whole-mounts (Figure 4.6A). P-cadherin, on the other hand, was virtually absent from the front and expressed only in superficial periderm cells and the basal layer of the surrounding epidermis.

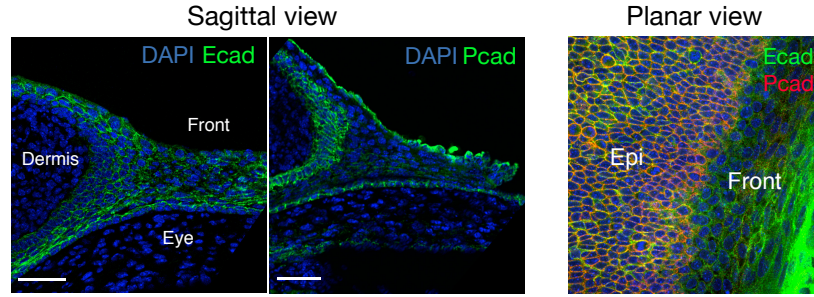
Disruption of adherens junction formation in the skin through loss of α -catenin is known to compromise eyelid closure (Vasioukhin et al., 2001), likely through an overall loss of epidermal integrity, but perhaps also through a role in cell migration (Drees et al., 2005). Taking advantage of the redundancy of E- and P-cadherin in the skin, I further reduced cell-cell adhesion in the eyelid without globally disrupting epidermal architecture by injecting E9.5 embryos with shRNAs against E-cadherin. Immunofluorescence analysis in mosaic regions of the eyelid epidermis revealed a specific, near-complete loss of E-cadherin in transduced cells (Figure 4.6B). Despite markedly diminishing E-cadherin in the eyelid front, however, cell intercalation and eyelid closure progressed similarly to wild-type embryos (Figure 4.6B). This is in contrast to the broader-scale intercalations of convergent extension in *Xenopus*, which require cadherins (Delarue et al., 1998). Interestingly, examination of eyelid morphology by whole-mount immunofluorescence even revealed a potential acceleration of the process in E-cadherin knockdown embryos, evidenced by an increased spreading of front cells over the eye at E15.5 (Figure 4.6C). However, this could also represent a minor defect in the coupling of cell intercalation to pulling forces, leading to increased spreading of front

4.1. INTEGRIN AND CADHERIN-BASED ADHESION IN EYELID CLOSURE

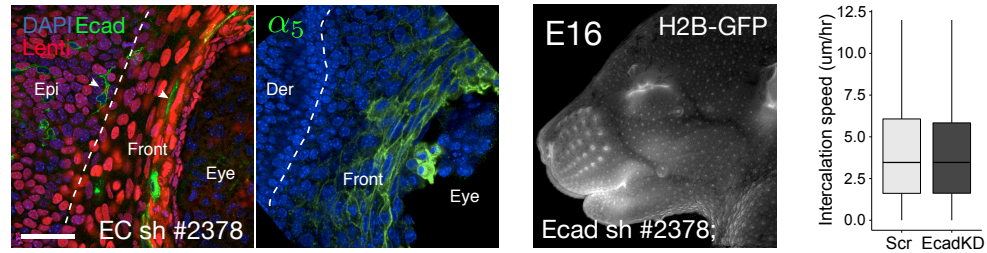
cells at the expense of forward movement of the eyelid. Additional quantitative analyses will be required to differentiate between these possibilities. Importantly, reducing E-cadherin did not cause cells in the surrounding epidermis to express α_5 integrin or to adopt morphological and motile properties of eyelid front cells, indicating that other signaling cues drive these events (Figure 4.6B). Conversely, knockdown of fibronectin or α_5 integrin did not lead to an obvious upregulation of E-cadherin in the eyelid based on immunofluorescence staining, arguing against a secondary role for these proteins in modifying cadherin levels (Figure 4.7).

To further explore the dependence of eyelid front cells on integrin rather than cadherin-based adhesion, I examined eyelid closure in mice lacking either P-cadherin alone or both E- and P-cadherin. Because these genes are tightly linked, classical transgenic technology cannot be used to create a double knockout. I therefore made use of a previously-generated E-cadherin conditional knockout line expressing a robust P-cadherin shRNA from the *K14* promoter (*Ecad^{fl/fl}; PcadRNAi*, Tinkle et al., 2008). *PcadRNAi* mice do not exhibit eyelid closure defects despite a substantial reduction of P-cadherin in embryonic skin (Figure 4.8). Loss of both E-cadherin and P-cadherin by injecting E9.5 *Ecad^{fl/fl}; PcadRNAi* embryos with *LV-Cre* causes clear defects in epidermal architecture, but only a partial defect in eyelid closure at E16.5 (less severe than that observed for myosin II, fibronectin, and α_5 integrin knockdown). These data suggest that cell intercalation in the eyelid is not driven by the dynamic remodeling of either E-cadherin or P-cadherin alone, and that cadherins instead may have a more general role in maintaining epithelial cohesion. To date, injection of *LV-K17-Cre* into *Ecad^{fl/fl}; PcadRNAi* to completely disrupt cell–cell adhesion only in front cells has not produced embryos with eyelid closure defects. While these experiments do not rule out an important role of cadherins in eyelid closure by mediating cell cohesion, they suggest that cell intercalation in the eyelid depends primarily on cell motility and integrin–ECM adhesion rather than on cell junction remodeling. This dependence is in line with the many other similarities between cell intercalation in the eyelid and convergent extension movements in

A Cadherin expression in the eyelid



B E-cadherin KD



C Accelerated eyelid closure in E-cad KD embryos

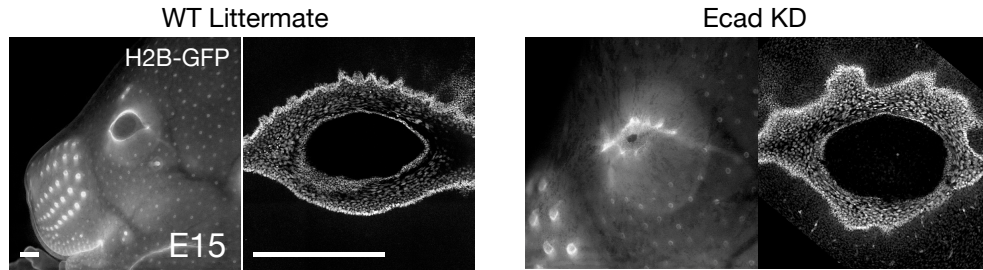


Figure 4.6: Eyelid closure primarily depends on integrin rather than on cadherin-based adhesion. (A) Expression of core adherens junction components in the eyelid (sagittal views). While E-cadherin is present throughout the front, P-cadherin is present in the periderm and surrounding epidermis but absent in front cells. (B) Lentiviral-mediated knockdown of E-cadherin results in near-complete loss of E-cadherin in the eyelid (H2B-RFP expression indicates transduced cells, arrowheads denote rare untransduced cells to indicate specificity). Note that α_5 integrin is still restricted to the eyelid front, indicating that loss of E-cadherin is not sufficient for epidermal cells to acquire the morphological and motile features of front cells (left panels). Eyelids fully close by E16.5 and cell intercalation speed is equivalent to that in embryos transduced with a scrambled-sequence control hairpin. (C) Indications of accelerated eyelid closure in E-cadherin KD embryos. Analysis of eyelid morphology by *K14-H2B-GFP* expression reveals that significantly more of the eye is covered by intercalating front cells in KD embryos than in WT littermates ($n = 4$ mutants, ≥ 6 WT). High-magnification images of the eye reveal that the border of KD eyelids is highly irregular, suggesting either that front cells are able to exert greater forces on the surrounding epidermis that accelerate eyelid closure, or that the coupling of cell intercalation to translational movement of the eyelid is defective, leading to tissue spreading. Scale bars, 50 μm .

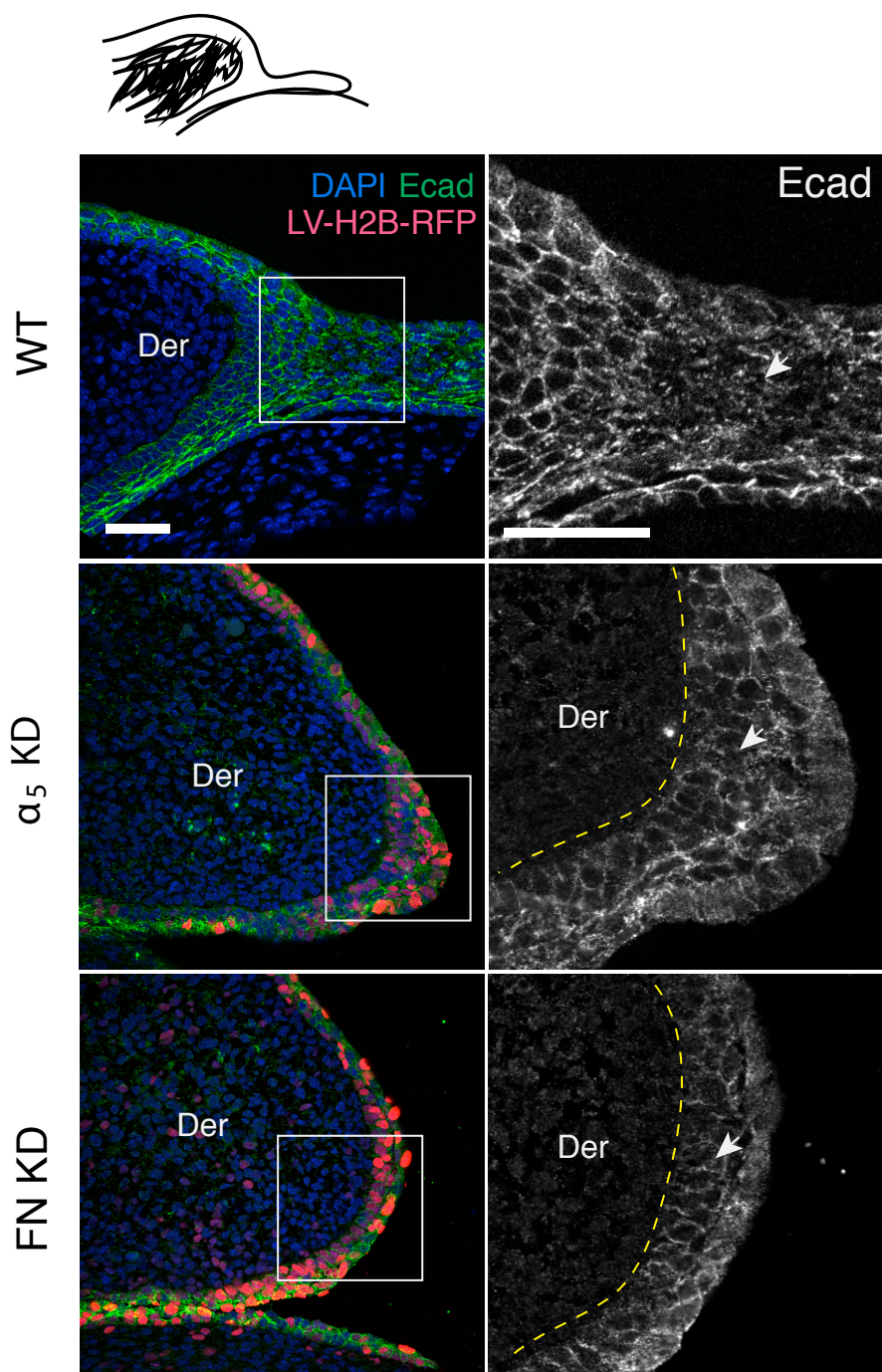


Figure 4.7: E-cadherin is not upregulated in the absence of fibronectin or α_5 integrin. Analysis of E-cadherin expression in sagittal sections of E15.5 fibronectin and α_5 integrin knockdown embryos does not reveal an obvious upregulation of E-cadherin. Left panels illustrate infectivity in the eyelid, right panels are magnified views of transduced cells in the front with normal E-cadherin levels. This suggests that integrin-fibronectin adhesion is directly required for cell intercalation rather than acting to reduce levels of cell-cell adhesion. Scale bars, 50 μ m.

mesodermal tissues.

4.2 Canonical and non-canonical Wnt signaling in eyelid closure

Both canonical and non-canonical Wnt signaling play essential roles in morphogenesis. Non-canonical Wnt signaling and the PCP pathway are well-known for their spatial control of actomyosin dynamics in epithelial and mesenchymal convergent extension movements and in the generation of polarized epithelial structures (Section 1.4.4). Canonical Wnts, on the other hand, are well-known upstream regulators of EMTs and drive many processes of cell migration, proliferation, and sorting, perhaps by a concurrent role in cell fate specification (Section 1.3.1). In eyelid closure, both are likely to play a role, as defects have been reported in mice harboring mutations in canonical (Gage et al., 2008; Wu et al., 2012) and non-canonical Wnts (Curtin et al., 2003a).

Following up on a study implicating Wnt/ β -catenin signaling in specifying migratory cells in the eyelid (Wu et al., 2012), I examined Wnt activity prior to and during eyelid closure in whole-mount and sagittal sections using BATGAL Wnt reporter mice and *LV-TOPGFP*, a lentiviral Wnt reporter (Beronja et al., 2013). At E14.5, BATGAL expression revealed a population of Wnt-responsive cells in the region of the eyelid that shows early expression of fibronectin and α_5 integrin and eventually gives rise to the front (Figure 4.9A). During closure, *LV-TOPGFP* expression revealed high Wnt activity both in the eyelid epidermis and throughout the front. This suggests an important role in the acquisition or maintenance of intercalary behavior in eyelid front cells. Given that fibronectin upregulation and E-cadherin downregulation are frequent consequences of Wnt signaling, a particularly compelling view is that it mediates the transcriptional changes underlying the transition of front cells to a motile fate. In agreement with this, live imaging E14.5 and E15.5 eyelids in which cells are sparsely-labeled with cytoplasmic YFP reveals occasional cells detaching from the eyelid epidermis and elongating along their mediolateral axis (Figure 4.9B). Localized Wnt signaling may therefore direct formation of the eyelid front by a process of

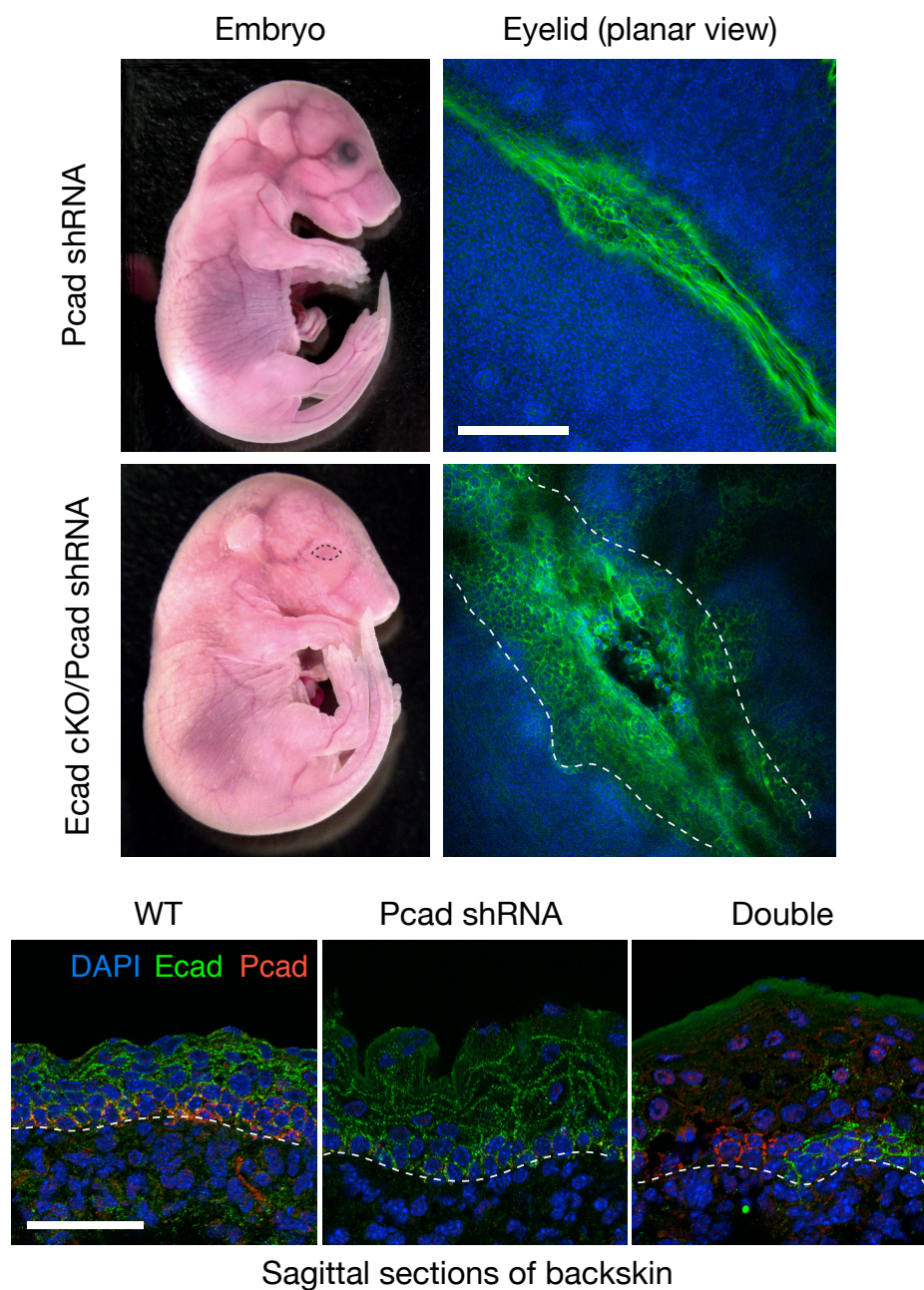


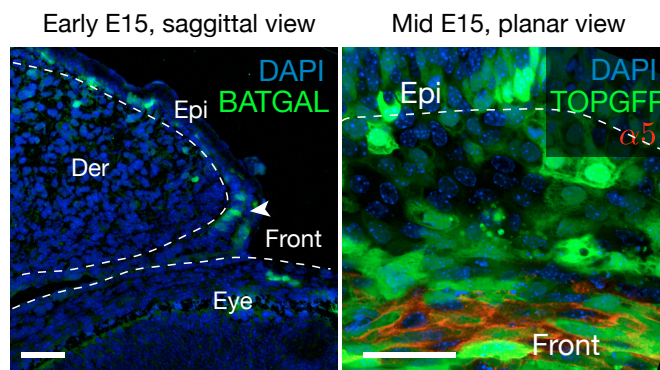
Figure 4.8: Epithelial cohesion is necessary for eyelid closure. Similar to loss of E-cadherin in the skin, knockdown of P-cadherin by the transgenic expression of a robust P-cadherin shRNA driven by the *K14* promoter has no eyelid closure phenotype. Loss of both E- and P-cadherin by injecting *LV-Cre* into *Ecad^{fl/fl}; PcadRNAi* mice, however, results in a partial eyelid closure defect at E16.5, as well as an overall loss of epidermal integrity (note the flaky appearance of the skin in the brightfield stereomicroscope image). This suggests that cadherins play a secondary role in eyelid closure by maintaining epithelial cohesion. Bottom panels illustrate the loss of E- and P-cadherin in embryonic skin in sagittal section. Scale bar, 300 μm (A), 50 μm (B).

stochastic delamination that occurs between E14.5 and E15.5.

In mice, non-canonical Wnt signaling plays an essential role in neural tube closure, where it regulates epithelial cell intercalation and apical constriction, polarization of stereocilia bundles in the inner ear, and the orientation of hair follicles in the skin (Section 1.4.4). Fzd3/Fzd6 double mutants (Stuebner et al., 2010), and mutants of *Celsr1* (Curtin et al., 2003b), *Vangl2* (Murdoch et al., 2001), *Dvl2* (Hamblet, 2002), and *Scribble* (Scrib, Murdoch et al., 2003), a protein typically associated with apical-basal polarity but that also functions in PCP and cell migration, also exhibit defects in eyelid closure. However, these mice exhibit multiple embryonic defects leading to early lethality, including craniorachischisis, in which the brain and spinal cord are fully exposed from failure to initiate neural tube closure, and gastroschisis, a protrusion of internal organs through the abdomen. It is thus unknown whether the eyelid closure defects are a secondary consequence of these other abnormalities. To address this, I performed lentiviral injections of shRNAs against *Celsr1*, *Vangl2*, and *Scrib* to achieve skin-specific knockdowns. In all three cases, embryos exhibited an eyelid closure defect at E16.5 in the absence of other gross defects (the representative example of *Vangl2* is shown in Figure 4.10A).

In the skin, *Celsr1* and *Vangl2* are planar polarized along the A–P faces of basal cell membranes (Devenport and Fuchs, 2008). As previously reported, disruption of a single core PCP protein is sufficient to disrupt planar polarity. For example, in the *Looptail* (*Lp*) mouse mutant, which harbors a point mutation in *Vangl2* leading to its degradation, *Celsr1* becomes uniformly localized at the cell membrane rather than along the A–P axis. To confirm that lentiviral knockdown of PCP proteins disrupts planar polarity in the skin, I therefore examined the localization of *Celsr1* in clones of *Vangl2* KD cells in embryonic backskin by whole-mount immunofluorescence. In contrast to its strong anterior-posterior enrichment in the cells of uninfected littermates, *Celsr1* localization was disrupted in *Vangl2* KD cells (Figure 4.10B). This indicates that lentiviral knockdown of PCP proteins in the skin faithfully disrupts PCP, and implies that PCP plays a specific role in eyelid closure.

A Wnt reporters



B Cell delamination in eyelid closure

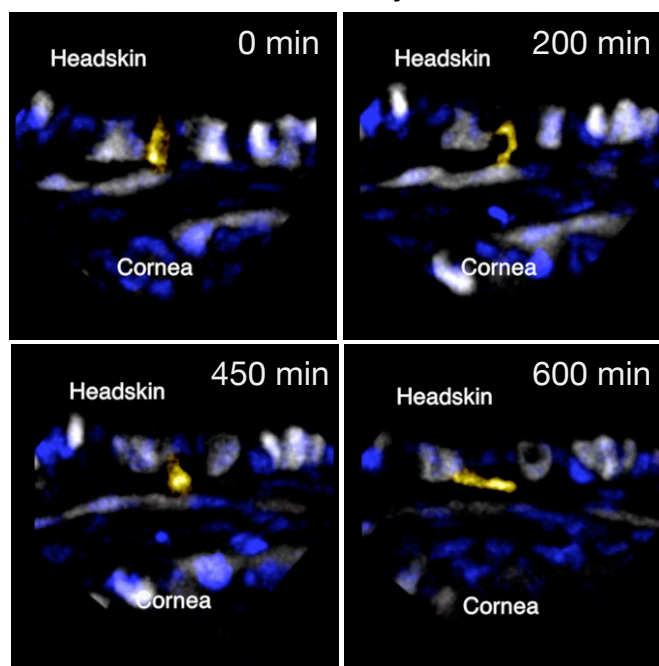


Figure 4.9: Canonical Wnt signaling in the eyelid. (A) Immunofluorescence analysis of Wnt reporter activity in the eyelid. Left, sagittal section of an eyelid from a BATGAL embryo at early E15, illustrating Wnt-responsive cells at the junction between the eyelid front and surrounding epidermis. Right, planar view of an E15.5 eyelid transduced with a lentiviral Wnt-reporter (*LV-TOPGFP*). Note the significant concentration of Wnt-responsive cells at the eyelid/epidermal junction as well as in the eyelid front. (B) Proposed role of Wnt signaling in the acquisition of intercalary behavior by front cells. Sparse-labeling cells in the eyelid front with cytoplasmic YFP by injecting *Rosa26^{YFP}* with low-titer LV-Cre and live imaging reveals the occasional detachment of cells from the eyelid epidermis. Upon entering the front, they rapidly elongate along their mediolateral axis. This phenomenon can also be observed at E14.5, raising the possibility that local Wnt signaling promotes the stochastic detachment of cells from the epidermis to form the eyelid front between E14.5 and E15.5. Scale bars, 50 μ m.

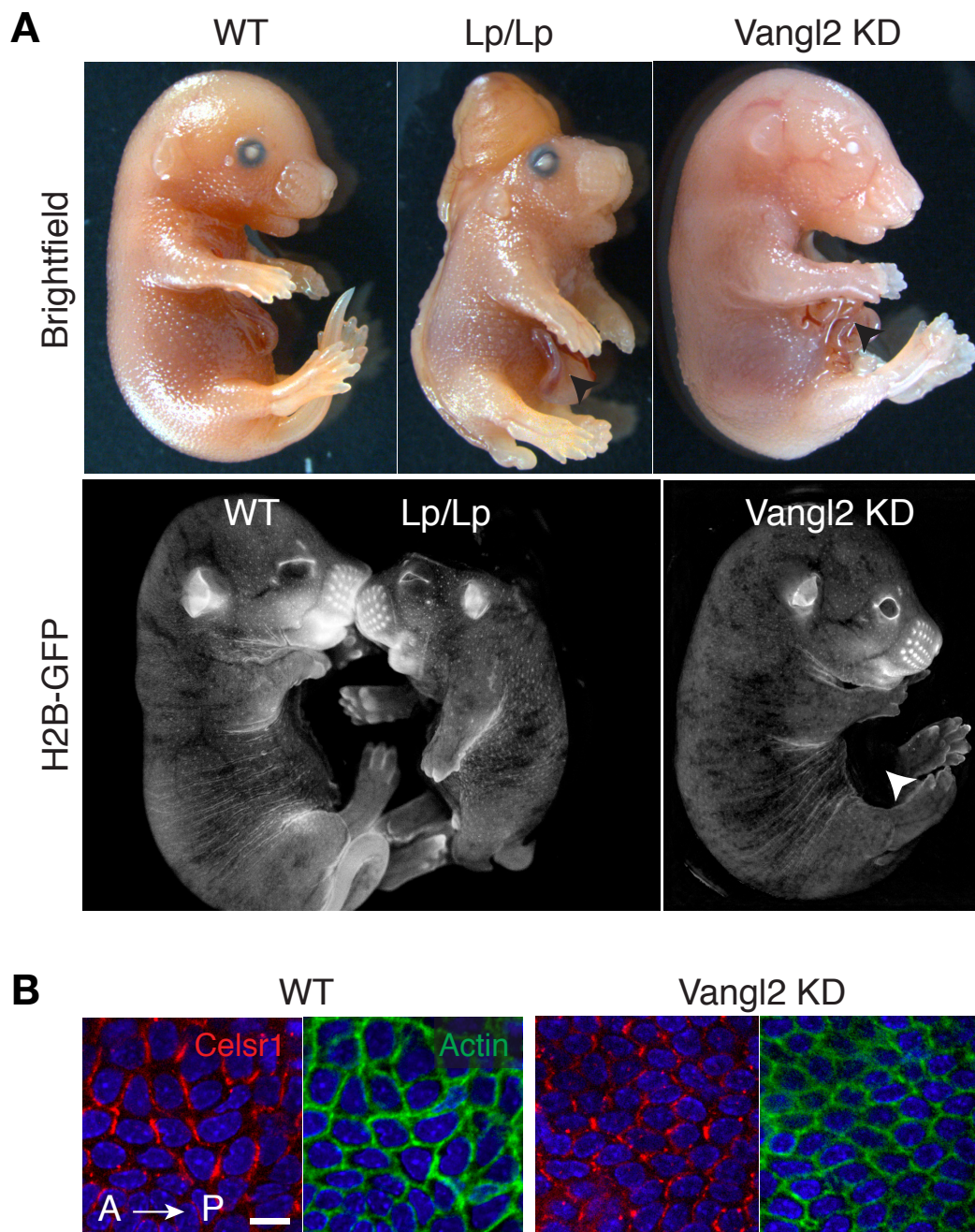


Figure 4.10: Non-canonical Wnts/PCP in the skin are required for eyelid closure. (A) Skin-specific knockdown of the core PCP protein, Vangl2 (Van gogh/Strabismus), results in an eyelid closure defect at E16.5. This indicates the eyelid closure defects of PCP mutants are not a secondary consequence of other embryonic abnormalities and that PCP has a specific function in regulating the process. (B) Whole-mount immunofluorescence of Celsr1 localization in embryonic headskin to confirm that lentiviral knockdown of Vangl2 disrupts PCP in the skin. In wildtype embryos, Celsr1 is strongly polarized along the A-P axis (left), but becomes uniformly distributed upon loss of Vangl2 (right). Scale bar, 50 μ m.

4.2. CANONICAL AND NON-CANONICAL WNTS

Lp mice exhibit the most severe defects of the available PCP mutants. To better understand the role of PCP in eyelid closure, I generated a *Lp/K14-H2B-GFP* mouse line, which allows the simple visualization of eyelid closure defects and avoids potential issues of mosaicism inherent to lentiviral injection. To my surprise, I found that loss of PCP delayed rather than prevented eyelid closure. Normally finished by mid E16.5, *Lp/H2B-GFP* mice instead complete the process by late E17.5 in spite of severe neural tube closure defects (Figure 4.11A). To ensure this delay was related to a specific effect on eyelid closure, I quantified proliferation and apoptosis in the skin by FACS. Using EdU incorporation and caspase-3 staining as readouts, I observed no differences compared to wild-type littermates (Figure 4.11B).

In *Xenopus* convergent extension, PCP is required both for the organization of the fibronectin matrix as well as for the mediolateral polarization of cell protrusions. In *XStbm* (*Vangl2*) mutants, cells in mesodermal explants fail to elongate mediolaterally and display random protrusive activity. I therefore analyzed the morphology of eyelid front cells in *Lp* embryos. Immunofluorescence in whole-mounts revealed that, similarly to knockdown of fibronectin and α_5 integrin, front cells still adopt a bipolar morphology and are highly elongated perpendicularly to the axis of closure (Figure 4.11B). They also express both K17 and fibronectin, indicating that their specification is fully intact. However, the presence of these cells in only a thin layer bordering the eye indicates that they fail to intercalate, suggesting a defect in cell movement or an upstream defect in fibronectin remodeling. Together, these results uncover a fascinating interplay between canonical Wnt signaling, which likely plays a role in the specification of the eyelid front, and non-canonical Wnts, which may play a role in the motility of front cells by regulating cell protrusive behavior or fibronectin matrix organization. A detailed analysis of global and individual cell behaviors in these mutants awaits future study.

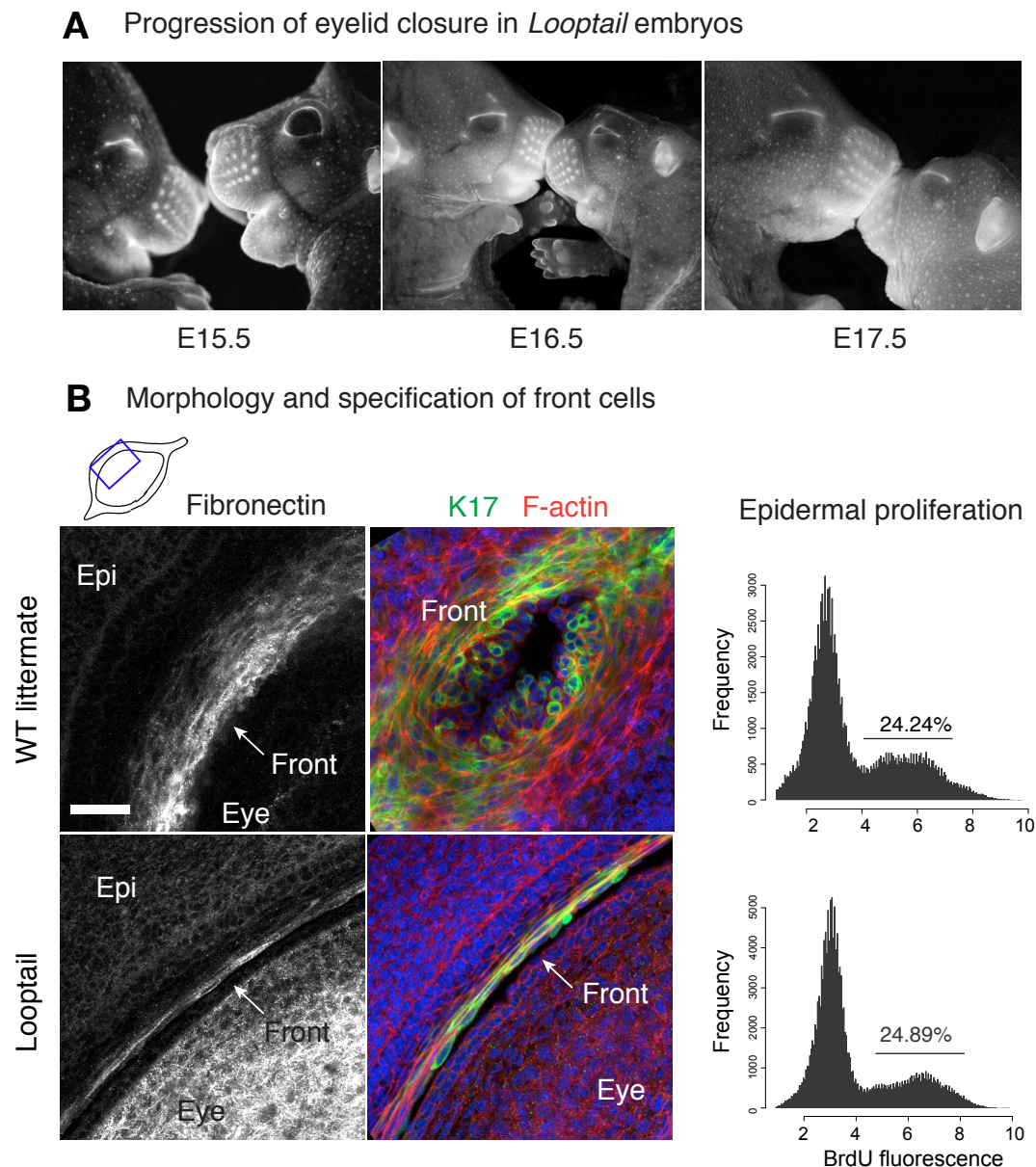


Figure 4.11: Eyelid front cells are specified but fail to intercalate in PCP mutants. (A) Eyelid closure is delayed, but not completely inhibited, in PCP mutants. Eyelid closure was monitored in *Looptail/K14-H2B-GFP* mice, revealing that the process is delayed by 24 h relative to wildtype littermates. Eyelids are fully fused by E17.5. (B) A defect in cell motility is likely responsible for the delay in eyelid closure of PCP mutants. Whole-mount immunofluorescence reveals that eyelid front cells of E15.5 *Looptail* mutants still express K17 and fibronectin, indicating proper specification, but fail to intercalate. The rate of cell proliferation in the backskin of mutant embryos was equivalent to wild-type, suggesting that loss of PCP in the skin does not cause widespread non-specific defects. Scale bar, 50 μ m.

4.3 Discussion

Cell intercalation is a paradox of sorts in that it requires cells to be connected enough to form a coherent tissue but loose enough to permit small relative movements whose sum leads to substantial tissue elongation. Epithelial tissues solve this by directing the remodeling of specific apical junctions while remaining connected ([Section 1.4.3](#)), while more loosely-connected mesodermal tissues appear to carefully tune levels of cell–cell adhesion through integrin signaling and to intercalate by polarizing their protrusive activity. Both mechanisms are regulated by the non-canonical Wnt/PCP pathway in certain contexts by localizing Dsh and compartmentalizing the activity of myosin II through ROCK, or actin polymerization through Rac and Cdc42. This, in turn, orients cell junction shrinkage, protrusive activity, or polarized ECM remodeling.

Both morphologically and in terms of its reliance on integrin-fibronectin adhesion, cell intercalation in the eyelid front bears more resemblance to the mediolateral intercalations of the dorsal mesoderm in *Xenopus*. Loss of fibronectin, α_5 integrin, and myosin IIA in the eyelid all result in eyelid closure defects without affecting the specification of front cells. In all three cases, cells adopt a highly elongated, bipolar morphology and express markers associated with the transition to a motile fate, including K17. Multiple lines of evidence suggest that integrin-fibronectin adhesion is directly required for cell intercalation, perhaps as a means for cells to gain traction on one another. Fibronectin expression is restricted to the eyelid front and is the only ECM with which these cells have contact. There are no signs of an organized basement membrane above or below the eyelid over which front cells can migrate—they rest directly on the corneal epithelium. While the local secretion of fibronectin could act as a signal to stimulate the transformation of cells in the surrounding epidermis to a migratory fate, the lack of a specification defect in knockdown mice argues against this. Similarly, loss of α_5 integrin or myosin II is expected to affect cell motility without disrupting the local signaling environment of the eyelid, and knockdown of α_5 integrin and fibronectin does not cause an obvious upregulation of E-cadherin. This argues against

a secondary role for integrin adhesion in reducing cadherin expression and suggests that it is directly required for cell intercalation.

While the requirement of cadherin-based cell–cell adhesion in eyelid closure is apparently complex, at minimum my studies argue that, fundamentally, the cell intercalation that occurs is integrin- rather than cadherin-dependent. In contrast to convergent extension in *Xenopus*, when E-cadherin is depleted in the skin, eyelid closure proceeds unaffected and even shows signs of acceleration. However, this experiment relies on the redundancy of E- and P-cadherin expression in the skin. Whereas both cadherins are expressed in the epidermis, only E-cadherin is substantially expressed in the eyelid front, and thus knockdown of E-cadherin is expected to reduce cell–cell adhesion in the eyelid without affecting the integrity of the epidermis as a whole. Low levels of P-cadherin in the eyelid could nevertheless represent a highly dynamic pool of cadherins whose remodeling underlies the observed cell intercalation. Diminishing P-cadherin in the skin by transgenic expression of a potent shRNA, however, also does not affect eyelid closure, suggesting that neither E-cadherin nor P-cadherin alone is necessary. Depletion of both cadherins does cause an eyelid closure defect, but at the same time results in a loss of epidermal integrity. The eyelid closure defect in this case is less severe than that observed for the knockdown of fibronectin, α_5 integrin, or myosin II, suggesting that cadherins are more important for their general role in maintaining epithelial cohesion than a specific one in eyelid closure.

Of course, in order for the pulling forces generated by cell intercalation to be transmitted to the eyelid, the front cells must be connected in some way to the surrounding epidermis. It will therefore be important to address the potential redundancy of E- and P-cadherin by using tools to specifically deplete them in the eyelid. Efforts are currently underway to generate a *K17-Cre* transgenic mouse line, which can be combined with *Ecad^{fl/fl}*; *PcadRNAi* mice to achieve the specific loss of both cadherins in the eyelid, although a lentiviral approach using either *LV-K17-Cre* or *LV-Pax6-Cre* may also prove suitable. While it would be surprising to find that cadherins are not necessary in the eyelid, it is possible that front cells are

4.3. DISCUSSION

primarily connected to the epidermis by desmosomes or strictly through integrin adhesion. Indeed, even when both E- and P-cadherin are depleted from the skin, desmosomes still form in normal numbers and some degree of epithelial cohesion is achieved (Tinkle et al., 2008). The loss of epidermal integrity appears to be the consequence of a combination of factors, including loss of polarity, disorganization of cortical actin, and a disruption of the keratin filament network leading to an overall loss of mechanical stability.

In the context of the eyelid, where a defining feature of front cells is the loss of apicobasal polarity and acquisition of some mesenchymal properties, desmosomes may be more than sufficient to tether them to the surrounding epidermis. It is also not altogether unreasonable that the layers of epidermis on top of and behind the eyelid front attach by means of integrins on their basal surface. In the skin, the epidermis is tightly connected to the dermis through integrin-based adhesion. Many large-scale tissue deformations in development also involve heterogeneous tissue interfaces—in gastrulation, the ectoderm and mesoderm are tightly linked by a layer of ECM, and this is sufficient to allow them to converge and extend together. A detailed analysis of cell adhesion in the eyelid by electron microscopy should shed some light on these important details. Likewise, overexpression of E-cadherin in the eyelid to increase cell–cell adhesion would shed light on whether cell–cell adhesion must be maintained within certain levels to allow productive cell intercalation. Regardless of how the front attaches to its surroundings, however, it is clear from the eyelid closure defect in mice lacking both E- and P-cadherin that epidermal cohesion is required for the forces from cell intercalation to be effectively transmitted to the eyelid.

The requirement of both canonical and non-canonical Wnt signaling for eyelid closure raises a number of questions about their relative role. Downregulation of E-cadherin and up-regulation of fibronectin are well-known consequences of canonical Wnt signaling (Jamora et al., 2003; ten Berge et al., 2008), and the pathway is indeed active in the eyelid, particularly at the junction where the front meets the surrounding epidermis. Previous studies have also shown that inhibition or overactivation of Wnt signaling lead to eyelid closure defects,

suggesting that it is carefully regulated both spatially and temporally in the region (Huang et al., 2009). At present, it is unclear if Wnt signaling is necessary for stimulating the secretion of fibronectin and reducing cell–cell adhesion, or whether these are consequences of a more extensive transcriptional program regulating cell motility. Either way, Wnts likely plays a role upstream of the cellular mechanisms physically driving eyelid closure. A particularly attractive hypothesis suggested by the observation of sporadic cell detachment from the epidermis is that localized Wnt signaling mediates the gradual formation of the eyelid front between E14.5 and E15.5. It should be possible to test this hypothesis in detail by combining live imaging with inhibition of Wnt signaling prior to or during eyelid closure by using a variety of conditional knockout mice (e.g. β -catenin, Tcf-3, or Lef-1) with an inducible Cre line (*K14-CreER* or *K14-rTTA/TRE-Cre*) to control the timing of inhibition. The availability of specific small molecule inhibitors of Wnt signaling could also prove useful (Liu et al., 2013).

The role of Wnt/ β -catenin signaling in *Xenopus* convergent extension and early development in general is in line with the notion that its primary role is in mediating the upstream transcriptional changes that drive morphogenesis. Wnt signaling has an early role in embryogenesis in establishing the organizer, a signaling center that controls cell fates and initiates the large-scale cell movements of gastrulation (Kiecker and Niehrs, 2003). Many of these events are triggered by downstream signaling through members of the TGF- β superfamily, such as Nodal and Vg1 (Varlet et al., 1997). In *Xenopus* convergent extension, Wnt signaling is required primarily for activating Nodal signaling rather than directly modulating cell–cell adhesion (Kühl et al., 2001). Interestingly, this was found to occur through Lef-1 rather than Tcf-3, similarly to a recent study of eyelid closure suggesting that the main role of Wnt/ β -catenin signaling is to inhibit Tcf-3’s repression of Lef-1 (Wu et al., 2012). The evidence thus points to a role in specification separate from the pathways that control the intercalary behavior of front cells.

Cell intercalation in epithelial and mesenchymal tissues is frequently controlled by the

4.3. DISCUSSION

non-canonical Wnt/PCP pathway, and eyelid closure is no exception. Using lentiviral injection to achieve skin-specific knockdown of core PCP genes, I found that this pathway has a specific role in eyelid closure. As the specification of front cells is intact, this suggests that PCP regulates cell intercalation either directly or through organization of the fibronectin matrix. Clues to its role come from studies of mediolateral intercalation in the *Xenopus* mesoderm and neural tissues. Unlike the eyelid, *Xenopus* mesodermal cells migrate along an external ECM, a fibronectin matrix assembled by cells of the blastocoel roof. It is thought that integrin adhesion to this polarized ECM suppresses protrusive activity along A–P surfaces, orienting it mediolaterally and promoting intercalation along this axis. Inhibiting integrin-fibronectin adhesion results in the randomization of protrusive activity and a failure of convergent extension (Davidson et al., 2006). PCP is believed to play both an indirect role in mediolateral intercalation by regulating the polarized assembly of fibronectin fibrils on the blastocoel roof as well as a direct role in polarizing the protrusive activity of mesodermal cells (Goto et al., 2005). In the case of fibrillogenesis, PCP signaling downstream of Wnt11 is believed to increase cadherin-based adhesion and tissue surface tension in the blastocoel roof through Rac and Pak, which is transmitted to integrin-fibronectin adhesions leading to multimerization of fibronectin monomers (Dzamba et al., 2009). Polarization of protrusive activity, on the other hand, is thought to function downstream of Dsh through Daam, Rho, and ROCK (Seifert and Mlodzik, 2007).

In eyelid closure, PCP could be involved in either or both of these processes. It is unclear to what extent the fibronectin matrix is organized in the eyelid front. Immunostaining of eyelid whole-mounts did not reveal a clear fibrillar organization, but this will need to be substantiated further by improved fixation and imaging protocols and by electron microscopy. However, whereas PCP controls fibronectin organization at least in part through a separate cell type, the blastocoel roof, this is not the case in the eyelid. Overlying cells of the periderm are not required for eyelid closure, and knockdown of fibronectin specifically in peridermal cells does not affect the process. Thus, if the polarized organization of a fibronectin matrix

is required, it is intrinsic to front cells. In PCP mutants, although fibronectin is still present at the front, it will be important to assess whether its organization is perturbed.

Complicating matters further is that PCP is known to regulate cell–cell adhesion through cadherin recycling. In zebrafish, increased recycling actually increases adhesion (Ulrich et al., 2005), but in other systems it could as easily lead to a decrease. Whether or not cadherins are necessary for cell intercalation in the eyelid, changes in adhesion and surface tension by PCP could modify the mechanical properties of the epidermis as a whole, affecting its ability to be towed by the front. Given that the role of PCP is highly context-dependent, deciphering its role will require carefully addressing each of these possible scenarios. Of particular importance will be an analysis of the dynamics of individual cells in both PCP and integrin/fibronectin mutants. This will immediately clarify whether these interdependent pathways regulate the orientation or frequency of cell protrusive activity.

The presence of tissue boundaries in development often regulates the extent of mediolateral versus radial intercalation, leading to different amounts of tissue thickening or thinning (Keller et al., 2008b). An intriguing possibility is that polarized fibronectin assembly in the eyelid front maintains a careful balance of mediolateral and radial intercalation to generate tissue compression and extension, enabling it to tow the surrounding epidermis. If PCP is involved in polarizing fibronectin assembly in the eyelid, its loss could lead to excessive tissue thickening at the expense of extension. This would result in a delay or failure to close the eyelid, even if cell intercalation speed is unaffected. By combining an analysis of the deformation of the front in 3D with measurements of intercalation speed and the frequency and orientation of protrusions, it will be possible to distinguish between these possible roles of PCP in eyelid closure. More importantly, with a basic understanding of eyelid closure in terms of its cellular behaviors and the extent to which it relies on integrin- and cadherin-mediated adhesion now in place, it will be possible to realize its full potential as a model system by uncovering novel roles of canonical and non-canonical Wnt signaling in mammalian tissue morphogenesis.

4.4. EXPERIMENTAL PROCEDURES

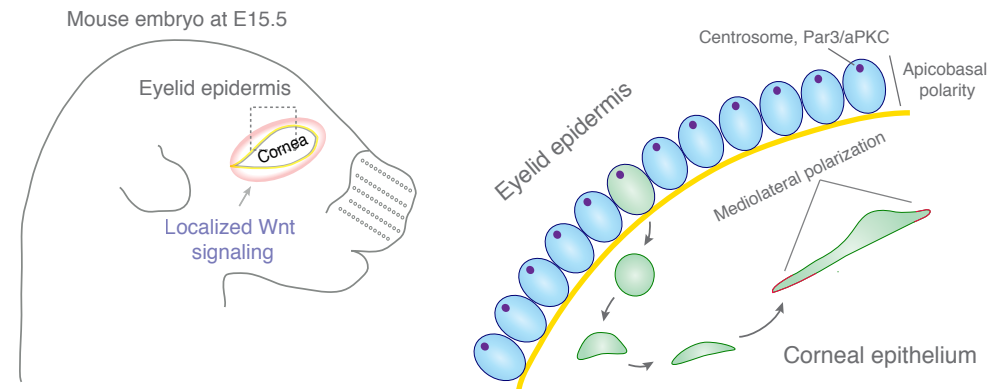
In total, my study of eyelid closure uncovers a novel mechanism of epithelial fusion in which intercalating cells act as a source of circumferential tension to tow the surrounding tissue (Figure 4.12). I propose that formation of the eyelid front is a process of stochastic delamination between E14.5 and E15.5 mediated by localized Wnt/ β -catenin signaling. Upon entering the region, cells adopt an elongated, bipolar morphology and intercalate perpendicularly to the axis of closure, in many ways resembling the convergent extension movements of mesodermal tissues. This intercalation depends on $\alpha_5\beta_1$ integrin/fibronectin and myosin II-dependent cell movement, potentially organized by non-canonical Wnt/PCP signaling and supported by a concomitant reduction in cadherins. As an example in which cells derived from a differentiating epidermis become migratory and undergo cell intercalations, eyelid closure becomes a paradigm for understanding how well-described mechanisms of collective cell movement can be tailored and combined to achieve morphogenetic processes in increasingly complex tissue environments.

4.4 Experimental procedures

4.4.1 Mouse lines

Myh9^{*fl/fl*} mice were purchased from EMMA (EM:02572). *BATGAL* mice were a gift from S. Piccolo (University of Padua, Padua, Italy), *Ecad*^{*fl/fl*} from R. Kemler (Max Planck Institute, Freiburg, Germany), *Looptail* (LPT/Le stock, Jackson Laboratories) from M.W. Kelley (NIDCD, NIH, Rockville, MD), and *Circletail* from R. Rachel (NCI, Frederick, MD). Generation of *Ecad*^{*fl/fl*}; *PcadRNAi* was described previously (Tinkle et al., 2008). To generate *Lp/Lp* or *Crc/Crc* mice expressing *K14-H2B-GFP*, I established *Lp/+; K14-H2B-GFP/+* and *Crc/+; K14-H2B-GFP/+* lines and mated double heterozygotes prior to experiments.

Formation of the eyelid front



Cells enter the region of the eye from the epidermis, lose apicobasal polarity, and adopt an elongated, bipolar morphology between E14 and E15.

Eyelid closure

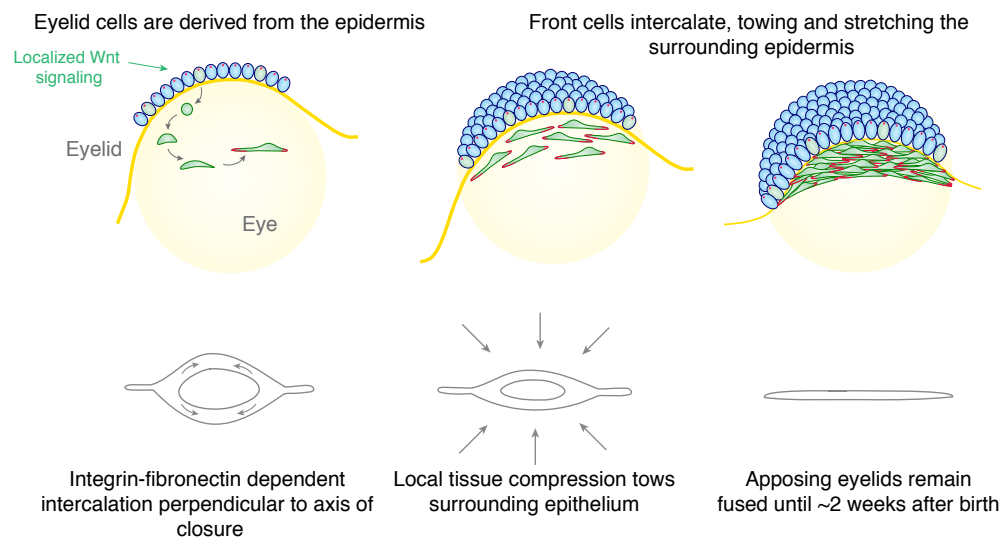


Figure 4.12: Proposed mechanism of eyelid closure. As the eye emerges and local (likely Wnt) signals are transmitted, a population of epidermal cells in the eyelid downregulates E-cadherin, upregulates fibronectin and α_5 integrin, and acquire mesenchymal features (top). They produce an elaborate actomyosin network and initiate intercalation movements, leading to localized compression and extension and enabling them to exert a net force on the surrounding epidermis. This elongates the epidermal cells within the sheet and pulls it over the eye (bottom). The process is regulated by the PCP pathway, and appears to depend directly on α_5 integrin/fibronectin rather than on cadherin-based adhesion.

4.4. EXPERIMENTAL PROCEDURES

4.4.2 Immunofluorescence

Immunostaining and imaging were performed as described earlier. Antibodies were used at the following dilutions: Celsr1 (guinea pig, 1:200, Fuchs lab), E-cadherin (rat, 1:500 sections, 1:50 whole-mount, Fuchs lab), P-cadherin (goat, 1:1000, Zymed), β -galactosidase (rabbit, 1:5000, Cappel), and GFP (chicken, 1:2000, Abcam).

4.4.3 Lentiviral constructs

All shRNAs were obtained from the Broad Institute’s Mission TRC-1 mouse library (Moffat et al., 2006). shRNAs were screened for knockdown efficiency in cultured keratinocytes by quantification of mRNA levels by RT-PCR. The best-performing hairpins were cloned into a pLKO.1 vector expressing H2B-RFP downstream of the PGK promoter using *BamHI* and *NsiI* sites (Beronja et al., 2010). Eyelid closure defects were confirmed using two different hairpins per gene.

Construction of the *LV-TOPGFP* Wnt reporter was described previously (Beronja et al., 2013). The *LV-K17-Cre* construct was created by PCR by amplifying the mouse K17 promoter from a K17-GFP construct provided by Pierre Coulombe and cloning it into the lab’s *LV-Cre* plasmid in place of the PGK promoter using *SacII* and *BamHI* sites. An identical strategy was used for generating *LV-Pax6-Cre*, except that the Pax6 promoter (the 64 bp upstream of exon 1) and the conserved 341 bp upstream enhancer were amplified from genomic DNA. All plasmids were sequenced prior to large-scale lentiviral production and injection into mice. The primer sequences used were as follows:

Pax6-Enhancer-F: 5'-CCGGCCGCGGGGTTACACCAGAAGCACCC-3'
Pax6-P0-R: 5'-GGATCCGCTCCGGCAGGCGCTAACTTTCCTTAATATCCACGCCAGCAAT-GCCCTCATTGTTGCCGGGCG-AGTAAGAAGTTCTGCCGAAC-3'
K17-F: 5'-CCGGCCGCGGGAATTCATCATTTGTCTGTTCAT-3'
K17-R: 5'-CCGGGGATCCGGAGCTGGAGGGCTTGGGAGG-3'

The target sequences for shRNAs used were as follows:

Scramble shRNA: 5'-CCTAAGGTTAAGTCGCCCTCG-3'

Fn1-8108: GCCTAGAAATACCTTTCTCTT-3'

Fn1-5056: GCCAGTTTCCATCAATTATAA-3'

Itga5-2548: CCTCAGCAAGAACCTGAACAA-3'

Itga5-1402: GCAAGATGAGTTCAGCCGATT-3'

Myh9-504: CGGTAAATTCATTCGTATCAA-3'

Myh9-507: GCGATACTACTCAGGGCTTAT-3'

Itgav-3359: CGTGTGTTCTTAGGGACTTAA-3'

Itgh1-363: GCACGATGTGATGATTTAGAA-3'

Ecad-2378: CGGGACAATGTGTATTACTAT-3'

Ecad-1957: GCCTCATATCATCACCATCTT-3'

4.4.4 Statistical analysis

All statistical analyses were performed as described in Chapter 2.

Chapter 5

Summary and Perspectives

Processes of cell movement underlie all tissue morphogenesis in development, homeostasis, and disease. These processes have fascinated biologists since cells were first observed under microscopes, and for more than a hundred years, we have been piecing together the puzzle of how cells of the early embryo give rise to the incredible diversity of tissues that make up an organism. This study has spanned multiple size regimes. We now not only understand the mechanics of how individual cells adhere to their surroundings and propel themselves forward, but how groups of cells interconnect, adjust their mechanical properties, and form discrete domains within an organism. Even more, we understand in great detail not only which cells of the early embryo give rise to which tissues in development, but the signaling pathways that drive the process (Solnica-Krezel, 2005). This has uncovered an intimate link between cell movement and cell fate. In many ways, tissue formation is simply a process in which cells are signaled to move away from other cells. Likewise, once formed, tissues are characterized by the extent to which their constituent cells are motile or adherent. Even the epithelial tissues that line the internal cavities and the outside of our bodies, providing a barrier and regulating the exchange of nutrients and chemicals with the environment, retain a remarkable capacity to mobilize their cells into adulthood (Martin, 1997). Without this, we would be unable to heal wounds or regenerate our tissues in response to internal and external stresses. And of course, aberrant or misregulated cell movement is the hallmark of many of the most devastating diseases of our generation, including metastatic cancer (Sahai,

2005). The study of cell movement is thus fundamental not only to our understanding of development, but also to basic processes relevant to human health and disease.

To carry out the vast demands placed on them, cells must coordinate their behaviors and migrate collectively. Such movements are both intricate and incredibly varied, and thus research into cell movement will continue well into the future. By studying cell movements in model morphogenetic processes, we can gain insight into the diversity of cellular behaviors that contribute to the shaping of embryos and organs, and to tissue homeostasis and disease. Elegant studies in model organisms including flies, fish, and mice have somewhat surprisingly revealed that a small number of evolutionarily conserved behaviors that differ only in details of execution underlies this diversity, both in different contexts within an organism and across species. Among them are convergent extension movements, in which cell intercalation drives the narrowing of a tissue along one axis and elongation along another; epithelial fusions, in which epithelial cells often assemble a contractile actomyosin purse string to squeeze a gap or wound closed; and variations of directed cell migration, in which individual or groups of cells coordinate their migration toward a signal ([Section 1.4](#)).

The study of such behaviors in model morphogenetic processes, such as dorsal closure and germband extension in *Drosophila*, convergent extension in the *Xenopus* dorsal mesoderm, and neural tube closure in mice has yielded enormous insight into the cellular and molecular mechanisms that drive them. Live imaging of gastrulation movements in frog, fish, and mouse embryos is now common practice, and every day we understand the details of their regulation in finer detail. A key challenge is to now understand to what extent these mechanisms operate outside of early development in processes of organogenesis, tissue homeostasis and repair, and the etiology of disease. Although we are only beginning to understand how different modes of collective migration are combined and tailored to achieve diverse morphogenetic tasks throughout the life of an organism, we continue to expand our knowledge through advances in imaging modalities, methods to maintain embryos and organs *ex vivo*, and techniques to visualize cells within adult animals. The picture that is

5.1. EYELID CLOSURE AS A MODEL SYSTEM

emerging is that no single mode of cell movement characterizes tissue morphogenesis in the increasingly complex tissue environments of late development and adulthood. Branching morphogenesis in the *Drosophila* trachea or mouse mammary gland, for example, integrates aspects of both cell intercalation and the specification of leader and follower cells characteristic of epithelial sheet movement (Lu and Werb, 2008). Live imaging of cancer cells within tumors in recent years has similarly revealed that cells invade adjacent tissues not as individual cells, but as sheets or strands (Friedl et al., 2012). Understanding the variations on conserved mechanisms of collective movement at play outside of early development is thus vital to understanding principles of morphogenesis in complex systems.

5.1 Eyelid closure as a model system

As a model system, eyelid closure is unique in that it is a process of epithelial fusion involving a differentiating epidermis, and that it occurs late in mammalian development. It thus has perhaps the most potential in providing insights applicable to human diseases involving aberrant or misregulated migration. The intercalation of eyelid front cells is, in a way, reminiscent of mesodermal tissues, raising the possibility that cells within a differentiating tissue can be induced to adopt modes of collective migration characteristic of early development, and that they can drive large-scale tissue movements. Eyelid closure is thus not only a convenient model of cell intercalation in a mammalian system, but a scenario in which basic, highly conserved mechanisms of cell movement are re-purposed. My studies have in large part only laid the groundwork, defining the basic players of the system and the extent of their reliance on integrin- and cadherin-based adhesion. With live imaging techniques and lentiviral tools now in place, deciphering the pathways that control cell intercalation in this system and uncovering novel regulators of collective migration should be well within reach.

Among the defining features of eyelid closure are a transformation of epidermal cells to a motile fate, which involves the acquisition of a highly elongated, bipolar morphology, a shift in integrin and keratin expression, and intercalation perpendicular to the axis

of closure. Whereas the formation of the migratory eyelid front appears to be mediated by Wnt/ β -catenin signaling, cell intercalation itself appears to be controlled separately by the non-canonical Wnt/PCP pathway. This may represent a general strategy of collective movement in late development and adulthood, as differentiating tissues such as the skin must simultaneously maintain a stable epidermal barrier and mobilize cells to heal wounds or regenerate epidermal structures. Specifying a small region of active cell migration or cell intercalation enables substantial, directional tissue movement without altering the properties of the majority of cells.

In addition to eyelid closure, such a mechanism appears to be at play in embryonic wound healing, recently shown to require PCP (Caddy et al., 2010). However, in this scenario, it is unclear if PCP mediates the formation of a contractile actomyosin cable, as observed in the chick wing bud, polarization of keratinocytes at the leading edge, shown to be regulated by PCP in tissue culture (Caddy et al., 2010; Dow et al., 2007), or cell intercalation. Similarly, wound healing in adult skin is thought to occur by the crawling of keratinocytes over an interstitial ECM and contraction of the wound bed (Martin, 1997), a process in which canonical Wnts are known to be important but in which the role of PCP has not yet been explored. Thus, to what extent a combination of canonical and non-canonical Wnt signaling is involved in specifying an active tissue region to achieve a morphogenetic task is ripe for future study both in the eyelid and in other systems. It will be particularly interesting to learn whether cell intercalation is involved in other processes, as it may represent an under-appreciated mechanism of epithelial sheet movement and fusion. In some scenarios, specifying a region of active cell intercalation may be preferable to a contractile actomyosin cable or directed migration, as it potentially allows a fine-tuning of tissue compression and extension, enabling varying degrees of tissue pulling, spreading and thinning, or thickening.

5.2 Cell intercalation in eyelid closure

The requirement of integrin–fibronectin adhesion in eyelid closure is intriguing not for its role in cell intercalation *per se*, but for its necessity in a case of epithelial intercalation. Cell intercalation is typically classified as being either epithelial, which involves the polarized, myosin II-dependent remodeling of apical junctions, or mesodermal, which involves polarized cell movements. Whereas the expectation is that epithelial cells depend predominantly on cadherins and mesodermal cells on integrins, the situation is significantly more complex than this. Mesodermal cells also require some degree of cadherin-based adhesion—either too much or too little results in defective convergent extension—and it turns out the same may be true of integrins and epithelial cells. Integrin- and cadherin-based adhesion are also highly interdependent, sharing a number of effectors, including the Rho GTPases, and links to the actin cytoskeleton, including vinculin and VASP (Harris and Tepass, 2010). In some contexts, they are antagonistic, as in processes of EMT (Thiery et al., 2009), but in other cases they appear to reinforce each other, likely by transmitting tension through the cytoskeleton (Dzamba et al., 2009). It is thus not surprising that integrin and cadherin-based adhesion cooperate in processes of cell intercalation.

In eyelid closure, this balance is heavily tilted in the direction of integrin adhesion. Although cadherins are required insofar as they maintain epidermal cohesion, the process of intercalation itself appears to rely directly on α_5 integrin and fibronectin, perhaps as a means for cells to gain traction on one another. This is somewhat surprising, because although they acquire some “mesenchymal” features and intercalate in the manner of mesodermal cells, eyelid front cells are nevertheless epidermal. This suggests that, regardless of cell type, there is some plasticity in the mode of cell intercalation employed. Indeed, a somewhat less appreciated mode of cell intercalation that occurs in the dorsal epidermis of *C. elegans* and in the notochord of ascidians and fish, which in these organisms is epithelial, involves basolateral protrusive activity leading to the wedging of cells between each other (Heid et al., 2001). In this scenario, protrusive activity likely represents a dynamic remodeling of cell-cell junctions

rather than a process of cell migration, similar to what occurs in the early stages of adherens junction formation (Vasioukhin et al., 2000). Thus, the directed actin polymerization that in some contexts leads to the zippering of cell membranes and the formation of stable junctions may mediate cell intercalation situations where cell–cell adhesion is fundamentally weaker.

Recent studies in *Xenopus* and mice further suggest that epithelial and mesodermal modes of cell intercalation are not mutually exclusive. In the *Xenopus* mesoderm, it was discovered that PCP can direct the myosin II-dependent remodeling of D–V-oriented junctions, driving intercalation by a T1 process as observed in the *Drosophila* germband (Shindo and Wallingford, 2014). This occurs concomitantly with mediolaterally-oriented protrusive activity, and it is unclear to what extent either or both are necessary for convergent extension. Mouse neural tube closure is similarly thought to involve a process of epithelial intercalation that generates anisotropic tension in the neuroectoderm, both narrowing the tissue and bending it to form a tube (Nishimura et al., 2012). However, a recent study documents both apical junction remodeling and basolateral protrusive activity that can independently form multicellular rosettes (Williams, et. al., in press). These appear to contribute equally to neural tube closure, suggesting that both cell protrusive activity and apical junction remodeling can simultaneously play a role in cell intercalation. Just as integrin- and cadherin-based adhesion can be thought of as manifestations of the same basic process, with the prevalence of one over the other depending on context, it appears that the two modes of cell intercalation may represent a common process and simply reflect differences in the local tissue environment or physical properties of cells.

The reliance of cell intercalation in the eyelid on integrins over cadherins implies that it is fundamentally a process of polarized motility, as originally proposed for mediolateral intercalation in mesodermal tissues. Such a process could, in theory, utilize only integrin–fibronectin adhesion. However, a detailed analysis of individual cell behaviors in the eyelid remains to be performed. It will be interesting to see how PCP is involved and whether it cooperates with integrin adhesion to orient cell protrusive activity, localizes myosin II to

shrink specific cell junctions, or both. Eyelid closure may thus prove to be a useful model not only for understanding how modes of collective movement are integrated to achieve a complex morphogenetic process, but how the basic cellular behaviors underlying them are regulated.

5.3 Beyond eyelid closure

Fully understanding a morphogenetic process requires probing the dynamics of cells at multiple levels of detail. Cell movement, proliferation, and shape change can all contribute in various ways and at different times. Live imaging techniques and computational analyses thus form a major part of the modern developmental biologist's toolbox. For the analysis of eyelid closure, I utilized a combination of H2B-GFP-expressing embryos to visualize and track global cell movements, sparse-labeling of cells with membrane-targeted GFP by lentiviral injection to visualize individual cell dynamics, and a combination of lentivirally-expressed shRNAs and conditional knockout mice for loss-of-function studies. In combination with live imaging techniques and quantitative image analysis, this constitutes a powerful set of tools that can easily be adapted to the study of any morphogenetic process in the skin. In addition to establishing eyelid closure as a model of epithelial fusion in the mouse and setting the stage for the future study of PCP in regulating cell intercalation, it is hoped that the work presented here will facilitate the study of other dynamic processes in the skin, including early hair follicle morphogenesis and asymmetric cell division in early epidermal stratification.

One relatively unexplored aspect of eyelid closure is the full set of transcriptional changes that accompany the transition of front cells to a motile fate. Although the process in general falls within the realm of EMT, characterized by the upregulation of integrins and fibronectin and downregulation of E-cadherin, classical markers such as vimentin are not obviously present. It is possible that front cells undergo an EMT to carry out eyelid closure and an MET subsequently to maintain a continuous epidermal seam, but more likely is that the

acquisition of motile properties by the skin takes a slightly different form. Transcriptional profiling to better characterize this transition would be extremely informative in light of the extensive data our lab has acquired about the downgrowth and cycling of hair follicles, which have many features in common with eyelid front cells.

The genome-wide transcriptional profiling of even small numbers of cells is becoming routine with low-input amplification methods. Our lab has had success performing Illumina sequencing starting with as little as 500 pg mRNA (from ~500 FACS purified cells). This level of sensitivity would allow profiling cells both prior to eyelid closure to understand the transcriptional changes required for formation of the eyelid front, and during eyelid closure to understand those required for cell migration. This has enormous potential for uncovering novel regulators not only of cell motility, collective migration, and intercalation, but pathways mediating the acquisition of motile or invasive properties. In this way, eyelid closure could have relevance beyond the closing of eyelids and into the realm of human health.

Bibliography

- Abercrombie, M., Heaysman, J. E., and Pegrum, S. M. The locomotion of fibroblasts in culture. I. Movements of the leading edge. *Exp Cell Res*, 59(3):393–398, Mar. 1970a.
- Abercrombie, M., Heaysman, J. E. M., and Pegrum, S. M. The locomotion of fibroblasts in culture. *Exp Cell Res*, 62(2-3):389–398, Oct. 1970b.
- Abercrombie, M., Joan, E., Heaysman, M., and Pegrum, S. M. The locomotion of fibroblasts in culture. *Exp Cell Res*, 60(3):437–444, June 1970c.
- Adams, R. H. and Alitalo, K. Molecular regulation of angiogenesis and lymphangiogenesis. *Nat Rev Mol Cell Biol*, 8(6):464–478, June 2007.
- Ahrens, M. B., Orger, M. B., Robson, D. N., Li, J. M., and Keller, P. J. Whole-brain functional imaging at cellular resolution using light-sheet microscopy. *Nat Meth*, 10(5):413–420, May 2013.
- Ahtiainen, L., Lefebvre, S., Lindfors, P. H., and Renvoisé, E. Directional Cell Migration, but Not Proliferation, Drives Hair Placode Morphogenesis. *Dev Cell*, 2014.
- Arboleda-Estudillo, Y., Krieg, M., Stühmer, J., Licata, N. A., Muller, D. J., and Heisenberg, C.-P. Movement Directionality in Collective Migration of Germ Layer Progenitors. *Curr Biol*, 20(2):161–169, Jan. 2010.
- Arias, A. M. and Jacinto, A. Dpp signalling orchestrates dorsal closure by regulating cell shape changes both in the amnioserosa and in the epidermis. *Mech Dev*, 124(11-12):884–897, Nov. 2007.
- Bahri, S., Wang, S., Conder, R., Choy, J., Vlachos, S., Dong, K., Merino, C., Sigrist, S., Molnar, C., Yang, X., Manser, E., and Harden, N. The leading edge during dorsal closure as a model for epithelial plasticity: Pak is required for recruitment of the Scribble complex and septate junction formation. *Development*, 137(12):2023–2032, June 2010.
- Baker, P. C. and Schroeder, T. E. Cytoplasmic filaments and morphogenetic movement in the amphibian neural tube. *Dev Biol*, 15(5):432–450, May 1967.

- Baker, R. E., Schnell, S., and Maini, P. K. Mathematical models for somite formation. *Curr Top Dev Biol*, 81:183–203, 2008.
- Bate, C. M. Pioneer neurones in an insect embryo. *Nature*, 260(5546):54–56, Mar. 1976.
- Behrndt, M., Salbreux, G., Campinho, P., Hauschild, R., Oswald, F., Roensch, J., Grill, S. W., and Heisenberg, C.-P. Forces driving epithelial spreading in zebrafish gastrulation. *Science*, 338(6104):257–260, Oct. 2012.
- Bement, W. M. Wound Healing in Model Organisms. *Annu Rev Cell Dev Biol*, 27(1):110301095425039, Oct. 2010.
- Bement, W. M., Mandato, C. A., and Kirsch, M. N. Wound-induced assembly and closure of an actomyosin purse string in *Xenopus* oocytes. *Curr Biol*, 9(11):579–587, June 1999.
- Beronja, S., Livshits, G., Williams, S., and Fuchs, E. Rapid functional dissection of genetic networks via tissue-specific transduction and RNAi in mouse embryos. *Nat Med*, 16(7):821–827, July 2010.
- Beronja, S., Janki, P., Heller, E., Lien, W.-H., Keyes, B. E., Oshimori, N., and Fuchs, E. RNAi screens in mice identify physiological regulators of oncogenic growth. *Nature*, 501(7466):185–190, Sept. 2013.
- Bertet, C., Sulak, L., and Lecuit, T. Myosin-dependent junction remodelling controls planar cell intercalation and axis elongation. *Nature*, 429(6992):667–671, 2004.
- Blanchard, G. B., Kabla, A. J., Schultz, N. L., Butler, L. C., Sanson, B., Gorfinkiel, N., Mahadevan, L., and Adams, R. J. Tissue tectonics: morphogenetic strain rates, cell shape change and intercalation. *Nat Meth*, 6(6):458–464, June 2009.
- Blankenship, J. T., Backovic, S. T., Sanny, J. S. P., Weitz, O., and Zallen, J. A. Multicellular rosette formation links planar cell polarity to tissue morphogenesis. *Dev Cell*, 11(4):459–470, Oct. 2006.
- Breitman, M. L., Rombola, H., Maxwell, I. H., Klintworth, G. K., and Bernstein, A. Genetic ablation in transgenic mice with an attenuated diphtheria toxin A gene. *Mol. Cell. Biol.*, 10(2):474–479, Feb. 1990.
- Brieher, W. M. and Gumbiner, B. M. Regulation of C-cadherin function during activin induced morphogenesis of *Xenopus* animal caps. *J Cell Biol*, 126(2):519–527, July 1994.
- Brock, J., Midwinter, K., Lewis, J., and Martin, P. Healing of incisional wounds in the embryonic chick wing bud: characterization of the actin purse-string and demonstration of a requirement for Rho activation. *J Cell Biol*, 135(4):1097–1107, Nov. 1996a.
- Brock, J. E., Midwinter, K., Lewis, J., and Martin, P. Healing of incisional wounds in the embryonic chick wing bud: characterization of the actin purse-string and demonstration of a requirement for Rho activation. *J Cell Biol*, 135(4):1097–1107, Oct. 1996b.

BIBLIOGRAPHY

- Brodland, G. W. The Differential Interfacial Tension Hypothesis (DITH): A Comprehensive Theory for the Self-Rearrangement of Embryonic Cells and Tissues. *J Biomech Eng*, 124 (2):188–197, Apr. 2002.
- Caddy, J., Wilanowski, T., Darido, C., Dworkin, S., Ting, S. B., Zhao, Q., Rank, G., Auden, A., Srivastava, S., Papenfuss, T. A., Murdoch, J. N., Humbert, P. O., Boulos, N., Weber, T., Zuo, J., Cunningham, J. M., and Jane, S. M. Epidermal Wound Repair Is Regulated by the Planar Cell Polarity Signaling Pathway. *Dev Cell*, 19(1):138–147, Feb. 2010.
- Cano, A., rez Moreno, M. A. P. e., Rodrigo, I., Locascio, A., Blanco, M. i. a. J., del Barrio, M. G., Portillo, F., and Nieto, M. A. The transcription factor Snail controls epithelial–mesenchymal transitions by repressing E-cadherin expression. *Nat Cell Biol*, 2(2):76–83, Feb. 2000.
- Carroll, J. M., Luetkeke, N. C., Lee, D. C., and Watt, F. M. Role of integrins in mouse eyelid development: studies in normal embryos and embryos in which there is a failure of eyelid fusion. *Mech Dev*, 78(1-2):37–45, Nov. 1998.
- Chen, X. and Gumbiner, B. M. Paraxial protocadherin mediates cell sorting and tissue morphogenesis by regulating C-cadherin adhesion activity. *J Cell Biol*, 174(2):301–313, July 2006.
- Chrzanowska-Wodnicka, M. and Burridge, K. Rho-stimulated contractility drives the formation of stress fibers and focal adhesions. *J Cell Biol*, 133(6):1403–1415, June 1996.
- Coulombe, P. A., Kerns, M. L., and Fuchs, E. Epidermolysis bullosa simplex: a paradigm for disorders of tissue fragility. *Journal of Clinical Investigation*, 119(7):1784–1793, July 2009.
- Curtin, J. A., Quint, E., Tsipouri, V., Arkell, R. M., Cattnach, B., Copp, A. J., Henderson, D. J., Spurr, N., Stanier, P., Fisher, E. M., Nolan, P. M., Steel, K. P., Brown, S. D. M., Gray, I. C., and Murdoch, J. N. Mutation of *Celsr1* Disrupts Planar Polarity of Inner Ear Hair Cells and Causes Severe Neural Tube Defects in the Mouse. *Curr Biol*, 13(13):1129–1133, July 2003a.
- Curtin, J. A., Quint, E., Tsipouri, V., Arkell, R. M., Cattnach, B., Copp, A. J., Henderson, D. J., Spurr, N., Stanier, P., Fisher, E. M., Nolan, P. M., Steel, K. P., Brown, S. D. M., Gray, I. C., and Murdoch, J. N. Mutation of *Celsr1* disrupts planar polarity of inner ear hair cells and causes severe neural tube defects in the mouse. *Curr Biol*, 13(13):1129–1133, July 2003b.
- da Silva, S. M. and Vincent, J. P. Oriented cell divisions in the extending germband of *Drosophila*. *Development*, 134(17):3049–3054, Aug. 2007.
- Damon, B. J., Mezentseva, N. V., Kumaratilake, J. S., Forgacs, G., and Newman, S. A. Limb bud and flank mesoderm have distinct ”physical phenotypes” that may contribute to limb budding. *Dev Biol*, 321(2):319–330, Sept. 2008.
- Danen, E. H. J. and Sonnenberg, A. Integrins in regulation of tissue development and function. *J. Pathol.*, 200(4):471–480, July 2003.

- Danjo, Y. and Gipson, I. K. Actin “purse string” filaments are anchored by E-cadherin-mediated adherens junctions at the leading edge of the epithelial wound, providing coordinated cell movement. *J Cell Sci*, 111:3323–3332, Nov. 1998.
- Davidson, L. A., Koehl, M. A., Keller, R., and Oster, G. F. How do sea urchins invaginate? Using biomechanics to distinguish between mechanisms of primary invagination. *Development*, 1995.
- Davidson, L. A., Marsden, M., Keller, R., and DeSimone, D. W. Integrin $\alpha 5 \beta 1$ and fibronectin regulate polarized cell protrusions required for *Xenopus* convergence and extension. *Curr Biol*, 16(9):833–844, May 2006.
- Davis, G. S., Phillips, H. M., and Steinberg, M. S. Germ-layer surface tensions and “tissue affinities” in *Rana pipiens* gastrulae: quantitative measurements. *Dev Biol*, 192(2):630–644, Dec. 1997.
- Davis, M. A., Ireton, R. C., and Reynolds, A. B. A core function for p120-catenin in cadherin turnover. *J Cell Biol*, 163(3):525–534, Nov. 2003.
- de Beco, S., Gueudry, C., Amblard, F., and Coscoy, S. Endocytosis is required for E-cadherin redistribution at mature adherens junctions. *Proc Nat Acad Sci*, 106(17):7010–7015, Apr. 2009.
- Delarue, M., Saez, F. J., Boucaut, J. C., Thiery, J. P., and Broders, F. Medial cell mixing during axial morphogenesis of the amphibian embryo requires cadherin function. *Dev Dyn*, 213(3):248–260, Nov. 1998.
- Denk, W., Piston, D. W., and Webb, W. W. Two-Photon Molecular Excitation in Laser-Scanning Microscopy. *Handbook of Biological Confocal Microscopy*, (Chapter 28):445–458, 1995.
- Devenport, D. and Fuchs, E. Planar polarization in embryonic epidermis orchestrates global asymmetric morphogenesis of hair follicles. *Nat Cell Biol*, Oct. 2008.
- Dow, L. E., Kauffman, J. S., Caddy, J., Peterson, A. S., Jane, S. M., Russell, S. M., and Humbert, P. O. The tumour-suppressor Scribble dictates cell polarity during directed epithelial migration: regulation of Rho GTPase recruitment to the leading edge. *Oncogene*, 26(16):2272–2282, Apr. 2007.
- Dowling, J., Yu, Q. C., and Fuchs, E. Beta4 integrin is required for hemidesmosome formation, cell adhesion and cell survival. *J Cell Biol*, 134(2):559–572, 1996.
- Drees, F., Pokutta, S., Yamada, S., Nelson, W. J., and Weis, W. I. Alpha-catenin is a molecular switch that binds E-cadherin-beta-catenin and regulates actin-filament assembly. *Cell*, 123(5):903–915, Dec. 2005.
- Duband, J. L., Monier, F., Delannet, M., and Newgreen, D. Epithelium-Mesenchyme Transition during Neural Crest Development. *Cells Tissues Organs*, 154(1):63–78, 1995.

BIBLIOGRAPHY

- Duchek, P., Somogyi, K., Jékely, G., Beccari, S., and Rorth, P. Guidance of cell migration by the Drosophila PDGF/VEGF receptor. *Cell*, 107(1):17–26, Oct. 2001.
- Durbin, L., Brennan, C., Shiomi, K., Cooke, J., Barrios, A., Shanmugalingam, S., Guthrie, B., Lindberg, R., and Holder, N. Eph signaling is required for segmentation and differentiation of the somites. *Genes & Development*, 12(19):3096–3109, Oct. 1998.
- Dzamba, B. J., Jakab, K. R., Marsden, M., Schwartz, M. A., and DeSimone, D. W. Cadherin adhesion, tissue tension, and noncanonical Wnt signaling regulate fibronectin matrix organization. *Dev Cell*, 16(3):421–432, Mar. 2009.
- Elul, T. and Keller, R. Monopolar protrusive activity: a new morphogenic cell behavior in the neural plate dependent on vertical interactions with the mesoderm in *Xenopus*. *Dev Biol*, 224(1):3–19, Aug. 2000.
- Etienne-Manneville, S. Polarity proteins in migration and invasion. *Oncogene*, 27(55):6970–6980, Nov. 2008.
- Ezratty, E. J., Stokes, N., Chai, S., Shah, A. S., Williams, S. E., and Fuchs, E. A role for the primary cilium in Notch signaling and epidermal differentiation during skin development. *Cell*, 145(7):1129–1141, June 2011.
- Fagotto, F., Rohani, N., Touret, A.-S., and Li, R. A molecular base for cell sorting at embryonic boundaries: contact inhibition of cadherin adhesion by ephrin/ Eph-dependent contractility. *Dev Cell*, 27(1):72–87, Oct. 2013.
- Farhadifar, R., Röper, J.-C., Aigouy, B., Eaton, S., and Jülicher, F. The influence of cell mechanics, cell-cell interactions, and proliferation on epithelial packing. *Curr Biol*, 17(24):2095–2104, Dec. 2007.
- Farooqui, R. and Fenteany, G. Multiple rows of cells behind an epithelial wound edge extend cryptic lamellipodia to collectively drive cell-sheet movement. *J Cell Sci*, 2005.
- Fernandez-Gonzalez, R., Simões, S. d. M., Roeper, J.-C., Eaton, S., and Zallen, J. A. Myosin II Dynamics Are Regulated by Tension in Intercalating Cells. *Dev Cell*, 17(5):736–743, Nov. 2009.
- Findlater, G. S., McDougall, R. D., and Kaufman, M. H. Eyelid development, fusion and subsequent reopening in the mouse. *J Anat*, 183 (Pt 1):121–129, Aug. 1993.
- Foty, R. A. and Steinberg, M. S. The differential adhesion hypothesis: a direct evaluation. *Dev Biol*, 278(1):255–263, Feb. 2005.
- Foty, R. A., Pflieger, C. M., Forgacs, G., and Steinberg, M. S. Surface tensions of embryonic tissues predict their mutual envelopment behavior. *Development*, 122(5):1611–1620, May 1996.
- Francis, G. W., Fisher, L. R., Gamble, R. A., and Gingell, D. Direct measurement of cell detachment force on single cells using a new electromechanical method. *J Cell Sci*, 87 (Pt 4):519–523, May 1987.

- Friedl, P. and Gilmour, D. Collective cell migration in morphogenesis, regeneration and cancer. *Nat Rev Mol Cell Biol*, 10(7):445–457, July 2009.
- Friedl, P., Locker, J., Sahai, E., and Segall, J. E. Classifying collective cancer cell invasion. *Nat Cell Biol*, 14(8):777–783, Aug. 2012.
- Fuchs, E. Skin stem cells: rising to the surface. *J Cell Biol*, 180(2):273–284, Jan. 2008.
- Fuchs, E. and Cleveland, D. W. A Structural Scaffolding of Intermediate Filaments in Health and Disease. *Science*, 279(5350):514–519, Jan. 1998.
- Fuchs, E. and Green, H. Changes in keratin gene expression during terminal differentiation of the keratinocyte. *Cell*, 19(4):1033–1042, Apr. 1980.
- Gage, P. J., Qian, M., Wu, D., and Rosenberg, K. I. The canonical Wnt signaling antagonist DKK2 is an essential effector of PITX2 function during normal eye development. *Dev Biol*, 317(1):310–324, May 2008.
- Gail, M. H. and Boone, C. W. The locomotion of mouse fibroblasts in tissue culture. *Biophys J*, 10(10):980–993, Oct. 1970.
- Garrod, D. and Chidgey, M. Desmosome structure, composition and function. *BBA - Biomembranes*, 1778(3):572–587, Mar. 2008.
- Gavard, J. and Gutkind, J. S. VEGF controls endothelial-cell permeability by promoting the beta-arrestin-dependent endocytosis of VE-cadherin. *Nat Cell Biol*, 8(11):1223–1234, Nov. 2006.
- Geiger, B. and Yamada, K. M. Molecular architecture and function of matrix adhesions. *Cold Spring Harb Perspect Biol*, 3(5):a005033, May 2011.
- Geiger, B., Tokuyasu, K. T., Dutton, A. H., and Singer, S. J. Vinculin, an intracellular protein localized at specialized sites where microfilament bundles terminate at cell membranes. *Proc Nat Acad Sci*, 77(7):4127–4131, July 1980.
- Geisbrecht, E. R. and Montell, D. J. Myosin VI is required for E-cadherin-mediated border cell migration. *Nat Cell Biol*, 4(8):616–620, Aug. 2002.
- George, E. L., Baldwin, H. S., and Hynes, R. O. Fibronectins are essential for heart and blood vessel morphogenesis but are dispensable for initial specification of precursor cells. *Blood*, 90(8):3073–3081, Oct. 1997.
- Ghabrial, A., Luschnig, S., Metzstein, M., and Krasnow, M. Branching Morphogenesis Of The Drosophila Tracheal System. *Annu Rev Cell Dev Biol*, 19(1):623–647, Nov. 2003.
- Gong, Y., Mo, C., and Fraser, S. E. Planar cell polarity signalling controls cell division orientation during zebrafish gastrulation. *Nature*, 430(7000):689–693, Aug. 2004.

BIBLIOGRAPHY

- Gorfinkel, N., Blanchard, G. B., Adams, R. J., and Martinez Arias, A. Mechanical control of global cell behaviour during dorsal closure in *Drosophila*. *Development*, 136(11):1889–1898, June 2009.
- Goto, T., Davidson, L., Asashima, M., and Keller, R. Planar cell polarity genes regulate polarized extracellular matrix deposition during frog gastrulation. *Curr Biol*, 15(8):787–793, Apr. 2005.
- Greenburg, G. and Hay, E. D. Epithelia suspended in collagen gels can lose polarity and express characteristics of migrating mesenchymal cells. *J Cell Biol*, 95(1):333–339, Oct. 1982.
- Grosshans, J. and Wieschaus, E. A genetic link between morphogenesis and cell division during formation of the ventral furrow in *Drosophila*. *Cell*, 101(5):523–531, May 2000.
- Gumbiner, B. M. Regulation of cadherin-mediated adhesion in morphogenesis. *Nat Rev Mol Cell Biol*, 6(8):622–634, Aug. 2005.
- Haas, P. and Gilmour, D. Chemokine Signaling Mediates Self-Organizing Tissue Migration in the Zebrafish Lateral Line. *Dev Cell*, 10(5):673–680, May 2006.
- Haigo, S. L., Hildebrand, J. D., Harland, R. M., and Wallingford, J. B. Shroom Induces Apical Constriction and Is Required for Hingepoint Formation during Neural Tube Closure. *Curr Biol*, 13(24):2125–2137, Dec. 2003.
- Hall, A. and Nobes, C. D. Rho GTPases: molecular switches that control the organization and dynamics of the actin cytoskeleton. *Philos. Trans. R. Soc. Lond., B, Biol. Sci.*, 355(1399):965–970, July 2000.
- Hamblet, N. S. Dishevelled 2 is essential for cardiac outflow tract development, somite segmentation and neural tube closure. *Development*, 129(24):5827–5838, Dec. 2002.
- Hammerschmidt, M. and Wedlich, D. Regulated adhesion as a driving force of gastrulation movements. *Development*, 135(22):3625–3641, 2008.
- Harding, C. R. The stratum corneum: structure and function in health and disease. *Dermatologic Therapy*, 17(s1):6–15, 2004.
- Harris, A. K. Is cell sorting caused by differences in the work of intercellular adhesion? A critique of the steinberg hypothesis. *J Theor Biol*, 61(2):267–285, Sept. 1976.
- Harris, M. J. and McLeod, M. J. Eyelid growth and fusion in fetal mice. *Anat Embryol*, 164(2):207–220, 1982.
- Harris, T. J. C. and Tepass, U. Adherens junctions: from molecules to morphogenesis. *Nat Rev Mol Cell Biol*, 11(7):502–514, July 2010.
- Hay, E. D. An overview of epithelio-mesenchymal transformation. *Acta Anat*, 154(1):8–20, 1995.

- Hayashi, T. and Carthew, R. W. Surface mechanics mediate pattern formation in the developing retina : Abstract : *Nature*. *Nature*, 2004.
- Heath, J. P. and Dunn, G. A. Cell to substratum contacts of chick fibroblasts and their relation to the microfilament system. A correlated interference-reflexion and high-voltage electron-microscope study. *J Cell Sci*, 29(1):197–212, Feb. 1978.
- Heid, P.J., Raich, W. B., Smith, R., Mohler, W. A., Simokat, K., Gendreau, S. B., Rothman, J. H., and Hardin, J. The Zinc Finger Protein DIE-1 Is Required for Late Events during Epithelial Cell Rearrangement in *C. elegans*. *Dev Biol*, 236(1):165–180, Aug. 2001.
- Hilgenfeldt, S., Eriskien, S., and Carthew, R. W. Physical modeling of cell geometric order in an epithelial tissue. *Proc Nat Acad Sci*, 105(3):907–911, Jan. 2008.
- Hirai, Y., Nose, A., Kobayashi, S., and Takeichi, M. Expression and role of E- and P-cadherin adhesion molecules in embryonic histogenesis. II. Skin morphogenesis. *Development*, 105(2):271–277, Feb. 1989.
- Horwitz, A., Duggan, K., Buck, C., Beckerle, M. C., and Burridge, K. Interaction of plasma membrane fibronectin receptor with talin [mdash] a transmembrane linkage. *Nature*, 320(6062):531–533, Apr. 1986.
- Hou, S. X., Zheng, Z., Chen, X., and Perrimon, N. The Jak/STAT pathway in model organisms: emerging roles in cell movement. *Dev Cell*, 3(6):765–778, Dec. 2002.
- Huang, J., Dattilo, L. K., Rajagopal, R., Liu, Y., Kaartinen, V., Mishina, Y., Deng, C.-X., Umans, L., Zwijsen, A., Roberts, A. B., and Beebe, D. C. FGF-regulated BMP signaling is required for eyelid closure and to specify conjunctival epithelial cell fate. *Development*, 136(10):1741–1750, May 2009.
- Huisken, J., Swoger, J., Del Bene, F., Wittbrodt, J., and Stelzer, E. H. K. Optical Sectioning Deep Inside Live Embryos by Selective Plane Illumination Microscopy. *Science*, 305(5686):1007–1009, Aug. 2004.
- Hutson, M. S., Tokutake, Y., Chang, M. S., Bloor, J. W., Venakides, S., Kiehart, D. P., and Edwards, G. S. Forces for morphogenesis investigated with laser microsurgery and quantitative modeling. *Science*, 300:145–149, 2003.
- Hyafil, F., Babinet, C., and Jacob, F. Cell-cell interactions in early embryogenesis: A molecular approach to the role of calcium. *Cell*, 26(3):447–454, Nov. 1981.
- Hynes, R. O. and Destree, A. T. Relationships between fibronectin (LETS protein) and actin. *Cell*, 15(3):875–886, Nov. 1978.
- Ilić, D., Damsky, C. H., and Yamamoto, T. Focal adhesion kinase: at the crossroads of signal transduction. *J Cell Sci*, 110 (Pt 4):401–407, Feb. 1997.
- Irvine, K. D. and Wieschaus, E. Cell intercalation during *Drosophila* germband extension and its regulation by pair-rule segmentation genes. *Development*, 120(4):827–841, Apr. 1994.

BIBLIOGRAPHY

- Iwano, M., Plieth, D., Danoff, T. M., Xue, C., Okada, H., and Neilson, E. G. Evidence that fibroblasts derive from epithelium during tissue fibrosis. *Journal of Clinical Investigation*, 110(3):341–350, Aug. 2002.
- Jacinto, A., Wood, W., Woolner, S., Hiley, C., and Turner, L. Dynamic analysis of actin cable function during *Drosophila* dorsal closure. *Curr Biol*, 2002a.
- Jacinto, A., Woolner, S., and Martin, P. Dynamic analysis of dorsal closure in *Drosophila*: from genetics to cell biology. *Dev Cell*, 3(1):9–19, July 2002b.
- Jamora, C. and Fuchs, E. Intercellular adhesion, signalling and the cytoskeleton. *Nat Cell Biol*, 4(4):E101–8, Apr. 2002.
- Jamora, C., DasGupta, R., Kocieniewski, P., and Fuchs, E. Links between signal transduction, transcription and adhesion in epithelial bud development. *Nature*, 422(6929):317–322, 2003.
- Jaqaman, K. K., Loerke, D. D., Mettlen, M. M., Kuwata, H. H., Grinstein, S. S., Schmid, S. L. S., and Danuser, G. G. Robust single-particle tracking in live-cell time-lapse sequences. *Nat Meth*, 5(8):695–702, Aug. 2008.
- Jiang, L. and Tsai, H. L. Femtosecond laser ablation: challenges and opportunities. *Proceeding of NSF Workshop on Research ...*, 2003.
- Jin, J.-Z. and Ding, J. Analysis of cell migration, transdifferentiation and apoptosis during mouse secondary palate fusion. *Development*, 133(17):3341–3347, Sept. 2006.
- Jockusch, B. M., Bubeck, P., Giehl, K., Kroemker, M., Moschner, J., Rothkegel, M., Rüdiger, M., Schlüter, K., Stanke, G., and Winkler, J. The molecular architecture of focal adhesions. *Annu Rev Cell Dev Biol*, 11(1):379–416, 1995.
- Jones, E., Crotty, D., Kulesa, P., Waters, C., Baron, M., Fraser, S., and Dickinson, M. Dynamic in vivo imaging of postimplantation mammalian embryos using whole embryo culture. *Genesis*, 34(4):228–235, 2002.
- Kaltschmidt, J., Lawrence, N., Morel, V., and Balayo, T. Planar polarity and actin dynamics in the epidermis of *Drosophila*. *Nat Cell Biol*, 2002.
- Kane, D. A., McFarland, K. N., and Warga, R. M. Mutations in half baked/E-cadherin block cell behaviors that are necessary for teleost epiboly. *Development*, 132(5):1105–1116, Mar. 2005.
- Kashiwagi, M. and Huh, N. Organ culture of developing mouse skin and its application for molecular mechanistic studies of morphogenesis. *Epidermal Cells*, 2005.
- Keller, P. J., Schmidt, A. D., Wittbrodt, J., and Stelzer, E. H. K. Reconstruction of zebrafish early embryonic development by scanned light sheet microscopy. *Science*, 322(5904):1065–1069, Nov. 2008a.

- Keller, P. J., Schmidt, A. D., Santella, A., Khairy, K., Bao, Z., Wittbrodt, J., and Stelzer, E. H. K. Fast, high-contrast imaging of animal development with scanned light sheet-based structured-illumination microscopy. *Nat Meth*, 7(8):637–642, Aug. 2010.
- Keller, R. Shaping the vertebrate body plan by polarized embryonic cell movements. *Science*, 298(5600):1950–1954, Dec. 2002.
- Keller, R., Cooper, M. S., Danilchik, M., Tibbetts, P., and Wilson, P. A. Cell intercalation during notochord development in *Xenopus laevis*. *J. Exp. Zool.*, 251(2):134–154, Aug. 1989.
- Keller, R., Davidson, L., Edlund, A., Elul, T., Ezin, M., Shook, D., and Skoglund, P. Mechanisms of convergence and extension by cell intercalation. *Philos. Trans. R. Soc. Lond., B, Biol. Sci.*, 355(1399):897–922, July 2000.
- Keller, R., Shook, D., and Skoglund, P. The forces that shape embryos: physical aspects of convergent extension by cell intercalation. *Phys Biol*, 5(1):15007, 2008b.
- Keller, R. E. The cellular basis of epiboly: an SEM study of deep-cell rearrangement during gastrulation in *Xenopus laevis*. *J. Embryol Exp Morph*, 60:201–234, Dec. 1980.
- Kiecker, C. and Niehrs, C. The role of Wnt signaling in vertebrate head induction and the organizer-gradient model dualism. *Wnt signaling in development*, 2003.
- Kiehart, D. P., Galbraith, C. G., Edwards, K. A., Rickoll, W. L., and Montague, R. A. Multiple forces contribute to cell sheet morphogenesis for dorsal closure in *Drosophila*. *J Cell Biol*, 149(2):471–490, Apr. 2000.
- Kim, H. Y. and Davidson, L. A. Punctuated actin contractions during convergent extension and their permissive regulation by the non-canonical Wnt-signaling pathway. *J Cell Sci*, 124(Pt 4):635–646, Feb. 2011.
- Kinoshita, N., Iioka, H., Miyakoshi, A., and Ueno, N. PKC delta is essential for Dishevelled function in a noncanonical Wnt pathway that regulates *Xenopus* convergent extension movements. *Genes & Development*, 17(13):1663–1676, July 2003.
- Kobielak, A. and Fuchs, E. α -catenin: at the junction of intercellular adhesion and actin dynamics. *Nat Rev Mol Cell Biol*, 5(8):614–625, Aug. 2004.
- Kobielak, A., Pasolli, H. A., and Fuchs, E. Mammalian formin-1 participates in adherens junctions and polymerization of linear actin cables. *Nat Cell Biol*, 6(1):21–30, Jan. 2004.
- Kölsch, V., Seher, T., Fernandez-Ballester, G. J., Serrano, L., and Leptin, M. Control of *Drosophila* gastrulation by apical localization of adherens junctions and RhoGEF2. *Science*, 315(5810):384–386, Jan. 2007.
- Kovacs, E. M., Ali, R. G., McCormack, A. J., and Yap, A. S. E-cadherin homophilic ligation directly signals through Rac and phosphatidylinositol 3-kinase to regulate adhesive contacts. *J Biol Chem*, 277(8):6708–6718, Feb. 2002.

BIBLIOGRAPHY

- Kraft, B., Berger, C. D., Wallkamm, V., Steinbeisser, H., and Wedlich, D. Wnt-11 and Fz7 reduce cell adhesion in convergent extension by sequestration of PAPC and C-cadherin. *J Cell Biol*, 198(4):695–709, Aug. 2012.
- Kreft, B., Berndorff, D., and Böttinger, A. LI-Cadherin-mediated Cell-Cell Adhesion Does Not Require Cytoplasmic Interactions. *J Cell Biol*, 1997.
- Krieg, M., Arboleda-Estudillo, Y., Puech, P. H., Kaefer, J., Graner, F., Mueller, D. J., and Heisenberg, C. P. Tensile forces govern germ-layer organization in zebrafish. *Nat Cell Biol*, 10(4):429–U122, Apr. 2008.
- Kühl, M., Geis, K., Sheldahl, L. C., Pukrop, T., Moon, R. T., and Wedlich, D. Antagonistic regulation of convergent extension movements in *Xenopus* by Wnt/beta-catenin and Wnt/Ca²⁺ signaling. *Mech Dev*, 106(1-2):61–76, Aug. 2001.
- Kwon, G. S., Viotti, M., and Hadjantonakis, A.-K. The Endoderm of the Mouse Embryo Arises by Dynamic Widespread Intercalation of Embryonic and Extraembryonic Lineages. *Dev Cell*, 15(4):509–520, Oct. 2008.
- Labelle, M., Begum, S., and Hynes, R. O. Direct Signaling between Platelets and Cancer Cells Induces an Epithelial-Mesenchymal-Like Transition and Promotes Metastasis. *Cancer Cell*, 20(5):576–590, Nov. 2011.
- Landsberg, K. P., Farhadifar, R., Ranft, J., Umetsu, D., Widmann, T. J., Bittig, T., Said, A., Jülicher, F., and Dahmann, C. Increased cell bond tension governs cell sorting at the *Drosophila* anteroposterior compartment boundary. *Curr Biol*, 19(22):1950–1955, Dec. 2009.
- le Duc, Q., Shi, Q., and Blonk, I. Vinculin potentiates E-cadherin mechanosensing and is recruited to actin-anchored sites within adherens junctions in a myosin II-dependent manner. *J Cell Biol*, 2010.
- Lechler, T. and Fuchs, E. Asymmetric cell divisions promote stratification and differentiation of mammalian skin. *Nature*, 437(7056):275–280, Sept. 2005.
- Lecuit, T. and Lenne, P.-F. c. o. Cell surface mechanics and the control of cell shape, tissue patterns and morphogenesis. *Nat Rev Mol Cell Biol*, 8(8):633–644, Aug. 2007.
- Lee, C. H. and Gumbiner, B. M. Disruption of gastrulation movements in *Xenopus* by a dominant-negative mutant for C-cadherin. *Dev Biol*, 171(2):363–373, Oct. 1995.
- Lee, J.-Y. and Harland, R. M. Actomyosin contractility and microtubules drive apical constriction in *Xenopus* bottle cells. *Dev Biol*, 311(1):40–52, Nov. 2007.
- Leise, W. F. and Mueller, P. R. Inhibition of the cell cycle is required for convergent extension of the paraxial mesoderm during *Xenopus* neurulation. *Development*, 131(8):1703–1715, Apr. 2004.

- Leptin, M. Gastrulation in *Drosophila*: the logic and the cellular mechanisms. *EMBO J*, 18(12):3187–3192, 1999.
- Letourneau, P. C. Cell-to-substratum adhesion and guidance of axonal elongation. *Dev Biol*, 44(1):92–101, May 1975.
- Levi, G., Gumbiner, B., and Thiery, J. P. The Distribution of E-Cadherin During *Xenopus*-*Laevis* Development. *Development*, 111(1):159–169, Jan. 1991.
- Li, A., Ma, Y., Yu, X., Mort, R. L., Lindsay, C. R., Stevenson, D., Strathdee, D., Insall, R. H., Chernoff, J., Snapper, S. B., Jackson, I. J., Larue, L., Sansom, O. J., and Machesky, L. M. Rac1 Drives Melanoblast Organization during Mouse Development by Orchestrating Pseudopod-Driven Motility and Cell-Cycle Progression. *Dev Cell*, 21(4):722–734, Oct. 2011.
- Lienkamp, S. S., Liu, K., Karner, C. M., Carroll, T. J., Ronneberger, O., Wallingford, J. B., and Walz, G. Vertebrate kidney tubules elongate using a planar cell polarity-dependent, rosette-based mechanism of convergent extension. *Nat Genet*, 44(12):1382–1387, Dec. 2012.
- Liu, J., Pan, S., Hsieh, M. H., Ng, N., Sun, F., Wang, T., Kasibhatla, S., Schuller, A. G., Li, A. G., Cheng, D., Li, J., Tompkins, C., Pferdekamper, A., Steffy, A., Cheng, J., Kowal, C., Phung, V., Guo, G., Wang, Y., Graham, M. P., Flynn, S., Brenner, J. C., Li, C., Villarroel, M. C., Schultz, P. G., Wu, X., McNamara, P., Sellers, W. R., Petruzzelli, L., Boral, A. L., Seidel, H. M., McLaughlin, M. E., Che, J., Carey, T. E., Vanasse, G., and Harris, J. L. Targeting Wnt-driven cancer through the inhibition of Porcupine by LGK974. *Proc Nat Acad Sci*, 110(50):20224–20229, Dec. 2013.
- Livet, J., Weissman, T. A., Kang, H., Draft, R. W., Lu, J., Bennis, R. A., Sanes, J. R., and Lichtman, J. W. Transgenic strategies for combinatorial expression of fluorescent proteins in the nervous system. *Nature*, 450(7166):56–62, Nov. 2007.
- Livshits, G., Kobiela, A., and Fuchs, E. Governing epidermal homeostasis by coupling cell-cell adhesion to integrin and growth factor signaling, proliferation, and apoptosis. *Proc Nat Acad Sci*, 109(13):4886–4891, Mar. 2012.
- Lu, H., Hesse, M., Peters, B., and Magin, T. M. Type II keratins precede type I keratins during early embryonic development. *Eur J Cell Biol*, 84(8):709–718, Sept. 2005.
- Lu, P. and Werb, Z. Patterning Mechanisms of Branched Organs. *Science*, 322(5907):1506–1509, Dec. 2008.
- Luetke, N. C., Qiu, T. H., Peiffer, R. L., Oliver, P., Smithies, O., and Lee, D. C. TGF alpha deficiency results in hair follicle and eye abnormalities in targeted and waved-1 mice. *Cell*, 73(2):263–278, Apr. 1993.
- Lynley, A. M. and Dale, B. A. The characterization of human epidermal filaggrin. *Biochimica et Biophysica Acta (BBA) - Protein Structure and Molecular Enzymology*, 744(1):28–35, Apr. 1983.

BIBLIOGRAPHY

- Maconnachie, E. A study of digit fusion in the mouse embryo. *J Embryol Exp Morph*, 49: 259–276, Jan. 1979.
- Maître, J.-L., Berthoumieux, H., Krens, S. F. G., Salbreux, G., Jülicher, F., Paluch, E., and Heisenberg, C.-P. Adhesion Functions in Cell Sorting by Mechanically Coupling the Cortices of Adhering Cells. *Science*, pages 253–256, Aug. 2012.
- Marchisio, P. C., Bondanza, S., Cremona, O., Cancedda, R., and De Luca, M. Polarized expression of integrin receptors ($\alpha 6 \beta 4$, $\alpha 2 \beta 1$, $\alpha 3 \beta 1$, and $\alpha v \beta 5$) and their relationship with the cytoskeleton and basement membrane matrix in cultured human keratinocytes. *J Cell Biol*, 112(4):761–773, Feb. 1991.
- Margolis, B. and Borg, J.-P. Apicobasal polarity complexes. *J Cell Sci*, 118(Pt 22):5157–5159, Nov. 2005.
- Marsden, M. and DeSimone, D. W. Integrin-ECM Interactions Regulate Cadherin-Dependent Cell Adhesion and Are Required for Convergent Extension in *Xenopus*. *Curr Biol*, 13(14):1182–1191, July 2003.
- Martin, A. C., Kaschube, M., and Wieschaus, E. F. Pulsed contractions of an actin | myosin network drive apical constriction. *Nature*, 457(7228):495–499, Nov. 2008.
- Martin, P. Wound healing - Aiming for perfect skin regeneration. *Science*, 276(5309):75–81, 1997.
- Martinez-Rico, C., Pincet, F., Thiery, J.-P., and Dufour, S. Integrins stimulate E-cadherin-mediated intercellular adhesion by regulating Src-kinase activation and actomyosin contractility. *J Cell Sci*, 123(5):712–722, Mar. 2010.
- Mathieu, J., Griffin, K., Herbomel, P., Dickmeis, T., Strähle, U., Kimelman, D., Rosa, F. M., and Peyri  ras, N. Nodal and Fgf pathways interact through a positive regulatory loop and synergize to maintain mesodermal cell populations. *Development*, 131(3):629–641, Feb. 2004.
- M’Boneko, V. and Merker, H. J. Development and Morphology of the Periderm of Mouse Embryos (Days 9–12 of Gestation). *Cells Tissues Organs*, 133(4):325–336, 1988.
- McCafferty, R. E. A physiological study of the amniotic fluid of the mouse. I. Volume and weight changes of the amniotic fluid compared with the weights of fetus and placenta during gestation. *Anat Rec*, 123(4):521–530, Dec. 1955.
- McCluskey, J., Hopkinson-Woolley, J., Luke, B., and Martin, P. A study of wound healing in the E11.5 mouse embryo by light and electron microscopy. *Tissue Cell*, 25(2):173–181, 1993.
- McGowan, K. M. and Coulombe, P. A. Onset of keratin 17 expression coincides with the definition of major epithelial lineages during skin development. *J Cell Biol*, 143(2):469–486, Oct. 1998.

- Miettinen, P. J., Berger, J. E., Meneses, J., Phung, Y., Pedersen, R. A., Werb, Z., and Derynck, R. Epithelial immaturity and multiorgan failure in mice lacking epidermal growth factor receptor. *Nature*, 376(6538):337–341, July 1995.
- Millard, T. H. T. and Martin, P. P. Dynamic analysis of filopodial interactions during the zipper phase of *Drosophila* dorsal closure. *Development*, 135(4):621–626, Feb. 2008.
- Mine, N. HB-EGF promotes epithelial cell migration in eyelid development. *Development*, 132(19):4317–4326, Oct. 2005.
- Minn, A. J., Gupta, G. P., Siegel, P. M., Bos, P. D., Shu, W., Giri, D. D., Viale, A., Olshen, A. B., Gerald, W. L., and Massagué, J. Genes that mediate breast cancer metastasis to lung. *Nature*, 436(7050):518–524, July 2005.
- Moffat, J., Grueneberg, D. A., Yang, X., Kim, S. Y., Kloepper, A. M., Hinkle, G., Piqani, B., Eisenhaure, T. M., Luo, B., Grenier, J. K., Carpenter, A. E., Foo, S. Y., Stewart, S. A., Stockwell, B. R., Hacohen, N., Hahn, W. C., Lander, E. S., Sabatini, D. M., and Root, D. E. A lentiviral RNAi library for human and mouse genes applied to an arrayed viral high-content screen. *Cell*, 124(6):1283–1298, Mar. 2006.
- Montcouquiol, M., Sans, N., Huss, D., Kach, J., Dickman, J. D., Forge, A., Rachel, R. A., Copeland, N. G., Jenkins, N. A., Bogani, D., Murdoch, J., Warchol, M. E., Wenthold, R. J., and Kelley, M. W. Asymmetric Localization of Vangl2 and Fz3 Indicate Novel Mechanisms for Planar Cell Polarity in Mammals. *J Neurosci*, 26(19):5265–5275, May 2006.
- Montell, D. J. Border-cell migration: the race is on. *Nat Rev Mol Cell Biol*, 4(1):13–24, Jan. 2003.
- Montell, D. J., Rorth, P., and Spradling, A. C. slow border cells, a locus required for a developmentally regulated cell migration during oogenesis, encodes *Drosophila* CEBP. *Cell*, 1992.
- Moore, S. W., Keller, R. E., and Koehl, M. A. The dorsal involuting marginal zone stiffens anisotropically during its convergent extension in the gastrula of *Xenopus laevis*. *Development*, 121(10):3131–3140, Oct. 1995.
- Munoz, R., Moreno, M., Oliva, C., Orbenes, C., and Larrain, J. Syndecan-4 regulates non-canonical Wnt signalling and is essential for convergent and extension movements in *Xenopus* embryos. *Nat Cell Biol*, 8(5):492–500, May 2006.
- Murdoch, J. N., Doudney, K., Paternotte, C., Copp, A. J., and Stanier, P. Severe neural tube defects in the loop-tail mouse result from mutation of *Lpp1*, a novel gene involved in floor plate specification. *Hum Mol Genet*, 10(22):2593–2601, Oct. 2001.
- Murdoch, J. N., Henderson, D. J., Doudney, K., Gaston-Massuet, C., Phillips, H. M., Paternotte, C., Arkell, R., Stanier, P., and Copp, A. J. Disruption of scribble (*Scrb1*) causes severe neural tube defects in the circletail mouse. *Hum Mol Genet*, 12(2):87–98, Jan. 2003.

BIBLIOGRAPHY

- Muzumdar, M. D. M., Tasic, B. B., Miyamichi, K. K., Li, L. L., and Luo, L. L. A global double-fluorescent Cre reporter mouse. *Genesis*, 45(9):593–605, Sept. 2007.
- Nakamura, D. H., Nakamura, H., Yasuda, M., and Yasuda, M. An electron microscopic study of periderm cell development in mouse limb buds. *Anat Embryol*, 157(2):121–132, 1979.
- Nakaya, Y., Sukowati, E. W., Wu, Y., and Sheng, G. RhoA and microtubule dynamics control cell-basement membrane interaction in EMT during gastrulation. *Nat Cell Biol*, 10(7):765–775, July 2008.
- Nikolaidou, K. K. and Barrett, K. A Rho GTPase Signaling Pathway Is Used Reiteratively in Epithelial Folding and Potentially Selects the Outcome of Rho Activation. *Curr Biol*, 14(20):1822–1826, Oct. 2004.
- Ninomiya, H., Elinson, R. P., and Winklbauer, R. Antero-posterior tissue polarity links mesoderm convergent extension to axial patterning. *Nature*, 430(6997):364–367, July 2004.
- Nishimura, T., Honda, H., and Takeichi, M. Planar Cell Polarity Links Axes of Spatial Dynamics in Neural-Tube Closure. *Cell*, 149(5):1084–1097, May 2012.
- Nishio, S., Tian, X., Gallagher, A. R., Yu, Z., Patel, V., Igarashi, P., and Somlo, S. Loss of oriented cell division does not initiate cyst formation. *J. Am. Soc. Nephrol.*, 21(2):295–302, Feb. 2010.
- Nobes, C. D. and Hall, A. Rho, Rac, and Cdc42 GTPases regulate the assembly of multi-molecular focal complexes associated with actin stress fibers, lamellipodia, and filopodia. *Cell*, 81(1):53–62, Apr. 1995.
- O'Donnell, M., Chance, R. K., and Bashaw, G. J. Axon Growth and Guidance: Receptor Regulation and Signal Transduction. *Annu Rev Neurosci*, 32(1):383–412, June 2009.
- Omelchenko, T., Vasiliev, J. M., Gelfand, I. M., Feder, H. H., and Bonder, E. M. Rho-dependent formation of epithelial "leader" cells during wound healing. *P Natl Acad Sci Usa*, 100(19):10788–10793, Sept. 2003.
- Osterfield, M., Du, X., Schüpbach, T., Wieschaus, E., and Shvartsman, S. Y. Three-dimensional epithelial morphogenesis in the developing *Drosophila* egg. *Dev Cell*, 24(4):400–410, Feb. 2013.
- Overduin, M., Harvey, T. S., Bagby, S., Tong, K. I., and Yau, P. Solution structure of the epithelial cadherin domain responsible for selective cell adhesion. *Science*, 1995.
- Ozawa, M. and Kemler, R. The membrane-proximal region of the E-cadherin cytoplasmic domain prevents dimerization and negatively regulates adhesion activity. *J Cell Biol*, 1998.
- Piliszek, A., Kwon, G. S., and Hadjantonakis, A.-K. Ex utero culture and live imaging of mouse embryos. *Methods Mol Biol*, 770:243–257, 2011.

- Plusa, B., Piliszek, A., Frankenberg, S., Artus, J., and Hadjantonakis, A.-K. Distinct sequential cell behaviours direct primitive endoderm formation in the mouse blastocyst. *Development*, 135(18):3081–3091, Sept. 2008.
- Pollard, T. D. and Borisy, G. G. Cellular motility driven by assembly and disassembly of actin filaments. *Cell*, 112(4):453–465, Feb. 2003.
- Pouille, P.-A. and Farge, E. Hydrodynamic simulation of multicellular embryo invagination. *Phys Biol*, 5(1):015005, Mar. 2008.
- Poujade, M., Grasland-Mongrain, E., Hertzog, A., Jouanneau, J., Chavrier, P., Ladoux, B., Buguin, A., and Silberzan, P. Collective migration of an epithelial monolayer in response to a model wound. *P Natl Acad Sci Usa*, 104(41):15988–15993, Oct. 2007.
- Pyrgaki, C., Trainor, P., Hadjantonakis, A.-K., and Niswander, L. Dynamic imaging of mammalian neural tube closure. *Dev Biol*, 344(2):941–947, Aug. 2010.
- R Core Team. *R: A Language and Environment for Statistical Computing*. R Foundation for Statistical Computing, Vienna, Austria, 2013. URL <http://www.R-project.org>.
- Radice, G. L. Precocious Mammary Gland Development in P-Cadherin-deficient Mice. *J Cell Biol*, 139(4):1025–1032, Nov. 1997.
- Raghavan, S., Bauer, C., Mundschau, G., Li, Q., and Fuchs, E. Conditional ablation of beta1 integrin in skin. Severe defects in epidermal proliferation, basement membrane formation, and hair follicle invagination. *J Cell Biol*, 150(5):1149–1160, Sept. 2000.
- Rauzi, M., Lenne, P.-F., and Lecuit, T. Planar polarized actomyosin contractile flows control epithelial junction remodelling. *Nature*, 468(7327):1110–1114, Dec. 2010.
- Rice, D. S., Hansen, G. M., Liu, F., Crist, M. J., Newhouse, M. M., Potter, D., Xu, N., Abuin, A., Vogel, P. J., and Zambrowicz, B. P. Keratinocyte Migration in the Developing Eyelid Requires LIMK2. *PLoS ONE*, 7(10):e47168, Oct. 2012.
- Ridley, A. J., Schwartz, M. A., Burridge, K., Firtel, R. A., Ginsberg, M. H., Borisy, G., Parsons, J. T., and Horwitz, A. R. Cell migration: integrating signals from front to back. *Science*, 302(5651):1704–1709, Dec. 2003.
- Rivera-Pérez, J. A., Jones, V., and Tam, P. P. L. Culture of whole mouse embryos at early postimplantation to organogenesis stages: developmental staging and methods. *Meth. Enzymol.*, 476:185–203, 2010.
- Rompolas, P., Deschene, E. R., Zito, G., Gonzalez, D. G., Saotome, I., Haberman, A. M., and Greco, V. supp. *Nature*, 487(7408):496–499, July 2012.
- Root, D. E., Hacohen, N., Hahn, W. C., Lander, E. S., and Sabatini, D. M. Genome-scale loss-of-function screening with a lentiviral RNAi library. *Nat Meth*, 3(9):715–719, Sept. 2006.

BIBLIOGRAPHY

- Sahai, E. Mechanisms of cancer cell invasion. *Curr Opin Genet Dev*, 15(1):87–96, Feb. 2005.
- Sahai, E. Illuminating the metastatic process. *Nat Rev Cancer*, 7(10):737–749, Oct. 2007.
- Savant-Bhonsale, S. and Montell, D. J. torso-like encodes the localized determinant of Drosophila terminal pattern formation. *Genes & Development*, 7(12B):2548–2555, Dec. 1993.
- Schmitz, G. and Muller, G. Structure and Function of Lamellar Bodies, Lipid-Protein Complexes Involved in Storage and Secretion of Cellular Lipids. *J Lipid Res*, 32(10):1539–1570, Oct. 1991.
- Schober, M., Schaefer, M., and Knoblich, J. A. Bazooka recruits Inscuteable to orient asymmetric cell divisions in Drosophila neuroblasts. *Nature*, 402(6761):548–551, Dec. 1999.
- Schoenwolf, G. C. Histological and ultrastructural studies of secondary neurulation in mouse embryos. *Am J Anat*, 169(4):361–376, 1984.
- Schwartz, M. and Simone, D. Cell adhesion receptors in mechanotransduction. *Current Opinion in Cell Biology*, June 2008.
- Seifert, J. R. K. and Mlodzik, M. Frizzled/PCP signalling: a conserved mechanism regulating cell polarity and directed motility. *Nat Rev Genet*, 8(2):126–138, Feb. 2007.
- Sennett, R. and Rendl, M. Mesenchymal-epithelial interactions during hair follicle morphogenesis and cycling. *Semin. Cell Dev. Biol.*, 23(8):917–927, Oct. 2012.
- Shih, J. and Keller, R. Cell Motility Driving Mediolateral Intercalation in Explants of Xenopus-Laevis. *Development*, 116(4):901–914, Dec. 1992.
- Shih, W. and Yamada, S. N-cadherin-mediated cell-cell adhesion promotes cell migration in a three-dimensional matrix. *J Cell Sci*, 125(Pt 15):3661–3670, Aug. 2012.
- Shimizu, Y., Thumkeo, D., Keel, J., Ishizaki, T., Oshima, H., Oshima, M., Noda, Y., Matsumura, F., Taketo, M. M., and Narumiya, S. ROCK-I regulates closure of the eyelids and ventral body wall by inducing assembly of actomyosin bundles. *J Cell Biol*, 168(6): 941–953, Mar. 2005.
- Shin, K., Fogg, V. C., and Margolis, B. Tight junctions and cell polarity. *Annu Rev Cell Dev Biol*, 22:207–235, 2006.
- Shindo, A. and Wallingford, J. B. PCP and septins compartmentalize cortical actomyosin to direct collective cell movement. *Science*, 343(6171):649–652, Feb. 2014.
- Shyer, A. E., Tallinen, T., Nerurkar, N. L., Wei, Z., Gil, E. S., Kaplan, D. L., Tabin, C. J., and Mahadevan, L. Villification: how the gut gets its villi. *Science*, 342(6155):212–218, Oct. 2013.

- Silver, D. L. and Montell, D. J. Paracrine signaling through the JAK/STAT pathway activates invasive behavior of ovarian epithelial cells in *Drosophila*. *Cell*, 107(7):831–841, Dec. 2001.
- Simões, S. d. M., Blankenship, J. T., Weitz, O., Farrell, D. L., Tamada, M., Fernandez-Gonzalez, R., and Zallen, J. A. Rho-Kinase Directs Bazooka/Par-3 Planar Polarity during *Drosophila* Axis Elongation. *Dev Cell*, 19(3):377–388, Sept. 2010.
- Simões, S. d. M., Mainieri, A., and Zallen, J. A. Rho GTPase and Shroom direct planar polarized actomyosin contractility during convergent extension. *J Cell Biol*, 204(4):575–589, Feb. 2014.
- Solnica-Krezel, L. Conserved patterns of cell movements during vertebrate gastrulation. *Curr Biol*, 15(6):R213–28, Mar. 2005.
- Solnica-Krezel, L. and Sepich, D. S. Gastrulation: Making and Shaping Germ Layers. *Annu Rev Cell Dev Biol*, 28(1):687–717, 2012.
- Solon, J., Kaya-Copur, A., Colombelli, J., and Brunner, D. Pulsed forces timed by a ratchet-like mechanism drive directed tissue movement during dorsal closure. *Cell*, 137(7):1331–1342, June 2009.
- Stein, K. and Rudix, I. Development of Mice Homozygous for the Gene for Looptail. *J Hered*, 44(2):59–69, Mar. 1953.
- Steinberg, M. S. On The Mechanism Of Tissue Reconstruction By Dissociated Cells, iii. Free Energy Relations And The Reorganization Of Fused, Heteronomic Tissue Fragments. *P Natl Acad Sci Usa*, 48(10):1769, Oct. 1962.
- Stuebner, S., Faus Kessler, T., Fischer, T., Wurst, W., and Prakash, N. Fzd3 and Fzd6 deficiency results in a severe midbrain morphogenesis defect. *Dev Dyn*, 239(1):246–260, 2010.
- Sweeton, D., Parks, S., Costa, M., and Wieschaus, E. Gastrulation in *Drosophila*: the formation of the ventral furrow and posterior midgut invaginations. *Development*, 112(3):775–789, July 1991.
- Takeichi, M. Functional correlation between cell adhesive properties and some cell surface proteins. *J Cell Biol*, 75(2):464–474, Nov. 1977.
- Tamada, M., Farrell, D. L., and Zallen, J. A. Abl Regulates Planar Polarized Junctional Dynamics through β -Catenin Tyrosine Phosphorylation. *Dev Cell*, 22(2):309–319, Feb. 2012.
- Tao, H., Shimizu, Y., Kusumoto, R., Ono, K., Noji, S., and Ohuchi, H. A dual role of FGF10 in proliferation and coordinated migration of epithelial leading edge cells during mouse eyelid development. *Development*, 132(14):3217–3230, July 2005.

BIBLIOGRAPHY

- ten Berge, D., Koole, W., Fuerer, C., Fish, M., Eroglu, E., and Nusse, R. Wnt signaling mediates self-organization and axis formation in embryoid bodies. *Cell Stem Cell*, 3(5): 508–518, Nov. 2008.
- Thielicke, W., and E. J. Stamhuis. *PIVLab: Time-Resolved Digital Particle Image Velocimetry Tool for MATLAB*, 2013.
- Thiery, J.-P., Acloque, H., Huang, R. Y. J., and Nieto, M. A. Epithelial-Mesenchymal Transitions in Development and Disease. *Cell*, 139(5):871–890, Nov. 2009.
- Thumkeo, D., Shimizu, Y., Sakamoto, S., Yamada, S., and Narumiya, S. ROCK-I and ROCK-II cooperatively regulate closure of eyelid and ventral body wall in mouse embryo. *Genes Cells*, 10(8):825–834, Aug. 2005.
- Tinkle, C. L., Lechler, T., Pasolli, H. A., and Fuchs, E. Conditional targeting of E-cadherin in skin: insights into hyperproliferative and degenerative responses. *P Natl Acad Sci Usa*, 101(2):552–557, Jan. 2004.
- Tinkle, C. L., Pasolli, H. A., Stokes, N., and Fuchs, E. New insights into cadherin function in epidermal sheet formation and maintenance of tissue integrity. *Proc Nat Acad Sci*, 105(40):15405–15410, Oct. 2008.
- Tomer, R., Khairy, K., Amat, F., and Keller, P. J. Quantitative high-speed imaging of entire developing embryos with simultaneous multiview light-sheet microscopy. *Nat Meth*, June 2012.
- Townes, P. L. and Holtfreter, J. Directed movements and selective adhesion of embryonic amphibian cells. *J Exp Zool*, 128(1):53–120, 1955.
- Tozluoglu, M., Tournier, A. L., Jenkins, R. P., Hooper, S., Bates, P. A., and Sahai, E. Matrix geometry determines optimal cancer cell migration strategy and modulates response to interventions. *Nat Cell Biol*, 15(7):751–762, July 2013.
- Tumbar, T., Guasch, G., Greco, V., Blanpain, C., Lowry, W. E., Rendl, M., and Fuchs, E. Defining the epithelial stem cell niche in skin. *Science*, 303(5656):359–363, Jan. 2004.
- Ulrich, F., Krieg, M., Schötz, E.-M., Link, V., Castanon, I., Schnabel, V., Taubenberger, A., Mueller, D., Puech, P.-H., and Heisenberg, C.-P. Wnt11 functions in gastrulation by controlling cell cohesion through Rab5c and E-cadherin. *Dev Cell*, 9(4):555–564, Oct. 2005.
- Vaezi, A., Bauer, C., Vasioukhin, V., and Fuchs, E. Actin Cable Dynamics and Rho/Rock Orchestrate a Polarized Cytoskeletal Architecture in the Early Steps of Assembling a Stratified Epithelium. *Dev Cell*, 3(3):367–381, Sept. 2002.
- Varlet, I., Collignon, J., and Robertson, E. J. nodal expression in the primitive endoderm is required for specification of the anterior axis during mouse gastrulation. *Development*, 124(5):1033–1044, Mar. 1997.

- Vasioukhin, V., Bauer, C., Yin, M., and Fuchs, E. Directed actin polymerization is the driving force for epithelial cell-cell adhesion. *Cell*, 100(2):209–219, Jan. 2000.
- Vasioukhin, V., Bauer, C., Degenstein, L., Wise, B., and Fuchs, E. Hyperproliferation and Defects in Epithelial Polarity upon Conditional Ablation of α -Catenin in Skin. *Cell*, 104(4):605–617, Feb. 2001.
- Vassar, R., Coulombe, P. A., Degenstein, L., Albers, K., and Fuchs, E. Mutant keratin expression in transgenic mice causes marked abnormalities resembling a human genetic skin disease. *Cell*, 64(2):365–380, Jan. 1991.
- Veeman, M. T., Nakatani, Y., Hendrickson, C., Ericson, V., Lin, C., and Smith, W. C. Chongmague reveals an essential role for laminin-mediated boundary formation in chor-date convergence and extension movements. *Development*, 135(1):33–41, Jan. 2008.
- Verma, S., Shewan, A. M., Scott, J. A., Helwani, F. M., den Elzen, N. R., Miki, H., Takenawa, T., and Yap, A. S. Arp2/3 Activity Is Necessary for Efficient Formation of E-cadherin Adhesive Contacts. *J Biol Chem*, 279(32):34062–34070, Aug. 2004.
- Vestal, D. J. and Ranscht, B. Glycosyl phosphatidylinositol-anchored T-cadherin mediates calcium-dependent, homophilic cell adhesion. *J Cell Biol*, 119(2):451–461, Oct. 1992.
- Vicente-Manzanares, M., Ma, X., Adelstein, R. S., and Horwitz, A. R. Non-muscle myosin II takes centre stage in cell adhesion and migration. *Nat Rev Mol Cell Biol*, 10(11):778–790, Nov. 2009.
- Viotti, M., Niu, L., Shi, S.-H., and Hadjantonakis, A.-K. Role of the Gut Endoderm in Relaying Left-Right Patterning in Mice. *PLoS Biol*, 10(3):e1001276, Mar. 2012.
- Vitorino, P. and Meyer, T. Modular control of endothelial sheet migration. *Genes & Development*, 22(23):3268–3281, Nov. 2008.
- Voiculescu, O., Bertocchini, F., Wolpert, L., Keller, R. E., and Stern, C. D. The amniote primitive streak is defined by epithelial cell intercalation before gastrulation. *Nature*, 449(7165):1049–1052, Oct. 2007.
- von der Hardt, S., Bakkers, J., Inbal, A., Carvalho, L., Solnica-Krezel, L., Heisenberg, C.-P., and Hammerschmidt, M. The Bmp gradient of the zebrafish gastrula guides migrating lateral cells by regulating cell-cell adhesion. *Curr Biol*, 17(6):475–487, Mar. 2007.
- Wallingford, J. B., Rowning, B. A., Vogeli, K. M., Rothbächer, U., Fraser, S. E., and Harland, R. M. Dishevelled controls cell polarity during *Xenopus* gastrulation. *Nature*, 405(6782):81–85, May 2000.
- Wang, N., Butler, J. P., and Ingber, D. E. Mechanotransduction across the cell surface and through the cytoskeleton. *Science*, 260(5111):1124–1127, May 1993.
- Wang, X., Bo, J., Bridges, T., Dugan, K. D., Pan, T.-c., Chodosh, L. A., and Montell, D. J. Analysis of cell migration using whole-genome expression profiling of migratory cells in the *Drosophila* ovary. *Dev Cell*, 10(4):483–495, Apr. 2006.

BIBLIOGRAPHY

- Wang, Y. The Role of Frizzled3 and Frizzled6 in Neural Tube Closure and in the Planar Polarity of Inner-Ear Sensory Hair Cells. *J Neurosci*, 26(8):2147–2156, Feb. 2006.
- Weaire, D. and Rivier, N. Soap, cells and statistics—random patterns in two dimensions. *Contemporary Physics*, 25(1):59–99, Aug. 2006.
- Wei, Y. and Mikawa, T. Formation of the avian primitive streak from spatially restricted blastoderm: evidence for polarized cell division in the elongating streak. *Development*, 127(1):87–96, Jan. 2000.
- Weston, J. A. A radioautographic analysis of the migration and localization of trunk neural crest cells in the chick. *Dev Biol*, 6(3):279–310, June 1963.
- Wickham, H. *ggplot2: elegant graphics for data analysis*. Springer New York, 2009. URL <http://had.co.nz/ggplot2/book>.
- Williams, S. E., Beronja, S., Pasolli, H. A., and Fuchs, E. Asymmetric cell divisions promote Notch-dependent epidermal differentiation. *Nature*, 470(7334):353–358, Feb. 2011.
- Wong, P. Loss of keratin 6 (K6) proteins reveals a function for intermediate filaments during wound repair. *J Cell Biol*, 163(2):327–337, Oct. 2003.
- Woodfield, R. J., Hodgkin, M. N., Akhtar, N., Morse, M. A., Fuller, K. J., Saqib, K., Thompson, N. T., and Wakelam, M. The p85 subunit of phosphoinositide 3-kinase is associated with beta-catenin in the cadherin-based adhesion complex. *Biochem J*, 360(Pt 2):335–344, 2001.
- Wu, C., Endo, M., Yang, B. H., Radecki, M. A., Davis, P. F., Zoltick, P. W., Spivak, R. M., Flake, A. W., Kirschner, R. E., and Nah, H.-D. Intra-amniotic Transient Transduction of the Periderm With a Viral Vector Encoding TGF- β 3 Prevents Cleft Palate in Tgf- β 3^{-/-} Mouse Embryos. *Mol Ther*, 21(1):8–17, Jan. 2013.
- Wu, C. I., Hoffman, J. A., Shy, B. R., Ford, E. M., Fuchs, E., Nguyen, H., and Merrill, B. J. Function of Wnt/ β -catenin in counteracting Tcf3 repression through the Tcf3- β -catenin interaction. *Development*, 139(12):2118–2129, May 2012.
- Xu, W., Baribault, H., and Adamson, E. D. Vinculin knockout results in heart and brain defects during embryonic development. *Development*, 125(2):327–337, Jan. 1998.
- Yalcin, H. C., Shekhar, A., and Nishimura, N. Two-photon microscopy-guided femtosecond-laser photoablation of avian cardiogenesis: noninvasive creation of localized heart defects. *Am J Physiol Heart Circ Physiol*, 2010.
- Yamada, S. and Nelson, W. J. Localized zones of Rho and Rac activities drive initiation and expansion of epithelial cell-cell adhesion. *J Cell Biol*, 178(3):517–527, July 2007.
- Yan, C., Grimm, W. A., Garner, W. L., Qin, L., Travis, T., Tan, N., and Han, Y.-P. Epithelial to mesenchymal transition in human skin wound healing is induced by tumor necrosis factor-alpha through bone morphogenic protein-2. *Am J Pathol*, 176(5):2247–2258, May 2010.

- Yang, J., Mani, S. A., Donaher, J. L., Ramaswamy, S., Itzykson, R. A., Come, C., Savagner, P., Gitelman, I., Richardson, A., and Weinberg, R. A. Twist, a master regulator of morphogenesis, plays an essential role in tumor metastasis. *Cell*, 117(7):927–939, 2004.
- Yang, J. T., Rayburn, H., and Hynes, R. O. Embryonic mesodermal defects in alpha 5 integrin-deficient mice. *Development*, 119(4):1093–1105, Dec. 1993.
- Yoshida, C. and Takeichi, M. Teratocarcinoma cell adhesion: Identification of a cell-surface protein involved in calcium-dependent cell aggregation. *Cell*, 28(2):217–224, Feb. 1982.
- Yoshida, M., Shimono, Y., Togashi, H., Matsuzaki, K., Miyoshi, J., Mizoguchi, A., Komori, T., and Takai, Y. Periderm cells covering palatal shelves have tight junctions and their desquamation reduces the polarity of palatal shelf epithelial cells in palatogenesis. *Genes Cells*, 17(6):455–472, June 2012.
- Yvon, A.-M. C., Walker, J. W., Danowski, B., Fagerstrom, C., Khodjakov, A., and Wadsworth, P. Centrosome Reorientation in Wound-Edge Cells Is Cell Type Specific. *Mol Biol Cell*, 13(6):1871–1880, June 2002.
- Zallen, J. A. Planar polarity and tissue morphogenesis. *Cell*, 129(6):1051–1063, June 2007.
- Zallen, J. A. and Wieschaus, E. Patterned gene expression directs bipolar planar polarity in *Drosophila*. *Dev Cell*, 6(3):343–355, Mar. 2004.
- Zenz, R., Scheuch, H., Martin, P., Frank, C., Eferl, R., Kenner, L., Sibilio, M., and Wagner, E. F. c-Jun regulates eyelid closure and skin tumor development through EGFR signaling. *Dev Cell*, 4(6):879–889, June 2003.
- Zhang, L., Wang, W., Hayashi, Y., Jester, J. V., Birk, D. E., Gao, M., Liu, C.-Y., Kao, W. W.-Y., Karin, M., and Xia, Y. A role for MEK kinase 1 in TGF- β /activin-induced epithelium movement and embryonic eyelid closure. *EMBO J*, 22(17):4443–4454, Sept. 2003.
- Zhang, S. and Murphy, T. H. Imaging the Impact of Cortical Microcirculation on Synaptic Structure and Sensory-Evoked Hemodynamic Responses In Vivo. *PLoS Biol*, 5(5):e119, Apr. 2007.
- Zhang, Y., Lam, O., Nguyen, M.-T. T., Ng, G., Pear, W. S., Ai, W., Wang, I.-J., Kao, W. W. Y., and Liu, C.-Y. Mastermind-like transcriptional co-activator-mediated Notch signaling is indispensable for maintaining conjunctival epithelial identity. *Development*, 140(3):594–605, Feb. 2013.
- Zhong, Y., Briher, W. M., and Gumbiner, B. M. Analysis of C-cadherin Regulation during Tissue Morphogenesis with an Activating Antibody. *J Cell Biol*, 144(2):351–359, Jan. 1999.